

Asia Pacific Research Initiative for Sustainable Energy Systems 2012 (APRISES12)

Office of Naval Research
Grant Award Number N00014-13-1-0463

Computational Fluid Dynamics (CFD) Applications at the School of Architecture, University of Hawaii: Development of an Internal CFD Work Process

Task 7

Prepared For
Hawaii Natural Energy Institute

Prepared By
Sustainable Design & Consulting LLC, UH Environmental Research and
Design Laboratory, UH Sea Grant College Program & HNEI

March 2015



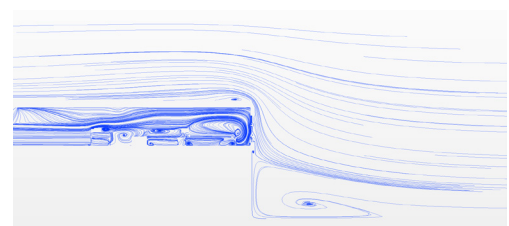
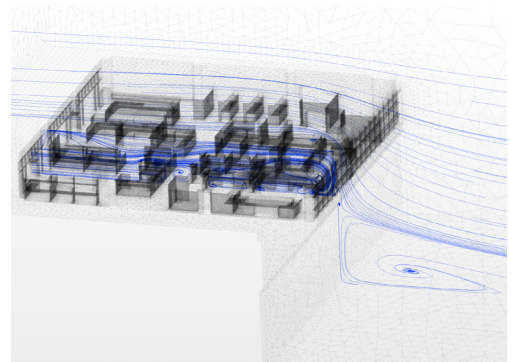
Project Phase 1- 7.B

REPORT ON DEVELOPMENT OF AN INTERNAL CFD WORK PROCESS

7.2

FINAL

March 30, 2015



Prepared by:

Manfred J. Zapka, PhD, PE (Editor)

Tuan Tran, D.Arch

Eileen Peppard, M. Sc.

Stephen Meder, D.Arch, Director

A. James Maskrey, MEP, MBA, Project Manager



Contract # N000-14-13-1-0463

Computational Fluid Dynamics (CFD) Applications at the School of Architecture,
University of Hawaii

Project Phase 1 – 7.B

Develop Skill Set for Internal CFD Analysis and Validation at the Building

Project Deliverable No. 7.2
Report on Development of an Internal CFD Work Process

FINAL

Prepared for Hawaii Natural Energy Institute

in support of

Contract #N000-14-13-1-0463

March 30, 2015

Prepared by:

Manfred J. Zapka, PhD, PE (Editor) (*)

Tuan Tran, D.Arch (**)

Eileen Peppard, M. Sc. (**)

Stephen Meder, D.Arch, Director (**)

A. James Maskrey, MEP, MBA, Project Manager (***)

(*) Sustainable Design & Consulting LLC

(**) Environmental Research and Design Laboratory (ERDL), School of Architecture, University of Hawaii at
Manoa

(***) Hawaii Natural Energy Institute (HNEI), University of Hawaii at Manoa

ACKNOWLEDGEMENTS

The authors would like to thank the staff of the Environmental Design & Research Laboratory (ERDL) for their assistance in carrying out parts of this research study.

The authors especially acknowledge the dedicated work and valuable input by research assistants Christian Damo and Reed Shinsato, and as well as Post-doctoral fellow Aarthi Padmanabhan.

TABLE OF CONTENTS

SECTION 1 – EXECUTIVE SUMMARY1

SECTION 2 – OBJECTIVES3

SECTION 3 – APPROACH OF DEVELOPING THE INTERNAL CFD WORKFLOW5

 3.1 Organizational Workflow and Project Team Responsibilities 5

 3.2 Required Proficiency of CFD Team Members 9

 3.3 Technical Aspects of the CFD Workflow 13

 3.4 CFD Best Practice Guidelines..... 17

SECTION 4 – METHODOLOGY.....21

 4.1 Description of Test Site Room Sinclair 301 and Instrumentation Used in Measurements 21

 4.2 Creating the Model Geometry with CAD Software..... 29

 4.3 Creating the Volume Mesh 32

 4.4 Determining the General Conditions that Affect Internal CFD Simulation..... 35

 4.5 Scope and Structure of CFD Test Scenarios 36

 4.6 Evaluating the Effects of Type and Resolution of the Applied Mesh..... 38

 4.9 Post-Processing – Visualization and Quantifying Internal Air Flow Phenomena 47

SECTION 5 - RESULTS AND DISCUSSION.....60

 5.1 Results of CFD simulations for Main Four Scenarios 60

 5.2 Presentation of the Test Measurements in Sinclair Room 301 65

 5.3 Comparing CFD Results with Actual Test Measurements..... 70

 5.4 Discussion and General Observation 85

SECTION 6 - PREFERRED CFD SETTINGS FOR INTERNAL CFD SIMULATIONS89

6.1 Model Geometry and Extent of Computational Domain..... 89

6.2 Meshing Procedure 90

6.3 Turbulence Models 91

6.4 Boundary conditions 91

6.5 Solver settings 92

REFERENCES93

ACRONYMS.....94

APPENDIX A - ILLUSTRATION OF MESHING PERTAINING TO CAD MODELING APPROACHES

APPENDIX B - RESULTS FROM CFD RUNS

SECTION 1 – EXECUTIVE SUMMARY

The present report on the development of an internal Computational Fluid Dynamics (CFD) work process is part of a CFD research program which is sponsored by the Hawaii Natural Energy Institute. The research program endeavors to develop advanced building modeling skills at the Environmental Design and Research Laboratory (ERDL) of the School of Architecture, University of Hawaii at Manoa.

The present report summarizes the work performed by the ERDL CFD research team developing a generic workflow process for internal CFD analysis at ERDL. This work process can be applied in subsequent CFD analysis work at ERDL. The term “Internal CFD” is referred to air flow occurrences and related physical properties inside an enclosed building space, in opposition to “external CFD” which is referred to as CFD analysis of wind movement and related physical properties outside and around the building.

The CFD research team could take advantage of the research site of another ERDL project, which was Room 301 inside the Sinclair Library on the University of Hawaii at Manoa campus. The Room 301 was equipped with temporary exhaust fans in conjunction with a ventilation and occupant comfort study for Room 301. This method of mechanical forced ventilation provided the CFD research team with the opportunity of using a well-defined air flow condition in Room 301, largely independent of external wind conditions, as a means of validating results obtained from theoretical CFD simulations.

A detailed geometry model of Room 301, including all relevant internal structural element and cubicle walls, was created in the 3D-CAD program Rhino3d. The 3D-CAD model was then exported to the CFD software Star-CCM+. The program Star-CCM+ was used to develop the theoretical VFD predictions of the air flow occurrences inside Room 301.

The CFD team tested the effects of decoupled and coupled domain approaches on the CFD simulation results. The CFD team opted to use a “semi-coupled” domain, where a limited portion of external air volume and the Sinclair Library Building was included in the computational domain. The “semi-coupled” approach proved to provide an effective way to model the inlet condition of Room 301, since only a small portion of the exterior space around Room 301 was included in the computational domain, thereby conserving computational resources. This approach allowed the CFD team to treat the openings of Room 301 as part of the computational domain and retain the ability to apply proper physical properties to the windward facing windows of Room 301. This approach thus allowed the inclusion of approaching wind conditions in defining the inlet conditions to Room 301, such as pressure build-up on the windward building side due to stagnation of wind.

The CFD team used a range of input values to benchmarking main CFD parameters, such as mesh type and size, type and extent of computational domain and solver settings. The CFD parameters used in benchmarking included the following:

- Type of computational domain, coupled or decoupled
- With or without furniture (structural elements such as columns were modeled in every case)
- Type of turbulence model
- Type of boundary condition for inlet of the domain
- Type of boundary condition for outlet (exhaust fans) of the internal space
- Air density and viscosity; either standard conditions (= CFD defaults) or value calculated from measured data at the site

The CFD team performed an initial 40 CFD runs and identified 18 test cases to evaluate the effects of benchmarking parameters in more detail. These 18 test cases included final eight test cases which included four test scenarios using two different turbulence models. The four test scenarios were established in Room 301 in full scale and included a combination of North facing windows of Room 301 either opened or closed and the exhaust fans either operating or not operating.

Air flow velocity and differential pressure conditions were measured in Room 301 using the four test scenarios and the results of the field measurements were used to validate the theoretical CFD predictions of the air flow conditions inside Room 301. The measurements of velocity and differential pressure in Room 301 as well as measurements of external wind conditions by means of a weather station were conducted during the three days of field tests. During these three days, incident wind conditions changed, which showed effects of air movement measured inside Room 301. The data obtained for the air velocity and differential pressures in Room 301 was statistically filtered and analyzed to provide representative description for the conditions inside Room 301. CFD simulations were conducted that used the exterior wind conditions as input wind conditions and the measured data was compared to the CFD simulations results.

The benchmarking and validation procedures carried out allowed the CFD team to develop a preferred work process for internal CFD analysis. This work process will be used by the CFD team for the subsequent project work of internal CFD.

SECTION 2 – OBJECTIVES

The objectives of the project work carried out under project task Task 7.b.2 “Development of an internal CFD work process” were as follows:

- Develop skills to perform CFD simulations of internal air movement and have an opportunity to validate theoretical CFD predictions with actually measured air flow phenomena in a controlled test environment.
- Utilize a large room on the University of Hawaii Manoa campus, Room 301 in Sinclair Library, to carry out full scale validation test of internal CFD simulations. Under another research project of ERDL, Room 301 was equipped with a temporary exhaust fan system. This test set up enabled the ERDL project team to assess the contribution of mechanical assist ventilation to the otherwise naturally ventilated Room 301. The exhaust system made it possible to control the airflow through Room 301 by selecting the windows on the windward side and operating the fans at different volume settings.
- Utilize the forced ventilation test set-up of Room 301 to provide the basis for test scenarios of internal airflow. The test scenarios created in Room 301 should represent combinations of inlet and outlet conditions, with different variations of inlet windows open and different combinations of exhaust fans operating, respectively.
- Conduct CFD benchmark simulations with varying CFD setting parameters, such as domain configuration, mesh configuration, solver setting and turbulence models, to determine the effects of these parameters on the convergence and air flow description performance.
- Determine what CFD settings in the benchmarking CFD simulations would provide the best convergence, calculation stability and air flow description performance for the test case. The most advantageous settings were then to be used in simulating the test scenarios which were established in the full scale Room 301 to induce s case specific internal air movement patterns.
- Determine the effectiveness of different post processing procedures of CFD simulations to obtain qualitative and quantitative determination of the CFD solutions.
- Use the measurement procedures for air velocity and pressure distribution in internal air flow, developed under the project task “Task 7.b.3: "Development and calibration of a data verification process for internal CFD simulations" to provide actual air velocity and differential pressures for the test scenarios.

- Utilize the data measured for air velocities and pressures under the test scenarios in Room 301 and compare the actual data with the theoretical CFD predictions. Acquire experience in interpreting validation of CFD results with actual air flow performance and obtain application knowledge in determining likely causes for different degrees of data consistence between theoretical predictions and actual measurements.
- On the basis of experience of the CFD work performed for this project phase, develop preferred domain geometry, mesh generation and CFD solver settings that should be used in subsequent internal CFD analysis.

SECTION 3 – APPROACH OF DEVELOPING THE INTERNAL CFD WORKFLOW

This section describes the approach taken in developing a work process for the study of internal air movement using the CFD software application.

3.1 Organizational Workflow and Project Team Responsibilities

This section describes the organizational structure and generic technical steps of the internal CFD workflow that have been adopted by the ERDL CFD team. The elements of the generic organization workflow are depicted in Figure 3.1. Figure 3.1 suggests two categories of process steps in the CFD workflow:

- Process steps (1) and (2) are decision steps in the work flow, which require setting of goals and objectives of the CFD calculation process and determining how close these goals have been achieved.
- Process steps (A) through (D) are part of four sequential CFD steps in the work process. This workflow elaborates the computational solution of the CFD problem. The work process steps (A) through (D) are basically the “tool-set” of the CFD calculation workflow. The validity of the process steps by themselves is not dependent on a suitably defined objective of the CFD project. This means while the calculation procedure might be correct, wrong input values can create inaccurate final results.

There are several different team functions for different phases in the CFD workflow. The responsibilities of the team members are described in this section.

Process step (1): At the start of the internal CFD work process the first step (1) is to set objectives for the CFD investigation, for example to determine the properties and phenomena that have to be determined on the basis of the internal air movement. Each objective might require specific physical settings and calculation procedures of the CFD analysis. At the conclusion of the process step (1) all relevant calculation parameters and requirements have been defined.

Responsibilities of project team members for process step (1) are shared between the principal investigator and project manager. The decision about the objectives has to be determined in close cooperation with the CFD project team. The CFD investigation has to serve the design objective at hand. The principal investigator needs to have a good understanding about the overall CFD work process to translate the project objectives into a viable CFD project approach.

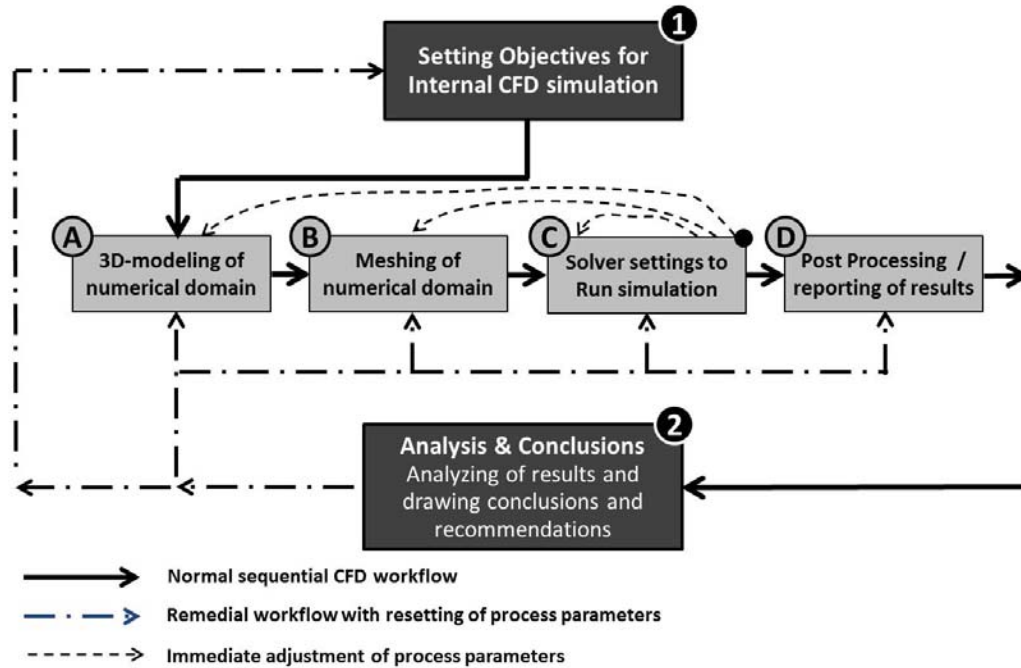


Figure 3.1: Generic organizational work process for internal CFD showing process steps involved

Process step (2): After the completion of a major CFD calculation iteration, the results obtained are examined regarding their consistency with the objectives, the estimated accuracy of the solution and the anticipated physical behavior of air-movement and related processes. Based on these findings, conclusions can be drawn about whether or not the CFD analysis produced quality data. The analysis assessment of results (2) determines whether the results appear to be valid or whether CFD results favorably compare to previous validation results. In case of a favorable review, the CFD analysis is accepted and the results allow conclusions to answer the objectives and goals. If the results appear to be questionable or a sensitivity analysis of certain parameter is needed, a new CFD calculation iteration is initiated. If the assessment of CFD results suggests that the objectives have not been met in a consistent way, the objectives might have to be revisited. In the more likely event a new CFD calculation procedure will be required along with changing geometry for the 3D-modelling of the central area of interest, meshing of the computational domain and the particular CFD solver settings.

Responsibilities of project team members for process step (2) are shared between the principal investigator and project manager. The results of the CFD calculation have to be adequate to allow meaningful answers and results to satisfy project objectives. The results of the CFD calculation may also need an appropriate degree of validation.

Process step (A)- 3D-Modelling: The initial step of the CFD workflow is the creation of a suitable geometry of the computational domain. The computational domain represents the volume of fluid which is subjected to the selected physics of the model and its boundary conditions. The fluid body is confined by the outer boundary of the domain as well as inner domain boundaries (e.g. solid structures inside the confinement of the outer domain boundaries). Typically the solid structures represent objects around which the fluid movement or effects of the fluid movement has to be determined. The geometry of the solid structures can either be created inside the CFD software or imported from a third party 3D-CAD program. The advantage of using a third party 3D-CAD program is that such programs typically allow the creation of a wide range of solid objects, which are composed of either straight or curved outer surfaces. Importing the 3D-geometries into the CFD program requires CAD interfaces that translate the CAD geometries into the format that can be used in the CFD program.

Responsibilities of project team members for process step (1) are shared between the principal investigator, the CAD operator and the CFD software operator. The CAD operator is responsible to create an accurate 3D-solid CAD model of the internal space as well as the part of the domain that is considered of affecting the air flow through the internal space (e.g. external buildings or other structures if a coupled domain approach is used). The principal investigator has to ascertain that the 3D-geometry is sufficient in detail but not too detailed to ensure an effective use of computation resources. Both the CFD software operator and the principal investigator need to ensure that the 3D-geometry is being correctly imported into the CFD software.

Process step (B) - Meshing: The second step of the CFD calculation procedure is the creation a suitable grid, or mesh, which represents the digitization of the numerical solution. For most of the high performance CFD software codes, the meshing occurs in two phases. The first phase is the preparation of an “impermeable” surface mesh where the surface has to be a continuous mesh that surrounds the solid objects. The mesh cannot “leak”; in other words, the entire mesh has to be a continuous assembly of individual 3D-faces or other 3D-solid geometry definitions, without discontinuities which would negatively affect the accuracy or convergence of the solution. The surface mesh basically represents the outside surface of the objects around which the fluid motion and other flow induced effects are analyzed. The second phase of meshing is the creation of the volume mesh which encompasses the extent of the fluid that is analyzed in the computational

domain. The volume of the fluid is discretized into a large number of cells for which the governing equations are solved.

Responsibilities of project team members for process step (2) are shared between the principal investigator and the CFD software operator. The CFD software operator is responsible in placing the 3D-geometry of the buildings and structures into the virtual wind tunnel, which is the outer extent of the computational domain. The CFD operator has to create the surface and the volume mesh required for the simulation. The principal investigator needs to review of software analytical checks to make sure that the surface is completely wrapped and the volume mesh is established in accordance to the CFD solver requirements (e.g. use the right type of cell geometries).

Process step (C) – Solver Settings & Simulation: The third step of the CFD calculation procedure is the solver setting to initiate and run the simulations. It is crucial that appropriate setting parameters are used for the simulation, otherwise the solution might not be precise or the solution might not converge. Important parameters to define are boundary conditions including surface roughness and the type and detailed parameters of the turbulence model. During the third step of the CFD workflow, the sensitivity of certain parameters can be evaluated. If the solution does not show robust convergence, some changes of the geometry, the mesh or the solver might have to be performed. Changes to the solver might include using a different type of turbulence model or varying coefficients of the turbulence model being used.

Responsibilities of project team members for process step (3) are shared between the principal investigator and the CFD software operator. The CFD software operator is responsible for entering all input variables which the principal investigator describes so that the physics of the simulations along with other required software parameters represent appropriate settings. An important solver setting is the choice of the turbulence model. The CFD operator and principal investigator monitor the convergence of the solution. In case the results appear non-conclusive, which could mean that the solution does not readily converge, the principal investigator and the CFD operator will attempt to improve the stability of the simulation by adjustments of the grid, a change in meshing or changing the solver settings. This means that the process steps (1), (2) and (3) might be revisited, with changed input data.

Process step (D) – Post Processing:

The fourth and final step of the CFD calculation procedure is post processing of the calculation solution in a way that can be easily interpreted to answer the objectives of the CFD calculation. A typical way to evaluate CFD post-process involves defining surfaces on which the physical properties such as wind velocity, pressure, temperature or derived properties such as predicted occupant comfort level are

visualized by colored contour maps. The post processing can also include other effective visualization means such as velocity vector fields or static or animated particle streamlines. Other options are 3D-contours of properties and integrating properties over a volume or area. While the results of CFD simulations typically represent many thousands or even millions of data points, a convenient visual representation of the data facilitates interpreting the results of the CFD simulation.

Responsibilities of project team members for process step (4) are shared between the principal investigator and the CFD software operator. The CFD software operator is responsible for performing the required software function to visualize the CFD results so that the principle investigator can determine the outcome of the simulation. The principal investigator might ask the CFD operator to create a variety of contoured surface maps, 3D-grid data or vector graphics; or the principal investigator might ask for tables or other statistical representation of the CFD simulation results.

3.2 Required Proficiency of CFD Team Members

A successful internal CFD analysis requires team members with appropriate proficiency to carry out the different functions of the workflow process. The different functions could potentially be carried out by the same person, such as for smaller CFD investigations, where the principle investigator might also perform the software technical aspects of the simulation. For larger projects, however, where CFD investigations are undertaken to provide input for solving design or compliance projects, the different team functions will most likely be carried out by different team members.

Table 3-1 shows function, responsibility and required proficiency of members of the CFD project team.

Table3-1 Function, responsibility and required proficiency of members of the CFD project team

Role in project team	Responsibility in CFD workflow	Required Proficiency	Training needs
Project manager	Responsible to translate projects needs to the type of CFD simulations that can solve the problems at hand. Responsible to use the CFD results to arrive at decisions that affect the design or compliance project.	Needs a high proficiency in overseeing project, setting project objectives and identifying how CFD can be used to satisfy project objectives	Has to be highly trained in managing complex projects that require considerable technology (e.g. projects that are in need of CFD simulations usually represent interdisciplinary solutions and technology integrations)
Principal investigator	Responsible for the technical and scientific approach used in the CFD investigation. Supervises the CAD and CFD operators. Assists and consults the project manager in decisions.	Needs a high proficiency in building physics and a comprehensive and detailed understanding of all aspects of the CFD workflow. Needs proficiency to supervise the CFD team to produce reliable CFD results and advise the project manager in realizing the project objectives.	Has to be highly trained in the scientific, technical and software application details of CFD simulations. Has to be trained in building physics and how CFD results can be used to serve specific problems in architecture and urban design.
CAD operator	Responsible for creating the 3D-CAD geometry from plans or building specifications, either within the CFD software or in generic 3D-solid CAD	Needs high technical proficiency in manipulating CAD geometry on the basis of plans and specifications. Needs to understand what level of	Has to be trained in operating 3D-CAD systems and create 3D drawings from plans.

Table3-1 Function, responsibility and required proficiency of members of the CFD project team

Role in project team	Responsibility in CFD workflow	Required Proficiency	Training needs
	software and importing the geometry into the CFD software. Works under the supervision of the principal investigator.	detail should be included. Needs good application knowledge of the CAD application used.	
CFD operator - meshing	Responsible for validating 3D-geometries for use in surface mesh and for creating volume mesh in accordance with mesh specifications. Works under the supervision of the principal investigator.	Needs proficiency to understand the importance of geometric representation of structures in the numeric domain. Needs proficiency to create effective meshes and select most appropriate cell geometries for the mesh. Needs good application knowledge of the CFD software.	Has to be trained to validate 3D-geometries or to import 3D-geometries from external CAD applications. Has to be trained in selecting and creating effective surface and volume meshes for a variety of CFD applications. Has to be trained in the CFD software product.
CFD operator - solver	Responsible to define all physical properties and settings for the fluid, boundary conditions and turbulence. Responsible to run the simulation and monitor	Needs high proficiency to understand the multiple settings and physical properties that have to be selected to run effective CFD calculations. Needs good application	Has to be trained in the solver settings of the CFD simulation. Has to be trained to understand the physical properties and settings and other required setting to run the simulation. Has to be trained in the

Table3-1 Function, responsibility and required proficiency of members of the CFD project team

Role in project team	Responsibility in CFD workflow	Required Proficiency	Training needs
	convergence.	knowledge of the CFD software.	CFD software product.
CFD operator – post processing	Responsible to create the type of CFD visualization, which is requested and required by the principal investigator and the project manager.	Needs proficiency in creating informative graphical representations of the CFD results. Needs flexible and good communication skills to serve the project teams with a variety of ways to show the CFD results.	Has to be trained in operating the post processor of the CFD software. Should be trained in other graphics software products that can integrate CFD results into high quality visualization.

3.3 Technical Aspects of the CFD Workflow

The technical phases and aspects of the internal CFD workflow process are illustrated in Figure 3.2. The internal CFD workflow process includes the following main phases:

1. Creation of the geometry of the model and boundaries.
2. Preprocessing: Meshing and setting Physics
3. Solution / Solver
4. Post processing

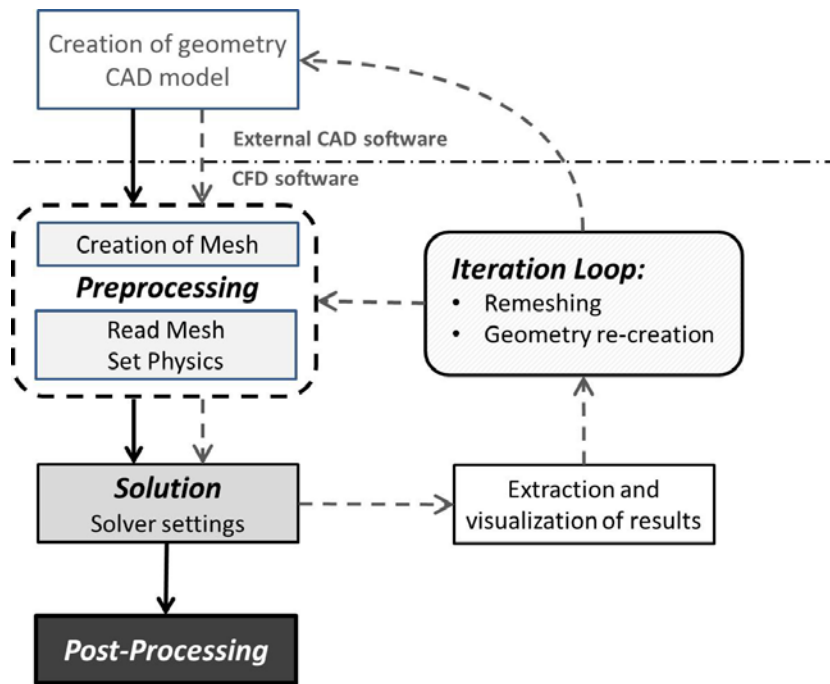


Figure 3.2: Technical phases and aspects of the internal CFD workflow

The approach used in the four phases is described in more detail below.

1. Creation of the geometry of the model and boundaries:

The geometry of the model and the boundaries of the computational domain are created with an appropriate modeling program. In the past, the most time consuming and frustrating part of the CFD process was the time and effort expended on creating a geometric model that integrates well with the CFD meshing functions.

The CFD software used for the internal workflow development offers three avenues to create the geometric model so that it can be handled in any of the following ways to facilitate downstream meshing:

- A. CAD Clients: CAD Clients directly transfers geometric and parametric information to the CFD software environment. This direct file transfer allows the CFD software to read user chosen design variables thus allowing the user to drive design changes from within the CFD software, or stay within the CAD software and simply push new geometries into the CFD simulation environment. Some CAD Clients also allow meshing within familiar CAD software applications thus eliminating or reducing the need to transfer or prepare the geometry further inside the CFD environment.
- B. CAD Import: The CFD software used for the project (Star-CCM+) work has the ability to import a wide variety of Neutral, CAD and PLM file formats. The user can either use the geometry as imported or these files can be read into the 3D-CAD function of the CFD software and the user can make parametric modifications to the geometry. When the best design is found the geometry can be exported back to the CAD environment.
- C. CAD Creation: The CFD software (Star-CCM+) has an internal fully parametric 3D feature-based modeler to modify existing or create new geometry. Geometry tools include sheet & solid creation, external and internal flow domain extraction, imprinting, exposing geometry parameters for downstream design exploration and optimization.

For the internal CFD workflow of the present project Option B “CAD import” was selected.

2. Meshing and Set Physics of the Computational domain:

After the geometry has been created the mesh of the computational domain is created. The process of meshing can be categorized into three distinct steps:

Surface preparation: Since solid surfaces are defined as a continuous system of surface primitives the imported CAD file has to be tested for consistency to allow subsequent volume meshing. The nature of surface primitives in CAD and CFD applications can differ, which can results in possible meshing inconsistencies. The imported geometry is referred to as “initial geometry”

which might require more or less refinement before launching the surface mesh generator. The CFD software (Star-CCM+) included several “surface repair tools” for surface preparation including: error diagnostics, fine grained manipulation of surface primitives, topological identification, defeaturing, boolean and imprinting operations on triangulated surfaces.

Automatic surface wrapping: After necessary repairs to the initial surface the step referred to as surface wrapping is used to create a quality surface mesh. A good surface mesh provides better region boundaries and a more accurate volume mesh. If the surface is not correctly closed and free edges or intersecting faces remain, volume meshing is negatively affected. The surface wrapping function of the software provides automatic closing proximity and poor quality faces refinement.

Volume mesh generation: A range of volume mesh types and shapes were available that included tetrahedral, trimmer and polyhedral. Polyhedral cells have certain advantages and this type of mesh cells have been primarily used for this study. For multi-domain studies, such as conjugate heat transfer, fully conformal meshes can automatically be created. Prism layer mesh cells are used mainly next to wall boundaries. A prism layer is defined by its thickness and the number of cells within the layer.

The CFD model requires setting of all the parameters and equations concerning the physical definition of the fluid analyzed. In our case the fluid is air. The software used (Star-CCM+) offers several real fluid definitions. For the simulations the simplest, the ideal gas model, has been adopted. The density and viscosity settings for air have to be adjusted to represent the prevailing climatic conditions in Hawaii. This means that the default setting of the software, which represents standard conditions, will have to be adjusted.

3. Solution / Solver

Setting of the solver parameters include selection of various values, including, but not limited to:

Turbulence models and Wall Functions: The air flow conditions in question for the investigations in Room 301 were inherently turbulent. This means the air flow acquired turbulent energy and eddies were generated resulting in a time variance of flow phenomena. With the transition to turbulence, chaotic oscillations appear in the flow, and it is no longer possible to assume that the flow is invariant with time. Therefore it is necessary to solve the problem in the time domain, and the mesh has to be fine enough to resolve the size of the smallest eddies in the flow. The flow problem can either be solved by means of Wall Functions or Turbulence models. The turbulent flow regime close to surfaces can be divided up into four regimes. Starting from the surface we have a viscous or laminar sublayer, where the velocity increases linearly from

zero velocity at the wall. Following is the buffer layer, where the flow begins to transition to turbulent. Both the viscous layer and buffer layer are relatively thin. The log-law region follows outward where the flow is fully turbulent and the average flow velocity is related to the log of the distance to the wall. The free-stream region is situated outside the log-law region.

Wall functions assume analytical solutions for the flow in the buffer region and on-zero fluid velocity at the wall. Wall functions have significantly lower computational requirements than turbulence models, which give a level of accuracy beyond what the wall function formulations provide.

There are numerous turbulence models available which augment the Navier-Stokes equations with an additional turbulent viscosity term, but they differ in how it is computed. The turbulence models considered by the CFD research team were as follows:

- **The k-epsilon model** solves for two variables: k ; the turbulent kinetic energy, and epsilon; the rate of dissipation of kinetic energy. Wall functions are used in this model. The k-epsilon is the standard turbulence model in many industrial applications and has good convergence performance and relatively low memory requirements. The model performs well for generic flow problems but does not very accurately compute flow fields that exhibit adverse pressure gradients or strong curvature to the fluid flow.
- **The k-omega model** is similar to the k-epsilon model. It also uses wall functions and therefore has comparable memory requirements, but it usually shows less tendencies of converging. The k-omega model is useful in cases where the k-epsilon model is not accurate, such as internal flows or flows that exhibit strong curvature.
- **The SST model** is a combination of the k-epsilon in the free stream and the k-omega models near the walls. It does not use wall functions and tends to be most accurate when solving the flow near the wall. The SST model does not always converge to the solution quickly, so the k-epsilon or k-omega models are often solved first to give good initial conditions.

Relaxation factor: Setting the appropriate relaxation factor U includes:

- $U < 1$ is under relaxation. This may slow down speed of convergence but increases the stability of the calculation, i.e. it decreases the possibility of divergence or oscillations in the solutions.
- $U = 1$ corresponds to no relaxation. One uses the predicted value of the variable.
- $U > 1$ is over relaxation. It can sometimes be used to accelerate convergence but will decrease the stability of the calculation.

Convergence criteria and Monitoring residuals:

- Always ensure proper convergence before using a solution:
- Solutions are converged when the flow field and scalar fields are no longer changing.
- It is most common to monitor the residuals;
 - If the residuals have met the specified convergence criterion but are still decreasing, the solution may not yet be converged.
 - If the residuals never meet the convergence criterion, but are no longer decreasing and other solution monitors do not change either, the solution is converged.
 - Low residuals do not automatically mean a correct solution, and high residuals do not automatically mean a wrong solution.
 - Final residuals are often higher with higher order discretization schemes than with first order discretization. That does not mean that the first order solution is better
 - BUT: It is practical to use other convergence monitors than residuals, such as force, temperature, pressure, air velocity or mass balance at important locations

Post processing: Post-processing provides complete insight into fluid dynamics simulation results.

There is a wide range of visualization methods available and the CFD practitioner can either use the internal CFD post-processor or can use dedicated post processor software application. The CFD research team used the following post processing methods:

1. XY plots (time/iterative history of residuals and
2. 2D contour plots (pressure, velocity, vorticity, eddy viscosity)
3. 2D velocity vectors
4. Streamlines and pathlines
5. Probes to determine exact values of properties at points of interest.

3.4 CFD Best Practice Guidelines

Several versions of CFD Best Practice Guidelines (BPG) were available to provide guidance to the CFD project team to carry out effective and valid internal CFD simulations. In any case, the project manager in conjunction with the principal investigator should review what BPG is most beneficial for the project. Several recurring topics presented in the BPGs for CFD work process include the following:

Identifying errors and uncertainties of the set-up of the problem:

- **Simplification of the CFD model:** CFD analysis should use simplification in the pre-processing (e.g. creating the CAD model) and mathematical description of the problem. Some wind movement phenomena in the urban environment and air movement through internal spaces are often too complex, both in spatial and time domains, to be precisely modeled. While detailed models might yield superior solutions, the required computational resources could be prohibitively expensive for most technical CFD applications. The overarching goal of simplifications is lowering the model complexity to a level that requires conservative computational resources while still allowing obtaining useful CFD results.
- **Physical boundary conditions:** The computational domain in internal CFD analysis can contain only the internal air volume surrounded by solid boundaries, or the domain can also contain a portion of the urban area that surrounds the internal space or the building. Therefore the choice of the boundaries of the computational domain significantly affects the results and can add to uncertainty and even errors of the simulation results.
- **Geometric boundary conditions:** The appropriately defined computational domain for the CFD analysis requires knowledge of the geometric details of the internal space to and/or the surrounding area, if the surrounding area is included in the domain. Furthermore, errors and uncertainties can result from the simplification of the geometrical complexity used in the CFD analysis experiment. In order to reduce the computational costs, geometric details can be omitted.

Identifying numerical errors and uncertainties:

- **Spatial and temporal discretization:** The spatial and temporal discretization is described as probably the most critical sources of numerical error. These errors are a result of the difference between the exact solution of the basic system of partial differential equations and the numerical solution obtained with finite discretization in space and time. With regard to the space discretization, it is not only the degree of resolution that is important but also the distribution of the grid points. Therefore the mesh used to discretize the space is of great importance for the accuracy of the results.
- **Iterative convergence:** A non-linear algebraic system that is formed by discretization of the partial differential equations is solved with an iterative method or by time integration towards a steady state. If the iteration or time integration is stopped too early, an iterative convergence error is introduced which is the difference between this intermediate solution and the exact solution of the algebraic system of equations. Assessment of the iterative convergence is based on the residuals obtain in solution iterations.

Recommendations to reduce errors and uncertainties:

- **Selection of target parameters:** The first step in a CFD analysis should be the definition of the target parameters, such as pressure and velocity, which are representative of the goals of the simulation.
 - **Selection of approximate equations describing the physics of the wind movement:** The selection of the basic equations has a significant impact on the simulation errors and uncertainties. The turbulent flow within the internal building and urban environments is generally modeled by Navier-Stokes equations. The most widely considered equations are Reynolds Averaged Navier-Stokes (RANS) equations, which are adequate representations of constant wind flow conditions. Interestingly, no best practice advice for the choice of the turbulence models is given. Rather, a verification strategy is proposed to evaluate the performance of the different turbulence models and determine what model should be used.
- **Selection of the geometrical representation of buildings and structures:** Buildings and structures acting as obstacles in the wind flow have the greatest impact on flow patterns and related physical phenomena. Wind flow obstacles created by vegetation and other surface characteristics (e.g. roads, grass, sand) have a lesser importance, though foliage can have significant effects on the wind regime around buildings. The level of detail required for individual buildings and structures is dependent on their distance from the central area of interest. The central area of interest should be reproduced with as much detail as possible. Buildings further away may normally be represented as simple blocks.
- **Selection of the computational domain:** For internal CFD analysis the computational domain can either be limited to the internal spaces to be modeled or the domain can further encompass surrounding external areas and air volumes. This distinction of domain types is referred to as “decoupled” and “coupled domain” approaches. For the coupled domain, the size of the entire computational domain in the vertical, lateral and flow directions depends on the extent to which the surrounding area is considered as contributing significantly to the solution.
- **Selection of boundary conditions of the external domain:** The boundary conditions represent the influence of the surroundings that have been cut off by the external computational domain. Their proper choice is very important since the solution depends on the appropriate choices of the boundary conditions. The following boundary conditions have to be identified:
 - Inflow boundary conditions, where the velocity and turbulence profile have to be defined.
 - Wall boundary conditions, depending on the shear stress conditions either no-slip, viscous sublayer or wall functions have to be defined.

- Top boundary conditions, usually defined constant shear stress
- Lateral boundary conditions, is usually defined as a symmetry plane with lateral distance from the built area of interest large enough to minimize effect of the boundary on the flow field.
- Outflow boundary conditions, are either outflow or constant static pressure boundary conditions

Selection of the computational grid: The grid (or mesh) is created in such a manner that it does not introduce significant errors. This means that the resolution of the grid should be fine enough to capture important physical phenomena like shear layers and vortices with sufficient resolution.

Selection of iterative convergence criteria: The iterative calculation process starts with an initial guess of the flow variables and then recalculates these variables in each of the iterations until the equations are solved up to a user-specified error. The termination criterion is usually based on residuals of the corresponding equations. These residuals should tend towards zero.

SECTION 4 – METHODOLOGY

This section describes the methodology that was applied in this investigation. This section describes the site of the investigation, the instrumentation used to collect and analyze velocity and pressure data in Room 301 and the methods to prepare, generate and visualize the CFD solution.

4.1 Description of Test Site Room Sinclair 301 and Instrumentation Used in Measurements

While the main objective of developing workflow was to establish procedures to carry out internal CFD investigations, the validation of the CFD results through on site measurements were an integral part of the project.

Description of the test site: The site for this investigation was Room 301, which is located in the third floor of Sinclair Library building, which in turn is part on the University of Hawaii Manoa campus, (Figures 4.1 and 4.2). The 123,000 square-foot Sinclair Library building was built in 1956. Although much of the building has been converted to air-conditioned space, the space used in this study, Room 301, is naturally-ventilated. Room 301 is a 4,800 square-foot open office on the third (top) floor on the west side of the building (Figures 4.3 and 4.4).

Figure 4.5 depicts Room 301 in a schematic layout. In order to provide controlled airflow conditions with a good approximation of mass flow rates two mechanical exhaust fan unit were installed on the South lanai. While keeping all windows on the South side close the exhaust fans provide a measurable and therefore determined mass flow out of Room 301. The air is entering the space through the windows on the North side.

The entire North side of Room 301 consists of pane windows and glass louvers (Figure 4.6). The entire south side consists of one pane window, three sets of sliding glass doors, a single glass door and the rest consists of wooden louvers (Figure 4.7). The South side opens onto a 12 feet wide lanai (veranda) which runs the entire width of the space. The roof overhang covers the lanai. The west wall of the office is brick and has no openings. The east wall is an interior wall with one opening consisting of a set of double doors, which were usually kept closed during regular business hours.

Figure 4.8 shows the two exhaust fan units which were custom built to accommodate two whole-house fans per exhaust fan unit. The exhaust fan units were installed on the South lanai and temporarily attached to louvered window frames with an air-tight seal. This allowed the exhaust fans to operate effectively and expel air from within the Room 301.

The interior of Room 301 included complex arrangements of work stations and cubicle walls. Figure 4.9 illustrates the complexity of the interior of Room 301. The ceiling height of Room 301 is 10' and

luminaries are set flush with the ceiling. The office has various cubicles with wall heights of 30", 37", 50", 44", 64", and 82".

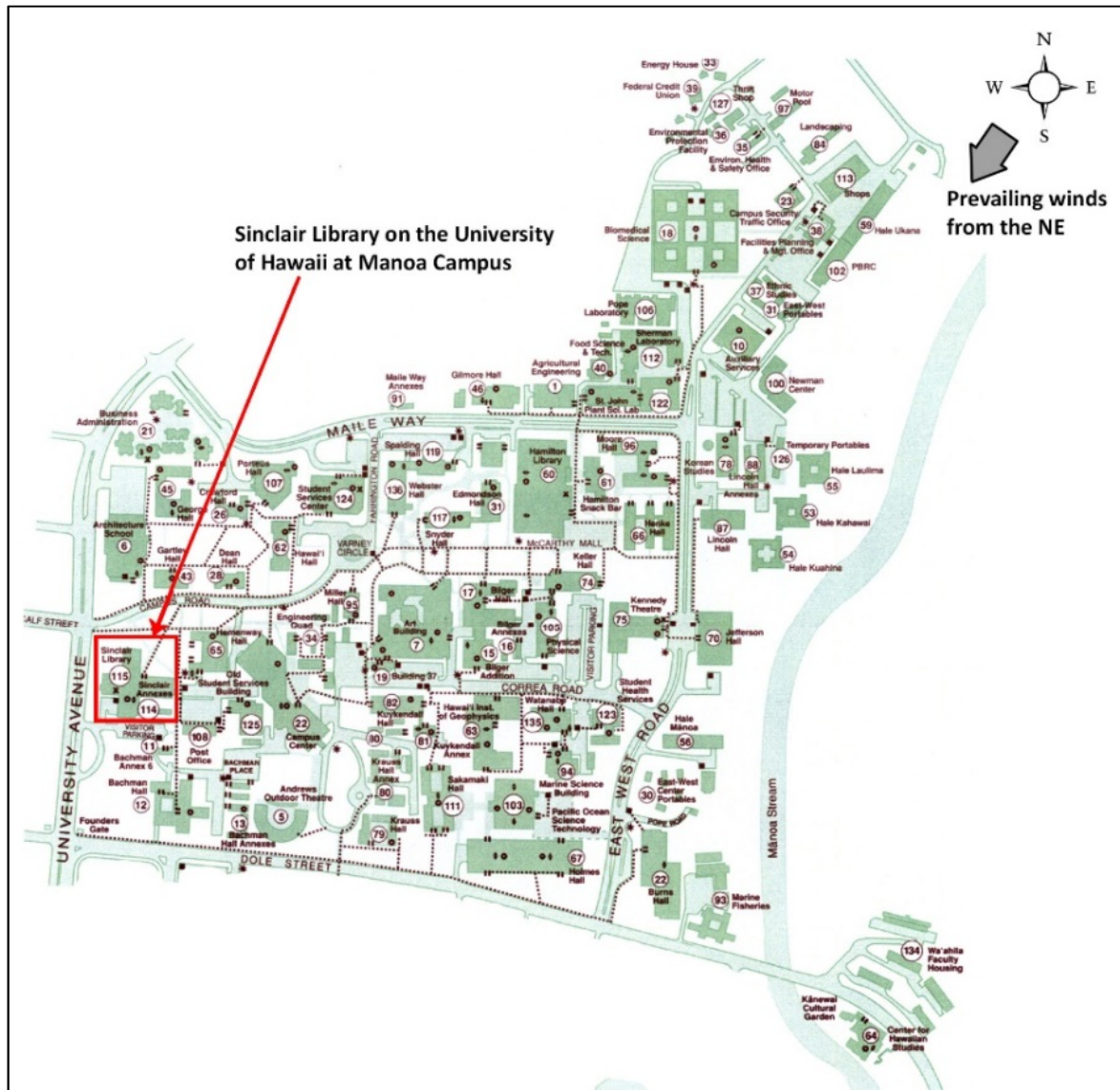


Figure 4.1: Vicinity map - Location of Sinclair Library on University of Hawaii Manoa Campus

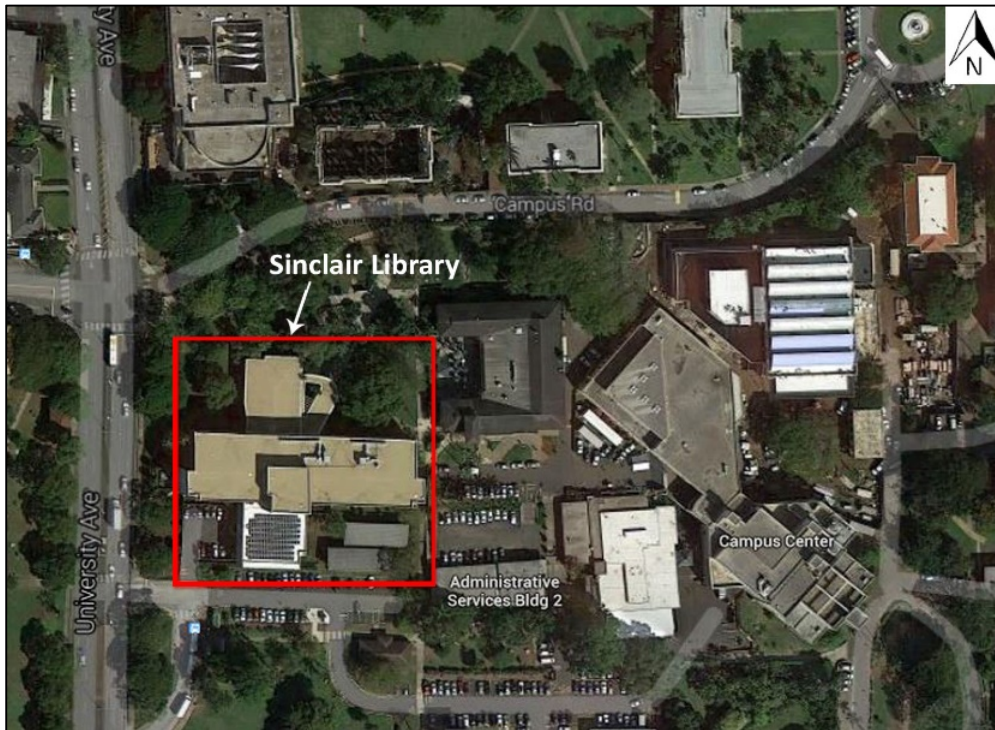


Figure 4.2: Aerial image of Sinclair Library

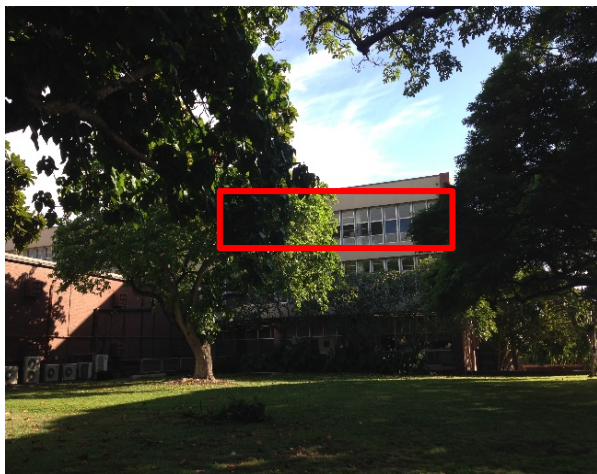


Figure 4.3: Sinclair room 301 north side



Figure 4.4: Sinclair room 301 south side

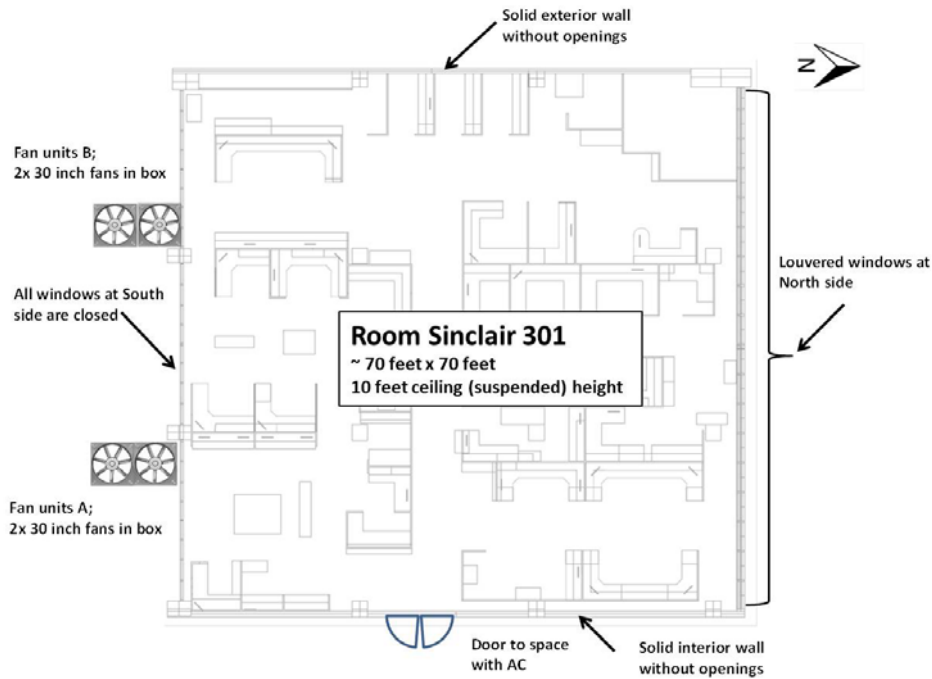


Figure 4.5: Layout sketch of Room Sinclair 301



Figure 4.6: North wall of Sinclair room 301 with window panes and glass louvers.



Figure 4.7: South wall of Sinclair room 301 with glass doors, wood louvers, and attached lanai.



(a)



(b)

Figure 4.8: Two exhaust fans units installed on the South lanai; (a) custom-built housing for two whole-house fans, (b) location of the two exhaust fan units (in red marks) on the South lanai of Room 301



(a)



(b)

Figure 4.9: Interior of Room 301 include complex arrangements of work station and partitions; (a) view toward the South wall, (b) view toward the North wall.

Instrumentation used to measure air velocity and differential pressures:

Three types of instruments were used to obtain data for validation of the CFD simulation of air movement through the room and differential pressures across inlet and outlet of Room 301.

Outside weather station to determine ambient climatic conditions: Wind velocity and wind direction were measured and logged with an Onset HOBO U30 installed on the west side of the roof of Sinclair, directly above room 301 (Figure 4.10). The sensors were 9'6" above the roof and 49'6" from the ground. Data rate resolution was set at 5 Hz.

Air velocity sensors: Air velocity was measured with Degree Controls Accusense hotwire anemometers model F900-0-5-1-9-2 with the XS blade which has a range of 0 - 5 m/s air velocity and an accuracy of 0.5 % of reading or 1% of full scale. (Figure

Pressure differentials: Pressure differentials were measured with two types of transducers. Three were the Setra Air Pressure Transducer Model 264 which has a range of zero to 0.1 inches of water column (zero to 25 Pascals) and 0.5% accuracy. The second type was one Halstrup Walcher P26 pressure transducer with a range of zero to 0.055 inches of water column (zero to 10 Pascals) and 0.5% accuracy of full range. The low and high pressure outlets of the differential pressure transducers were connected to flexible vinyl tubing ($\frac{3}{16}$ " internal diameter for the Setras and $\frac{1}{4}$ " for the Halstrup Walcher). The pressure tubing extended to pressure tubing terminals, which were PVC pipe sections with holes drilled in and brass barbed fitting to connect the pressure tubing. Tubing was color-coded to track which tubing was to be connected to the high or low side of the pressure transducer. Figure 4.12 shows the unit to measure differential pressures, including transducer, pressure tubing and pressure tubing terminals.

Instrumentation and data acquisition set up: The sensors were arranged in the room as illustrated in Figure 4.13. The orange rectangle in the center indicates the USB device (multiplexer) and laptop computer used for data acquisition. The sensor ID number, ai-01 for example, was based on the position in which it was connected to the data acquisition device. The data acquisition software used this position as a default ID. The height above floor of the air velocity sensors (anemometer) or terminal end of tubing (pressure transducer) is indicated in brackets, e.g. 4'-0" as an example. Multiple anemometers installed at different heights at the same location were attached to the same stand. Sensors ID ai-09, ai-10, ai-12, and ai13 indicate the four Setra differential pressure transducers were used, and ai-11 indicate the one Halstrup Walcher differential pressure transducer.

The red dotted lines in Figure 4.13 indicate the vinyl tubing for the pressure transducers which were attached to the “high” or the “low” pressure ports on the differential pressure transducers, labeled H or L respectively. The grey lines indicate the cubicle partitions. The L0 are the wood louvers on the south side and remained closed for the studies (except for those at the face of the fans which always remained open). The L1 through L4 on the north side indicate the glass louvers. The L1 louvers were in the director’s office, which was locked during the tests and therefore the louvers in this part of Room 301 were kept closed all the time for this study. That cubicle had the highest wall height of 82”. The exhaust fans units are indicated by “Fan A” and “Fan B” and each fan unit had a pair of two fans in the same fan unit housing. When a fan unit was used, both fans in the unit were turned onto the “high” setting. The prevailing wind was from the North side. The reference wind was measured by the weather station on the roof. This wind data was used as input variable for the CFD simulations.

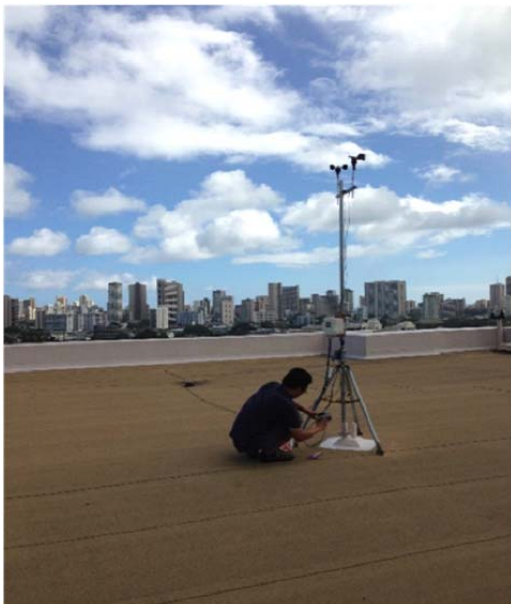


Figure 4.10: Weather station (Onset Hobo U30 data logger) with wind velocity and direction sensors installed on roof of Sinclair library during measurements



Figure 4.11: Anemometer tip held at 4’ height using wire attached to stand

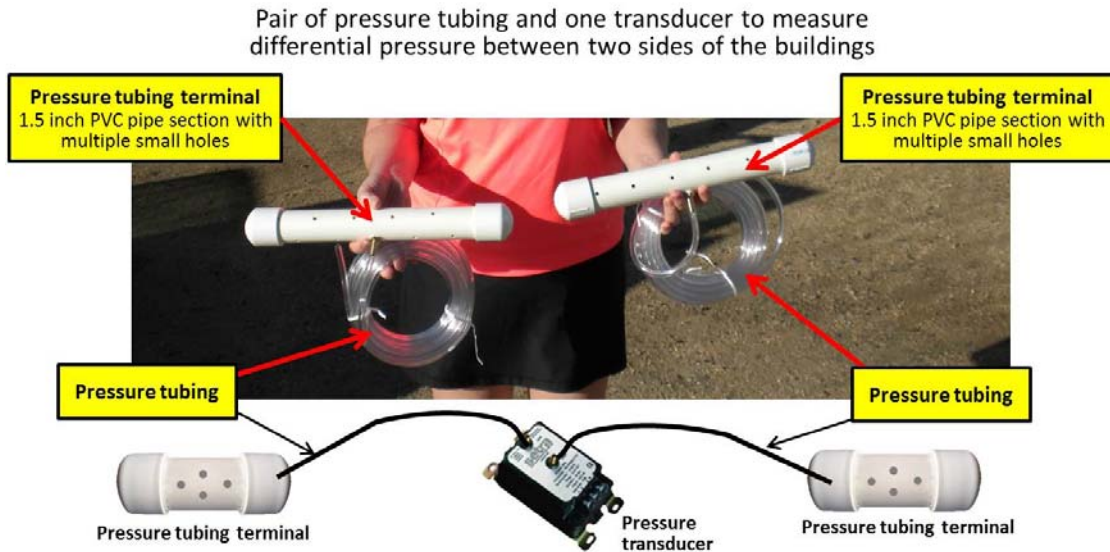


Figure 4.12: unit to measure differential pressures, including transducer, pressure tubing and pressure tubing terminals

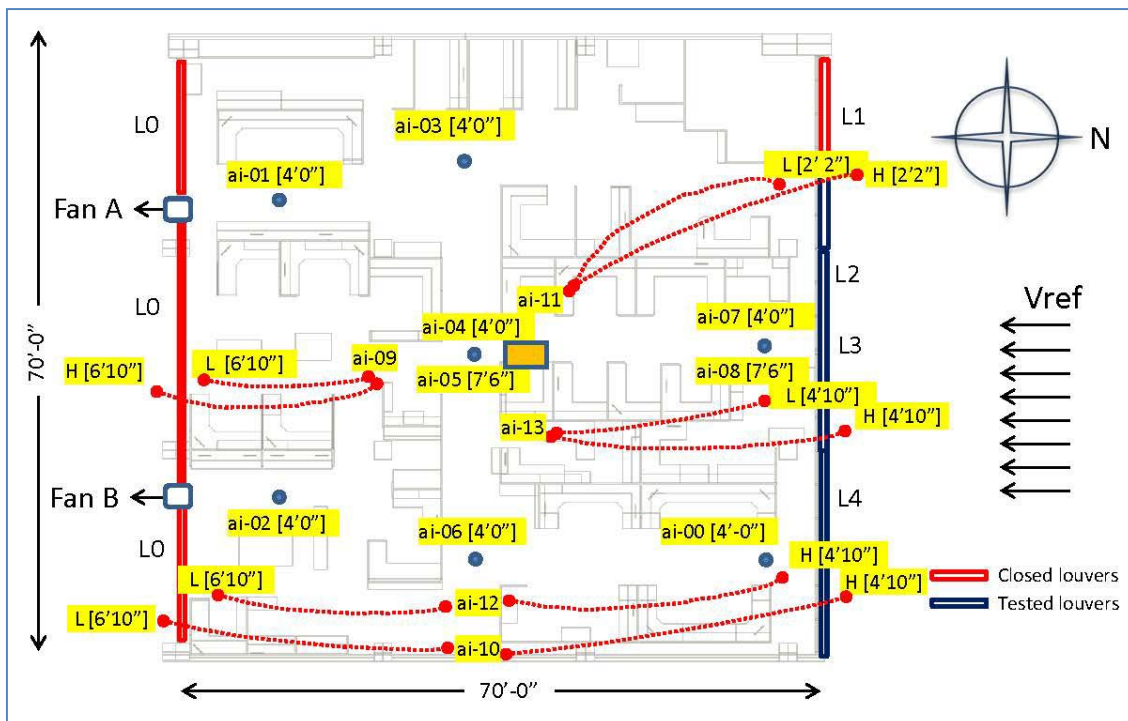
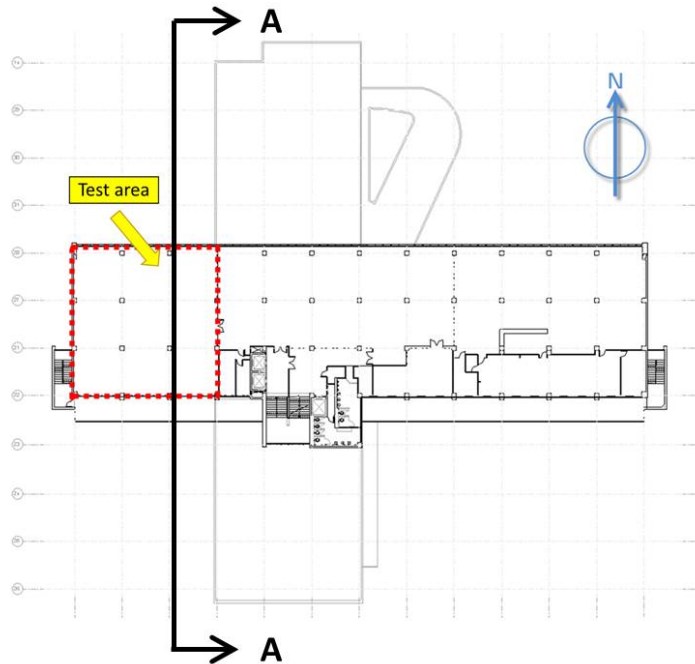


Figure 4.13: Set-up of instrumentation and data acquisition system in Room 301

4.2 Creating the Model Geometry with CAD Software

During previous phases of the CFD research program, the research team had experimented with different 3D-CAD interfaces and found that an efficient way of CAD 3D-modeling was using Rhino 3D application to model highly detailed architectural 3D models for use as CFD model geometry. The 3D-model was subsequently imported into the CFD software application CFD’s mesher to create the mesh. Figure 4.14 shows the extent of Room 301 and the geometry of the surrounding geometry which was considered under the coupled domain approach.



(a) Geometry of test site modeled in CAD software, plan view



(b) Geometry of test site modeled in CAD software, Section A-A

Figure 4.14: Test site modelled in 3D-CAD

An important step in the 3D-CAD modeling process is the modeling of the computational domain. The research team decided to test two domain modeling approaches, “decoupled domain” and “coupled domain” approaches. The first approach, decouple domain modeling approach, is the simpler one of the two, by which the fluid volume of interest (air in this case) is defined as the internal computational domain (interior space). When performing internal CFD analysis under the decoupled approach, the boundary conditions of the internal computational domain, e.g. openings in the walls of the space, are either derived from solutions of previous external CFD simulations or by assumptions of mass flow rate through the wall opening. The second approach, coupled domain, involves modeling a single computational domain including interior and exterior space, thus capturing a larger influence from the external space in solving the internal airflow. This approach, therefore, requires a higher level of complexity of 3D CAD modeling and more extensive computational resources.

The interior of Room 301 had numerous cubicle walls, which significantly complicated the internal airflow characteristics. A 3D-CAD modeling sequence was applied, allowing for testing the model of Room 301 with and without cubicle walls. This resulted in the following test cases, decoupled domain without cubicle walls, coupled domain without cubicle walls and coupled domain with cubicle walls. In order to test the capability of the CFD’s mesher to handle 3D geometry models at a reasonable processing time and computational resources, different level of geometry complexity were tested as follows:

- Decoupled domain CFD (computational domain extended only to the internal walls of Room 301) without cubicle walls. This domain setting is the simpler domain model for which only the internal space inside Room 301 represented the computational domain. For the decoupled domain no cubicle walls were included in the 3D geometry. The inlet boundary condition (e.g. the windows on the North wall of Room 301) was assigned a constant air velocity V_{ref} . Figure 4.15 illustrates the geometry of model under the decoupled domain approach.
- Coupled domain CFD without cubicle walls: The computational domain includes both internal and external volumes. The inlet boundary condition was assigned at the external computational domain, using log wind profile being consistent with the atmosphere boundary layer condition at the test site measured by the weather station. The coupled computational domain allows modelling the effects of approaching wind on the windward openings of Room 301 (e.g. the north facing windows of Room 301). No cubicle walls were included in the model to reduce the complexity. Figure 4.16 illustrates the geometry of model under the coupled domain approach.
- Coupled domain CFD with cubicle walls: The same external geometry as the coupled case without cubicle walls was used. The internal space, however, included cubicle walls. The addition of the internal geometry greatly increases the need for computational resources. Figure 4.17 illustrates the geometry of the computational domain under this simulation case.

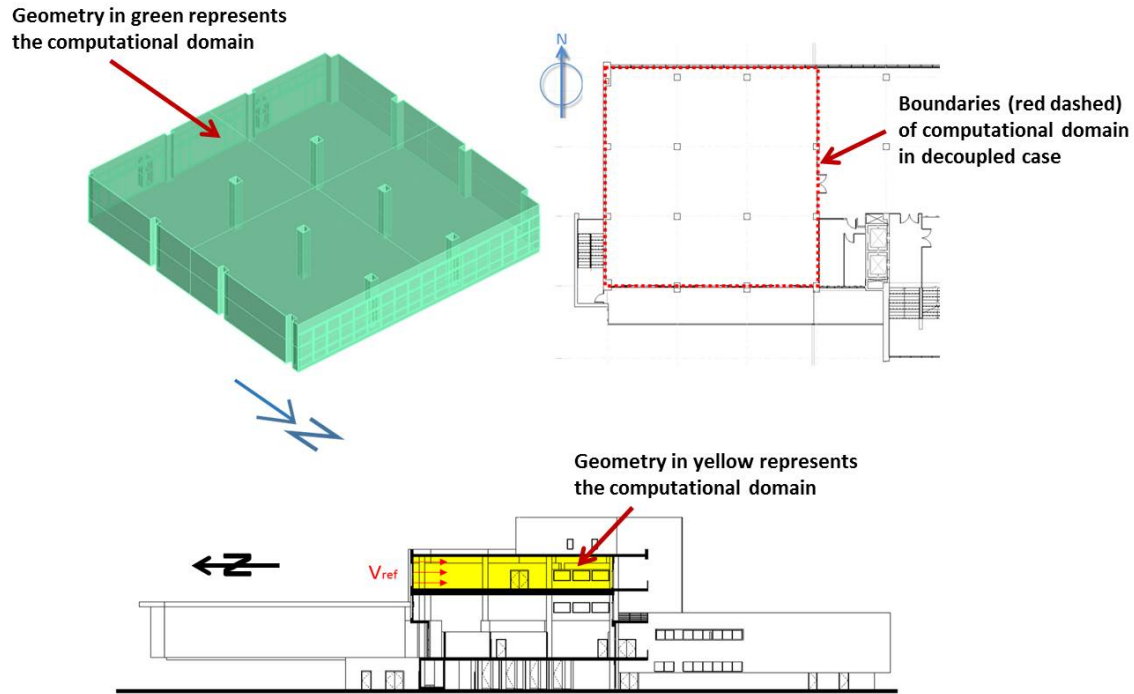


Figure 4.15: Geometry modeled for the decoupled domain case

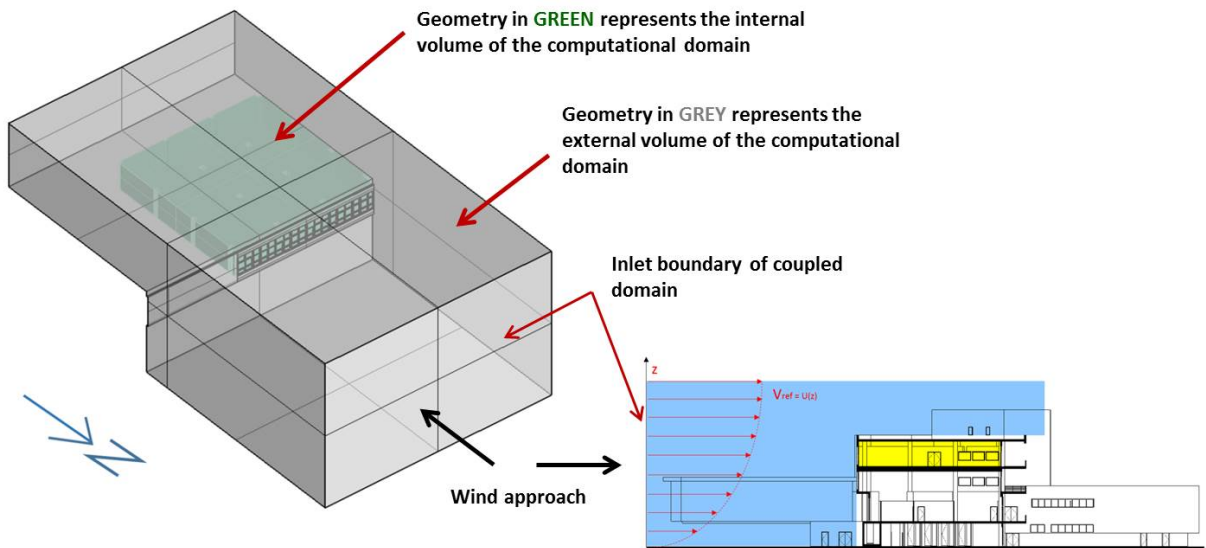


Figure 4.16: 3D CAD model illustration of the coupled domain CFD; case without furniture

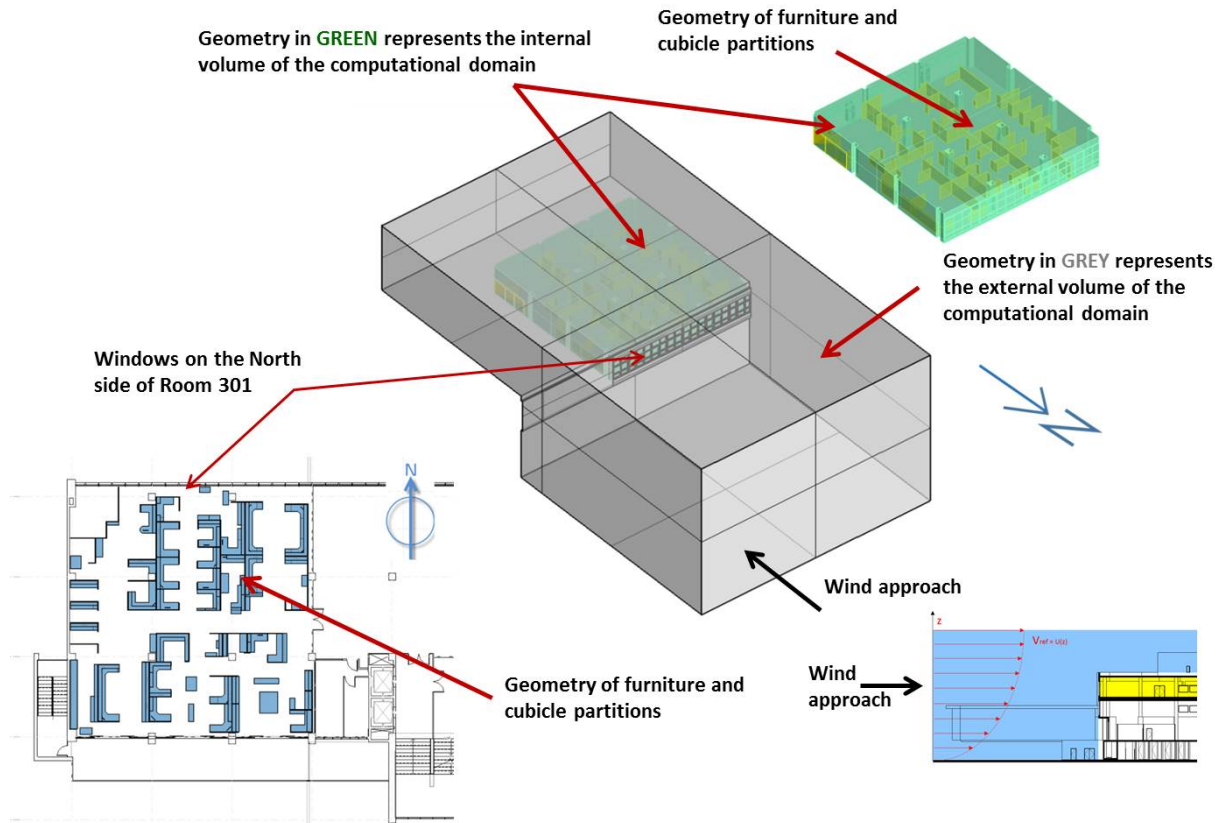


Figure 4.17: 3D CAD model illustration of the coupled domain CFD; case WITH furniture

4.3 Creating the Volume Mesh

An effective mesh provides the appropriate discretization of the numerical solution. The *Surface mesher*, *Trimer* and *Prism Layer Mesher* function from the CFD software use for the study (e.g. STAR-CCM+) were chosen for generating the volume mesh of this study. Figure 4.18 shows a user interface with option provided by the CFD software used for this study. In order to enhance the quality of meshing, a process was also used to control mesh resolution in vicinity of the small objects or at the location of the interest in the computational domain. Examples of surface meshing and volume cells of three different domain modeling approaches are shown in Figures 4.19 through 4.21. A detailed description of the meshing process used in this project and the grid quality assessment are presented in the Appendix A.

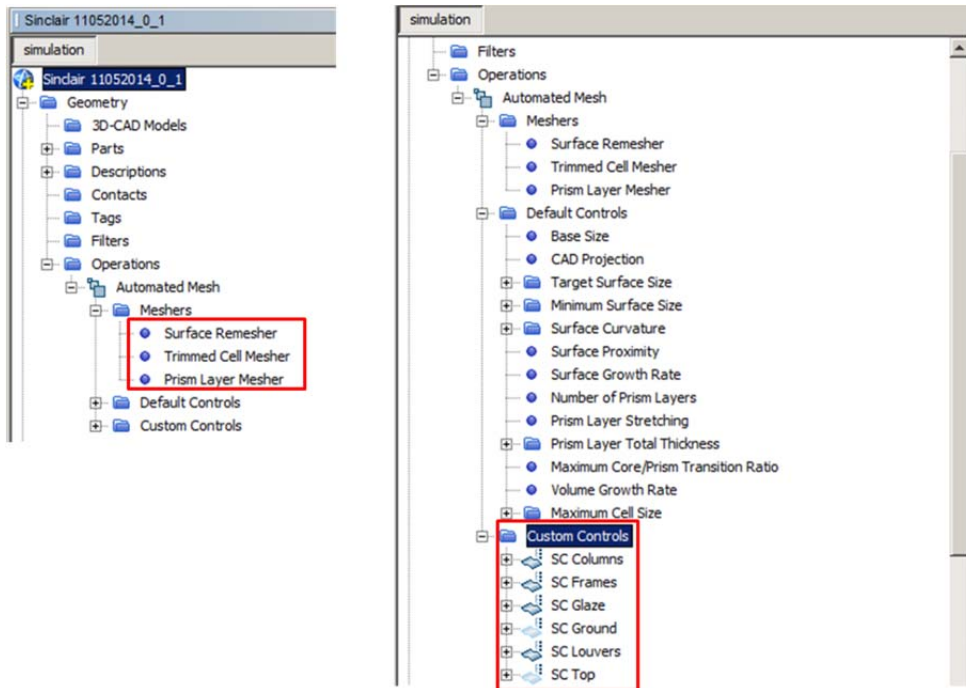
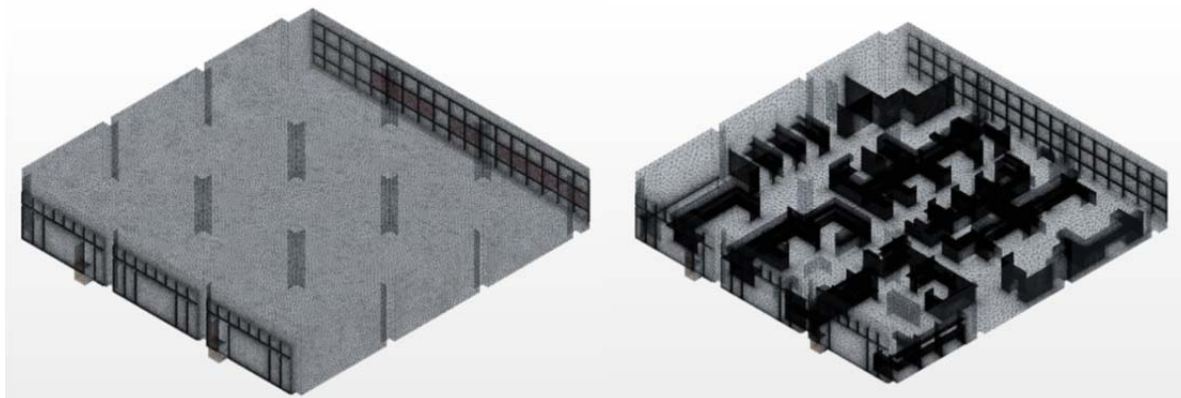


Figure 4.18: Screen shot of CFD software - Control options for surface and volume mesher chosen and custom control for the mesh settings



- (a) Surface mesh generated in the Decoupled Domain modeling approach; computational domain is limited to the internal space
- (b) Surface mesh generated in the Coupled Domain (with furniture) modeling approach; only internal space is shown as part of the computational domain.

Figure 4.19: Illustration of surface meshing of decoupled domain modeling approach (a) vs. the coupled domain modeling approach (b)

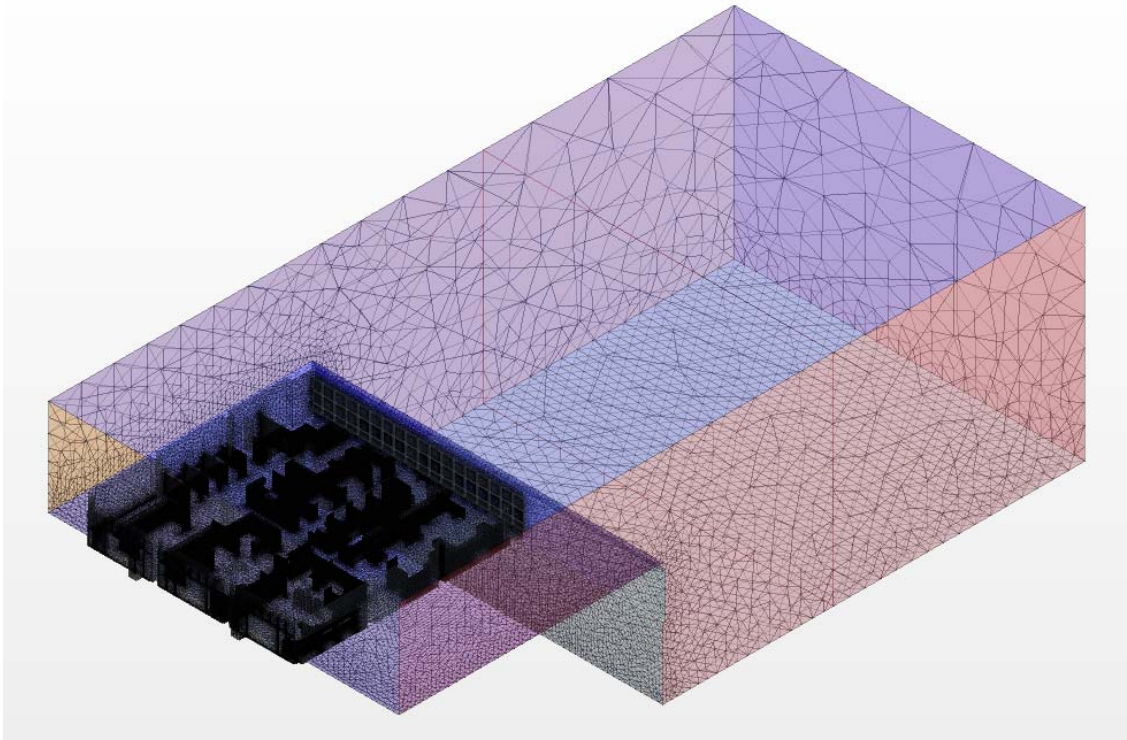


Figure 4.20: Illustration of surface meshing of coupled domain modeling approach, internal AND external portions of the domain are shown.

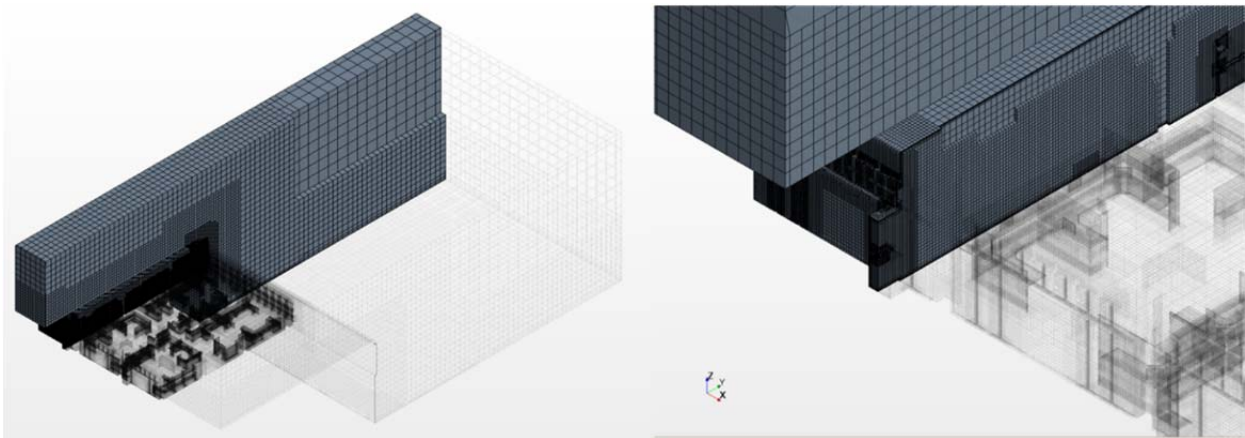


Figure 4.21: Illustration of volume mesh of coupled domain modeling approach, internal AND external portion of the domain is shown.

4.4 Determining the General Conditions that Affect Internal CFD Simulation

The parameters, which affect internal CFD results, have to be well understood for CFD modeling and validation through measurements at the test site. Perhaps the most important difference between internal CFD and external CFD is the low velocity of wind movement inside a space compared to outside wind movement around a building. By necessity, air movement inside spaces is significantly less than outside wind movement since the very basic function of a building is to provide adequate shelter from outside weather conditions. Energy contained in external wind movement is lost while the air enters the building, overcoming flow obstructions and pressure losses created by opening. In addition, interior walls and openings, furniture and equipment and occupant significantly affect the flow energy while the air is moving through internal spaces.

Internal airflow movement generated by either natural ventilation or mechanical fans typically results in low air velocities. The maximum of air velocity measured at the test site (e.g. inside Room 301) was approximately 1m/s. Most of the time, wind velocities were significantly lower than the maximum, especially at locations away from openings or exhausting fans. Low air velocity typically causes larger wake regions, increasing the uncertainty of the internal CFD since wakes generated interact with internal flow obstructions (e.g. cubicle walls). As a consequence a higher level of uncertainty of field validation measurements can be anticipated with slow internal air movement.

Since the test site is an office space with many cubicle walls, support columns and office equipment, the research team had to decide which of the internal flow obstructions had to be included or excluded in the geometry. Increasing the resolution (e.g. the number of objects and details of their geometry) of the internal flow obstructions increases complexity of the model and the demand on computational resources. Therefore the CFD research team chose to preserve the most significant internal features of Room 301 model (e.g. the support columns and the cubicle walls) in order to avoid unnecessary complexity of the CFD model and limiting demand on computational resources.

Thermal effect affects internal air movement through the generation of localized heat plumes and possibly stratification. Even though the building's thermal mass is very low (building construction is medium weight type), the heat from lighting fixtures and the roof slab being heated up during the daytime causes higher ceiling surface temperatures than the indoor ambient temperature. Some computer desktops and LCD monitors can also add to the thermal signature of the room. These temperature differences between different parts of the air volume would then induce buoyancy effects and affect internal air movement. As stated in the scope of this study, thermal diffusion was excluded since the main driving force of internal air movement was wind pressure and exhaust fans. Excluding thermal effects in the model introduced some minor degree of uncertainty which was deemed acceptable by the CFD research team. It also should be noted that the flow measurements in Room 301

were carried out during off-hours when most of the heat producing equipment, such as computers or other electric loads) was turned off.

When modeling the coupled CFD domain, some part of the surroundings had to be included in the model to represent part of the external conditions. The external geometry, though truncated to a volume in the vicinity of the air intake of Room 301 (e.g. windows on the North side of Room 301), approximated approaching wind conditions with certain turbulence and vortex characteristics before impinging on the North wall of the building and entering into Room 301. Sinclair Library, where the Outreach office test site located, had foliage with large canopy affecting the prevailing northeasterly wind. In order to eliminate the complexity of the CFD model, these foliage characters were not included in the model. The main objective of including external areas in the coupled domain was to be able to define the openings of Room 301 as part of the domain, therefore avoiding approximations of the mass flow rate through the windows of Room 301.

4.5 Scope and Structure of CFD Test Scenarios

The following parameters were used in the CFD analysis of Room 301:

Computational domain size and representation of characteristics of the test site:

- The computational domain focuses on the interior office space of the Outreach Office room 301 of Sinclair Library.
- All fixed and large furniture, office equipment, cubicles (partitions) were modeled.
- Moveable and small objects (e.g. books, boxes, etc.) were excluded in the CFD models.
- Other parts of the building are air-conditioning spaces with all windows closed and therefore were partial modeled as solid walls with wall-type boundary condition.

Steady RANS equation and turbulence model:

- Only velocity and wind velocity-driven pressure differentials are within the interest of the study.
- No heat transfer (radiant heat transfer) model included in the solution.
- Reynolds-Average Navier-Stokes (RANS) flow equation was solved in this study using either most popular turbulence model the Realizable k - ϵ and Shear Stress Transport (SST) k - ω .

Approximately 40 initial CFD runs were conducted to narrow the documented benchmarking process to 18 test cases. Figure 4.22 shows the 18 test cases under which the CFD simulation runs were conducted. Each simulation run represents a combination of the following parameters:

- Type of computational domain, coupled or decoupled
- With or without furniture (structural elements such as columns were modeled in every case)
- Type of turbulence model

- Type of boundary condition for inlet of the domain
- Type of boundary condition for outlet (exhaust fans) of the internal space
- Air density and viscosity; either standard conditions (= CFD defaults) or value calculated from measured data at the site

Test case groups D (D1 – D4) and E (E1 – E4) represent CFD simulations that corresponded to the four test scenarios which were established in Room 301 by a combination of having the north-facing louvered windows of Room 301 either closed or opened and the exhaust fans either on or off. The resulting air flow conditions in Room 301 were measured in Room 301 and the results of theoretical CFD simulations and actually measured air velocities and differential pressures for these four test scenarios were compared.

The parameter matrix for the 18 CFD simulation runs are depicted in Figure 4.23.

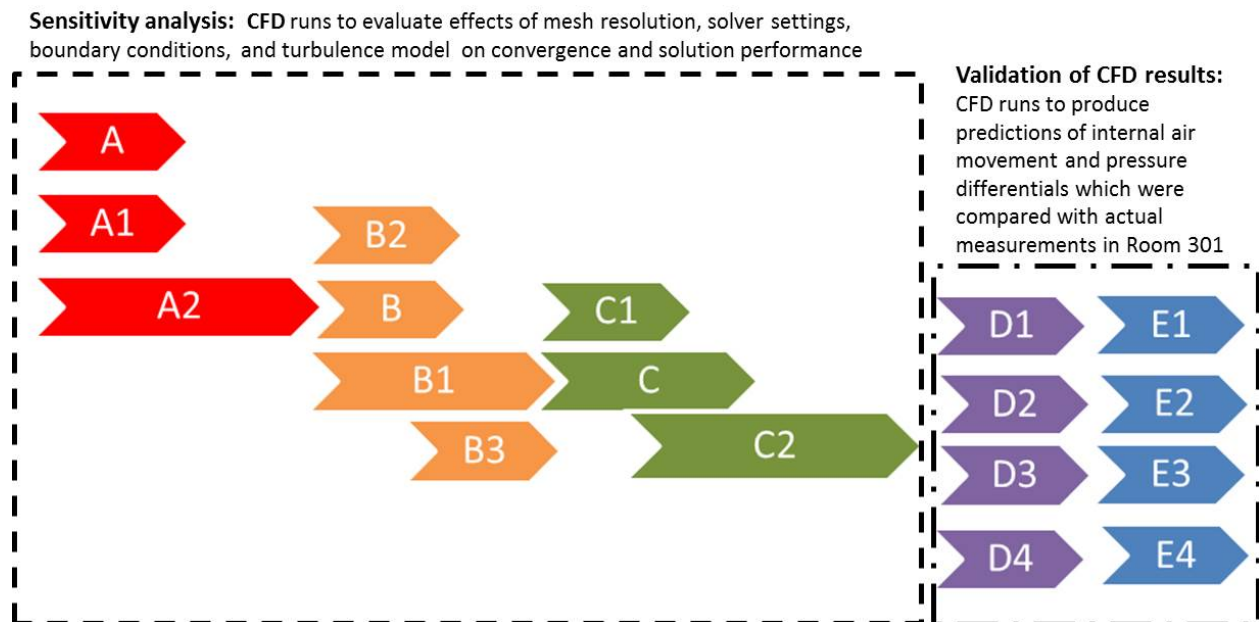


Figure 4.22: Structure of test cases under which CFD simulation runs were conducted

4.6 Evaluating the Effects of Type and Resolution of the Applied Mesh

The volume meshing process was a time consuming part of the CFD modeling process. The quality of the volume meshes affected the convergence of the solution. The “Trimmed cell mesher” function of the CFD software (STAR-CCM+) was used throughout the research based on its capability to produce a high-quality mesh, which could be effectively aligned to architectural structures of the model. Prism layers were used to create prism volume cells in the near wall regions of building’s surfaces and the ground surface. The total numbers of volume cells for three types of CFD domains are listed in the Table 4.1.

Table 4.1: Number of volume cells for meshes used in three different CFD domains

	Decoupled domain	Coupled domain without furniture	Coupled domain with furniture
Total number of cells	2,481,517	4,347,720	15,820,425

Mesh quality checks were performed to evaluate two quality criteria, consisting of face validity and volume change. Good cells should have cell validity of 1.0 and volume change close to 1.0 (less changing in volume in comparison to that of its neighbors). Table 4.2 shows the results of the volume change and cell validation test of three different CFD domains. All of the meshes were found satisfactory.

4.6 Evaluating the Effects of Turbulence Models on Convergence and Simulation Performance

Two turbulence models were used in the CFD simulations runs, the conventional k-epsilon (k-ε) and the SST k-ω turbulence model.

The k-epsilon (k-ε) turbulence model is a two-equation model in which transport equations are solved for the turbulent kinetic energy (k) and its dissipation rate (ε). Various forms of the k-ε model have been in use for several decades, and it has become the most widely used model for industrial applications. One of the improved versions of the standard k-ε model is the Realizable two layer k-ε, which was used in this study. The Realizable k-ε model contains a transport equation for the turbulence dissipation rate ε and substituting the constant C_μ in the standard model to a formula expressing a function of mean flow and turbulence properties. The Realizable k-ε model utilizes the two-layer approach to model explicitly the turbulence airflow in the far field and viscous sublayer as follows: “the computation is divided into two layers. In the layer next to the wall, the turbulent dissipation rate and the turbulent viscosity are specified as functions of wall distance. The values of specified in the near-wall layer are

blended smoothly with the values computed from solving the transport equation far from the wall. The equation for the turbulent kinetic energy is solved in the entire flow.” (STAR-CCM+ Manual V.9.02).

Solution ID	Coupled / Decoupled	With furniture	Turbulence model	Inlet	Outlet	Air density and dynamic viscosity	Test Scenario
A	Decoupled	No	k-ε	Constant velocity	Pressure outlet (0 Pa)	default	N/A
A1	Decoupled	No	k-ω	Constant velocity	Pressure outlet (0 Pa)	default	N/A
A2	Decoupled	No	k-ε	Constant velocity	Constant massflow rate (4.359kg/s)	default	N/A
B	Coupled	No	k-ε	Wind log profile	Constant massflow rate (4.359kg/s)	default	N/A
B1	Coupled	No	k-ε	Wind log profile	Fan curve	default	N/A
B2	Coupled	No	k-ω	Wind log profile	Fan curve	default	N/A
B3	Coupled	No	k-ε	Wind log profile	Fan curve	Actual test condition	N/A
C	Coupled	Yes	k-ε	Wind log profile	Fan curve	default	N/A
C1	Coupled	Yes	k-ω	Wind log profile	Fan curve	default	N/A
C2	Coupled	Yes	k-ε	Wind log profile	Fan curve	Actual test condition	N/A
D1	Coupled	Yes	k-ε	Wind log profile	Fan curve	Actual test condition	Scenario 1
D2	Coupled	Yes	k-ε	Wind log profile	Fan curve	Actual test condition	Scenario 2
D3	Coupled	Yes	k-ε	Wind log profile	Fan curve	Actual test condition	Scenario 3
D4	Coupled	Yes	k-ε	Wind log profile	Fan curve	Actual test condition	Scenario 4
E1	Coupled	Yes	k-ω	Wind log profile	Fan curve	Actual test condition	Scenario 1
E2	Coupled	Yes	k-ω	Wind log profile	Fan curve	Actual test condition	Scenario 2
E3	Coupled	Yes	k-ω	Wind log profile	Fan curve	Actual test condition	Scenario 3
E4	Coupled	Yes	k-ω	Wind log profile	Fan curve	Actual test condition	Scenario 4

Figure 4.23: CFD study model matrix

Table 4.2: Volume Change and Cell validation check of three different CFD domain

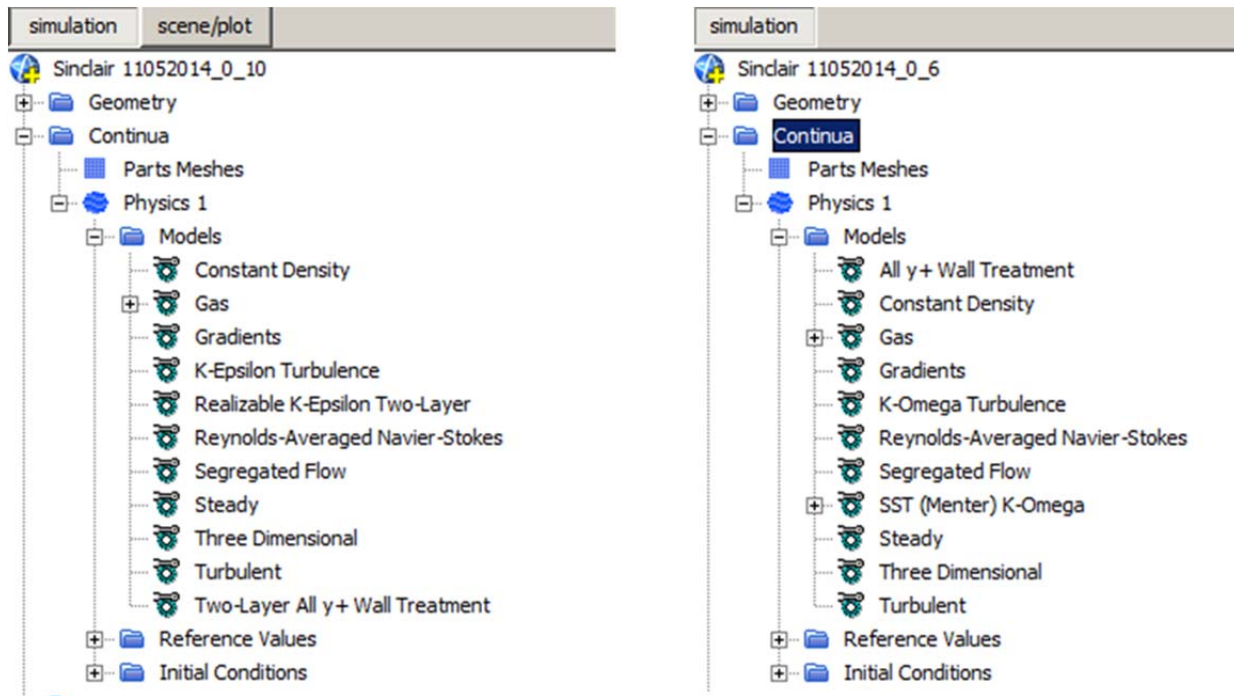
Volume Change		Decoupled CFD		Coupled CFD without furniture		Coupled CFD with furniture	
		# cells	%	# cells	%	# cells	%
	<= 1e-6	0	0.000%	0	0.000%	1	0.000%
1e-6	1e-5	0	0.000%	0	0.000%	1	0.000%
1e-5	1e-4	0	0.000%	1	0.000%	7	0.000%
1e-4	1e-3	5	0.000%	4	0.000%	50	0.000%
1e-3	1e-2	786	0.032%	1519	0.035%	4635	0.029%
1e-2	1e-1	16893	0.681%	31763	0.731%	175969	1.112%
1e-1	1.0	2463833	99.287%	4314433	99.234%	15639762	98.858%
Total number of volume cells		2481517	100%	4347720	100%	15820425	100%

Cell validation		Decoupled CFD		Coupled CFD without furniture		Coupled CFD with furniture	
		# cells	%	# cells	%	# cells	%
	<= 0.5	0	0.000%	0	0.000%	0	0.000%
0.5	0.6	0	0.000%	0	0.000%	0	0.000%
0.6	0.7	0	0.000%	0	0.000%	0	0.000%
0.7	0.8	0	0.000%	0	0.000%	0	0.000%
0.8	0.9	0	0.000%	0	0.000%	1	0.000%
0.9	0.95	0	0.000%	0	0.000%	46	0.000%
0.95	1.0	2481517	100.000%	4347720	100.000%	15820378	100.000%
Total number of volume cells		2481517	100%	4347720	100%	15820425	100%

The k-omega (k- ω) turbulence model a two-equation eddy-viscosity model to solve transport equations for the turbulent kinetic energy (k) and specific dissipation rate omega ($\omega \sim \epsilon / k$). The k- ω turbulence model is claimed to be advantageous in comparison to the k- ϵ model in handling the adverse pressure gradients at boundary layers (STAR-CCM+ Manual). These conditions are often found in architecture-related forms inheritably having many edges serving as separation points of separation airflow.

The k- ω model used in the study is the SST k- ω turbulence model. Using this model can avoid problems of sensitivity of the flow to inlet free-stream/inlet condition, which the standard k- ω model is prone to. In the SST k- ω model, the ϵ transport equation from the standard k- ϵ model is transformed into an omega transport equation by variable substitution and adding an additional non-conservative cross-diffusion term.

Figure 4.24 shows the physics property settings for the two turbulence models used in the CFD simulation test runs.

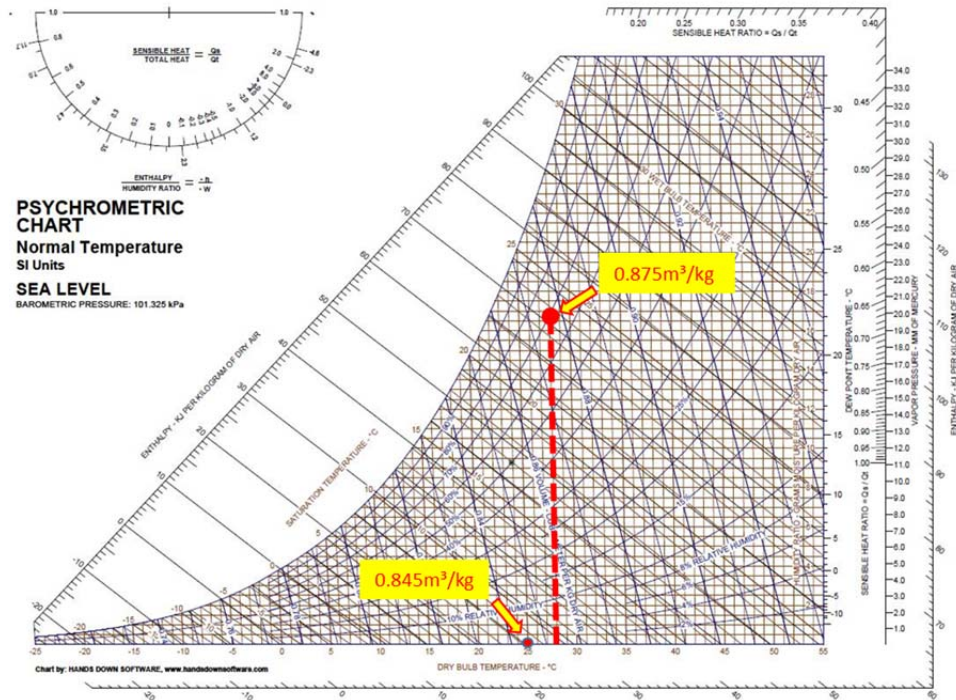


(a) Physic property settings used for k-ε turbulence model (b) Physic property settings used for SST k-ω turbulence model

Figure 4.24: Physic property setting for two turbulence models used in the CFD simulation runs

4.7 Evaluating the Air Properties to be used in the CFD Simulations

The CFD software (Star CCM+) uses default values of physic properties, such as density, dynamic viscosity, specific heat, thermal conductivity, latent heat of vaporization, etc. for air, reflecting standard conditions, e.g. 100,000 Pa and 20°C. For example, the default values of air density and dynamic viscosity, which are important for the internal CFD analysis, were set at 1.184 kg/m³ and 1.855058e-5 Pa-s, respectively. However, tests conducted at the site revealed an average air temperature and relative humidity of 28°C and 70% relative. Based on these test conditions, the air density and dynamic viscosity used in the CFD scenarios D1 through D4 and E1 through E4 were set to 1.143kg/m³ and 1.85144e-5 Pa-s, respectively. As indicated in Figures 4.25 and 4.26, the actual air density and dynamic viscosity used in the CFD simulations runs for scenarios D and E differed 4% and 0.2 % from the software default values, respectively.



At normal pressure (1 at or 101.325 kPa):

STAR-CCM+ default	$T_o = 25^{\circ}C$ $RH_o = 0\%$ $\rho_o = \frac{1}{0.845} = 1.184kg/m^3$	Test condition	$T = 28^{\circ}C$ $RH = 70\%$ $\rho = \frac{1}{0.875} = 1.143kg/m^3$
$\Delta\rho = \frac{\rho_o - \rho}{\rho} \approx 4\%$			

Figure 4.25: Difference of values of actual air density at the test site and default air density used in the CFD software

Sutherland Viscosity Law

Sutherland's viscosity law resulted from a kinetic theory by Sutherland (1893) using an idealized intermolecular-force potential. The formula is specified using two or three coefficients.

Sutherland's law with two coefficients has the form

$$\mu = \frac{C_1 T^{3/2}}{T + C_2} \quad (8.4-5)$$

For air at moderate temperatures and pressures, $C_1 = 1.458 \times 10^{-6} \text{ kg/m-s-K}^{1/2}$, and

$$C_2 = 110.4 \text{ K.}$$

μ = the viscosity in kg/m-s

T = the static temperature in K

C_1 and C_2 = the coefficients

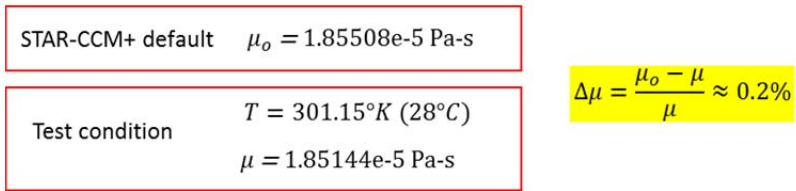


Figure 4.26: Difference of values of actual air dynamic viscosity at the test site and default air dynamic viscosity used in the CFD software

4.8 Evaluating the Effect of Inlet and Outlet Boundary Conditions

The boundary conditions of the three computational domains included the atmosphere boundary layers (logarithmic profile wind for velocity inlet, constant pressure outlet), the ground surface, surfaces inside building (including cubicle walls) and pressure outlet with electric fan performance curve.

- Inlet conditions for the coupled domain case: The inlet boundary condition was approximated by approaching wind with a logarithmic wind velocity profile distribution wind for velocity for

North-East wind direction. The wind velocity U_z (m/s) was assumed to vary with the elevation z (m) based on log-law formula as follows:

$$U(z) = \frac{U_{ABL}^*}{k} \ln \left(\frac{z - z_{ground} + z_0}{z_0} \right)$$

$$k(z) = \frac{U_{ABL}^{*2}}{\sqrt{C_\mu}}$$

$$\varepsilon(z) = \frac{U_{ABL}^{*3}}{k(z + z_0)}$$

Where k is the Karman constant ($=0.42$), z_0 is the roughness parameter and U_{ABL}^* is the atmospheric boundary layer friction velocity can be calculated as:

$$U_{ABL}^* = \frac{kU_r}{\ln((z_r + z_0)/z_0)}$$

Therefore,

$$U(z) = U_r \ln \left(\frac{z - z_{ground} + z_0}{z} \right) / \ln \left(\frac{z_r + z_0}{z} \right)$$

Where z is the height, z_{ground} is the ground elevation, z_0 is the aerodynamic roughness length selected from Table 4.3, U_r is the reference velocity at the reference height z_r . For SST k - ω turbulent model, ω can be obtained by using the approximation $\omega \sim \varepsilon/k$ and therefore:

$$\omega = \frac{U_{ABL}^* \sqrt{C_\mu}}{k(z + z_0)}$$

- Pressure outlet for the coupled domain case: Outlet boundary condition was set as pressure outlet on the West and South external domain surfaces (refer to Figure 4.26) with static pressure assigned as 0 Pascal (Pa).

Class	Short terrain description	z_0 (m)
1	Open sea, fetch at least 5 km	0.000 2
2	Mud flats, snow; no vegetation, no obstacles	0.005
3	Open flat terrain; grass, few isolated obstacles	0.03
4	Low crops; occasional large obstacles, $x/H > 20$	0.10
5	High crops; scattered obstacles, $15 < x/H < 20$	0.25
6	Parkland, bushes; numerous obstacles, $x/H = 10$	0.5
7	Regular large obstacle coverage (suburb, forest)	1.0
8	City centre with high- and low-rise buildings	≈ 2

Note: Here x is a typical upwind obstacle distance and H is the height of the corresponding major obstacles. For more detailed and updated terrain class descriptions see Davenport and others (2000) (See also Part II, Chapter 11, Table 11.2).

Table 4.3: Aerodynamic roughness length z_0 , based on the terrain classification (Davenport, 1960) (Source: MO Guide to Meteorological Instruments and Methods of Observation WMO-No. 8 page 1.5-12)

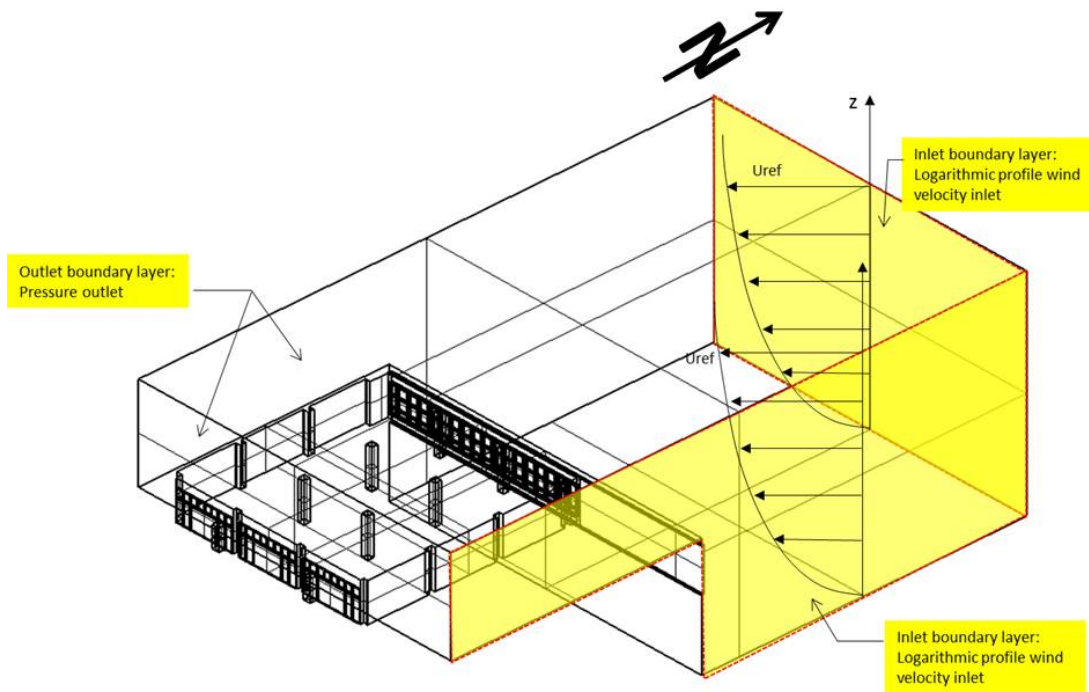


Figure 4.26: Outlet boundary condition for the West and South domain surfaces.

- The fan performance curve for outlet boundary conditions of Room 301, for coupled and decoupled cases: The exhaust fans draw air out of Room 301, thus increasing the ventilation performance of the office above the natural ventilation rate. Since the vendor of the whole house fans, which were used in this investigation, could not provide the exact fan curve the performance curve was estimated based on comparable fan performance curves for propeller type fans found in the literature. The outlet boundary condition with the two exhaust fan units is depicted in Figure 4.27. The whole house fan and the interpolated fan curve used in the CFD analysis are depicted in Figure 4.28.

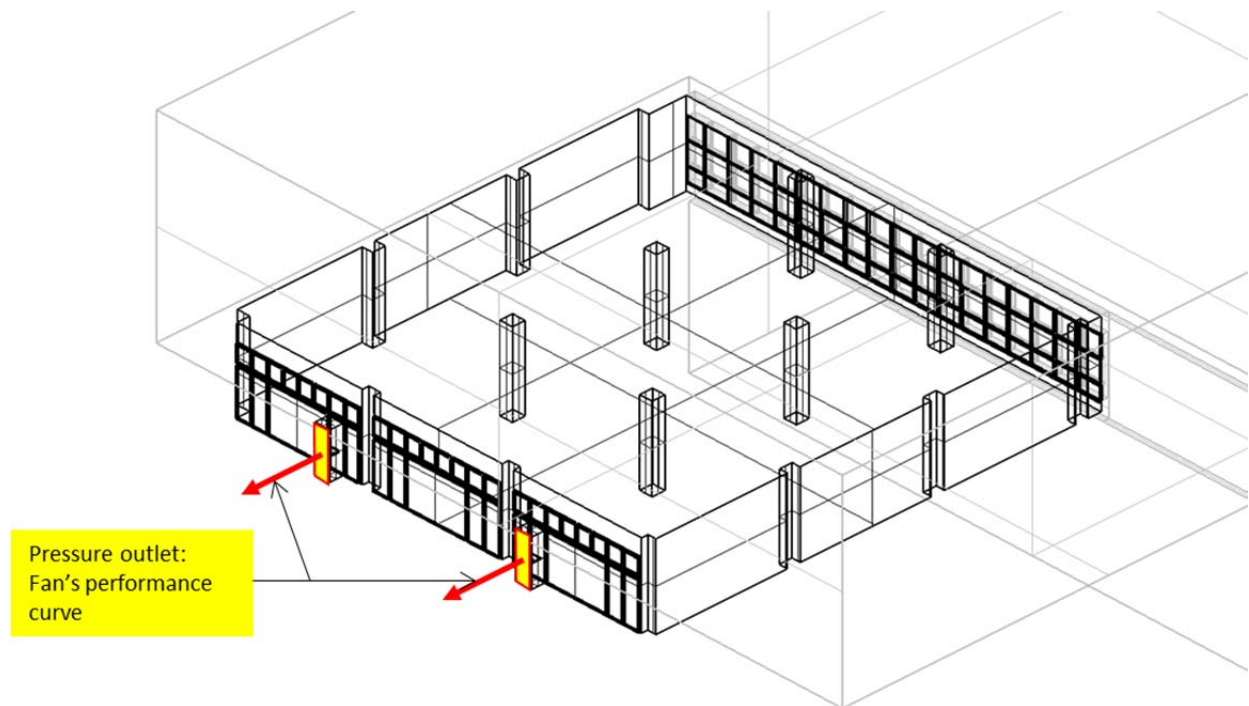


Figure 4.27: Pressure outlet boundary conditions for the exhaust fans located on the South lanai adjacent to Room 301.

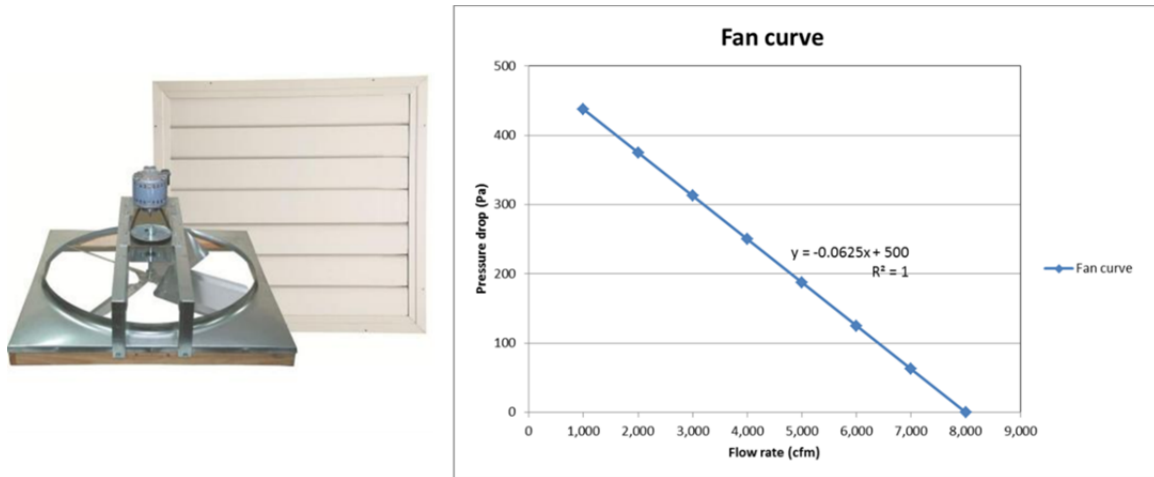


Figure 4.28: Type of exhaust fan used (total of four exhaust fans) in Room 301; fan curve depicts typical pressure versus exhaust volume performance of these propeller type fans.

4.9 Post-Processing – Visualization and Quantifying Internal Air Flow Phenomena

Post-processing of CFD results consisted of creating visualizations of the air flow and pressure fields and obtaining values of air velocities and pressure differentials at locations of interest within the computational domain.

Airflow and related properties visualization involved creating 2D contoured maps of velocities and pressures on (map) slices defined inside the computational domain or generating contoured maps of air velocity or air pressures in a the outside surface of objects, such as the building envelope. Contoured maps allowed for intuitively understanding of air movement patterns or wind induced air pressures at different testing scenarios. The present study used 2D slices extensively.

The present CFD study also used streamline plots to visualize the 2D air movement within the computation domain. In addition to the air flow direction at points on the streamlines the length of velocity vector were given as an indication of the air flow velocity.

For each of the 18 CFD cases, A through E (see Figure 4.23: “CFD study model matrix” for the description of the 18 cases), six images were created for each case in order to allow a ready comparison between the different cases. Figure 4.29 through 4.34 show six sample images of one of the 18 cases. Similar images were generated for each of the 18 cases and are presented in [Appendix B](#). Images with more details of the post-processing are depicted in Figures 4.35 through 4.40.

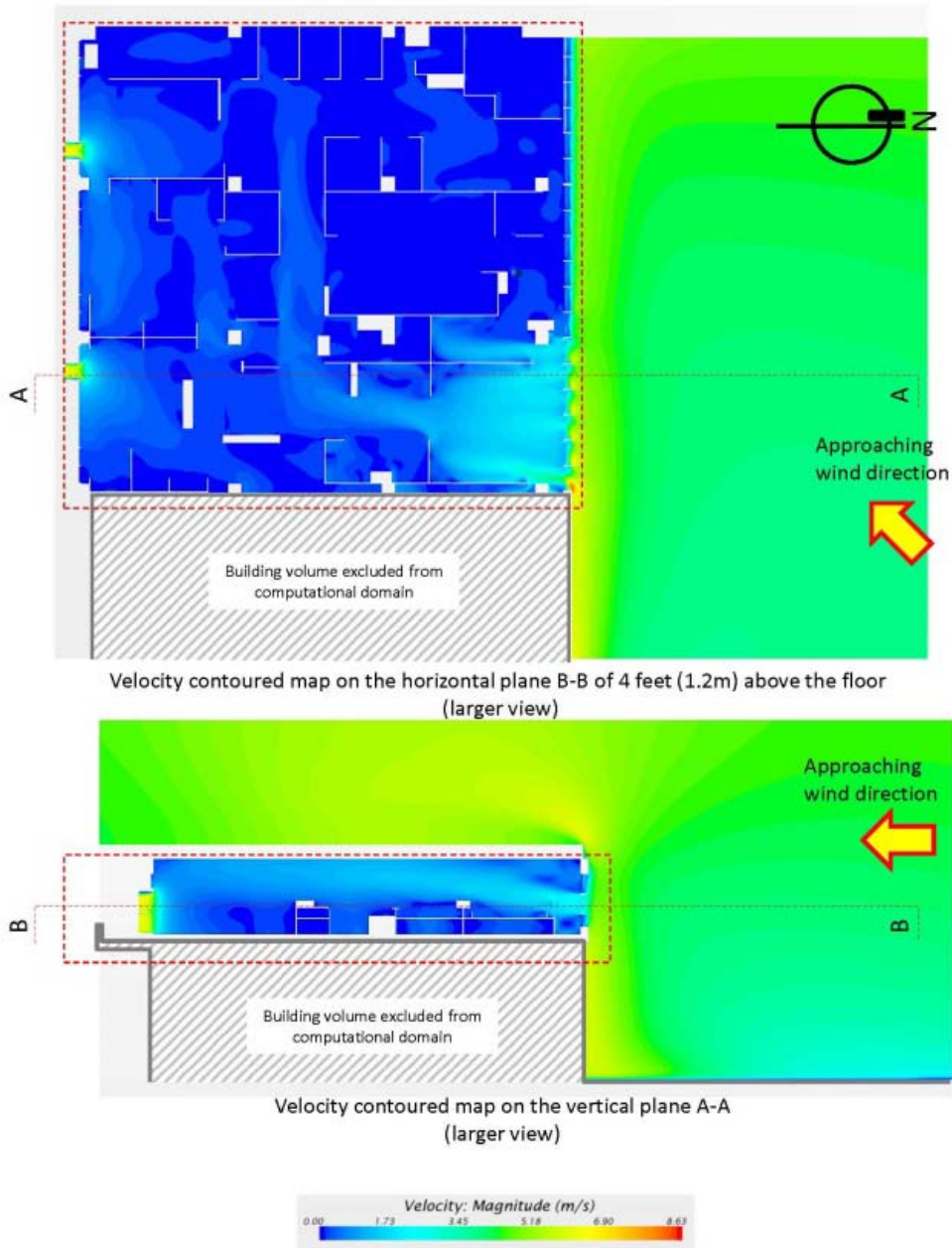


Figure 4.29: Sample plot of the visualization of the internal velocity field through colored contour map

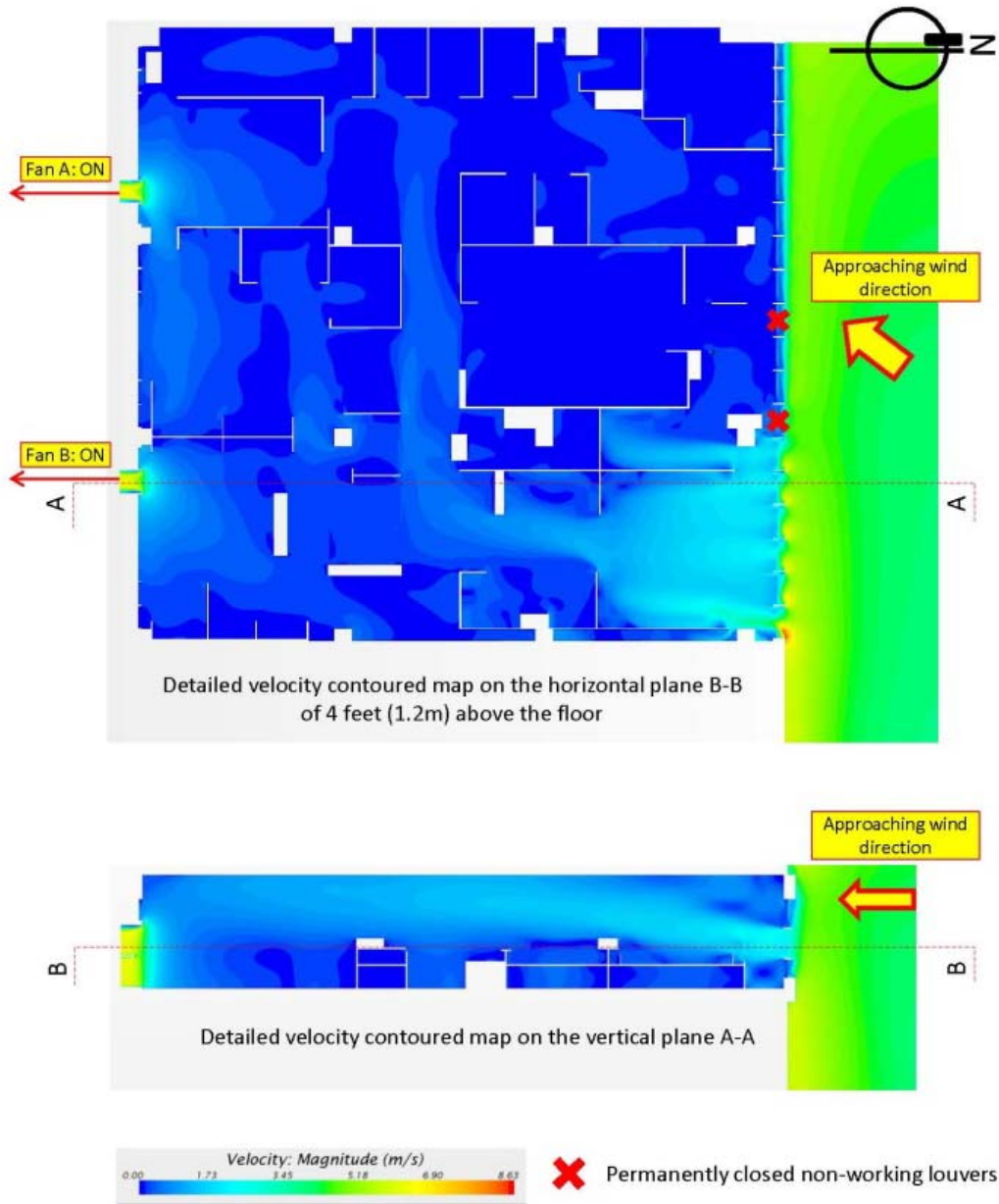


Figure 4.30: Sample plot of the visualization of the internal velocity field through colored contour map; detailed view

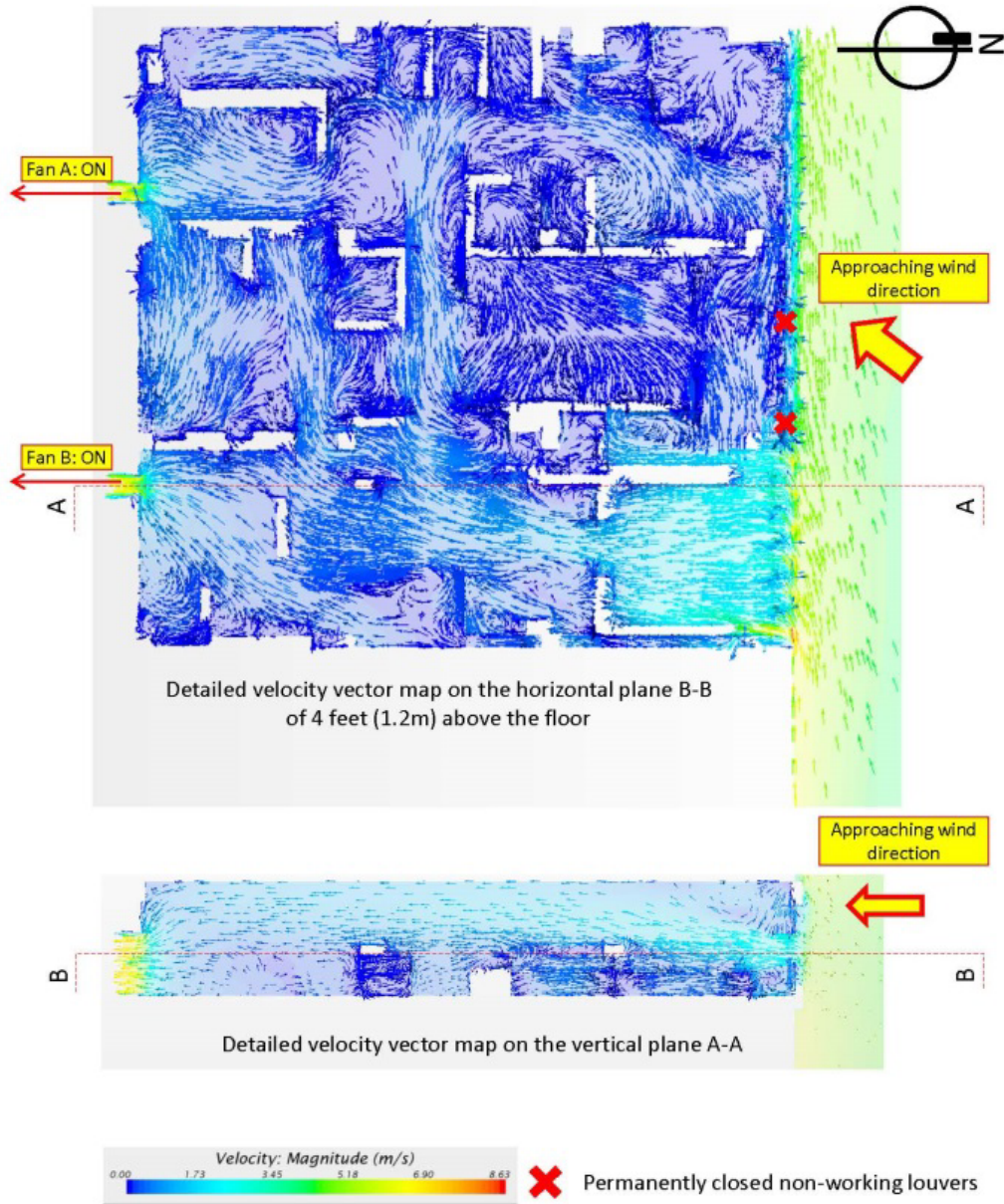


Figure 4.31: Sample plot of the visualization of the internal velocity field through scaled air velocity vector plot

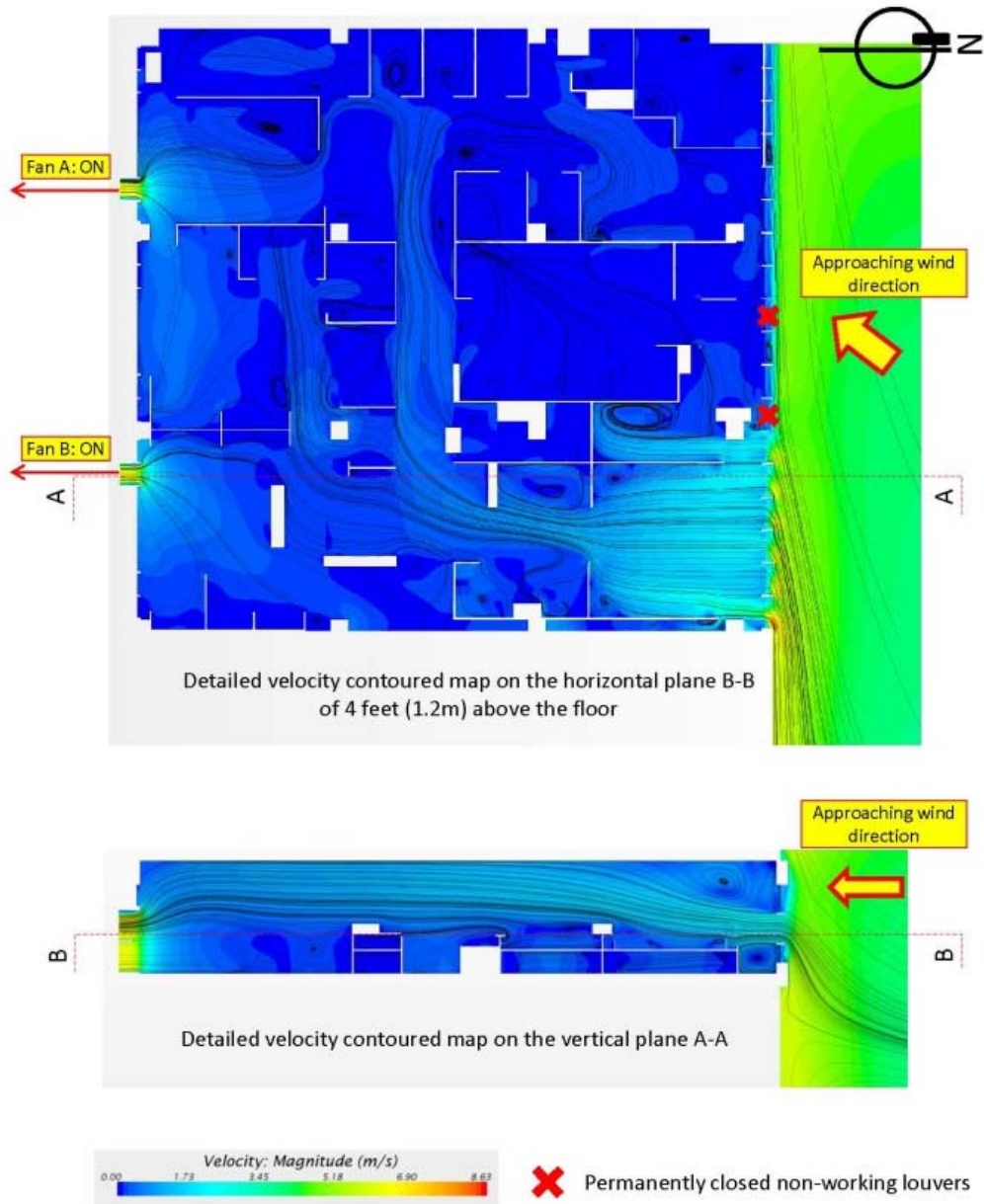


Figure 4.32: Sample plot of the visualization of the internal velocity field through colored contour map with overlaid streamline image

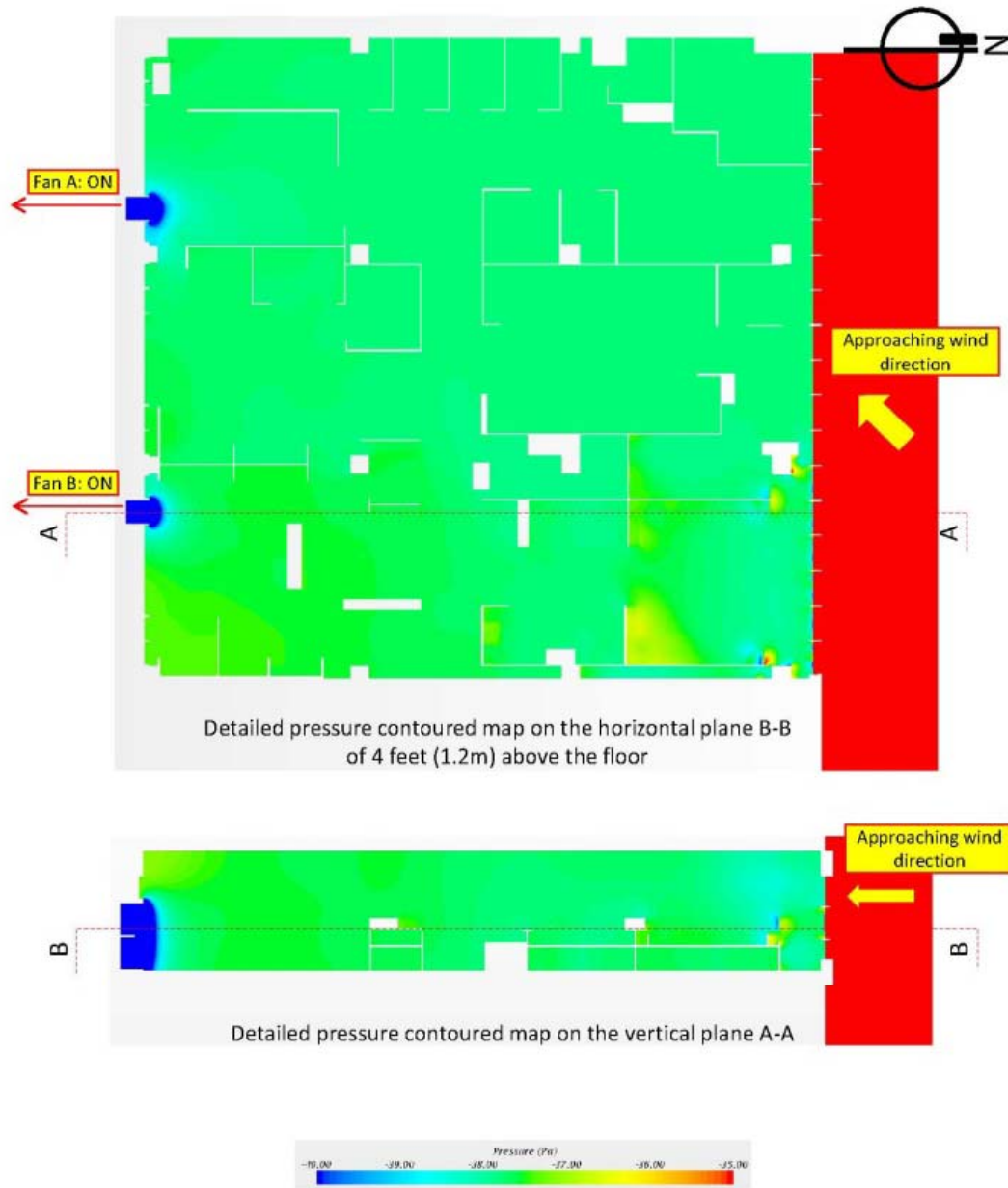
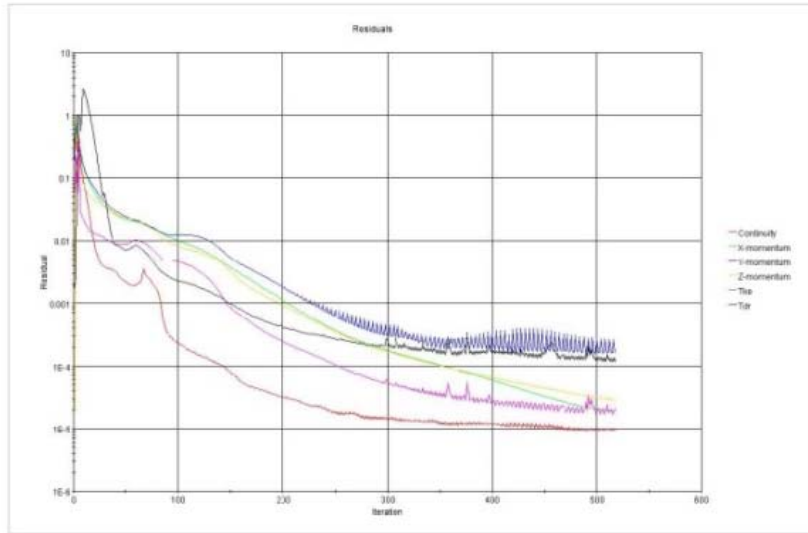
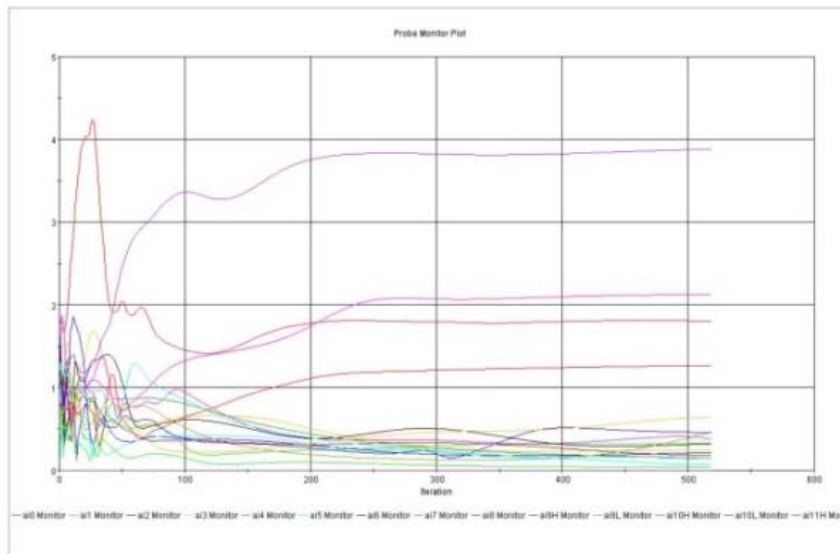


Figure 4.33: Sample plot of the visualization of the internal pressure field through colored contour map



Residual plot



Monitoring plot of wind speed at the locations for placement of sensors for convergence checking

Figure 4.34: Sample plot of the solution performance plots, through plot of residuals per iteration and monitoring of resulting velocities at locations of interest.

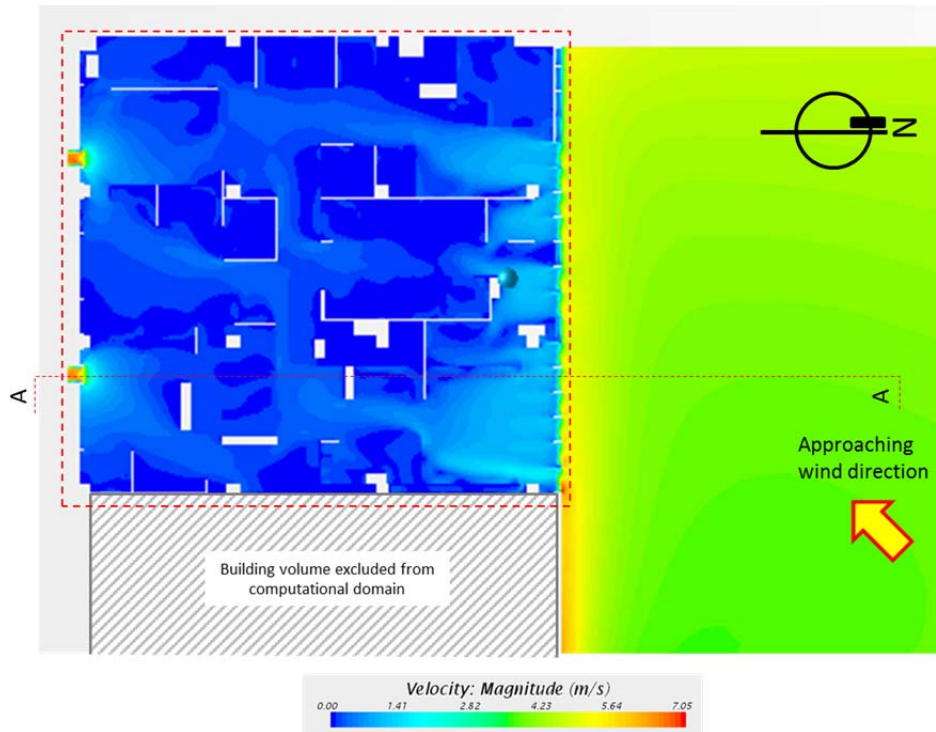


Figure 4.35: An example of the CFD result simulating the Scenario 1 (all north-facing windows were opened except non-working ones). Velocity contoured map on the horizontal plane B-B of 4 feet (1.2m) above the floor showing both internal and external wind flow (larger view)

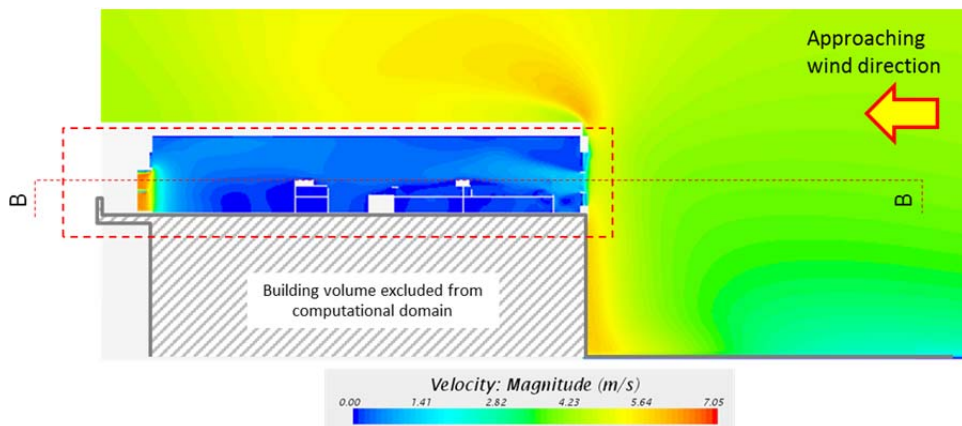


Figure 4.36: An example of the CFD result simulating the Scenario 1 (all north-facing windows were opened except non-working ones). Velocity contoured map on the vertical plane A-A (larger view).

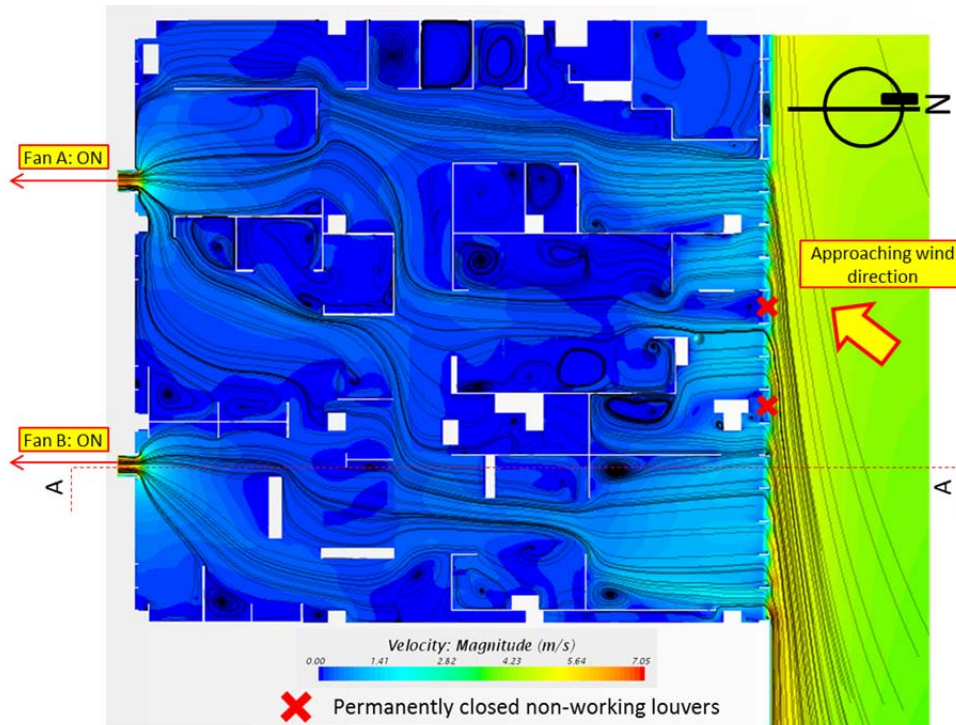


Figure 4.37: Figure: An example of the CFD results simulating the Scenario 1 (all north-facing windows were opened except non-working ones). Velocity streamlines overlaid on velocity contoured map on the horizontal plane B-B of 4 feet (1.2m) above the floor showing internal wind flow (detailed view).

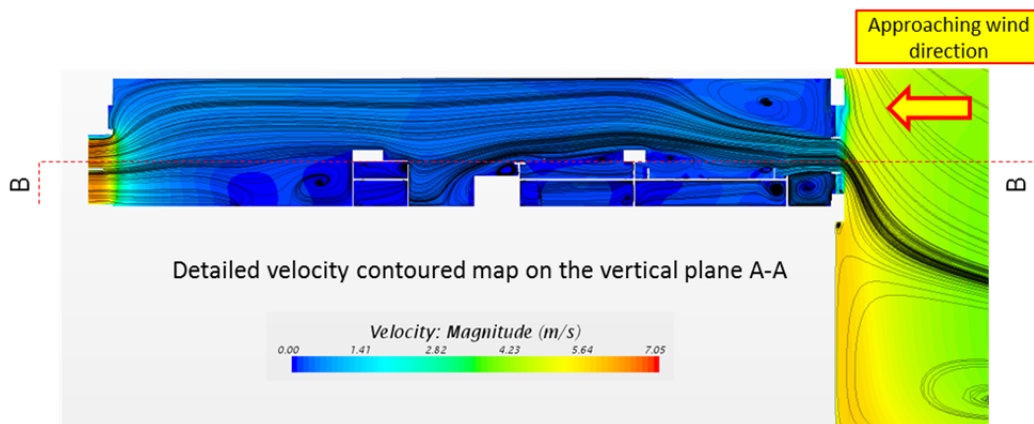


Figure 4.38: An example of the CFD result simulating the Scenario 1 (all north-facing windows were opened except non-working ones). Velocity streamlines overlaid on velocity contoured map on the vertical plane A-A showing internal wind flow (detailed view).

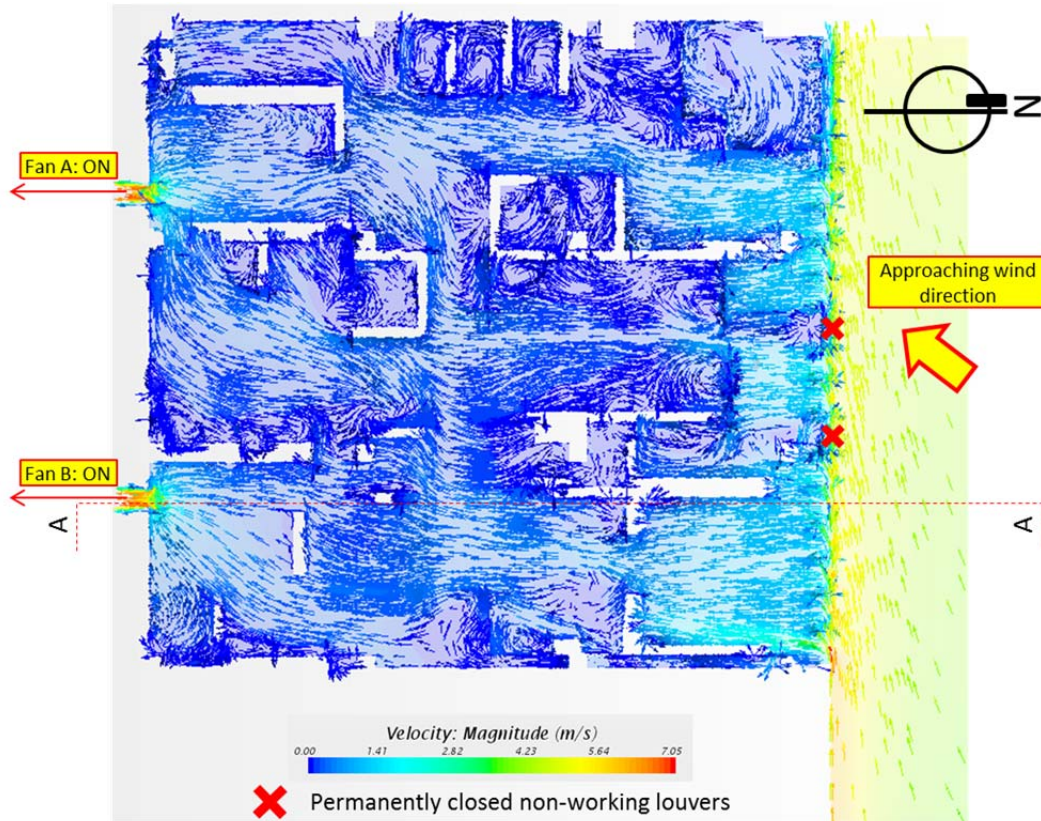


Figure 4.39: An example of the CFD result simulating the Scenario 1 (all north-facing windows were opened except non-working ones). Velocity vector map on the horizontal plane B-B of 4 feet (1.2m) above the floor showing internal wind flow (detailed view).

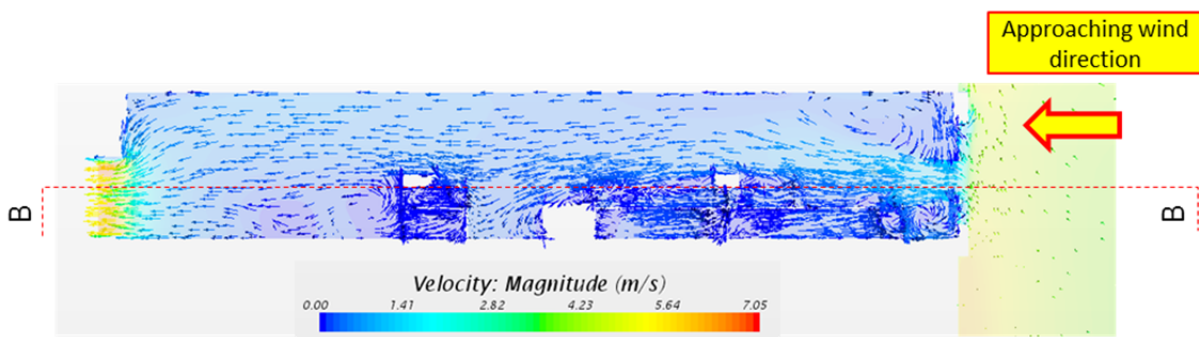


Figure 4.40: An example of the CFD result simulating the Scenario 1 (all north-facing windows were opened except non-working ones). Velocity vector map on the vertical plane A-A showing internal wind flow (detailed view).

Assessing specific values of air velocities and pressure differentials at locations of interest: So-called “probes” can be defined in the CFD software application to determine accurate values at locations of interest inside the computational domain. The values of air velocity and pressures obtained by the CFD probes can then be compared with values measured in the field at the corresponding locations. In this way the CFD results can be validated against real-world measurements.

Figure 4.41 shows the type of CFD probe that was used in the CFD research to determine air velocity values and pressures. The CFD team referred the customized probe as “presentation matrix”, a 1 foot by 1 foot grid probe with an average of 36 data points. The values obtained for the data points were averaged to determine a representative air velocity at this location.

Figures 4.42 and 4.43 show the locations and identify the coordinates of air velocity and pressure measurements points in Room 301. These locations correspond with the location of various probes in the CFD computational domain.

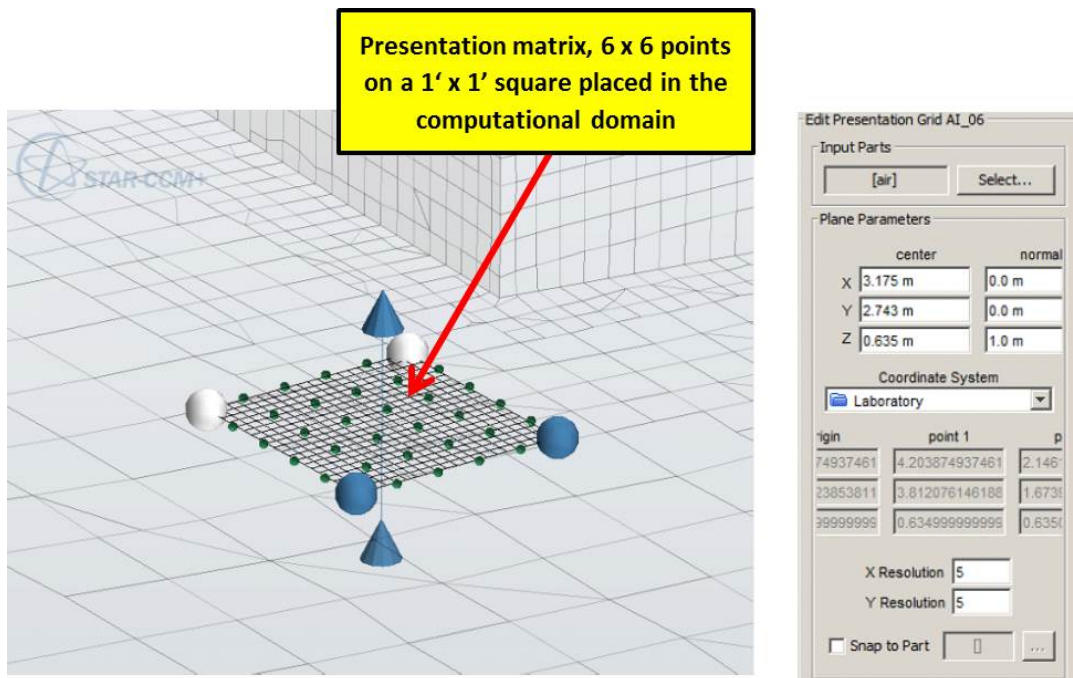


Figure 4.41: Typical presentation matrix, (a 1 foot by 1 foot grid probe) to obtain representative values for air velocity at that location in the computational domain

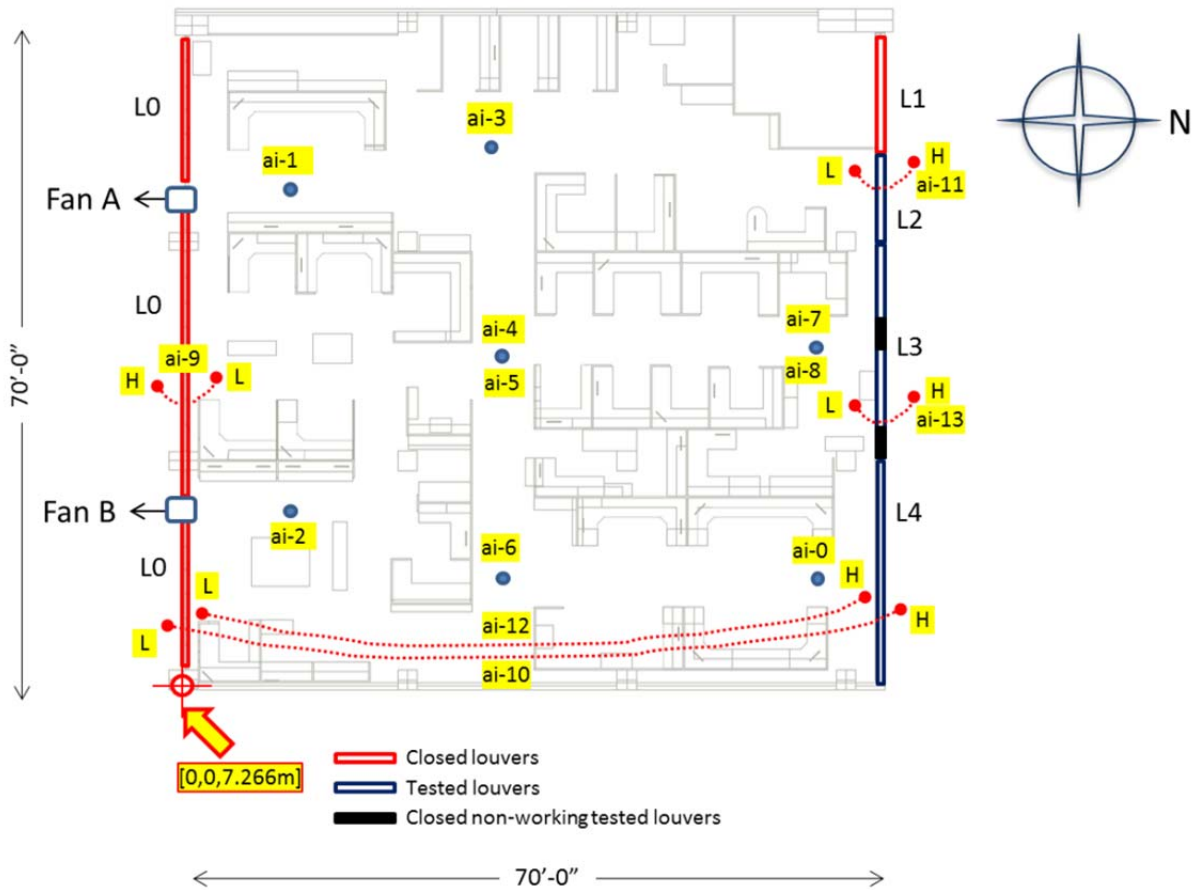


Figure 4.42: The sensor IDs and their indication of locations at the test site; these locations correspond with the locations of the CFD probes inside the computational domain

ID	Type		Unit	Coordinate
ai0	Anemometer		m/s	[17.67, 19.65, 8.53]
ai1	Anemometer		m/s	[5.49, 3.19, 8.53]
ai2	Anemometer		m/s	[15.55, 3.19, 8.53]
ai3	Anemometer		m/s	[4.19, 9.46, 8.53]
ai4	Anemometer		m/s	[10.72, 9.79, 8.53]
ai5	Anemometer		m/s	[10.72, 9.79, 9.60]
ai6	Anemometer		m/s	[17.66, 9.83, 8.53]
ai7	Anemometer		m/s	[11.10, 19.58, 8.53]
ai8	Anemometer		m/s	[11.10, 19.58, 9.60]
ai9	Pressure	Low	in. w.c.	[11.10, 0.20, 9.10]
		High		[11.10, -0.36, 9.10]
ai10	Pressure	High	in. w.c.	[17.96, 21.84, 7.98]
		Low		[17.73, -0.36, 9.10]
ai11	Pressure	High	in. w.c.	[5.40, 21.84, 7.98]
		Low		[5.40, 21.28, 7.98]
ai12	Pressure	High	in. w.c.	[17.96, 21.28, 7.98]
		Low		[17.73, 0.20, 9.10]
ai13	Pressure	High	in. w.c.	[11.10, 21.84, 8.83]
		Low		[11.10, 21.28, 8.83]

Figure 4.43: Coordinate of sensors’ locations in the computational domain (coordinate origin is indicated in Figure 4.35), CFD probes were deployed at these locations to extract data from simulation for validation against measurement

SECTION 5 - RESULTS AND DISCUSSION

This section presents and discusses the result of the CFD simulations and compares the results to the actual field data obtain from measurements in Room 301.

5.1 Results of CFD simulations for Main Four Scenarios

The development of the internal CFD workflow process included executing 40 CFD simulations during which 18 have test cases were indexed. The 18 test cases benchmarked the CFD simulation performance against the six parameters, which are listed below:

- Type of computational domain, coupled or decoupled
- With or without furniture (structural elements such as columns were modeled in every case)
- Type of turbulence model
- Type of boundary condition for inlet of the domain
- Type of boundary condition for outlet (exhaust fans) of the internal space
- Air density and viscosity; either standard conditions (= CFD defaults) or value calculated from measured data at the site

After the initial benchmarking four CFD simulations scenarios were used to investigate the effect of different turbulence models. The four CFD scenarios resembled four actual test scenarios established in Room 301 by combinations of windows on the North side of the Room 301 either open and closed and of having either both exhaust fans working or only one of the two. Figure 5.1 illustrates the four test scenarios. The same test conditions used in the CFD simulations and in the actual field test allowed direct validation of the theoretical CFD predictions. The results obtained for four scenarios are presented in detail later in this section.

Two different turbulence models, the realizable $k-\epsilon$ and the SST $k-\omega$ turbulence models, were the main parameters that distinguished the eight cases under groups E and F, which means cases E1 through E-4 and F-1 through F4, respectively. Four test scenarios were conducted with two turbulence models, thus totaling the weight test cases of groups E and F.

The Realizable $k-\epsilon$ turbulence model showed a faster and more stable convergence performance than the SST $k-\omega$ turbulence model. Realizable $k-\epsilon$ turbulence model, however, appeared to no produce detailed predictions of the air flow patterns within the Room 301 internal geometry, which featured numerous edges, and thus in many reverse pressure gradient and airflow separation.

The **SST $k-\omega$ turbulence model** showed slower and less stable convergence than the $k-\epsilon$ turbulence model and required a larger number of iterations until convergence was deemed to be satisfactory.

The use of the SST k- ω turbulence model produced a more defined prediction of the flow field with higher complex flow field geometry than the Realizable k- ϵ mode. The SST k- ω turbulence model could produce resolutions of weak airflow in some air pockets inside Room 301, whereas such air pockets and local low air flows were undetectable when using the Realizable k- ϵ turbulence model.

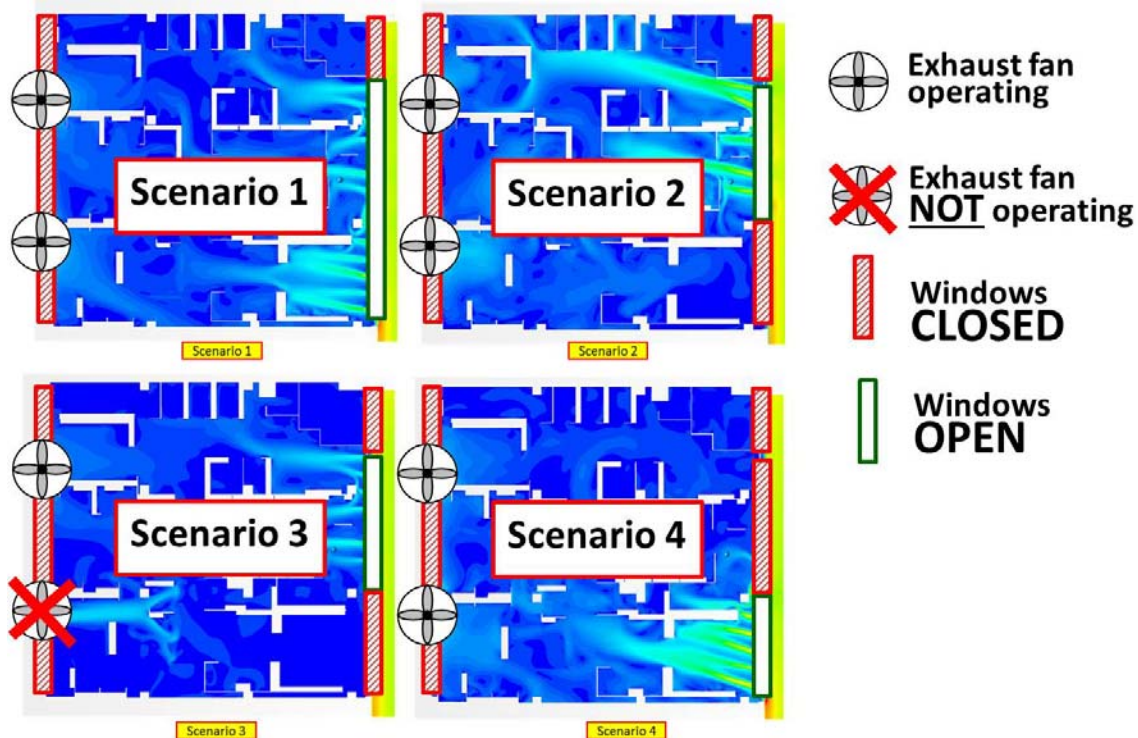
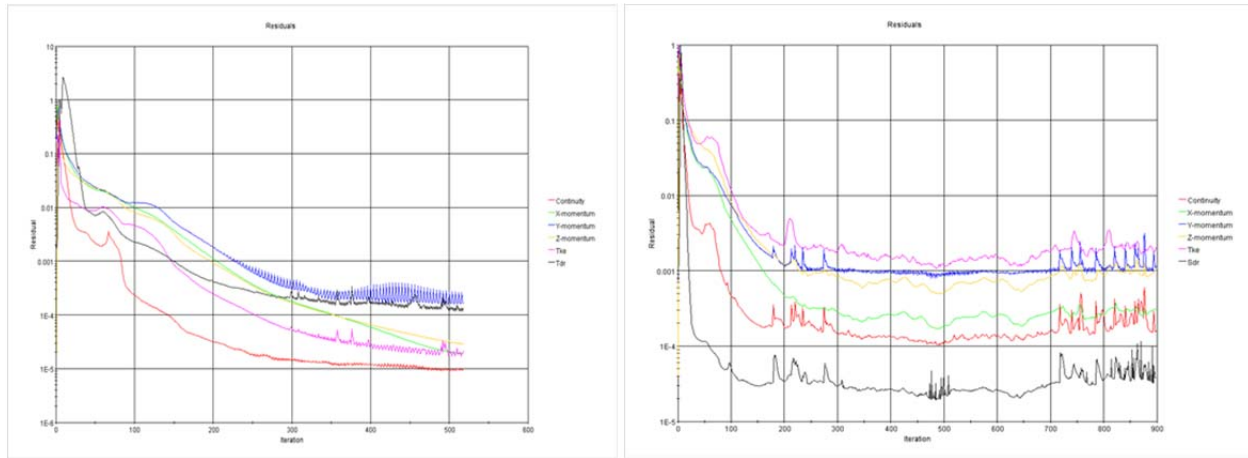


Figure 5.1: Definition of the four (4) test scenarios

Figure 5.2 shows typical convergence performances of CFD simulation runs with the Realizable k- ϵ (a) and the SST k- ω (b) turbulence models. The figure suggests the Realizable k- ϵ turbulence model has a faster and more stable convergence performance than the SST k- ω model.

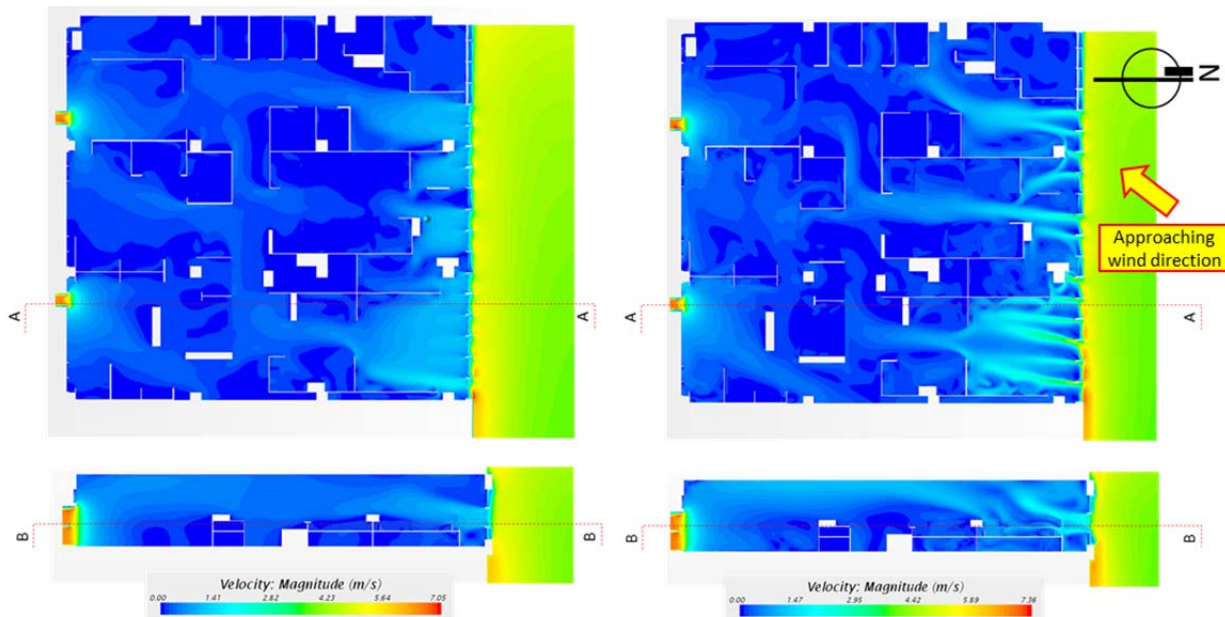
Figure 5.3 illustrates the horizontal (e.g. in x-y plane) flow distribution in Room 301. Figure 5.3 suggests that the use of the SST k- ω turbulence model produces flow descriptions with significantly better resolution than the Realizable k- ϵ turbulence model. The figure shows that the CFD simulation runs using the SST k- ω turbulence model could predict detail flow paths close to the North facing windows of Room 301.



(a) Realizable k-ε turbulence model

(b) SST k-ω turbulence model

Figure 5.2: Residuals plot of CFD solutions of two different turbulence models.



(a) Realizable k-ε turbulence model

(b) SST k-ω turbulence model

Figure 5.3: An example of airflow pattern from simulation results of two different turbulence models from the same CFD scenario (e.g. the same boundary conditions of all north-facing louvered windows kept open (Case D1 and E1).

Exhaust fans: The CFD simulation runs considered clearly defined boundary conditions on the South side of Room 301. During the test runs the windows on the South side of Room 301 were closed and two exhaust fans with two large propeller fans each extracted air from Room 301 and therefore augmented the driving force for ventilation of Room 301 from the North to the South.

Figure 5.4 illustrates the air flow pattern inside Room 301 under the four scenarios, Scenarios 1 through 4. As can be seen, the presence of exhausting fans were improving the ventilation performance of the indoor space. In comparison to the three other scenarios there were more stagnant pockets and less air movement under Scenario 3, when the exhaust fan B was turn off. In Scenario 2 (L2 closed, L3 and L4 opened) and Scenario 4 (L2 opened, L3 and L4 closed) the highest local air velocities were detected close to the North facing windows, which was the air inlet to Room 301. Under these two test scenarios only a portion of the North facing windows were left open, which reduced the air inlet area. At locations away from the North facing windows inside Room 301 smaller air velocities were measured air movement. Scenario 1 (all L2, L3 and L4 opened) showed a more even distributed air movement throughout Room 301m, when all North facing windows of Room 301 were left open.

Figure 5.5 shows the detailed CFD predictions of the air flow conditions of Scenario 3. Under this scenario the exhaust fan B was turned off. While the propeller fans were not moving and therefore not discharging air from Room 301, the opening through the fans housing was not sealed off. Therefore air could enter Room 301 from the South. This condition is clearly indicated by the scaled streamlines in Figure 5.5. Figure 5.4 also suggested higher air flow originating from the open fan box B. Figure 5.4 does, however, only provide the magnitude of internal air flow velocities without indicating the air flow direction. The CFD simulation could therefore successfully predict the condition where lower pressure in the internal space, generated by the exhaust fans, was drawing air from the Southern boundary into Room 301.

Under prevailing natural ventilation conditions, with trade winds coming from the North-West, a positive pressure gradient across the North and the South building envelope would be established. Under this natural ventilation scenario a higher pressure would exist inside Room 301 than on the South building envelope. The exhaust fans, on the other hand, create pressure gradients required for the expulsion of air from the space, and therefore the pressure inside Room 301 was calculated to be lower than on the South side of the building. Both pressure and air movement conditions could be successful predicted with the CFD simulations.

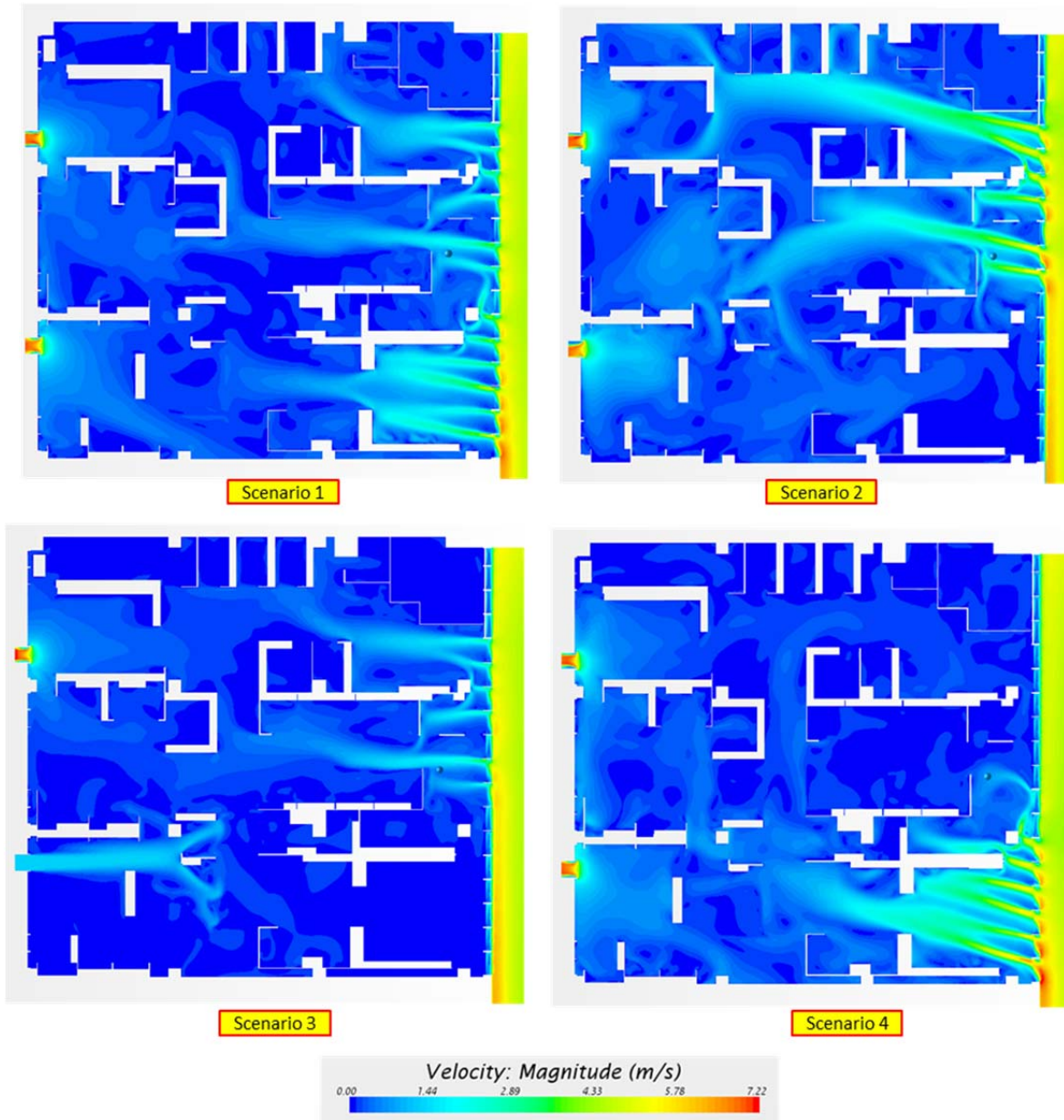


Figure 5.4: Velocity contoured map of four CFD scenarios runs using the same SST k- ω turbulence model (from E1 to E4). The upper range of the legend was not the maximum value of the simulation scenarios but adjusted accordingly for comparison reason.

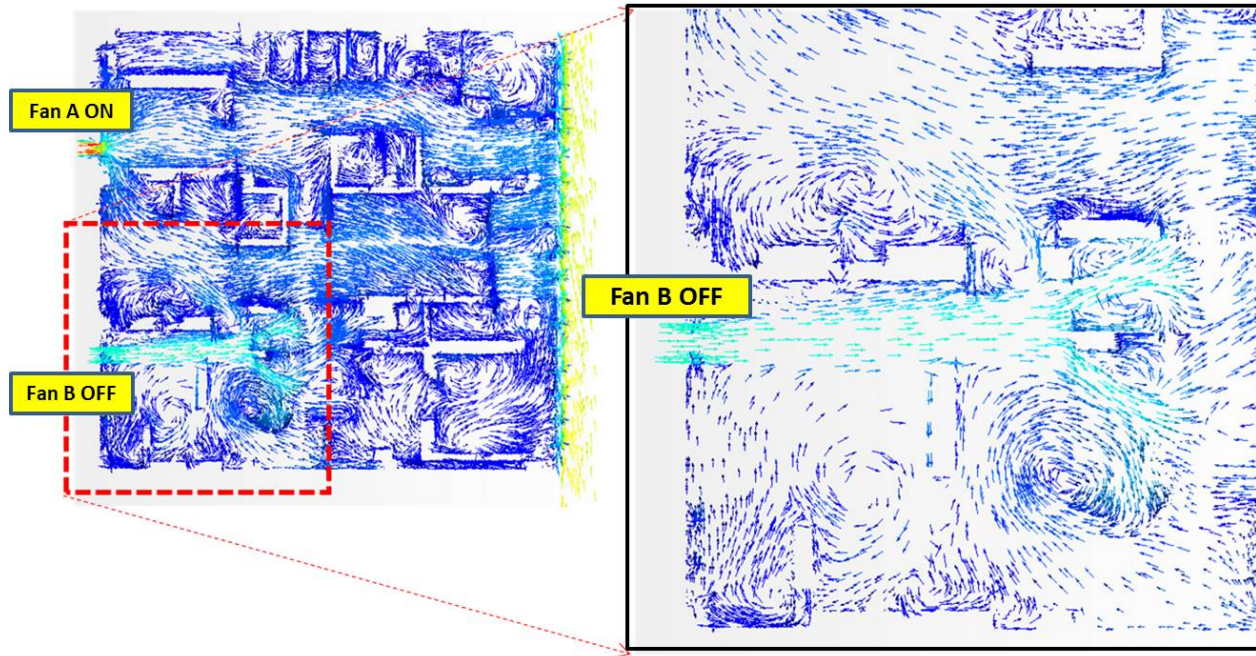


Figure 5.5: Airflow simulation from Scenario 3 (E3), under which the air flows into the interior through the non-operating exhausting fan B; the air flow vector map shows air flow direction and velocity on the section plane at 4 feet above the floor (a) and detailed view around the exhausting fan B (b).

5.2 Presentation of the Test Measurements in Sinclair Room 301

This section is a brief summary of the more detailed presentation of the test measurements in project report “Deliverable 8, Task 7.b.3: Report to Develop and Calibrate a Data Verification Process for Internal CFD simulations”.

The test measurements comprised three different types of data:

1. Presentation of weather station data for external wind movement
2. Presentation of air velocity data inside Room 301
3. Presentation of air pressure differential data across locations in Room 301

Presentation of weather station data for external wind movement: Data obtained with the weather station was filtered for wind velocity ≥ 0.05 m/s and direction 30-60 degrees. The median values for each scenario are presented in Table 5.1. The values shown in the table were used in the CFD simulation as the reference wind conditions. Figure 5.6 shows an example of a “wind rose” created

with the weather station data; the example in the figure depicts the conditions under test Scenario 1. The distance from the center represents the velocity in m/s. Figure 5.7 depicts the data record and trend line for the wind velocity during Scenario 1.

Table 5.1: Median wind direction and velocity, and number of total data points N for all four scenarios after weather station data was filtered for velocity > 0.05 m/s and for wind direction ranging from 30 to 60 degrees (North = 0 degree)

Scenario	Median Wind Direction (degrees)	Median Wind Velocity (m/s)	N
1	47.0	3.78000	504.0
2	49.1	4.28000	798.0
3	47.7	4.28000	854.0
4	49.1	3.78000	602.0

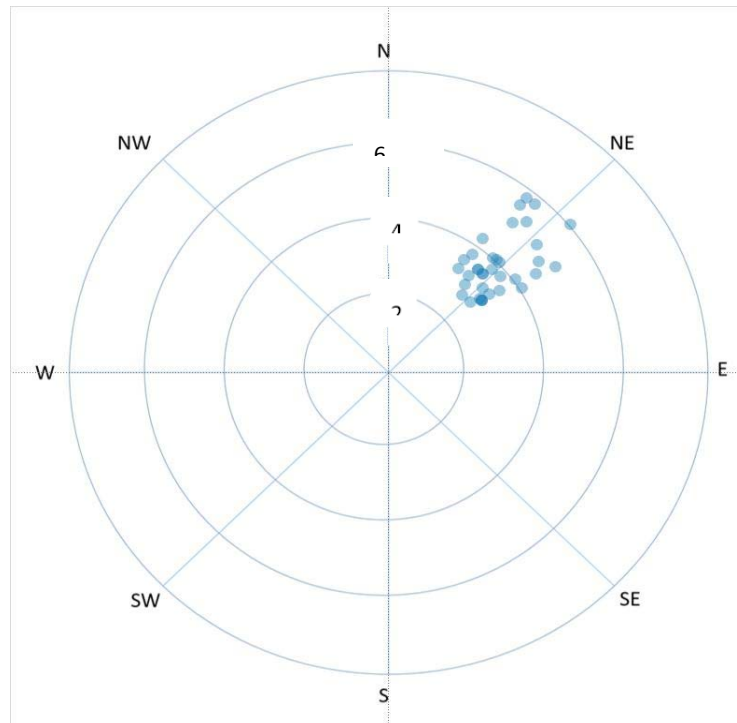


Figure 5.6: Sample of a Wind rose created with the weather station data, sample shows wind velocity (m/s; after filtering to > 0.05 m/s) and wind direction (after filtering for 30 – 60 degrees) measured by weather station during scenario

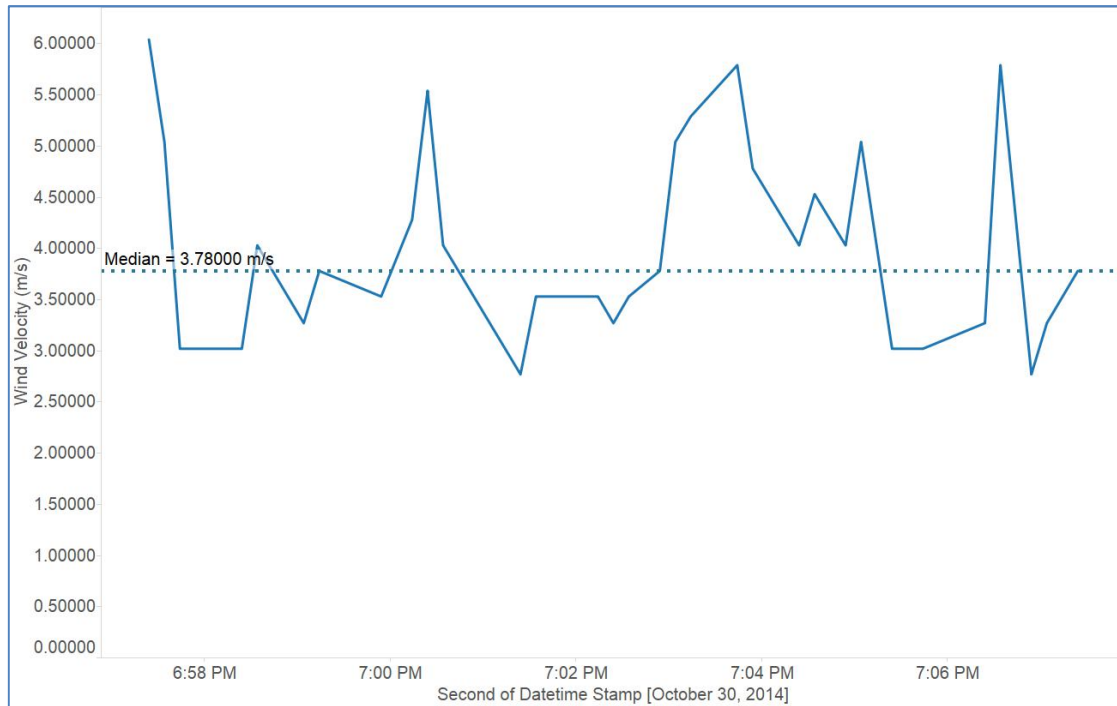


Figure 5.7: Time record and trend line for wind velocity measurement; after filtering velocity to > 0.05 m/s and wind direction to 30 – 60 degrees, measured by weather station during scenario 1

Presentation of air velocity data inside Room 301: Median air velocities calculated from anemometer data for all four test scenarios are shown in Table 5.2. All data was filtered to remove negative values, and filtered to keep only data from timestamps that correspond to filtered weather station data (wind velocity >0.05 m/s and direction 30-60 degrees). Figure 5.8 depicts the data record and trend line for air velocity data from anemometer ai0 during Scenario 1.

Presentation of air pressure differential data across locations in Room 301: Median pressure differentials measured with differential pressure transducer data for all four scenarios are shown in Table 5.3. The data was filtered to remove negative values for the Setra transducers only (but not ai11, the bi-directional Halstrup Walcher sensor), and filtered to keep only data from timestamps that correspond to filtered weather station data (wind velocity >0.05 m/s and direction 30-60 degrees). Figure 5.9 shows a data record trend line for pressure differential data from pressure transducer ai10 during Scenario 1.

Table 5.2: Median air velocities (m/s) for anemometers during all four scenarios

Sensor Id	scenario			
	1	2	3	4
ai0	0.67010		0.00494	1.04626
ai1	0.38909	0.56566	0.37840	0.32290
ai2	0.88446	0.85034	0.40430	0.86597
ai3	0.10444	0.19139	0.12458	0.06847
ai4	0.17902	0.61870	0.37265	0.21623
ai5	0.44745	0.87849	0.34220	0.16132
ai6	0.62387	0.00763	0.00064	0.73733
ai7	0.11854	0.25523	0.08442	
ai8	0.34113	0.45583	0.19601	

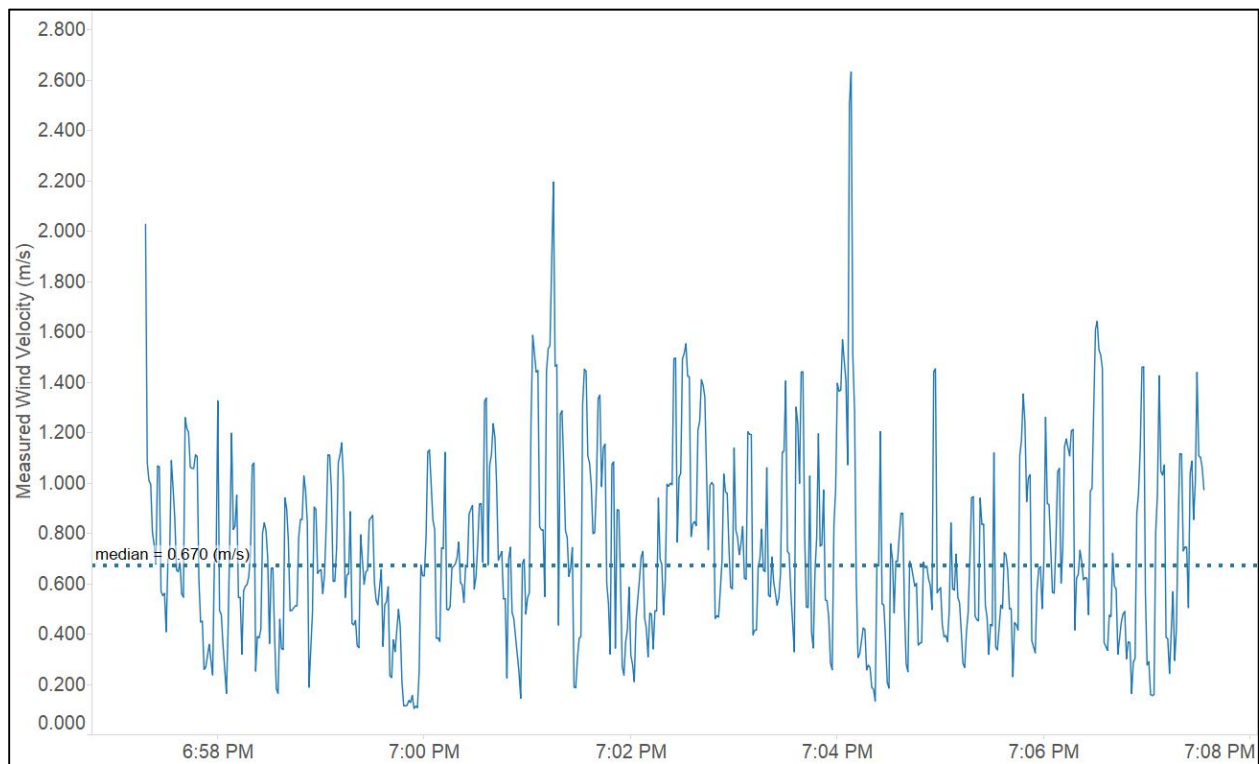


Figure 5.8 : Data record and trend line for air velocity data from anemometer ai0 during Scenario 1.

Table 5.3: Median differential pressures (in. w.c.) for pressure transducers during all four scenarios

Sensor Id	scenario			
	1	2	3	4
ai9	0.00831	0.01193	0.00862	0.01292
ai10	0.01278	0.01301	0.01360	0.01183
ai11	0.00913	0.03016	0.00796	0.01498
ai12	0.00100	0.00042	0.00086	0.00075

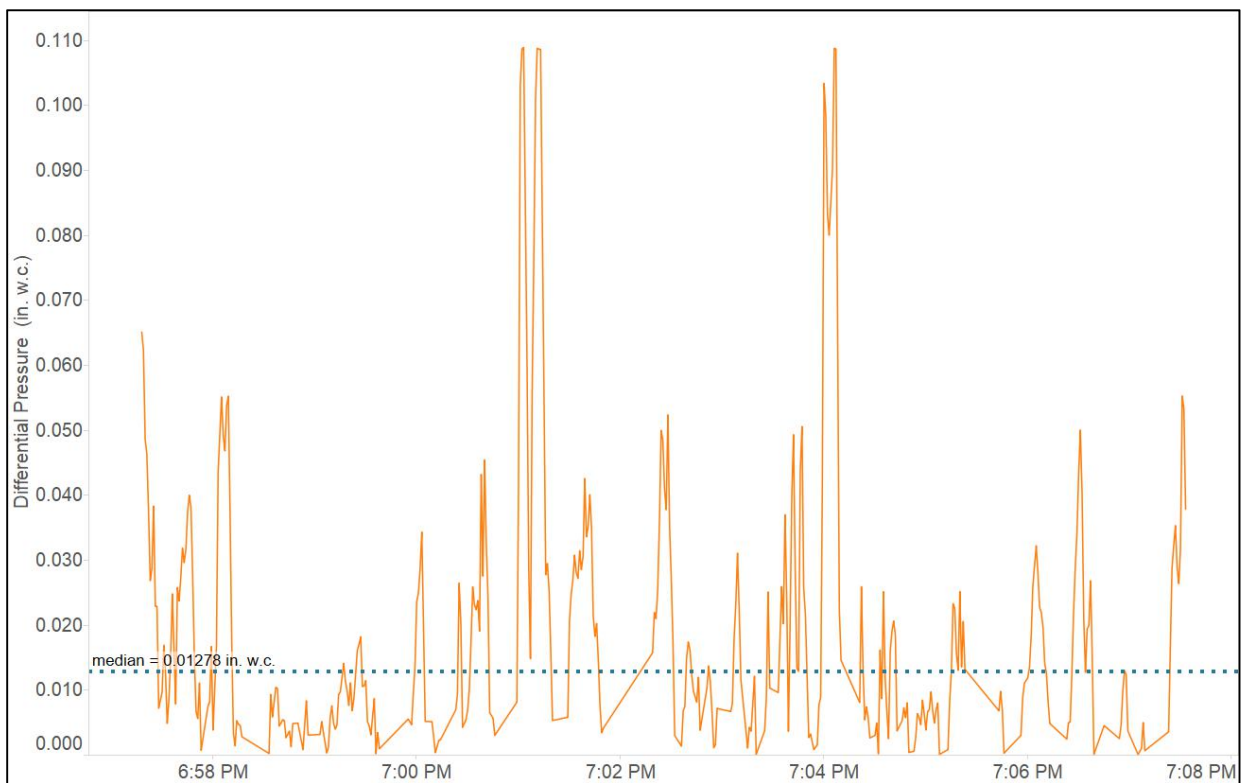


Figure 5.9: Data record trend line for pressure differential data from pressure transducer ai10 during Scenario 1.

5.3 Comparing CFD Results with Actual Test Measurements

This section presents the comparison of air flow velocities and pressure differentials obtained by CFD simulations and actual measurements in Room 301.

Comparing theoretical CFD results with actually measured air flow velocities in Room 301: Table 5.4 shows a comparison for air velocity data in Room 301 at selected locations obtained with CFD simulations and actual measurements.

Table 5.4: Comparison of CFD prediction of air velocities at the locations of anemometers and actual test measurements of wind velocities, results for Realizable k-ε and the SST k- ω turbulence models are shown.

Sensor Id	Unit	Scenario 1			Scenario 2			Scenario 3			Scenario 4		
		Measurement	k-e	k-w									
ai0	{m/s}	0.670	0.995	0.626	0.012	0.110	0.135	0.021	0.058	0.042	1.046	1.805	0.947
ai1	{m/s}	0.389	0.330	0.346	0.566	0.237	0.268	0.378	0.316	0.359	0.323	0.330	0.350
ai2	{m/s}	0.884	0.207	0.309	0.850	0.252	1.000	0.404	2.370	1.274	0.866	0.213	0.365
ai3	{m/s}	0.114	0.235	0.088	0.195	0.338	0.415	0.129	0.240	0.114	0.078	0.251	0.093
ai4	{m/s}	0.180	0.209	0.255	0.618	0.657	1.207	0.373	0.388	0.273	0.216	0.378	0.193
ai5	{m/s}	0.448	0.275	0.445	0.879	0.684	0.923	0.343	0.200	0.437	0.165	0.143	0.157
ai6	{m/s}	0.623	0.278	0.244	0.033	0.152	0.193	0.042	0.165	0.097	0.737	0.319	0.272
ai7	{m/s}	0.155	0.875	0.701	0.267	1.595	0.818	0.136	0.472	0.397	0.004	0.140	0.508
ai8	{m/s}	0.351	0.374	0.169	0.457	0.664	1.106	0.218	0.473	0.721	0.014	0.176	0.456

Figure 5.10 through 5.13 present comparisons between measured data and CFD simulation results for the four test scenarios at the locations of the anemometers ai0 through ai8. The locations of the “virtual anemometers” (e.g. used to extract the CFD results of air flow velocities) correspond to the actual anemometer placements in Room 301. These locations of the anemometers were selected in the initial phases of the project.

The results of the CFD predictions at the “virtual anemometer locations” were obtained with a “presentation grid”, a customized CFD probe setting which averaged the CFD results of air velocities on a 1 by 1 foot grid. The CFD simulations were conducted with both the SST k- ω (k-w) and the Realizable k-ε (k-e) turbulence models. The results shown in Figures 5.10 through 5.13 suggest that theoretical CFD predictions of air velocities inside Room 301 have a varying degree of consistency with actual measurements, ranging from good to fair data consistency.

Comparison of measured and predicted air velocities in Room 301—SCENARIO 1 (CFR runs E-1 and F-1)

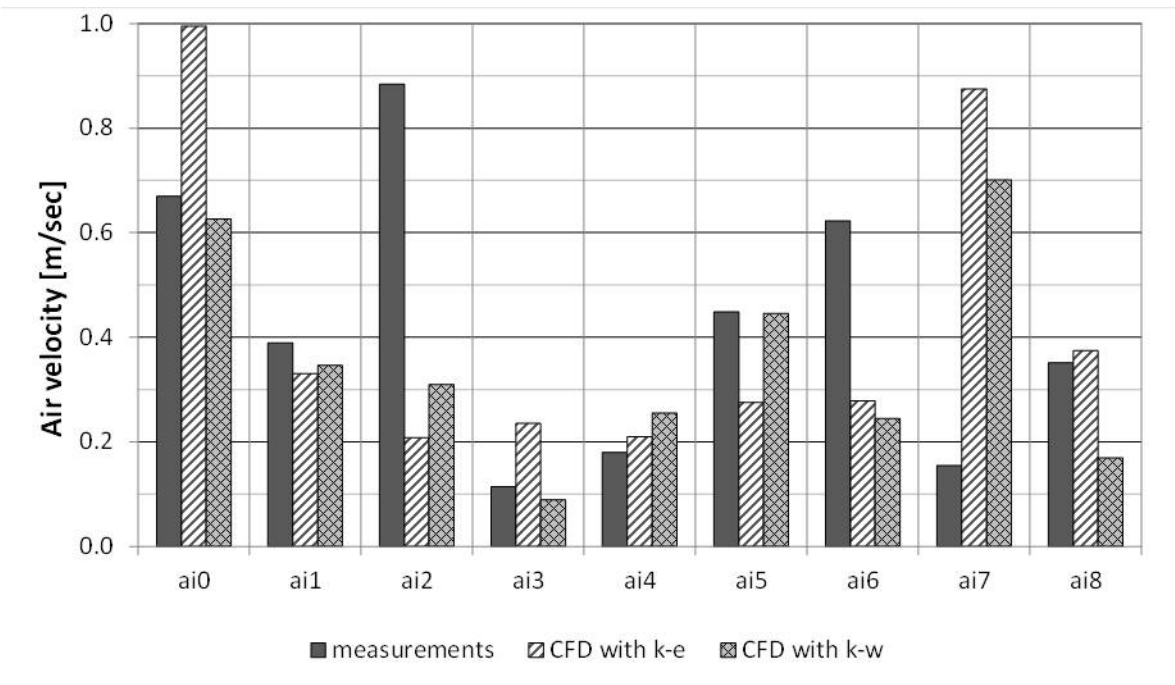
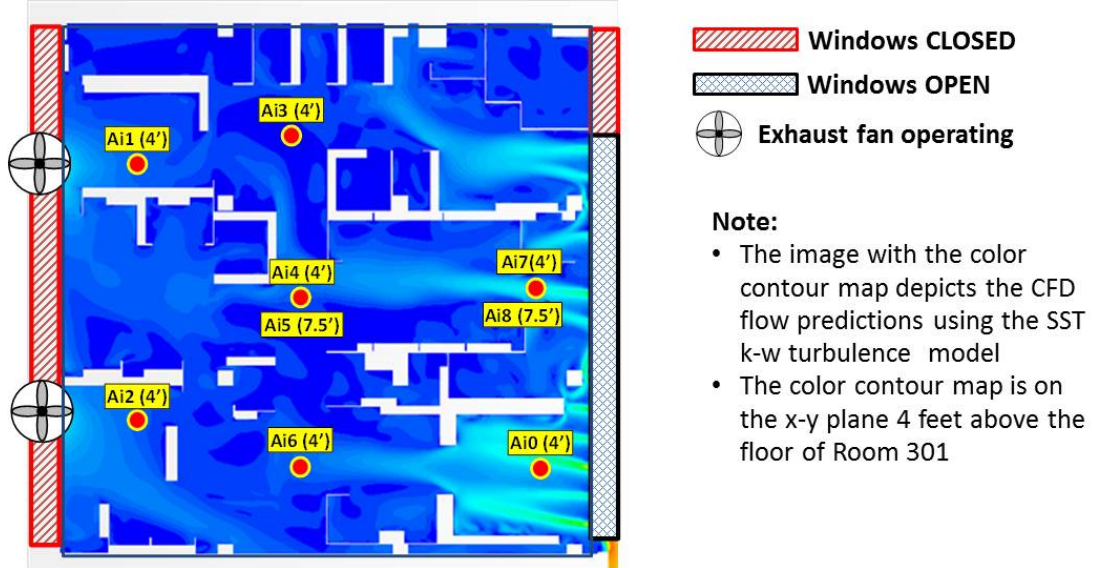


Figure 5.10: Comparison between measured air flow velocities and CFD predictions; **SCENARIO 1**

Comparison of measured and predicted air velocities in Room 301—SCENARIO 2 (CFR runs E-2 and F-2)

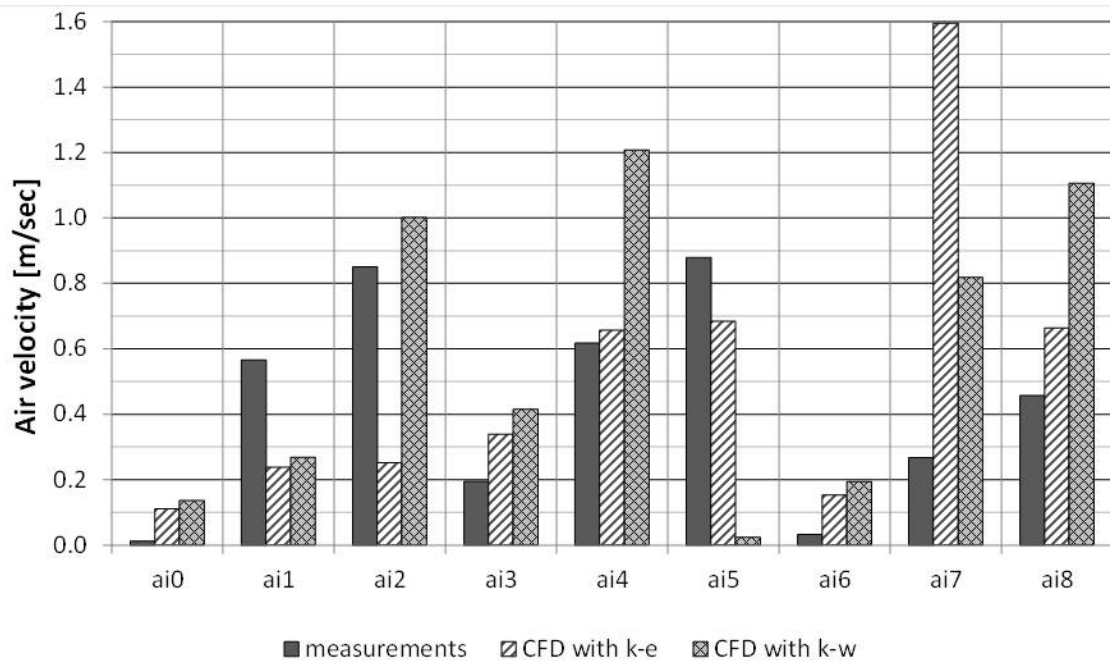
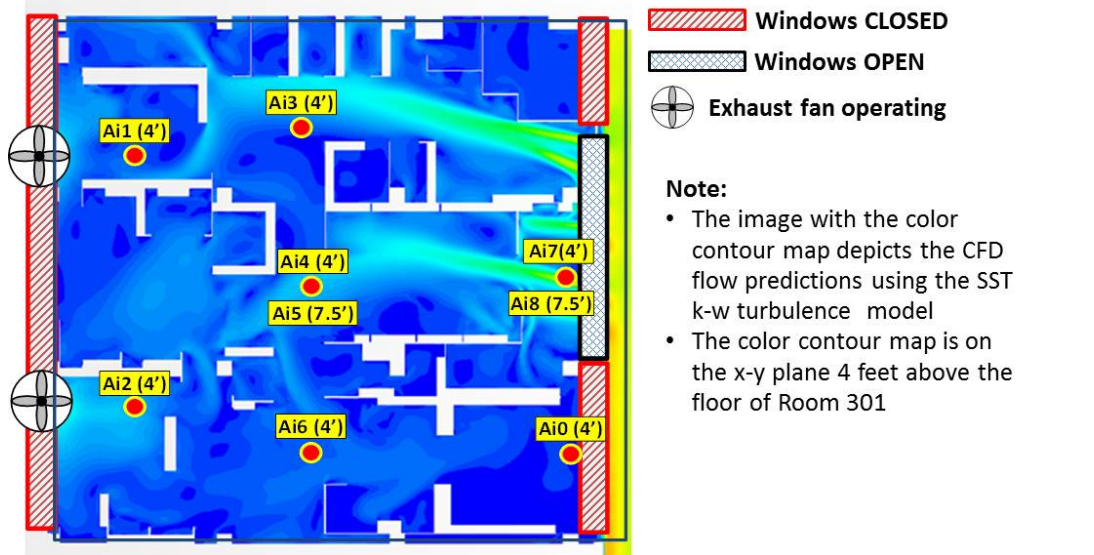


Figure 5.11: Comparison between measured air flow velocities and CFD predictions; **SCENARIO 2**

Comparison of measured and predicted air velocities in Room 301—SCENARIO 3 (CFR runs E-3 and F-3)

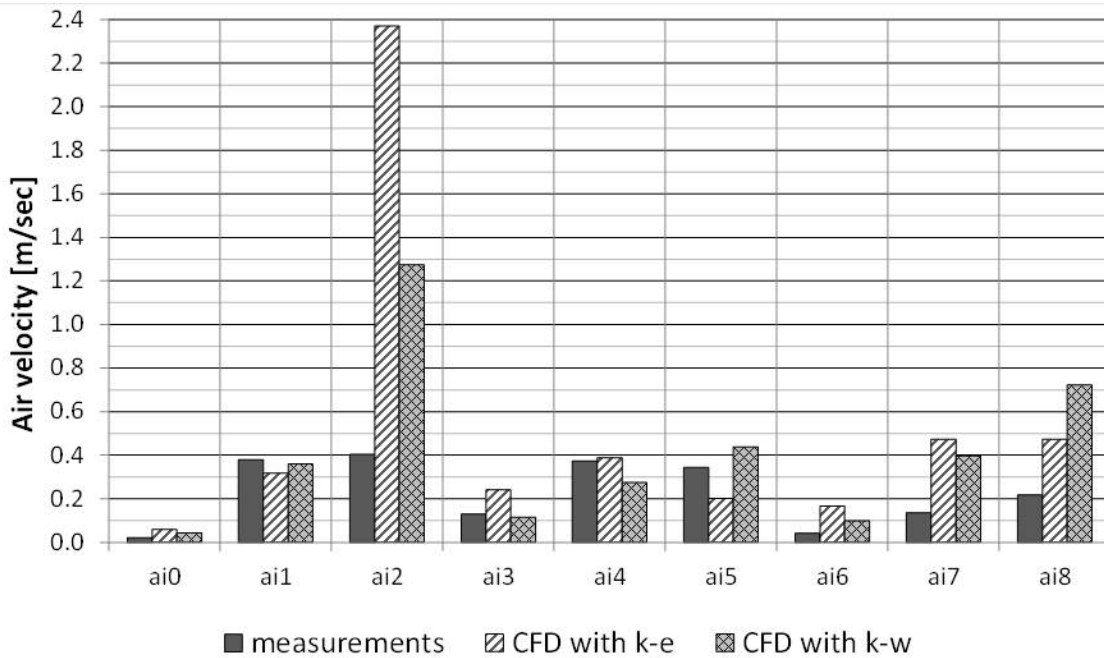
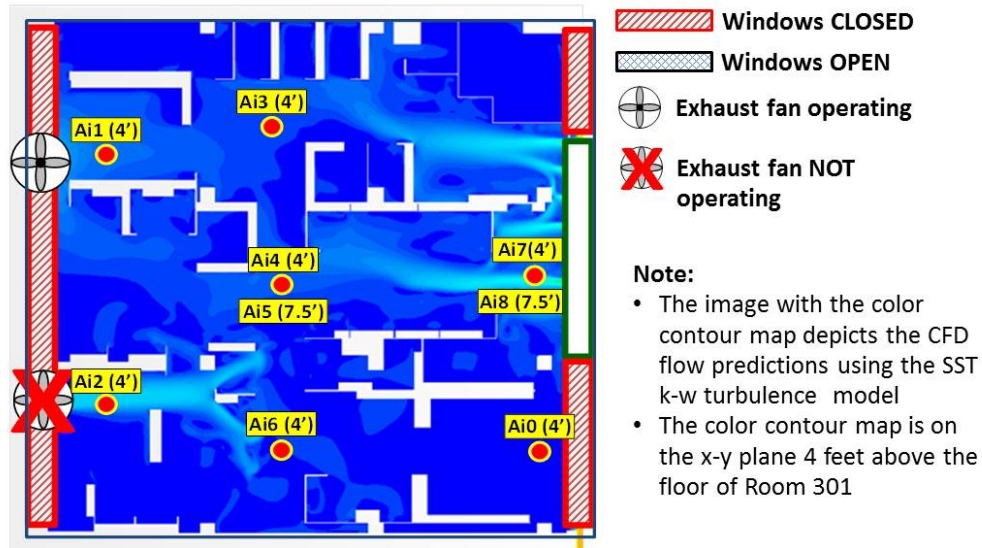


Figure 5.12: Comparison between measured air flow velocities and CFD predictions; **SCENARIO 3**

Comparison of measured and predicted air velocities in Room 301—SCENARIO 4 (CFR runs E-4 and F-4)

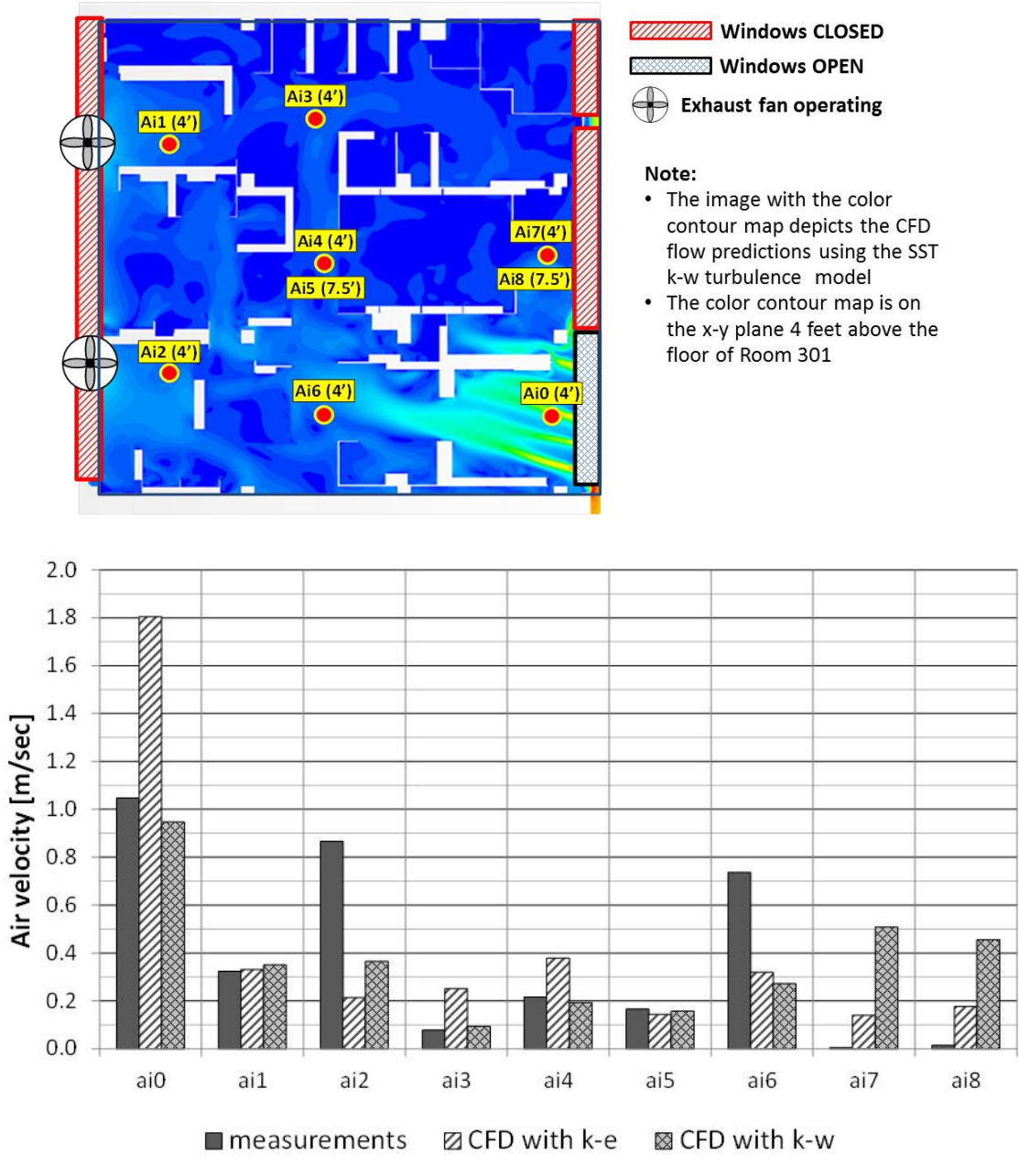


Figure 5.13: Comparison between measured air flow velocities and CFD predictions; **SCENARIO 4**

Figures 5.14 through 5.17 show comparisons of CFD predictions of air velocities for the four test scenarios obtained by the two different turbulence models, the SST k- ω and the Realizable k- ϵ turbulence models.

Scenario 1 (CFD runs E-1 and F-1): The results depicted in Figure 5-14 suggest that the use of the Realizable k- ϵ turbulence model results in higher predicted air velocities than the use of the SST k- ω model in regions of higher airflow, e.g. at anemometer located closer to the louvered windows on the North wall of Room 301, with stations ai0, ai7 and ai8. This deviation of results could be the inherent inaccuracy of the CFD models in predicting the complicated airflow at the wake region right downstream of the open louvered windows. For all other anemometer locations under this test scenario the two turbulence models suggest good to medium data consistency.

Scenario 2 (CFD runs E-2 and F-2): The results depicted in Figure 5-15 suggest that there is low consistency of air velocity predictions between CFD runs using SST k- ω and the Realizable k- ϵ turbulence models for the anemometers ai2, ai4, ai5, ai7 and ai8. All other results under this test scenario compare well between the two turbulence models.

Scenario 3 (CFD runs E-3 and F-3): The results depicted in Figure 5-16 suggest good data consistency of air velocity predictions between CFD runs using SST k- ω and the Realizable k- ϵ turbulence models for all anemometers except ai2. The anemometer ai2 measures the air flow that is entering the Room 301 through the not operating exhaust fan unit B. As mentioned earlier, air enters Room 301 through the partly open exhaust fan casings. Both turbulence models provide air velocity values that are supporting the qualitative flow pattern assessment.

Scenario 4 (CFD runs E-4 and F-4): The results depicted in Figure 5-17 suggest good to medium data consistency of air velocity predictions between CFD runs using SST k- ω and the Realizable k- ϵ turbulence models for all anemometers. Both turbulence models provide air velocity values that are supporting the qualitative flow pattern assessment.

Overall, the SST k- ω turbulence models (case E1-4) suggest a better data consistency to the actual test measurement in comparison of those to the k- ϵ models (case F1-4). The sensors locating in the high air velocity regions suggest a better validation agreement between actual test measurement and simulations. The SST k- ω turbulence model had the highest data consistency in regions of high air velocities.

Comparison of turbulence models SST k- ω and Realizable k- ϵ - SCENARIO 1 (CFR runs E-1 and F-1)

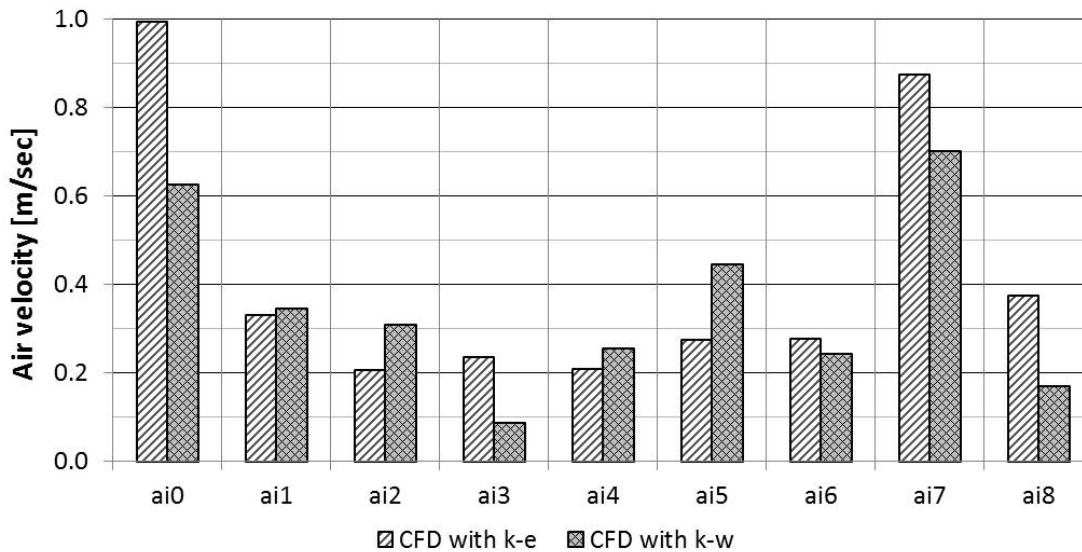
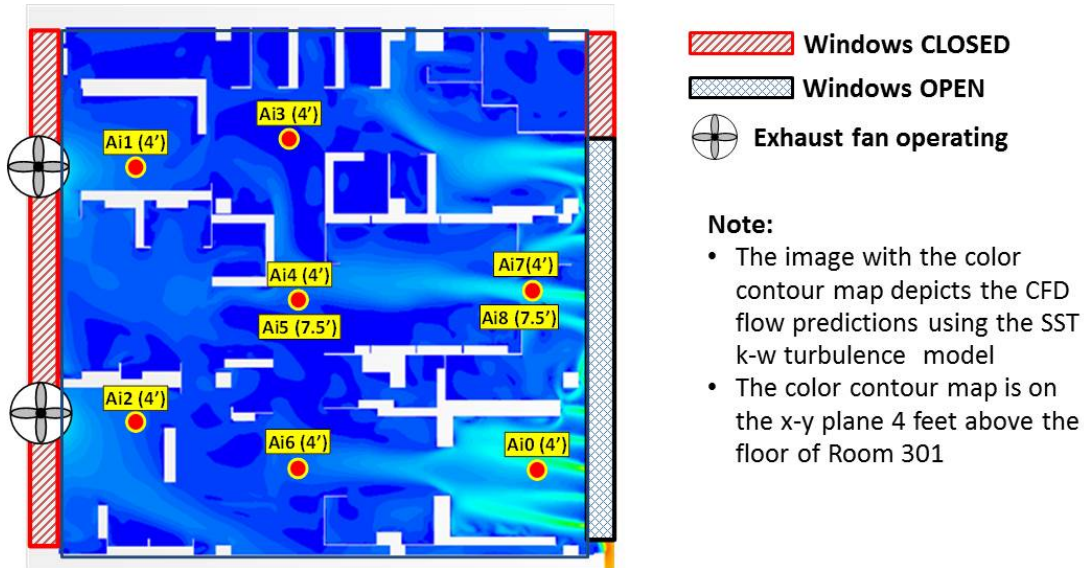


Figure 5.14: Comparison between turbulence models used in the CFD simulations; **SCENARIO 1**

Comparison of turbulence models SST k- ω and Realizable k- ϵ - SCENARIO 2 (CFR runs E-2 and F-2)

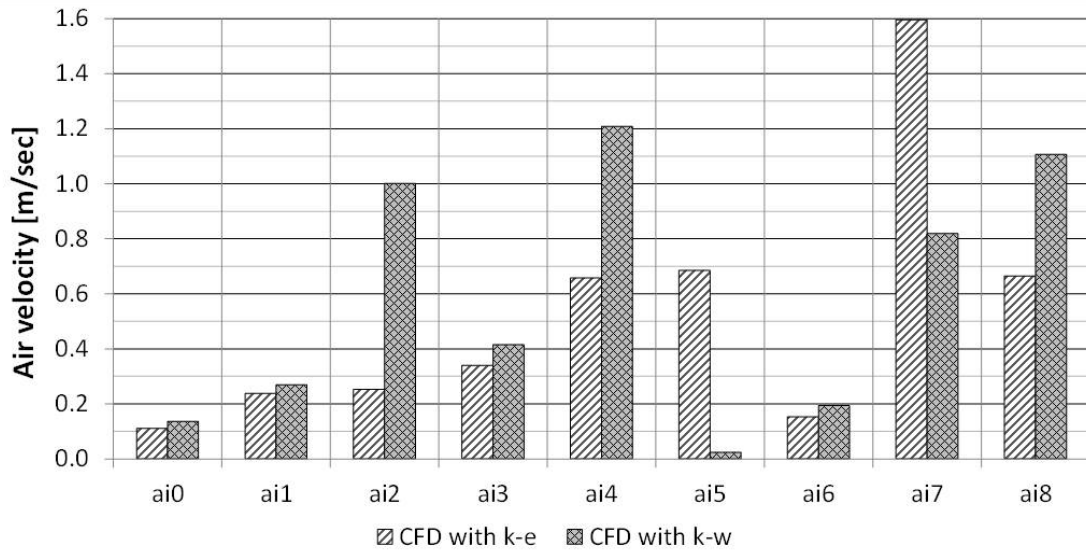
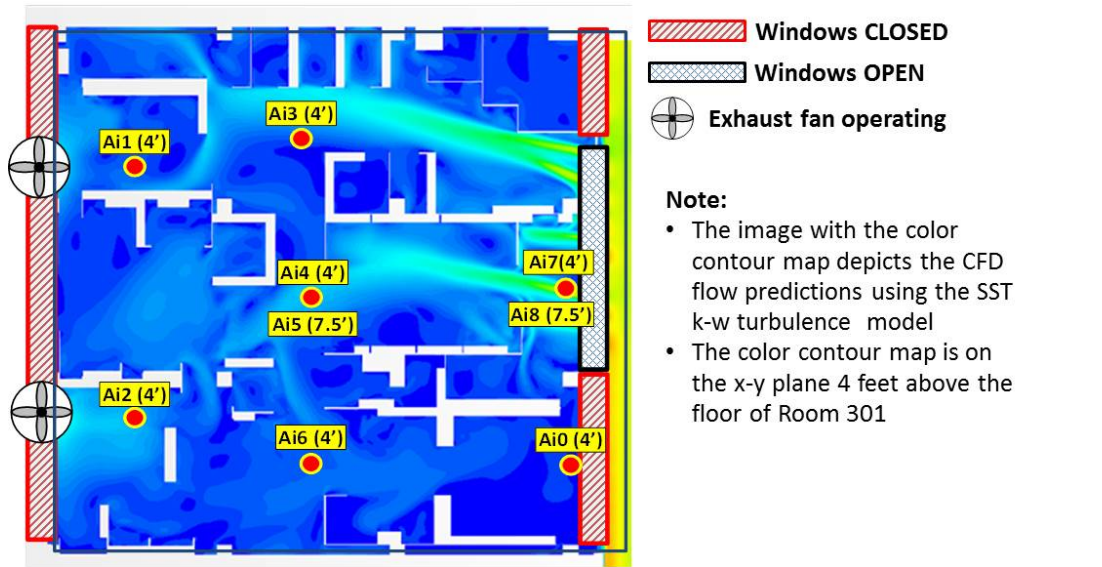


Figure 5.15: Comparison between turbulence models used in the CFD simulations; **SCENARIO 2**

Comparison of turbulence models SST k- ω and Realizable k- ϵ - SCENARIO 3 (CFR runs E-3 and F-3)

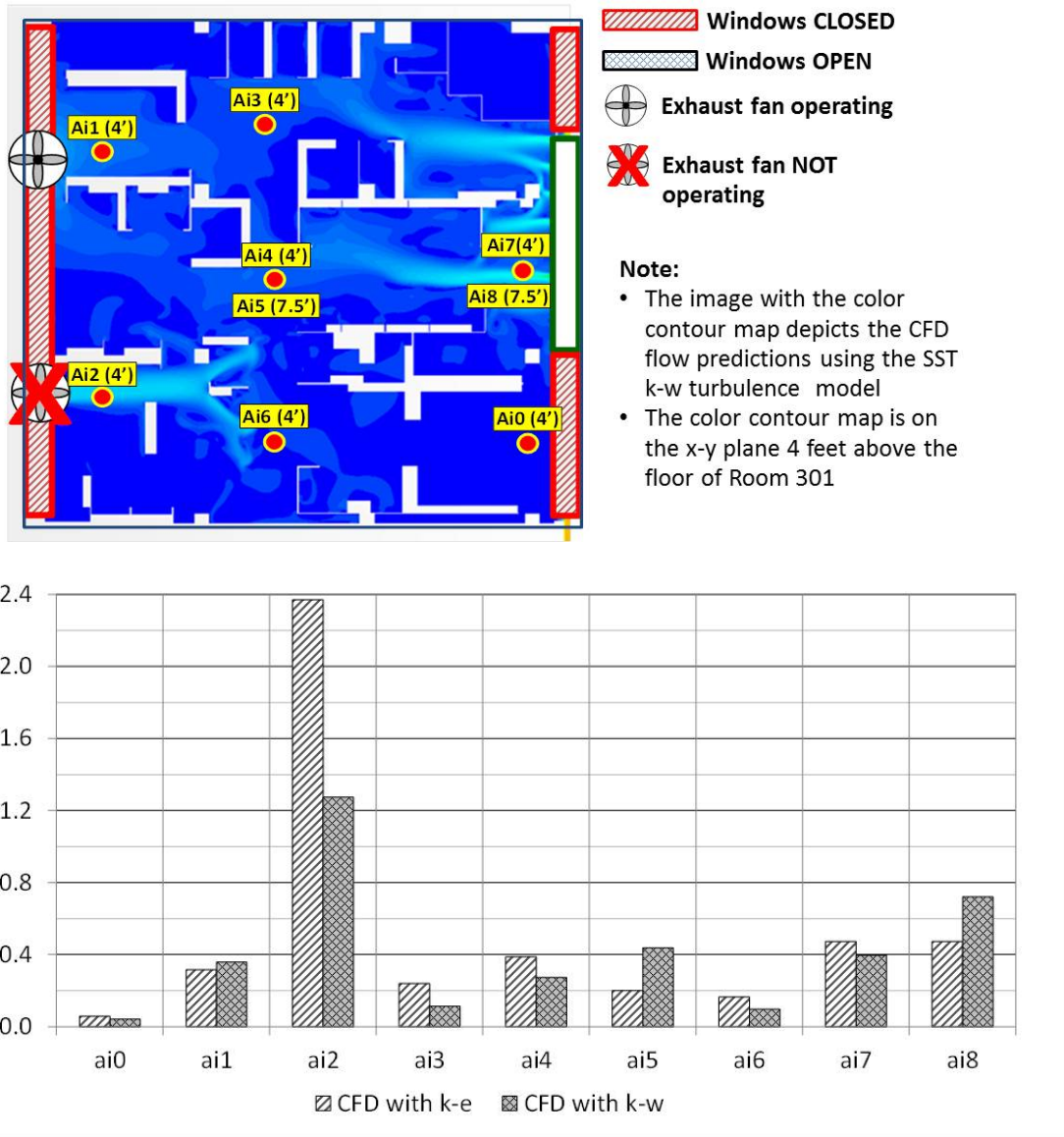


Figure 5.16: Comparison between turbulence models used in the CFD simulations; **SCENARIO 3**

Comparison of turbulence models SST k- ω and Realizable k- ϵ - SCENARIO 4 (CFR runs E-4 and F-4)

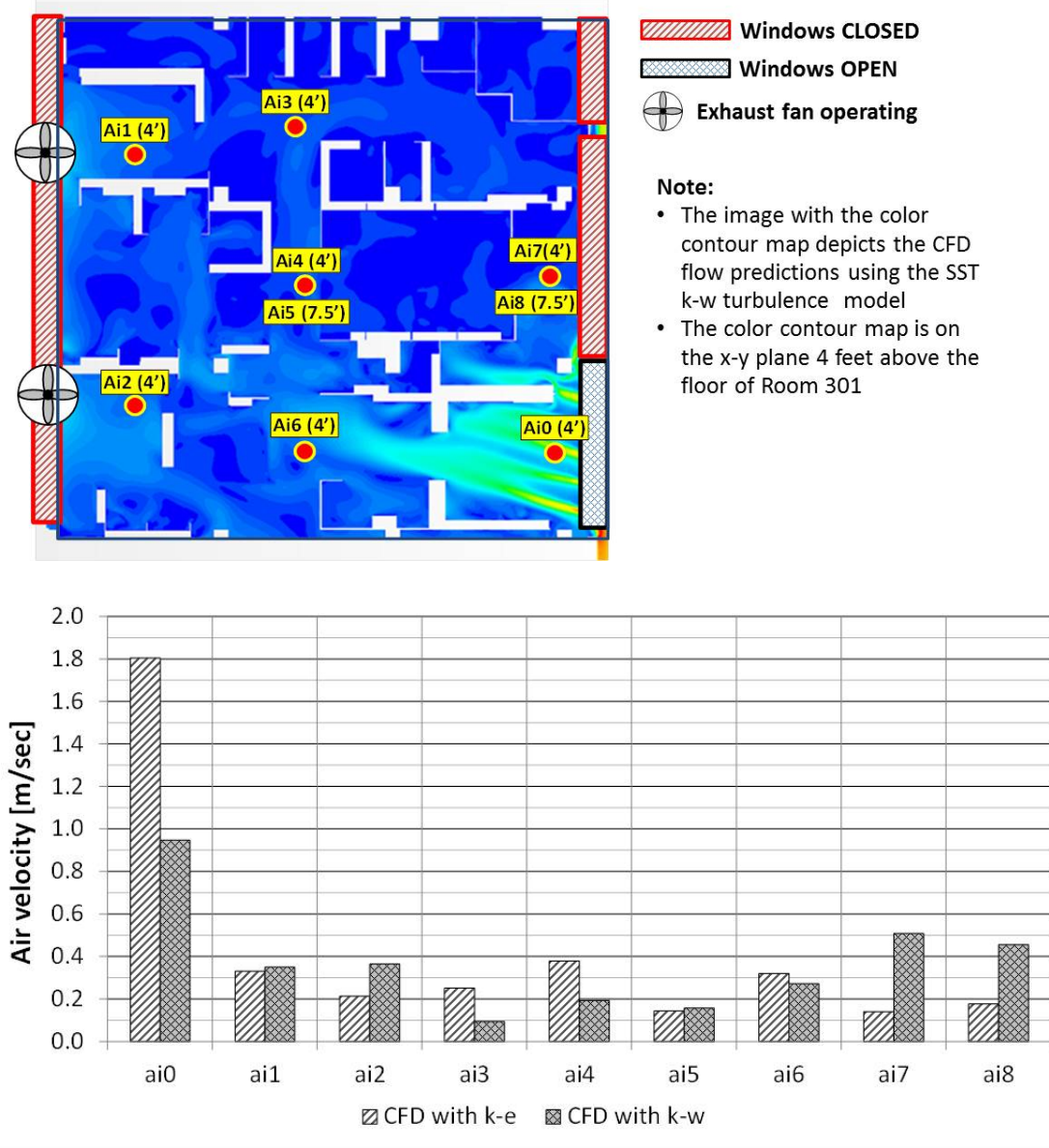


Figure 5.17: Comparison between turbulence models used in the CFD simulations; **SCENARIO 4**

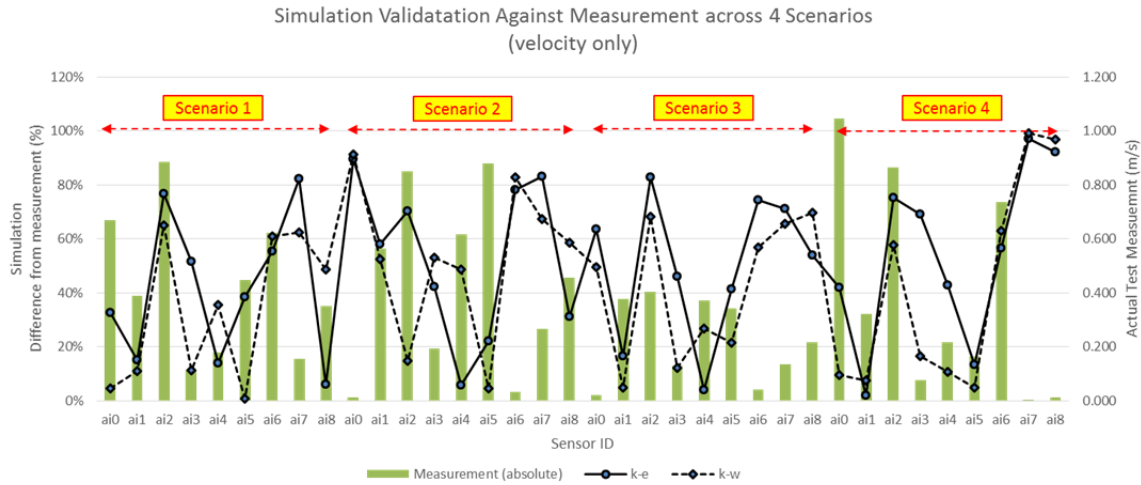


Figure 5.18: Overall Comparison between actual air velocity measurements and CFD runs using two different turbulence models for all 4 scenarios.

Comparing Theoretical CFD Results with Actually Measured Pressure Differentials: CFD estimates were obtained for pressure differentials between sets of relevant points at the perimeter and inside Room 301. Five sets of pressure differential points were investigated in this CFD analysis. The pressure differential measurements only yielded conclusive values for two of the five pressure sets, ai11 and ai12. Table 5.5 shows the pressure differentials obtained from CFD simulations and actual field data.

Table 5.5: Comparison of CFD predictions of pressure differentials obtained by actual test measurements and CFD simulations using the Realizable k-ε and the SST k-ω turbulence models

Sensor Id	Unit	Scenario 1			Scenario 2			Scenario 3			Scenario 4		
		Measurement	k-ε	k-ω	Measurement	k-ε	k-ω	Measurement	k-ε	k-ω	Measurement	k-ε	k-ω
ai9	{Pa}	2.070	n/a	n/a	2.979	n/a	n/a	2.147	n/a	n/a	3.218	n/a	n/a
ai10	{Pa}	3.188	n/a	n/a	3.181	n/a	n/a	3.388	n/a	n/a	2.947	n/a	n/a
ai11	{Pa}	2.558	1.447	1.021	7.311	0.885	1.494	2.538	1.393	2.879	3.756	1.224	1.333
ai12	{Pa}	0.249	-0.306	-0.233	0.102	-0.235	-0.599	0.214	-0.047	0.024	0.187	-0.184	-0.395
ai13	{Pa}	n/a	n/a	n/a	n/a	n/a	n/a	n/a	n/a	n/a	n/a	n/a	n/a

Figures 5.19 through 5.22 show comparisons between CFD results and actual measurements for pressure differentials in Room 301. The CFD results were obtained with two different turbulence models, the SST k-ω and the Realizable k-ε turbulence models. The CFD simulations in Figures 5.19 through 5.22 refer to CFD runs numbers E-1 and F-1 through E-4 and F-4. As a general observation, the

pressure differences across the windward windows (e.g. the ai11 pressure point set) showed reasonable consistency between CFD simulations and measurements. The pressure differences between the points of set ai12 were always very small, supporting the assumption that very small pressure differentials are present inside North and South side of Room 301. Overall, there was very little variation between the differential pressure values obtained in the CFD simulation using the two different turbulence models.

Comparison of measured and predicted pressure differences –SCENARIO 1 (CFR runs E-1 and F-1)

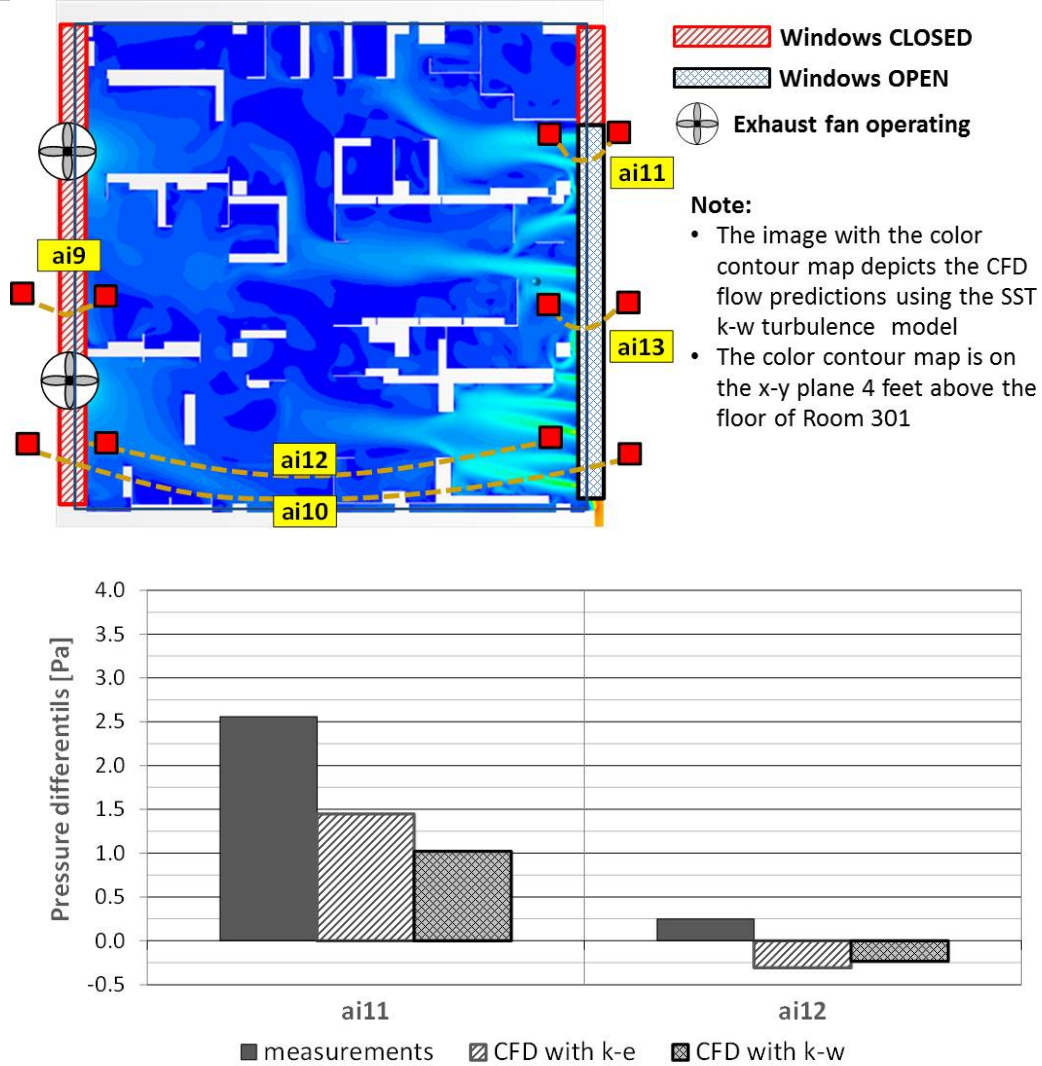


Figure 5.19: Comparison between measured pressure differences and CFD predictions; **SCENARIO 1**

Comparison of measured and predicted pressure differences –SCENARIO 2 (CFR runs E-2 and F-2)

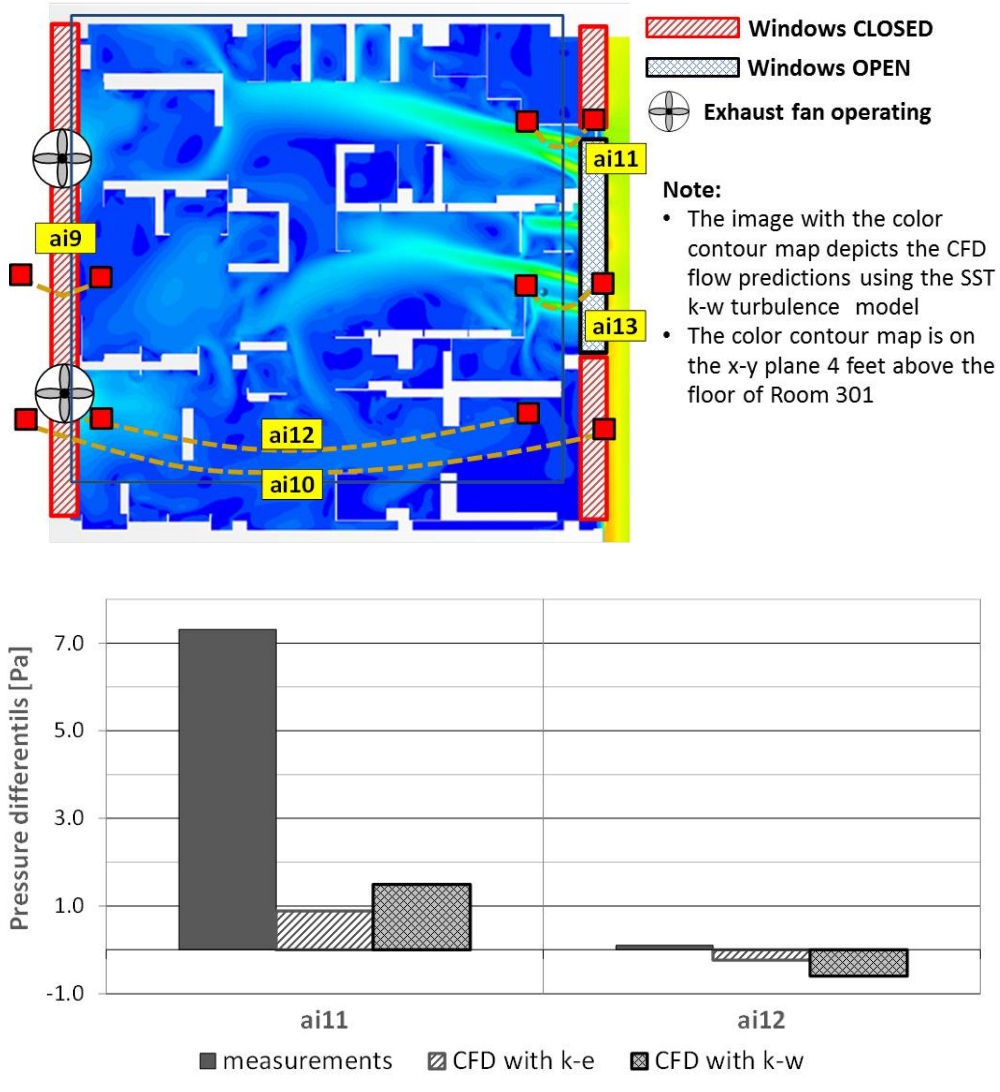


Figure 5.19: Comparison between measured pressure differences and CFD predictions; **SCENARIO 2**

Comparison of measured and predicted pressure differences –SCENARIO 3 (CFR runs E-3 and F-3)

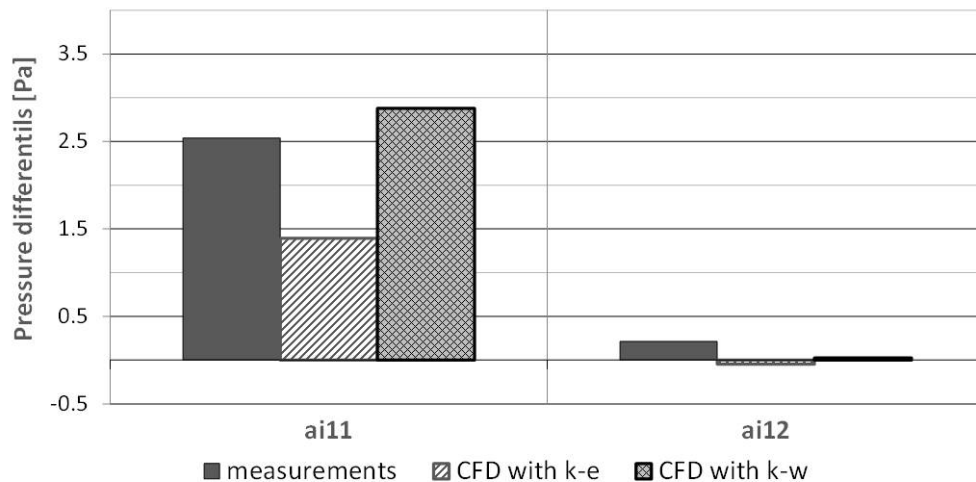
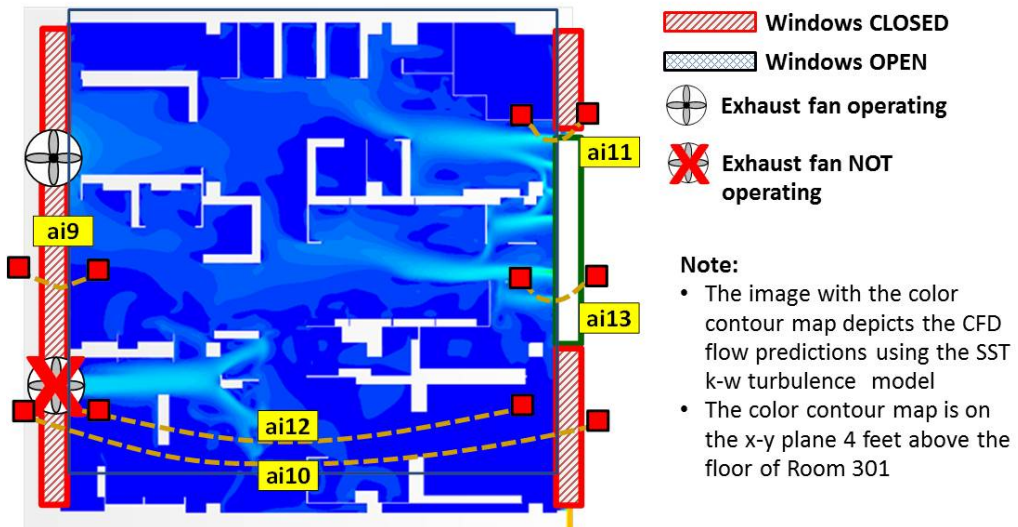


Figure 5.19: Comparison between measured pressure differences and CFD predictions; **SCENARIO 3**

Comparison of measured and predicted pressure differences –SCENARIO 4 (CFR runs E-4 and F-4)

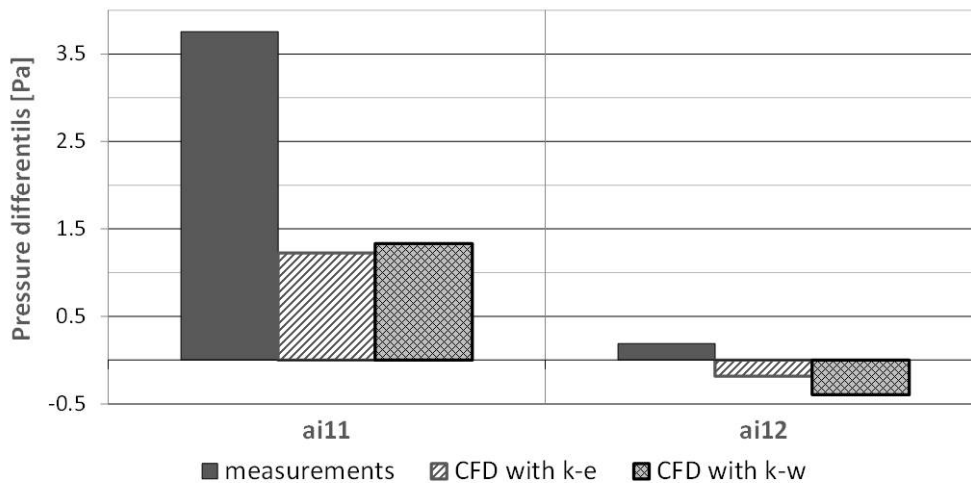
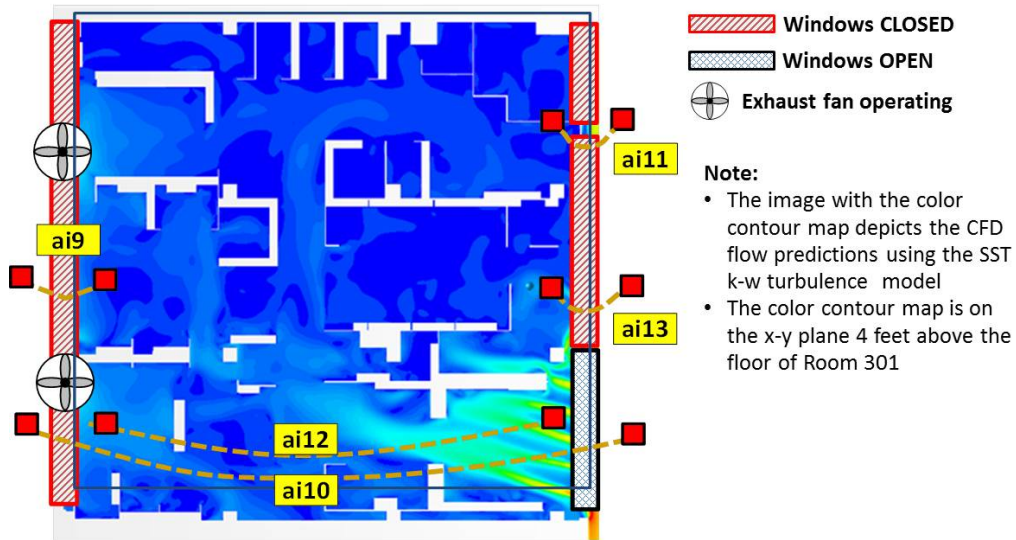


Figure 5.19: Comparison between measured pressure differences and CFD predictions; **SCENARIO 4**

5.4 Discussion and General Observation

The results of the CFD study and validation of CFD results through actual measurements in Room 301 suggest the following general conclusions:

- The presence of large exhaust fans in Room 301 provided the CFD research team with a unique opportunity to investigate complicated internal air movement under inflow and outflow conditions that could be controlled by four large propeller type exhaust fans. The development of internal CFD workflow methodologies combined with the ability to validate theoretical flow predictions with actual measurement in Room 301 presented the CFD team with a valuable research opportunity, since no other comparable full scale test site was available.
- The degree of data validation consistency between the CFD simulation results and actual measurements was generally limited and ranged from good to low. There were numerous likely causes that could have contributed to the deviation of theoretical results and actually measured observation of the flow patterns in Room 301. Causes, which the CFD team identified included complicated internal geometry, varying outside wind conditions, fluctuations in the exhaust volume and limited sensitivity of anemometer and differential pressure sensor, especially at low air movement.
- The geometry of internal structures of Room 301 and boundary conditions were complex and the resulting effects of inlet and outlet conditions as well as of numerous structural elements, cubicle walls and furniture on the internal flow patterns was perhaps too complicated for the type of benchmarking and parametric studies of the internal workflow development.
- The internal flow patterns showed significant interactions of flow separation, eddies and areas of small or no air movement in flow constrained areas. It is assumed that the detected highly unsteady velocity and differential pressure readings attest to the significant unsteady and random flow occurrence in the room.
- The CFD study suggested that the level of convergence of solution can be detected by relevant physical property parameter residuals monitors, including air velocity and pressures, and that residuals do not have to be the primary test of convergence. The CFD work used virtual monitors and probes to detect and quantify relevant parameters at locations of interest. The level and quality of convergence was then evaluated by evaluating the time step dependent patterns over the iterations. In doing so, while residuals could have depicted variation and sectional non-convergence, pertinent physical parameters showed good asymptotic convergence performance.
- The choice of the turbulence model is an important determinant of the resulting CFD simulation and the description of the internal flow field. The CFD team had applied two well-known turbulence models, the SST k- ω and the Realizable k- ϵ turbulence models, in the CFD analysis

for this report. Both turbulence models have advantages and disadvantages in describing internal air flow phenomena and related physical properties. Depending on the complexity of the geometry of the internal space and keeping convergence and computational resources in mind, both turbulence models have case specific advantages and disadvantages. The selection of what turbulence model to use in internal CFD investigations should be done by the CFD team on a case-by-case manner.

- In general, velocity was deemed to be a more reliable indicator of flow occurrences and overall level of validation was more consistent when using air velocities than using differential pressures. This observation follows recommendations found in the literature. Therefore, in order to measure actual flow performance and validate theoretical CFD results, air velocity should be the preferred validation parameter over differential pressure measurements. In general, the pressure differences in naturally ventilated and large spaces, as opposed to constricted flow through ducts in general HVAC applications, are typically very small. Measuring differential pressure in the range of 1 to 5 Pa, as was detected in the internal flow conditions of this study, is challenging and prone to errors and measurement side effects of the sensor and pressure tubing. Velocity measurements, on the other hand, are less prone to side effects and measurement uncertainties.
- The procedure used of creating the 3D geometry model with third party CAD software and importing the geometry model into the CFD software was effective. The CAD geometry modeling with the CAD software Rhino3D, importing it into the CFD software application and subsequently carrying out the meshing process was effective and resulted in high quality meshes, which required little surface repair.
- The boundary conditions of Room 301 in regard to inflow and out flow conditions exhibited more uncertainties than was initially anticipated. For example, the windows facing the South lanai could not be sealed as thoroughly as was assumed. Leakage consequently resulted in some quantity of air intrusion from the South. The degree to which the air intrusion affected the internal air flow conditions could not be determined.
- The fan curves of the propeller type exhaust fans were not available from the vendor (e.g. the CFD team had to use locally available inexpensive residential whole house fan with a simple plane propellers. The CFD team assumed a generic propeller type fan curve as the input variable for the CFD outlet condition. The CFD team considered that this approximation was reasonably accurate.
- The type of computational domain was a “semi-coupled” domain. As was identified in the literature (refer to the literature review of internal CFD, project deliverable No. 6) a preferred way to model the inlet of the internal space was to include a portion of the external domain, without including a significant extent of the exterior building and adjacent structure geometry. By including a portion of the external building geometry in the domain a “stagnation inlet”

condition could be established instead of using a constant mass flow inlet conditions used in the decoupled domain case. The “stagnation” approach allowed inclusion of momentum transfer in addition to pressure gradient as the inlet conditions, thereby increasing the reliability and robustness of the air inlet condition for the internal CFD analysis of Room 301.

- Following recommendations in the literature (as delineated in the literature review of internal CFD carried out earlier phase in the project; project deliverable No. 6) it was concluded that this approach of defining the inlet boundary conditions represents an effective and reliable internal CFD workflow procedure.
- The density and dynamic viscosity of air under typical Hawaii temperature and humidity conditions is different from standard air conditions used as default setting in the CFD software. The research team benchmarked Hawaii specific density and viscosity against standard conditions as a part of the CFD work of this study. Typical air density for Hawaii (e.g. at average Hawaii temperatures and humidities) and the standard air condition used as CFD default values vary about 3%. This variation is considered significant enough to warrant specific Hawaii climate values for air in the CFD calculations.
- The size of the mesh was found to be significant if all small detail flow obstructions were modeled with high resolutions. The CFD team had created large meshes of up to 30 million cells. While the solution resolution was good the required computational resources were challenging. Therefore the CFD team chose medium size meshes as preferable and according to benchmark simulations conducted for this CFD project, medium size meshes are not necessarily inferior to very large meshes.
- The post processing procedure of using color contour maps was found effective and provided the CFD team with the ability to observe the entire flow field and to obtain qualitative estimates of the overall air flow pattern.
- Additional post processing procedure included extracting specific values of air velocities and differential pressures at locations of interest within the computational domain. The CFD team used customized probes in the computational domain made of 1x1 feet matrixes which provided the team with the ability to determine average velocity and pressure values.
- The CFD software used of the investigation performed well and the developed internal CFD workflow uses a wide range of standard and customized features of the CFD software. This advantage will be used to advantage of the CFD research team for subsequent investigations.
- The experiences gained by the CFD research team during the development of the internal CFD workflow provided the team with a range of tested measures to carry out internal CFD simulations in subsequent phases of this research program.
- The CFD team concluded that the complex air flow conditions in Room 301 were not ideal to develop generic internal CFD workflow procedures. The CFD team, however, opted to utilize Room 301 as a test case since the exhaust fans were already installed Room 301 and provided

the team with a unique opportunity to establish actual flow conditions in an internal space and perform measurements. The CFD research team understands that the combination of CFD simulations in complex internal room geometry, highly unsteady internal air flow conditions and unavoidable instrumentation and data acquisition limitation, could bring about significant deviations between theoretical and actually measured flow patterns. These recognized limitations and resulting small data consistency between theoretical and actual test conditions, while sobering at times, were also unavoidable side effects of complex CFD analysis and the ability of the CFD team to recognize and accept unavoidable data deviations is part of good CFD working procedure.

SECTION 6 - PREFERRED CFD SETTINGS FOR INTERNAL CFD SIMULATIONS

This section summarizes the main conclusions of this study as they relate to preferred settings of an ERDL workflow process for internal CFD applications. With the development of preferred settings and the generic CFD workflow process for subsequent simulations of internal air flow occurrences, the ERDL CFD research team has successfully completed the main objective of this project phase. Much of the detail workflow procedures are documented in notes kept by the CFD team and only main points are presented hereafter.

6.1 Model Geometry and Extent of Computational Domain

- Creation of geometry and 3D-CAD applications: The 3D geometry models of the computational domain should be created externally of the CFD program since the building and internal space geometries are typically too complicated to be created with the CFD internal 3D-modelling software application, which has limited functionality. The CFD team will create 3D-CAD models in Rhino3d modeling software which is widely used by engineering and architecture practitioners and students. Rhino3d offers a wide range of CAD file formats for exporting the model into other software applications, including stereo lithography file format (stl). The CFD team has been successfully using importing “stl” files into the CFD software STAR-CCM+.
- The detailed level of the CAD model: The detail level of the CAD model should such that the geometries created emphasize large components affect the airflow. The relevant internal geometries should include main internal structural components as well as large outfitting, such as cubicle walls and other internal walls or room dividers, in order to limit the complexity of the model. Relevant external air flow obstructions and building components that can affect the external air flow should be limited to the immediate vicinity of the building. The objective of modelling external space for internal CFD investigation should to provide a procedure to make the inlet opening of the internal space a part pf the domain, (See “semi-coupled” domain approach in the subsequent paragraph). Some Foliage close to inlet openings of the building or internal space to be modeled might impact on the approaching wind flow, changing turbulence characteristic, wind direction and velocity of the airflow before entering into the internal space. Foliage, however, increases the complexity of the model and therefore foliage should not be considered as part of the computational domain.
- Extent of computational domain: The CFD research team has used both coupled and decoupled domain approaches and has built CAD models accordingly. Using decoupled domains in internal CFD investigations has the advantage of limiting the size of the domain, since the extent of the

computational domain on decoupled domains is the size of the interior space. A challenge in using decoupled domains is to correctly define the inlet and outlet boundary conditions. When using coupled domains the geometry of computational domain includes both internal and external air volumes and structures, which means that the size of the domain and the required computational resources has to be increased. The advantage of coupled domains is that the air inlet and outlets of the internal space are part of the domain. As a consequence the air flow properties of openings of the internal space can be modelled and have not to be arbitrarily assigned in terms of mass flow or pressures, for inlet and outlet boundary, respectively.

By using a coupled CFD domains approach the CFD team needs to make a good selection of the extent of the exterior air space to be included in the domain. Ideally, the exterior of the entire building in which the internal space is located should be included as well as adjacent buildings and other flow obstructions. If only a section of the immediate vicinity of the building is included in the model, such as was used in the CFD analysis of Room 301, one can speak about a “semi-coupled” domain. The selection of the extent of the exterior space to be included in the coupled domain should be done by the CFD team in a case-by-case manner.

6.2 Meshing Procedure

- Surface wrapping mesher: The “Surface wrapping mesher function” of STAR-CCM+ is a robust and effective meshing software tool that allows fixing sophisticated CAD geometry models by wrapping the exterior CAD surface with a new surface mesh of higher quality than the CAD model, while maintaining its original geometric features. The “Surface wrapping mesher” function should be used in the meshing procedure of the internal CFD simulation workflow.
- Trimmer: The Star-CCM+ “Trimmer” function is a reliable and robust mesher tool that provides good meshing quality. The Trimmer function creates cube-type volume cells that have a good alignment with building’s surfaces and therefore the resulting mesh is suitable for architecture-related geometric models. The “Trimmer” function should be used in the meshing procedure of the internal CFD simulation workflow.
- Memory requirements for meshing with STAR-CCM+: 3D-CAD modeling and meshing are among of the most time-consuming processes of the CFD simulation workflow. Having sufficient memory is important to set up optimal meshing parameters to accommodate both meshing quality and computational resource availability. According to Cd-Adapco (the vendor of the CFD software STAR-CCM+ that was used for the CFD analysis work of this report) the memory requirement is 0.5GB per million surface triangles for surface meshing, 0.5 GB per million trimmed cells. The CFD

team had benchmarked different mesh sizes ranging from small to very large (~ 30 million cell) meshes.

6.3 Turbulence Models

- Recommendation for the use of Realizable k- ϵ and SST k- ω turbulence models: The k- ϵ turbulence model is a two-equation model in which transport equations are solved for the turbulent kinetic energy (k) and its dissipation rate (ϵ). Realizable two layer k- ϵ , an improved version of the standard k- ϵ turbulence model was used in this CFD work of this study. The CFD team found that the SST k- ω model provided superior results in terms of flow pattern resolution than the k- ϵ model. The SST k- ω model appeared to be more suited in handling the adverse pressure gradients at boundary layers. Such conditions are often found in architecture-related internal air flow obstructions, which typically have edges serving as separation points of the airflow. The SST k- ω turbulence model provided better resolution in the flow field with small velocities. It was found that the Realizable k- ϵ typically showed faster convergence for the CFD solutions than the SST k- ω model, which the latter showed some difficulties to achieve convergence in some cases. The decision whether to select the Realizable k- ϵ or SST k- ω turbulence model should be done on a case-by-case basis.

6.4 Boundary conditions

- Inlet boundary: The coupled domain modeling approach is preferred, since the effects of the approaching wind conditions (e.g. wind direction and speed) are considered in determining the inlet conditions of the internal space. The applicable inlet boundary condition for the coupled domain is the inlet wind condition upstream of the internal space. This inlet boundary condition should use vertical logarithmic wind profile and reference wind velocity from a weather station record.
- Defining the performance of mechanical exhaust fans: In case of using mechanical fans for the internal CFD study, a performance prediction (e.g. fan curve) from fan manufacturers should be obtained for use in the CFD program. In case fan performance curves are not available, other information such as maximum volume flow and actual test measurement at the site can be helpful to estimate the performance curve.
- The CFD wall treatment: Wall treatment should be used in the internal CFD for accurately solving the near-wall flow regions. The wall treatment needs to include the number and sizes of prism layers, while considering equivalent grain roughness height, which can be converted from aerodynamic roughness length of the test area.

6.5 Solver settings

- Type of flow regime to be modeled: Segregated flow models solve the flow equations in a segregated manner in which each velocity and pressure component is initially solved independently and later corrected using a predictor-corrector approach. This approach is generally applicable to CFD investigation of internal space. Under constant-density flows, where wind speed is small and air flow is considered incompressible, segregated flow approach is recommended for both internal and external CFD simulations. In terms of computation resources for solver, segregated flow model requires only 0.5 GB of memory per 1 million cells while coupled explicit flow model and coupled implicit flow model require between 1 GB and 2 GB per million cells (according to Cd-Adapco Star-CCM+ Technical Manual).
- Unsteady versus steady flow regime: Steady-state CFD simulation has been used in this study to solve the inherent unsteady flow conditions of the indoor spaces. As the main interest of our investigations was determining mean velocity conditions in internal spaces, which makes the time-related air flow description inside internal spaces a lesser importance. Steady-state models require significantly less computational resources than simulating unsteady air flow conditions. For the simulation of air flow in internal spaces steady state flow solutions still provide sufficiently accurate answers while avoiding very much higher demands on computational resources.

REFERENCES

Previous research reports and notes elaborated under this research program, and literature cited in these previous reports, have been used in this report without giving reference.

ACRONYMS

3D	Three Dimensional
3D-Cad	Three Dimensional Computer Aided Design
ABL	Atmospheric Boundary Layer
CFD	Computational Fluid Dynamics
ERDL	Environmental Research and Design Laboratory
HNEI	Hawaii Natural Energy Institute
HVAC	Heating, Ventilating, and Air Conditioning
ID	Identification Index of Descriptor
LES	Large Eddy Simulation
Room 301	Room 301 of the Sinclair Library, University of Hawaii Manoa campus
V	Velocity
WS	Weather Station

Unit:

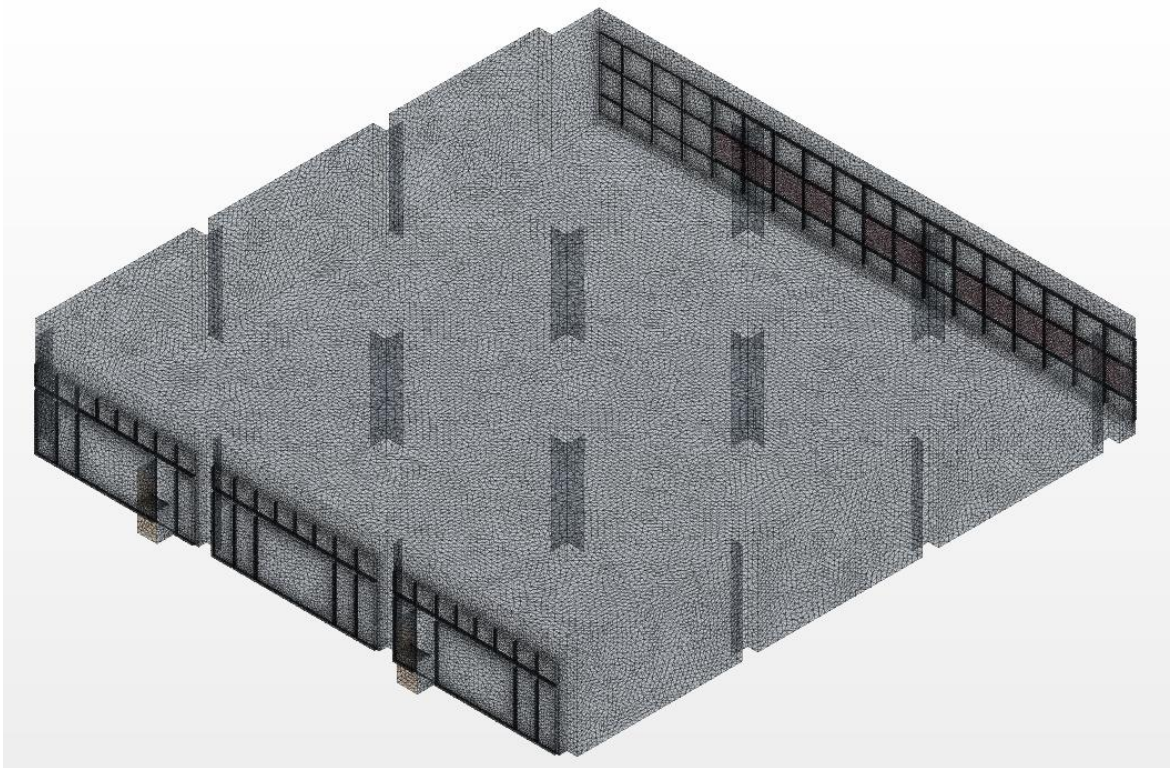
DC	Direct Current
ft	Foot or feet
hz	Hertz
m	Meter
m/s	Meter per second
mph	Miles per Hour
Pa	Pascal
sqft	Square Feet

APPENDIX A

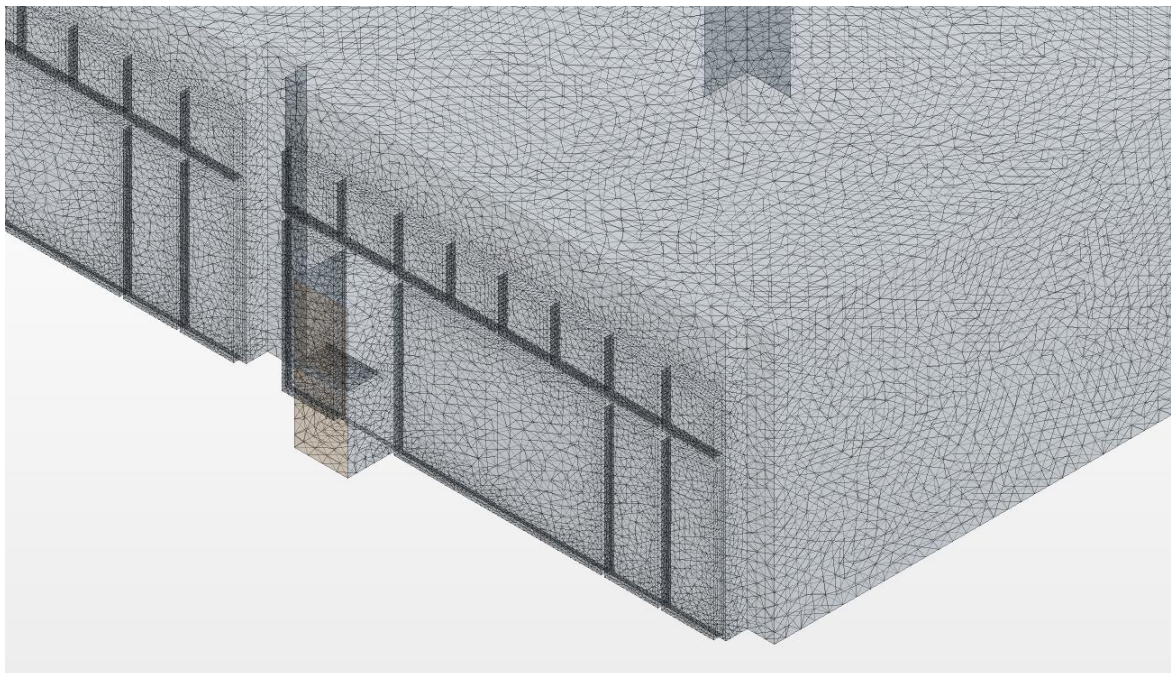
ILLUSTRATION OF MESHING PERTAINING TO CAD MODELING APPROACHES

This appendix showed the visualizations of three different CAD modeling approaches ranging from the most simplicity to the highest complexity: Decoupled domain, Coupled domain without furniture and Couple domain with furniture as well as their associated grid quality assessment.

Decoupled Domain Approach

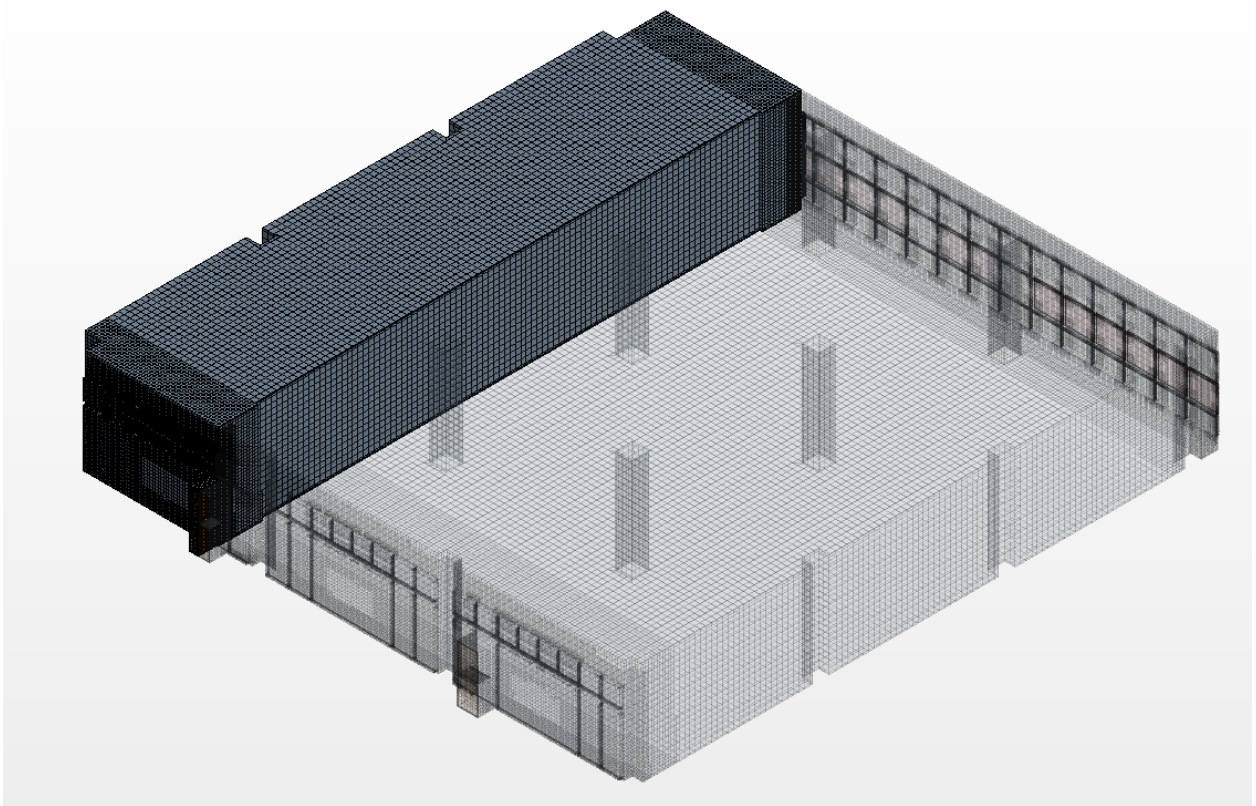


Visualization of the surface meshing (overall view)



Visualization of the surface meshing (detailed view)

Decoupled Domain Approach



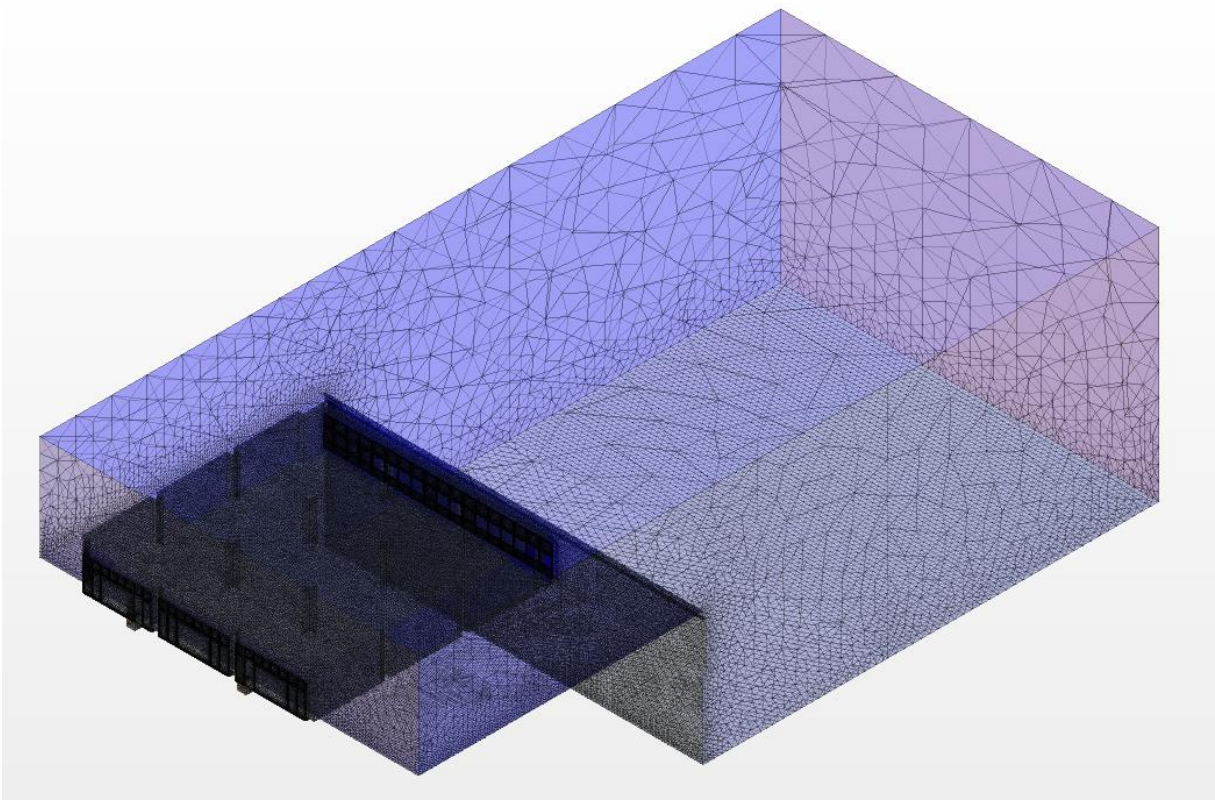
Visualization of the volume cells and partial computational domain resulted from the vertical virtual section plane

Volume Change		Number of cells	Percentage
	$\leq 1e-6$	0	0.000%
1e-6	1e-5	0	0.000%
1e-5	1e-4	0	0.000%
1e-4	1e-3	5	0.000%
1e-3	1e-2	786	0.032%
1e-2	1e-1	16893	0.681%
1e-1	1.0	2463833	99.287%
Total number of volume cells		2481517	100%

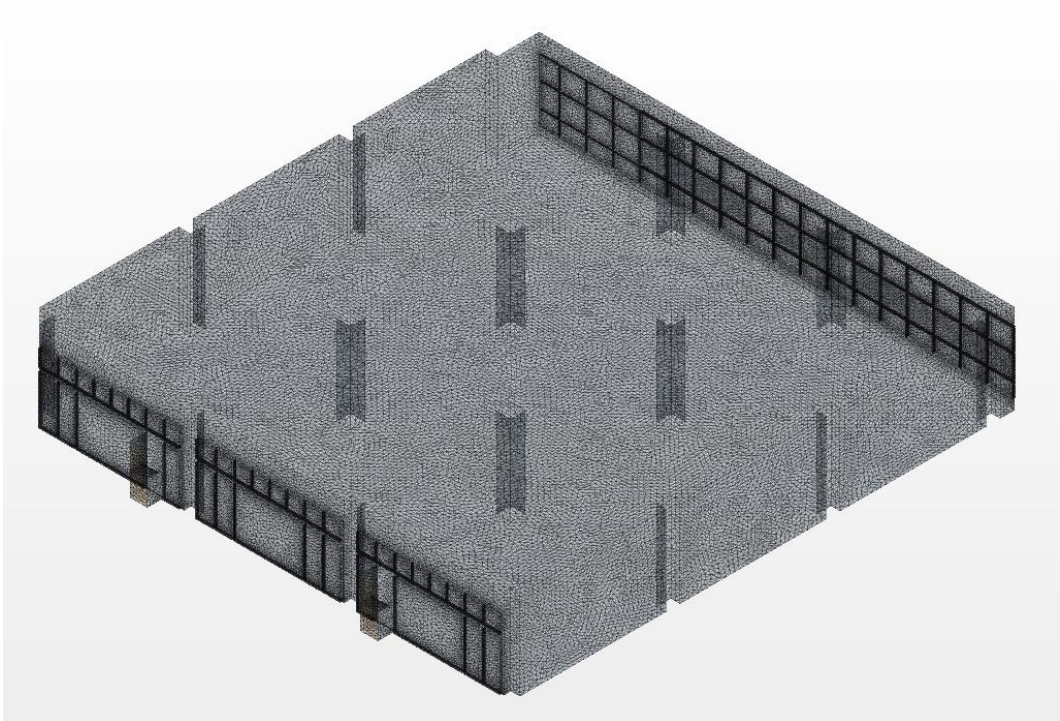
Cell validation		Number of cells	Percentage
	≤ 0.5	0	0.000%
0.5	0.6	0	0.000%
0.6	0.7	0	0.000%
0.7	0.8	0	0.000%
0.8	0.9	0	0.000%
0.9	0.95	0	0.000%
0.95	1.0	2481517	100.000%
Total number of volume cells		2481517	100%

Grid quality assessment (volume change and cell validation) from the meshing model

Coupled Domain without Furniture Approach

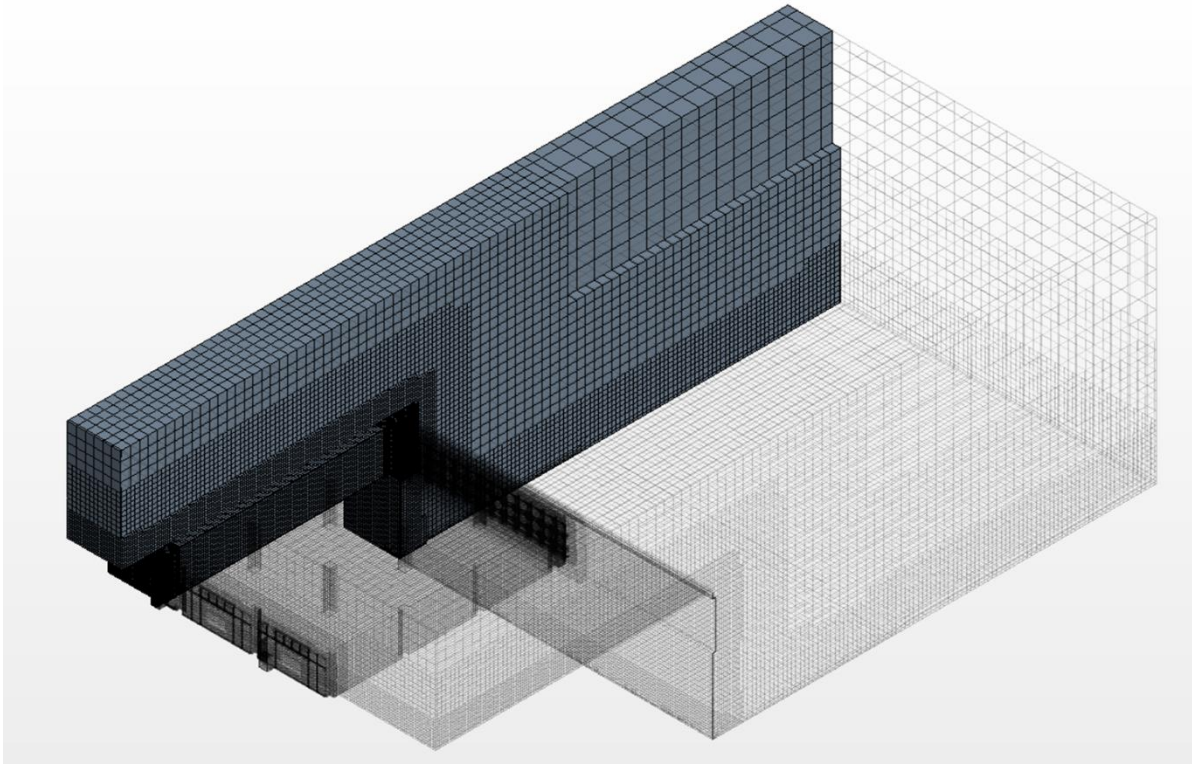


Visualization of the surface meshing (overall view)



Visualization of the surface meshing (detailed view)

Coupled Domain without Furniture Approach



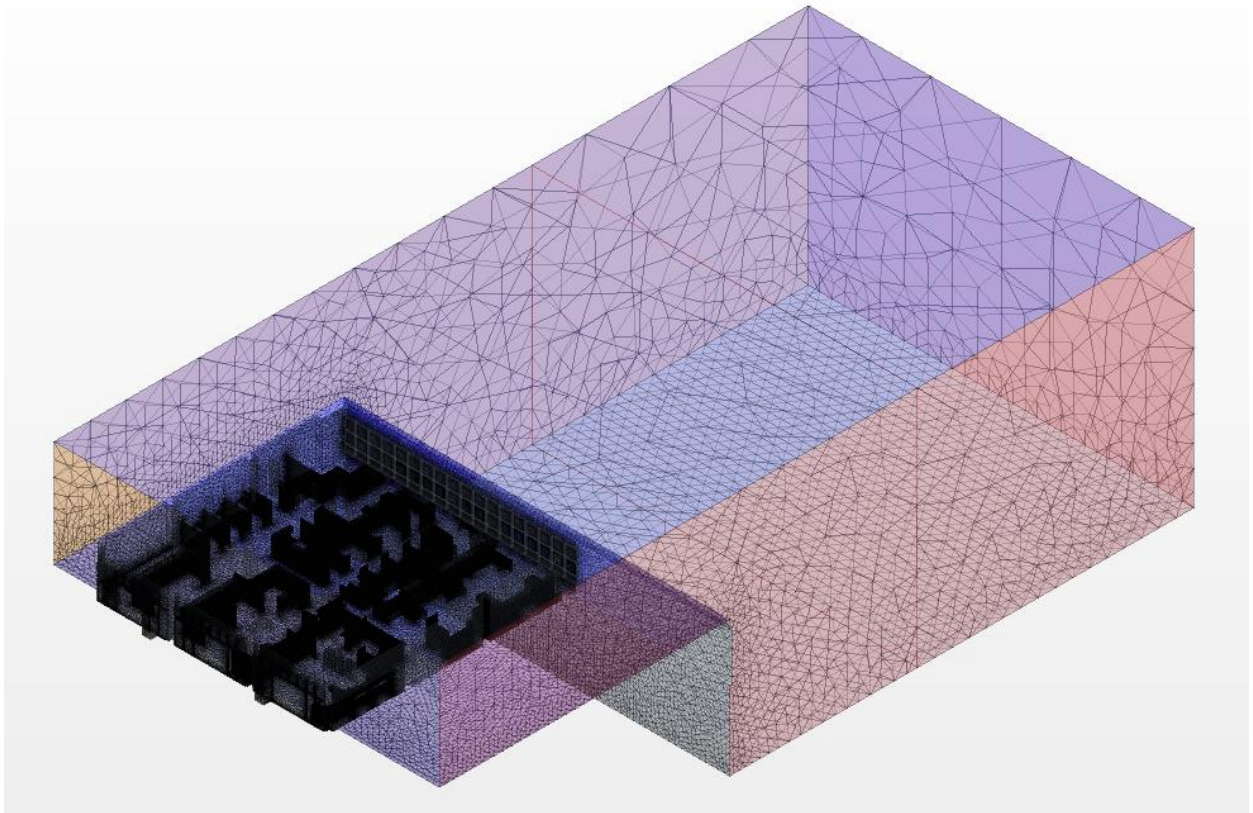
Visualization of the volume cells and partial computational domain resulted from the vertical virtual section plane

Volume Change		Number of cells	Percentage
	$\leq 1e-6$	0	0.000%
1e-6	1e-5	0	0.000%
1e-5	1e-4	1	0.000%
1e-4	1e-3	4	0.000%
1e-3	1e-2	1519	0.035%
1e-2	1e-1	31763	0.731%
1e-1	1.0	4314433	99.234%
Total number of volume cells		4347720	100%

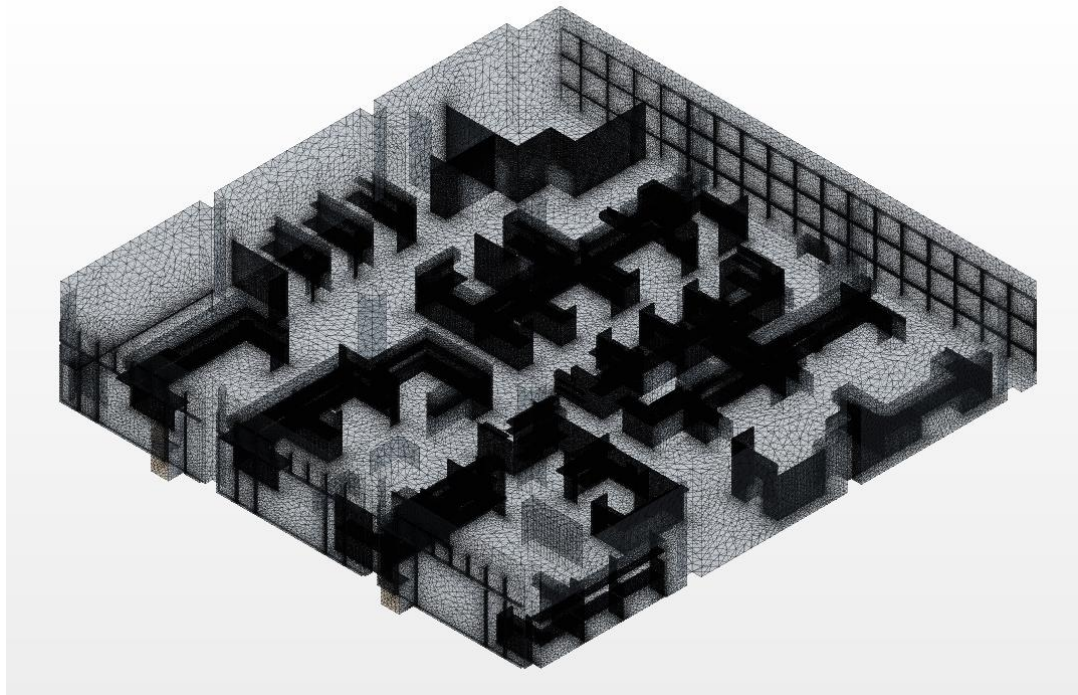
Cell validation		Number of cells	Percentage
	≤ 0.5	0	0.000%
0.5	0.6	0	0.000%
0.6	0.7	0	0.000%
0.7	0.8	0	0.000%
0.8	0.9	0	0.000%
0.9	0.95	0	0.000%
0.95	1.0	4347720	100.000%
Total number of volume cells		4347720	100%

Grid quality assessment (volume change and cell validation) from the meshing model

Coupled Domain including Furniture Approach

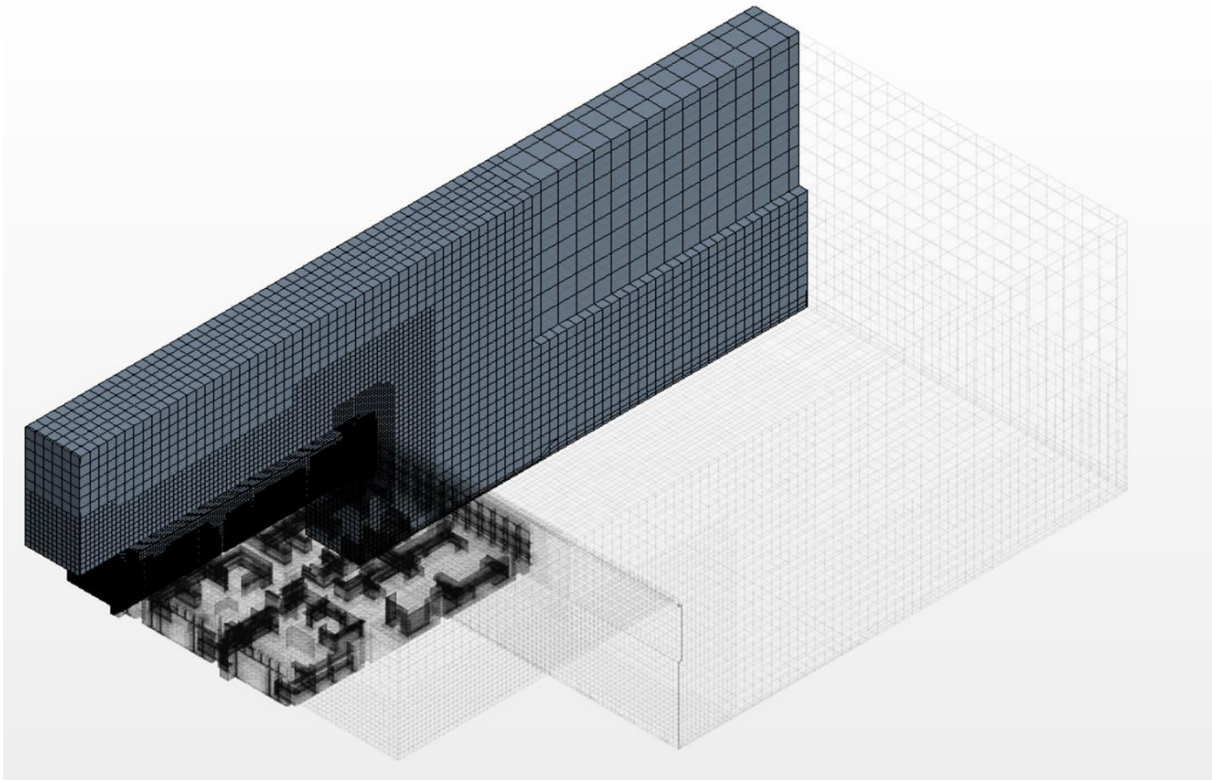


Visualization of the surface meshing (overall view)

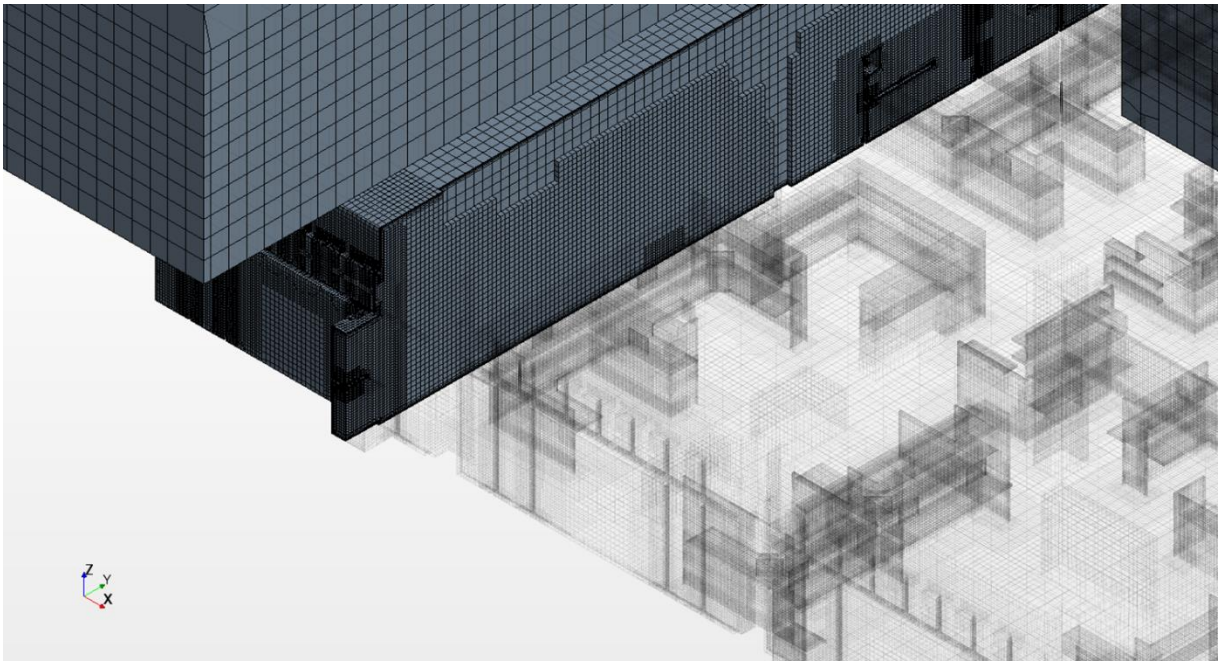


Visualization of the surface meshing (detailed view)

Coupled Domain including Furniture Approach



Visualization of the volume cells and partial computational domain resulted from the vertical virtual section plane (overall view)



Visualization of the volume cells and partial computational domain resulted from the vertical virtual section plane (detailed view)

Coupled Domain including Furniture Approach

Volume Change		Number of cells	Percentage
	<= 1e-6	1	0.000%
1e-6	1e-5	1	0.000%
1e-5	1e-4	7	0.000%
1e-4	1e-3	50	0.000%
1e-3	1e-2	4635	0.029%
1e-2	1e-1	175969	1.112%
1e-1	1.0	15639762	98.858%
Total number of volume cells		15820425	100%

Cell validation		Number of cells	Percentage
	<= 0.5	0	0.000%
0.5	0.6	0	0.000%
0.6	0.7	0	0.000%
0.7	0.8	0	0.000%
0.8	0.9	1	0.000%
0.9	0.95	46	0.000%
0.95	1.0	15820378	100.000%
Total number of volume cells		15820425	100%

Grid quality assessment (volume change and cell validation)
from the meshing model

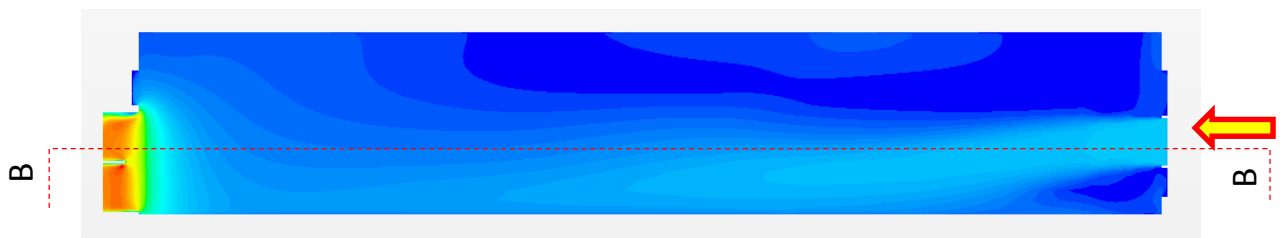
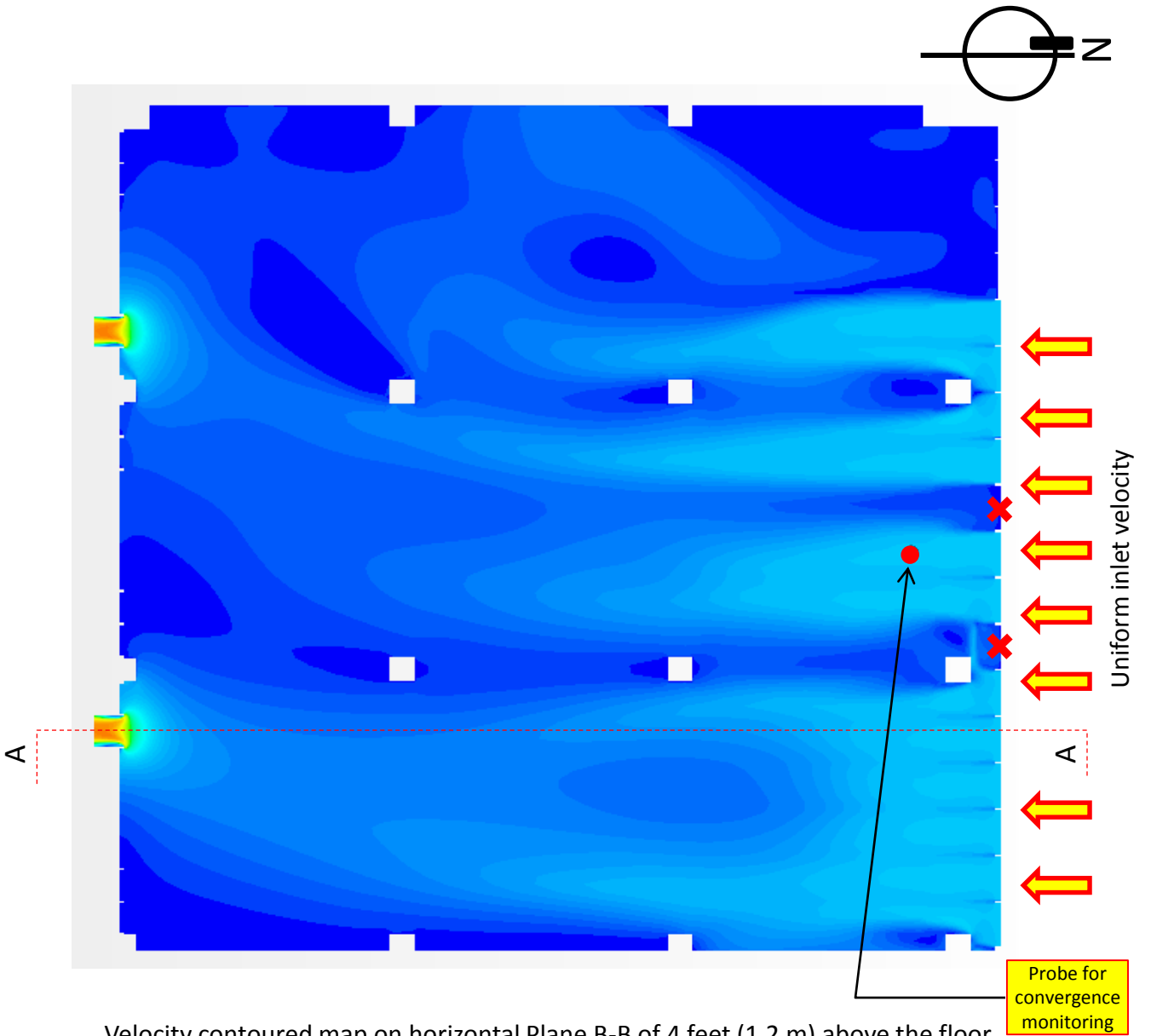
APPENDIX B

RESULTS FROM CFD RUNS

This appendix showed the results of 18 CFD runs pertaining to CAD modeling strategies, turbulence model and boundary condition testing, settings related at site test's environmental conditions as well as defined measurement scenarios.

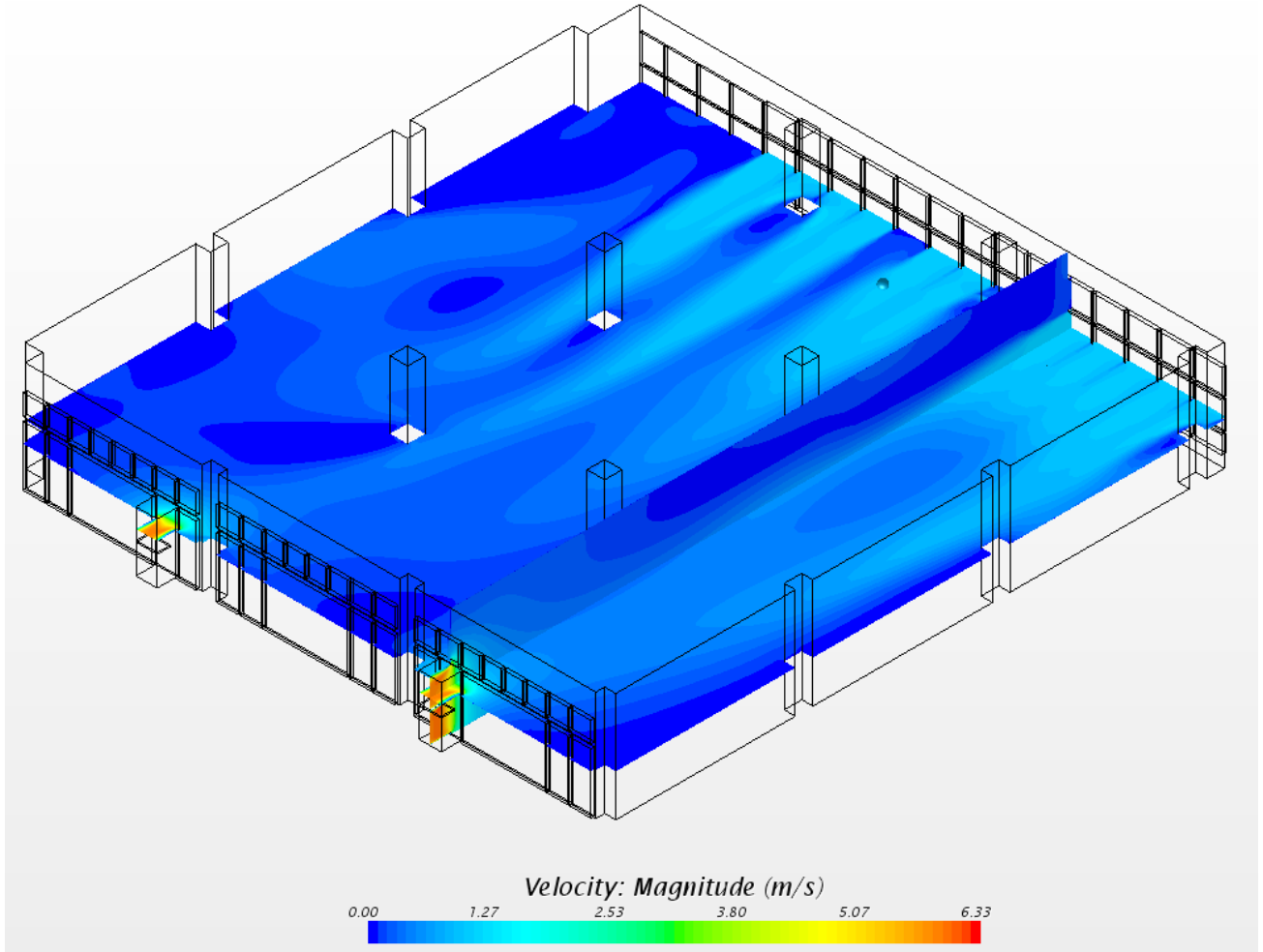
Solution ID	Coupled / Decoupled	With furniture	Turbulence model	Inlet	Outlet	Air density and dynamic viscosity	Test Scenario
A	Decoupled	No	k-ε	Constant velocity	Pressure outlet (0 Pa)	default	N/A
A1	Decoupled	No	k-ω	Constant velocity	Pressure outlet (0 Pa)	default	N/A
A2	Decoupled	No	k-ε	Constant velocity	Constant massflow rate (4.359kg/s)	default	N/A
B	Coupled	No	k-ε	Wind log profile	Constant massflow rate (4.359kg/s)	default	N/A
B1	Coupled	No	k-ε	Wind log profile	Fan curve	default	N/A
B2	Coupled	No	k-ω	Wind log profile	Fan curve	default	N/A
B3	Coupled	No	k-ε	Wind log profile	Fan curve	Actual test condition	N/A
C	Coupled	Yes	k-ε	Wind log profile	Fan curve	default	N/A
C1	Coupled	Yes	k-ω	Wind log profile	Fan curve	default	N/A
C2	Coupled	Yes	k-ε	Wind log profile	Fan curve	Actual test condition	N/A
D1	Coupled	Yes	k-ε	Wind log profile	Fan curve	Actual test condition	Scenario 1
D2	Coupled	Yes	k-ε	Wind log profile	Fan curve	Actual test condition	Scenario 2
D3	Coupled	Yes	k-ε	Wind log profile	Fan curve	Actual test condition	Scenario 3
D4	Coupled	Yes	k-ε	Wind log profile	Fan curve	Actual test condition	Scenario 4
E1	Coupled	Yes	k-ω	Wind log profile	Fan curve	Actual test condition	Scenario 1
E2	Coupled	Yes	k-ω	Wind log profile	Fan curve	Actual test condition	Scenario 2
E3	Coupled	Yes	k-ω	Wind log profile	Fan curve	Actual test condition	Scenario 3
E4	Coupled	Yes	k-ω	Wind log profile	Fan curve	Actual test condition	Scenario 4

Solution ID	Coupled / Decoupled	With furniture	Turbulence model	Inlet	Outlet	Air density and dynamic viscosity	Test Scenario
A	Decoupled	No	k-ε	Constant velocity	Pressure outlet (0 Pa)	Default	N/A



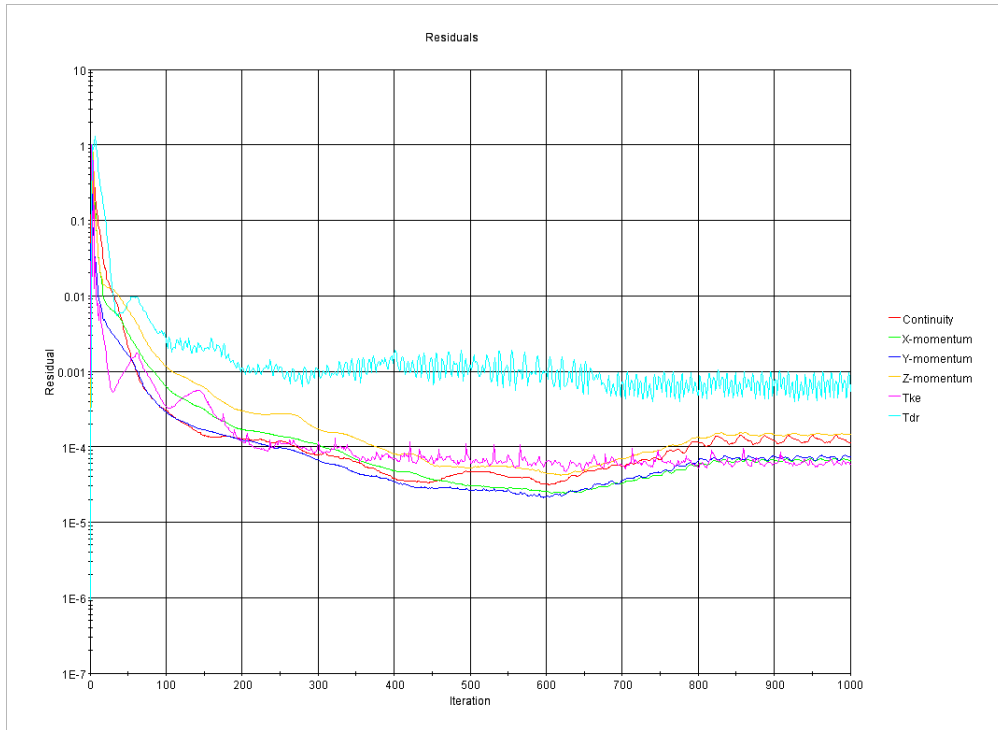
✘ Permanently closed non-working louvers

Solution ID	Coupled / Decoupled	With furniture	Turbulence model	Inlet	Outlet	Air density and dynamic viscosity	Test Scenario
A	Decoupled	No	k-ε	Constant velocity	Pressure outlet (0 Pa)	Default	N/A

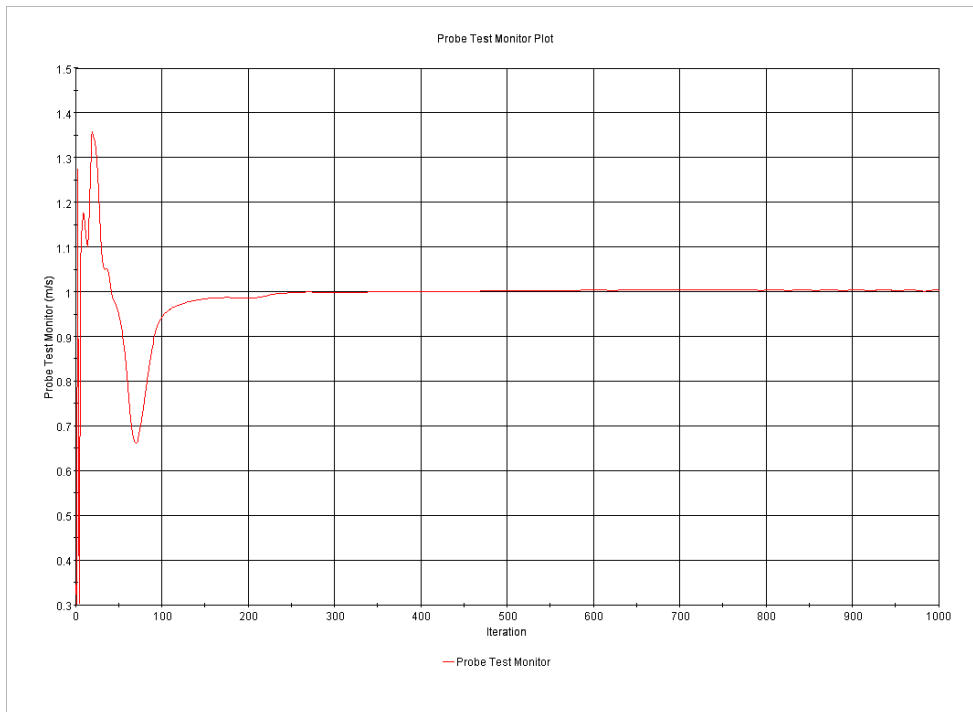


Velocity contoured maps (Axonometric SE View)

Solution ID	Coupled / Decoupled	With furniture	Turbulence model	Inlet	Outlet	Air density and dynamic viscosity	Test Scenario
A	Decoupled	No	k-ε	Constant velocity	Pressure outlet (0 Pa)	Default	N/A

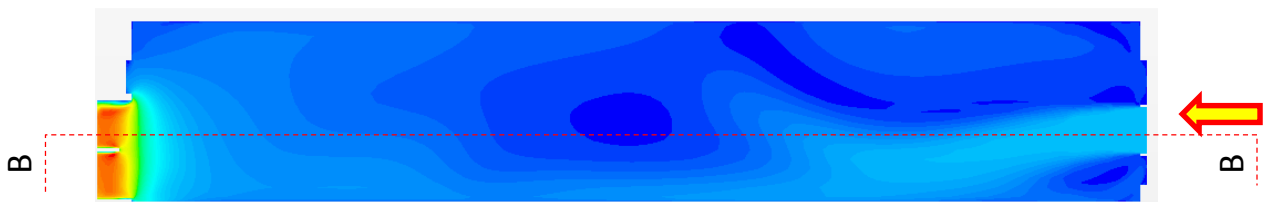
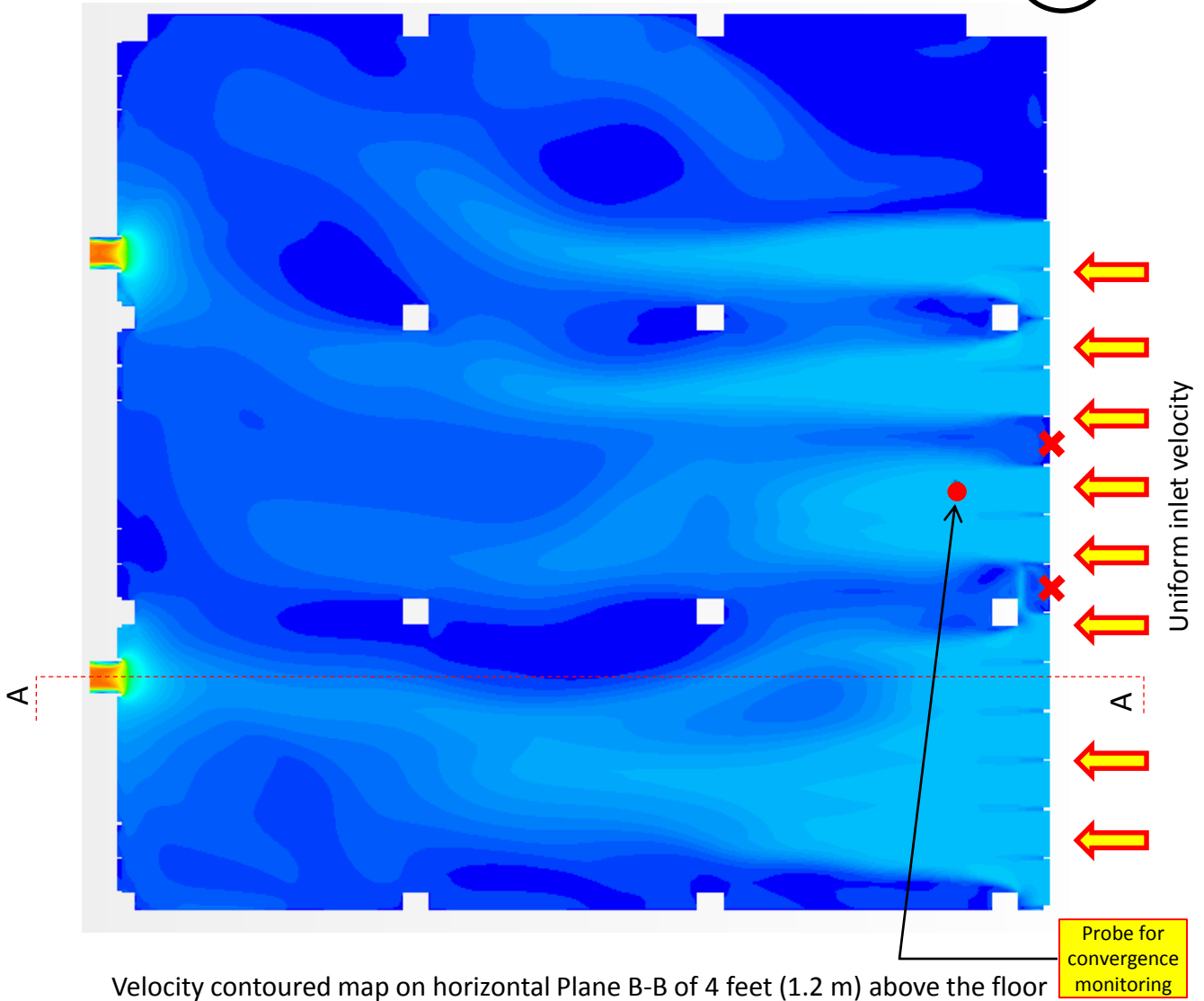
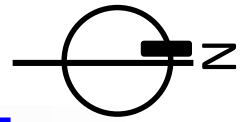


Residual plot



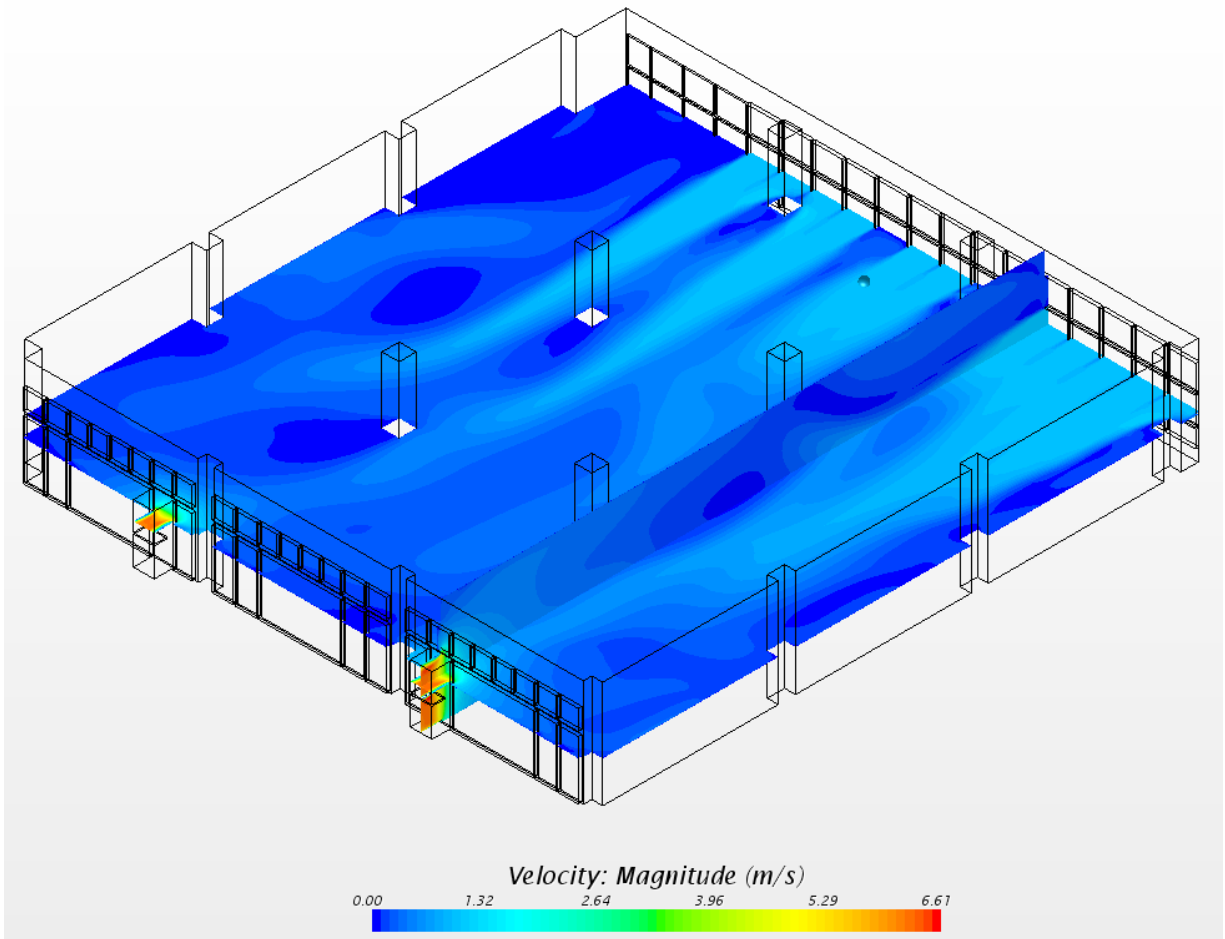
Monitoring plot of wind speed at the point-type probe for convergence checking

Solution ID	Coupled / Decoupled	With furniture	Turbulence model	Inlet	Outlet	Air density and dynamic viscosity	Test Scenario
A1	Decoupled	No	k- ω	Constant velocity	Pressure outlet (0 Pa)	Default	N/A



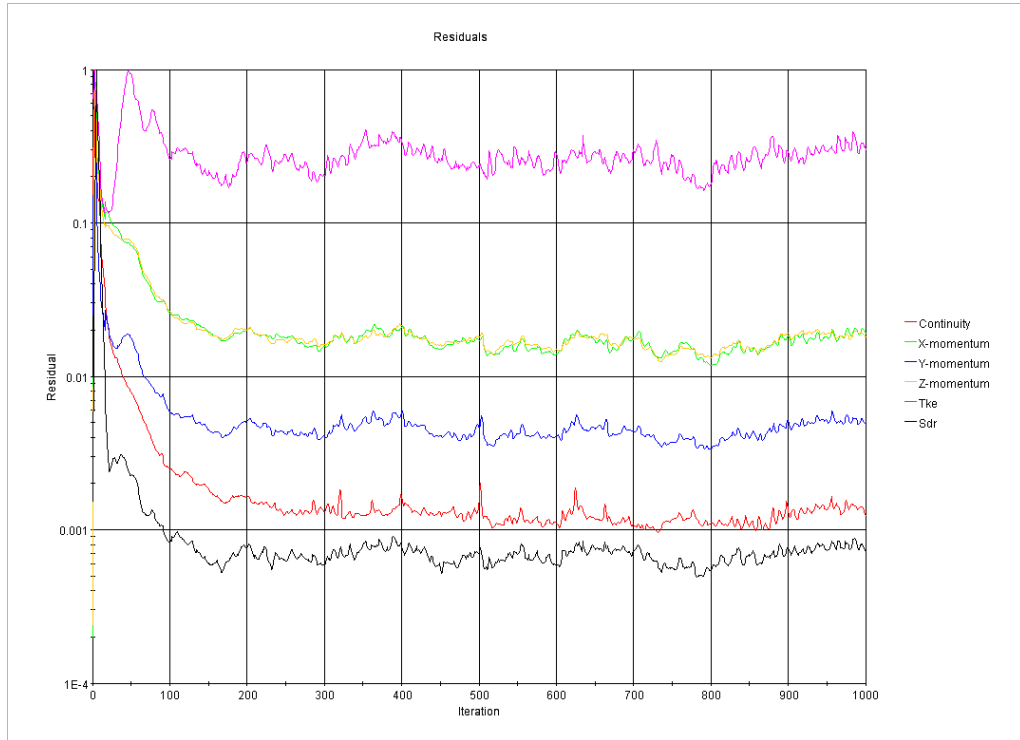
✘ Permanently closed non-working louvers

Solution ID	Coupled / Decoupled	With furniture	Turbulence model	Inlet	Outlet	Air density and dynamic viscosity	Test Scenario
A1	Decoupled	No	k- ω	Constant velocity	Pressure outlet (0 Pa)	Default	N/A

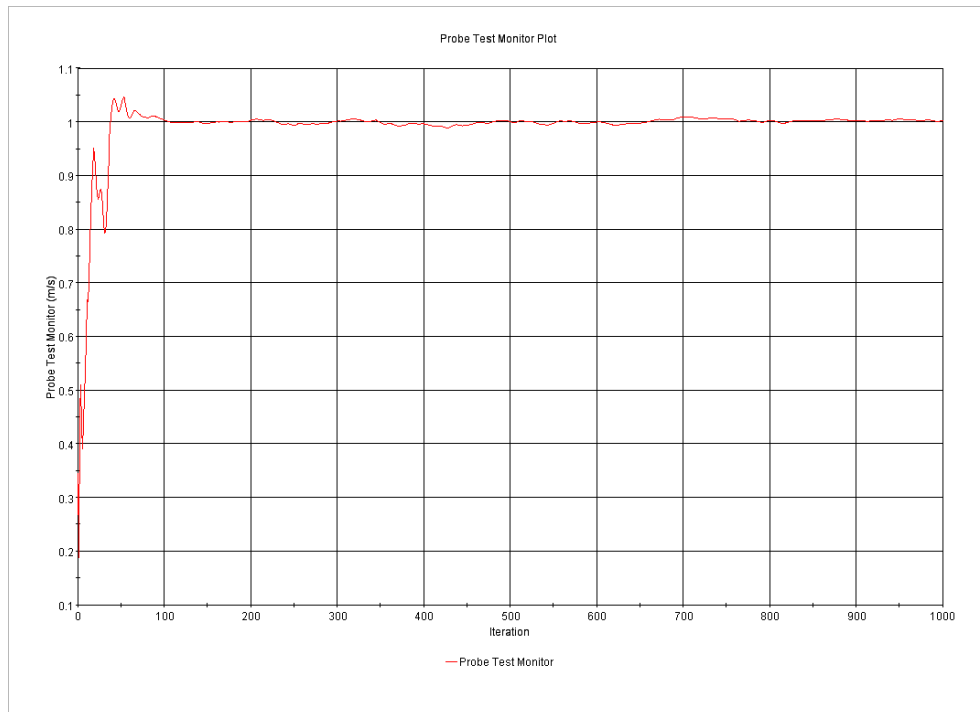


Velocity contoured maps (Axonometric SE View)

Solution ID	Coupled / Decoupled	With furniture	Turbulence model	Inlet	Outlet	Air density and dynamic viscosity	Test Scenario
A1	Decoupled	No	k- ω	Constant velocity	Pressure outlet (0 Pa)	Default	N/A

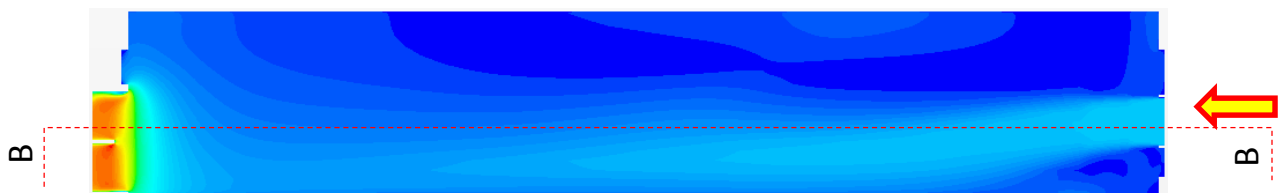
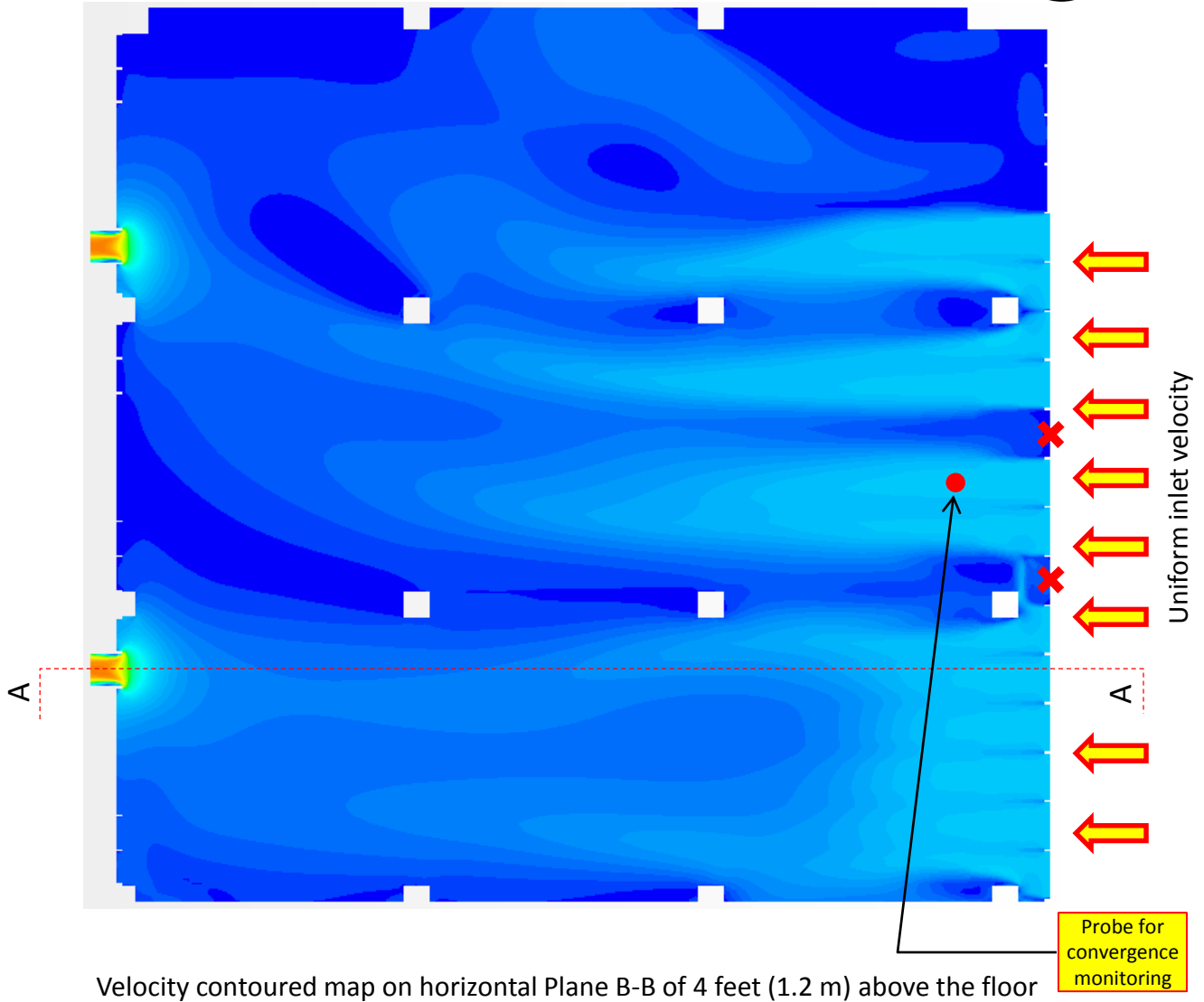
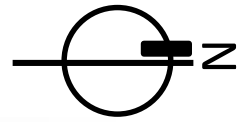


Residual plot



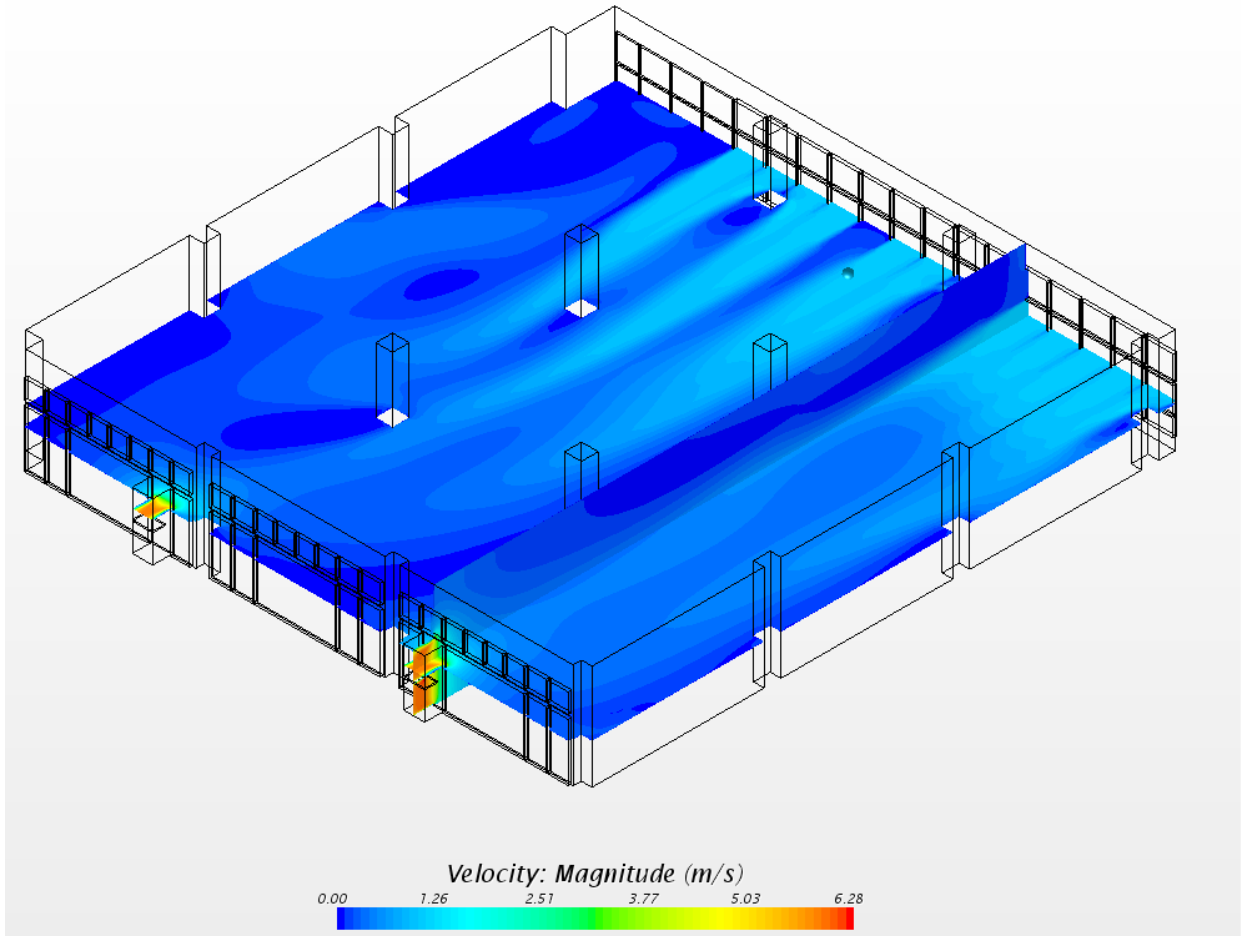
Monitoring plot of wind speed at the point-type probe for convergence checking

Solution ID	Coupled / Decoupled	With furniture	Turbulence model	Inlet	Outlet	Air density and dynamic viscosity	Test Scenario
A2	Decoupled	No	k-ε	Constant velocity	Constant mass flow rate (4.359kg/s)	Default	N/A



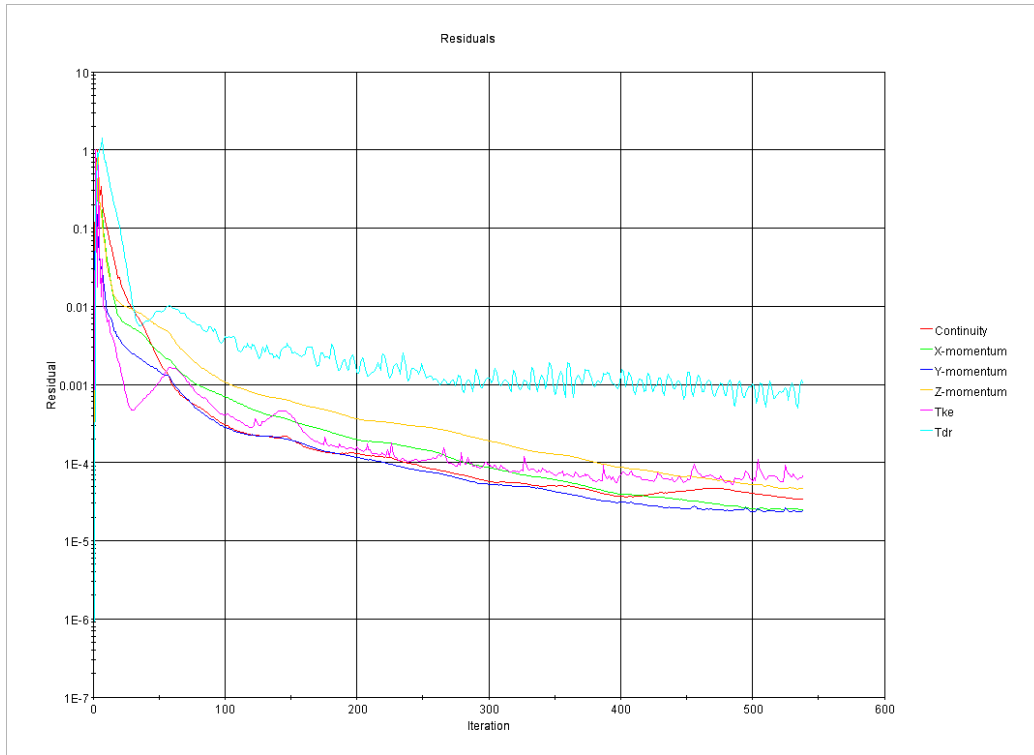
✘ Permanently closed non-working louvers

Solution ID	Coupled / Decoupled	With furniture	Turbulence model	Inlet	Outlet	Air density and dynamic viscosity	Test Scenario
A2	Decoupled	No	k-ε	Constant velocity	Constant mass flow rate (4.359kg/s)	Default	N/A

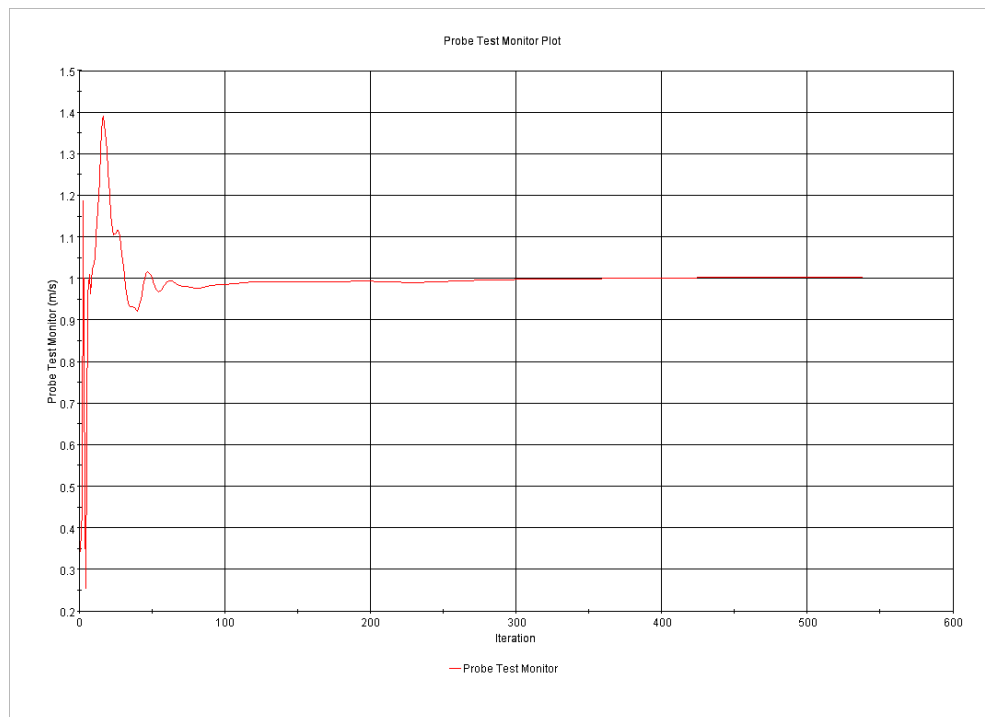


Velocity contoured maps (Axonometric SE View)

Solution ID	Coupled / Decoupled	With furniture	Turbulence model	Inlet	Outlet	Air density and dynamic viscosity	Test Scenario
A2	Decoupled	No	k-ε	Constant velocity	Constant mass flow rate (4.359kg/s)	Default	N/A

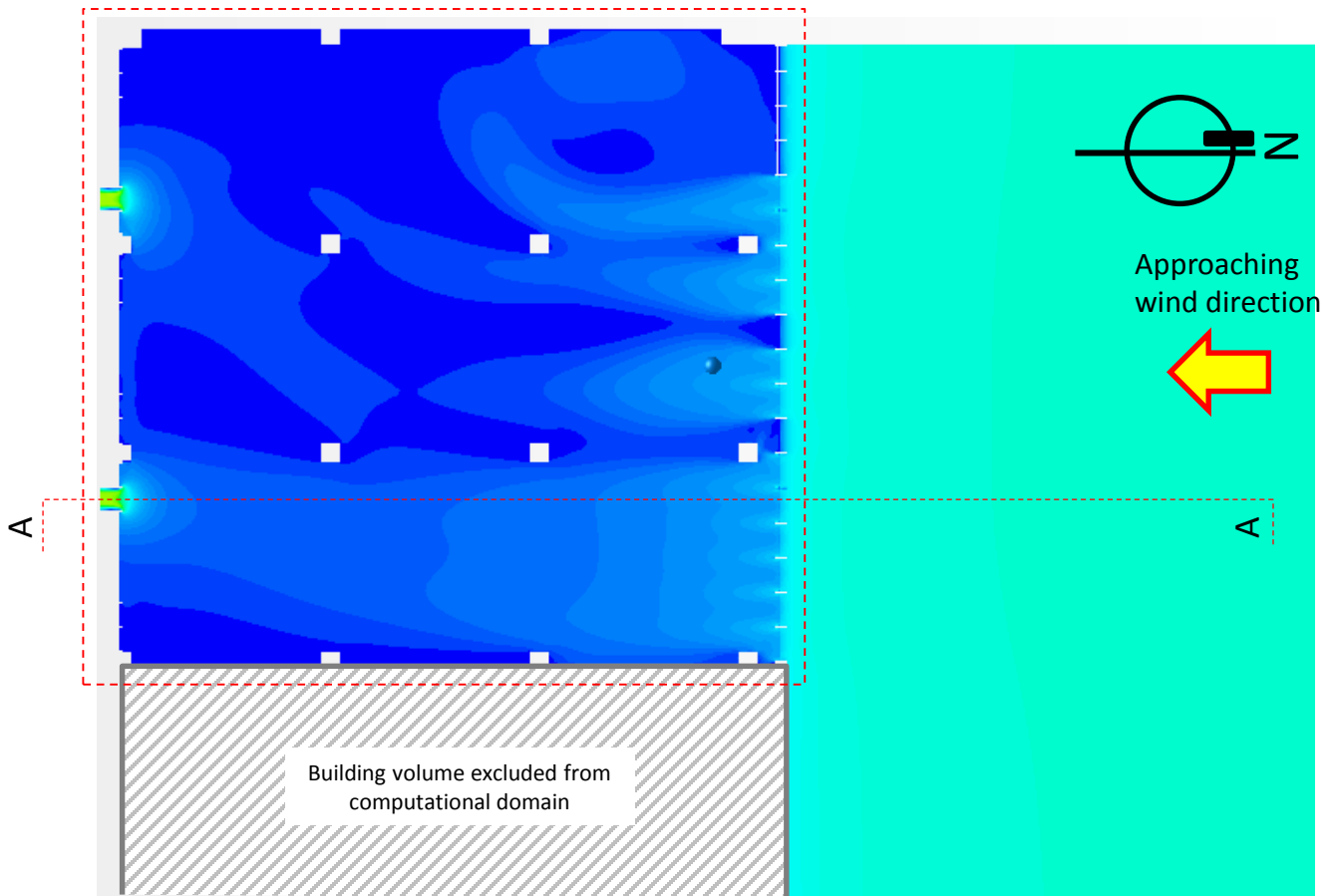


Residual plot

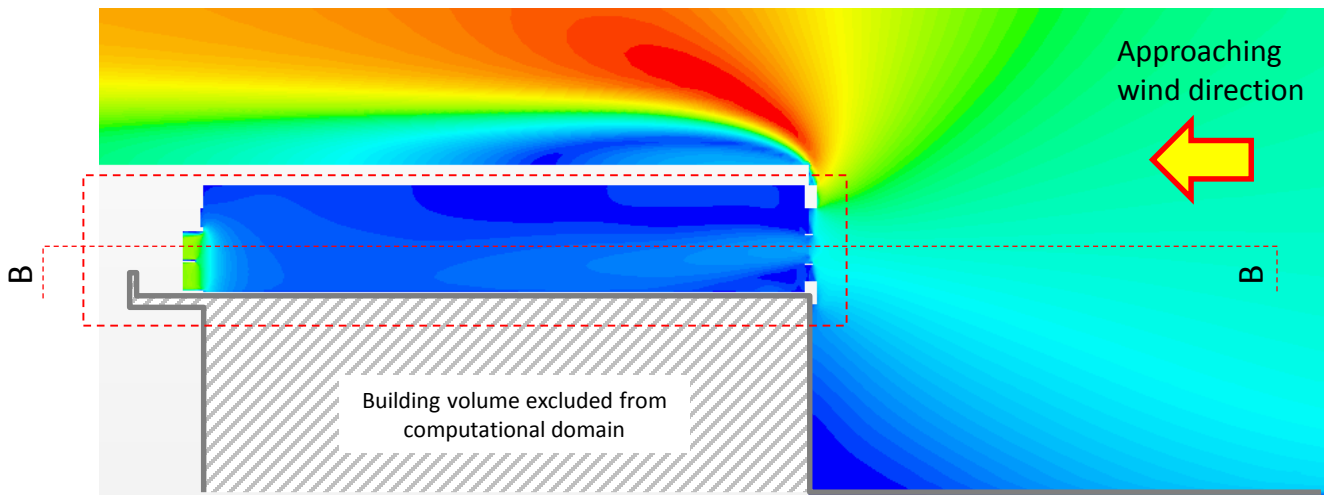


Monitoring plot of wind speed at the point-type probe for convergence checking

Solution ID	Coupled / Decoupled	With furniture	Turbulence model	Inlet	Outlet	Air density and dynamic viscosity	Test Scenario
B	Coupled	No	k-ε	Wind log profile	Constant mass flow rate (4.359kg/s)	Default	N/A



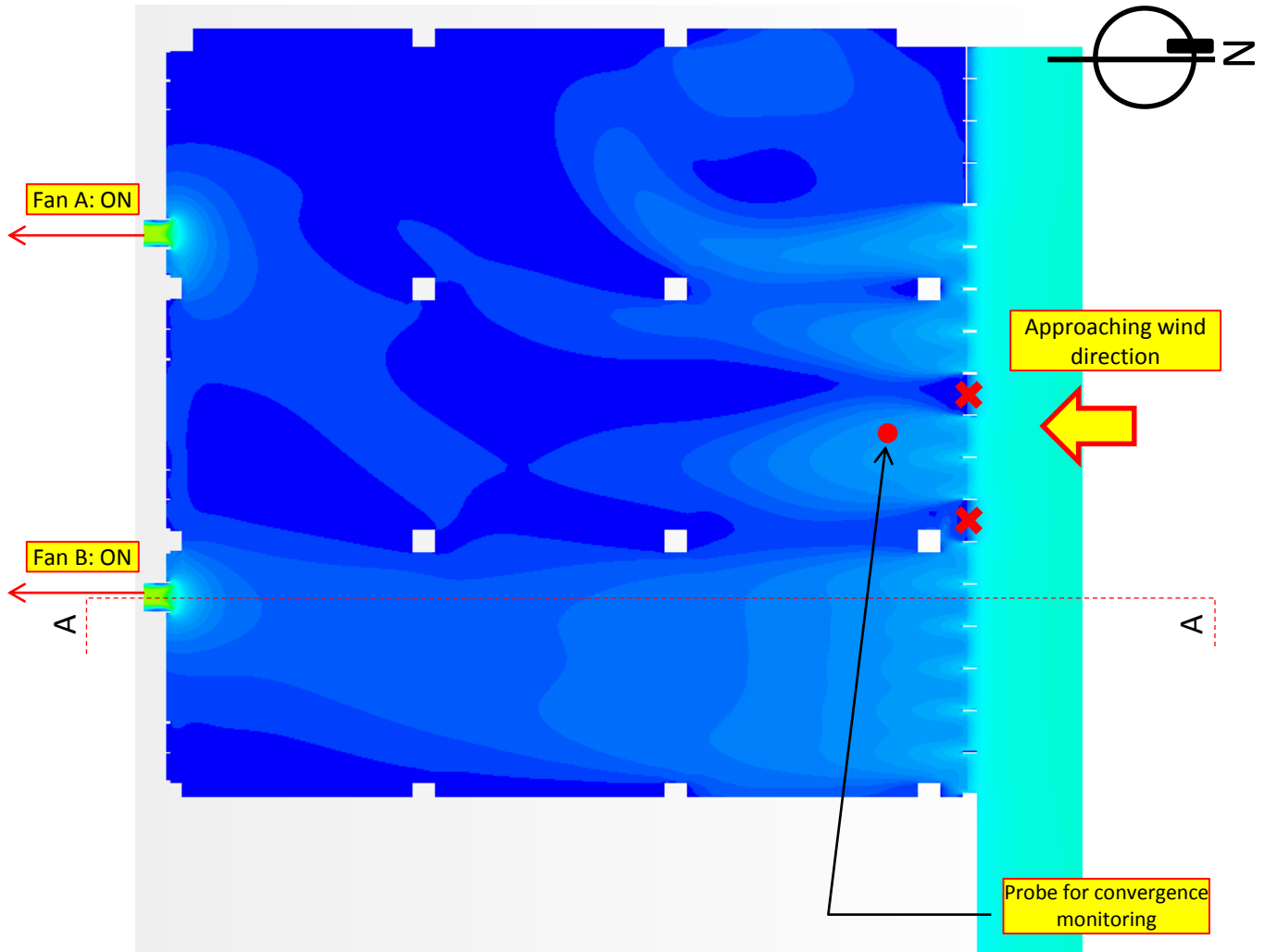
Velocity contoured map on the horizontal plane B-B of 4 feet (1.2m) above the floor (larger view)



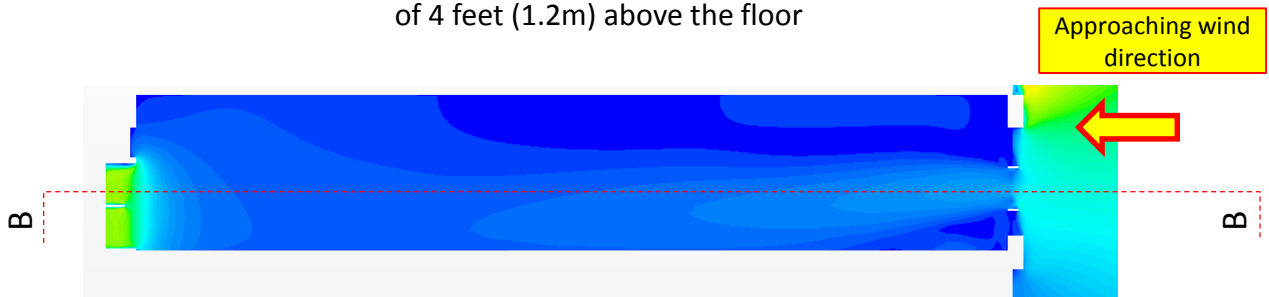
Velocity contoured map on the vertical plane A-A (larger view)



Solution ID	Coupled / Decoupled	With furniture	Turbulence model	Inlet	Outlet	Air density and dynamic viscosity	Test Scenario
B	Coupled	No	k-ε	Wind log profile	Constant mass flow rate (4.359kg/s)	Default	N/A



Detailed velocity contoured map on the horizontal plane B-B of 4 feet (1.2m) above the floor

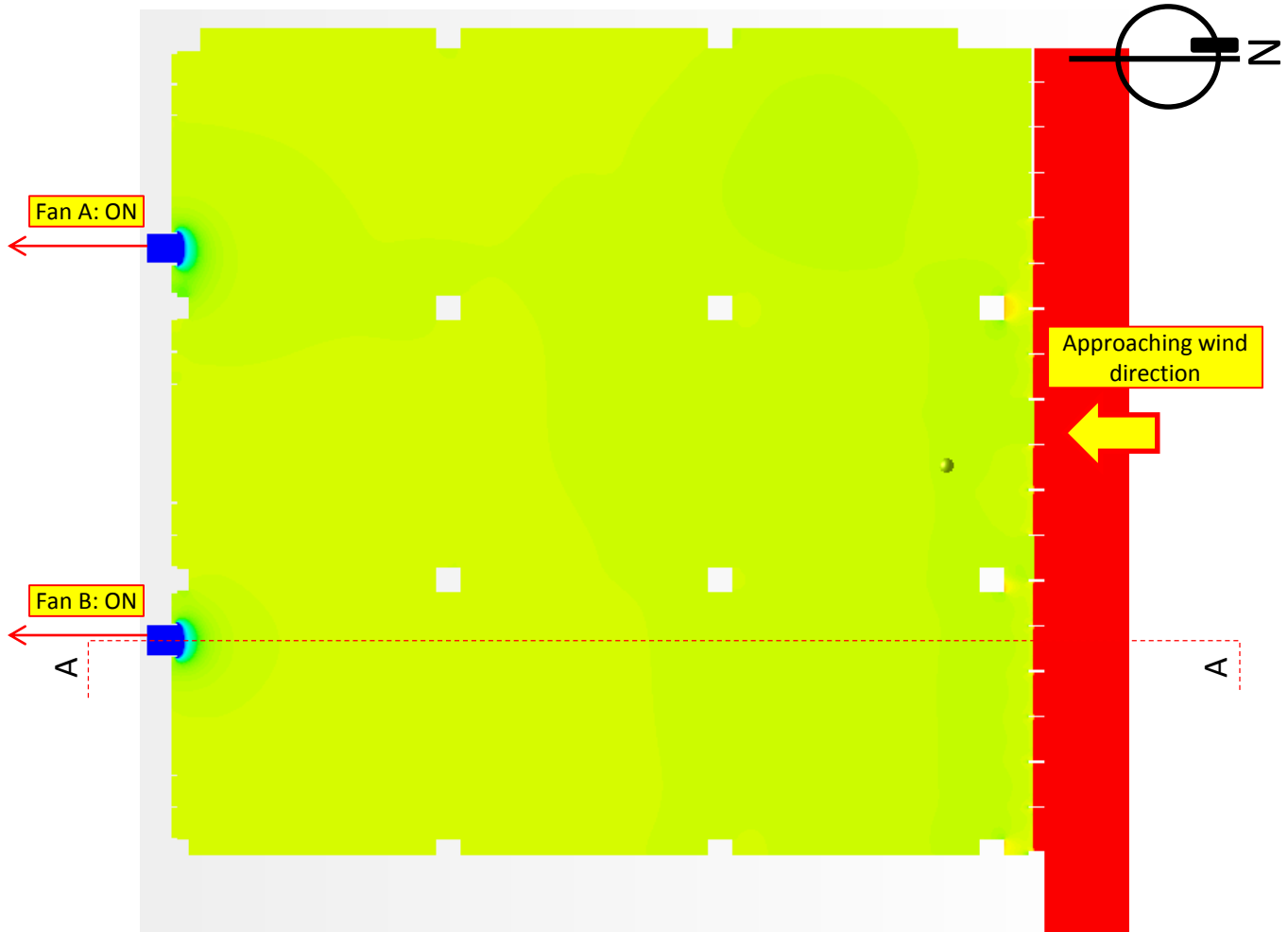


Detailed velocity contoured map on the vertical plane A-A



✘ Permanently closed non-working louvers

Solution ID	Coupled / Decoupled	With furniture	Turbulence model	Inlet	Outlet	Air density and dynamic viscosity	Test Scenario
B	Coupled	No	k-ε	Wind log profile	Constant mass flow rate (4.359kg/s)	Default	N/A



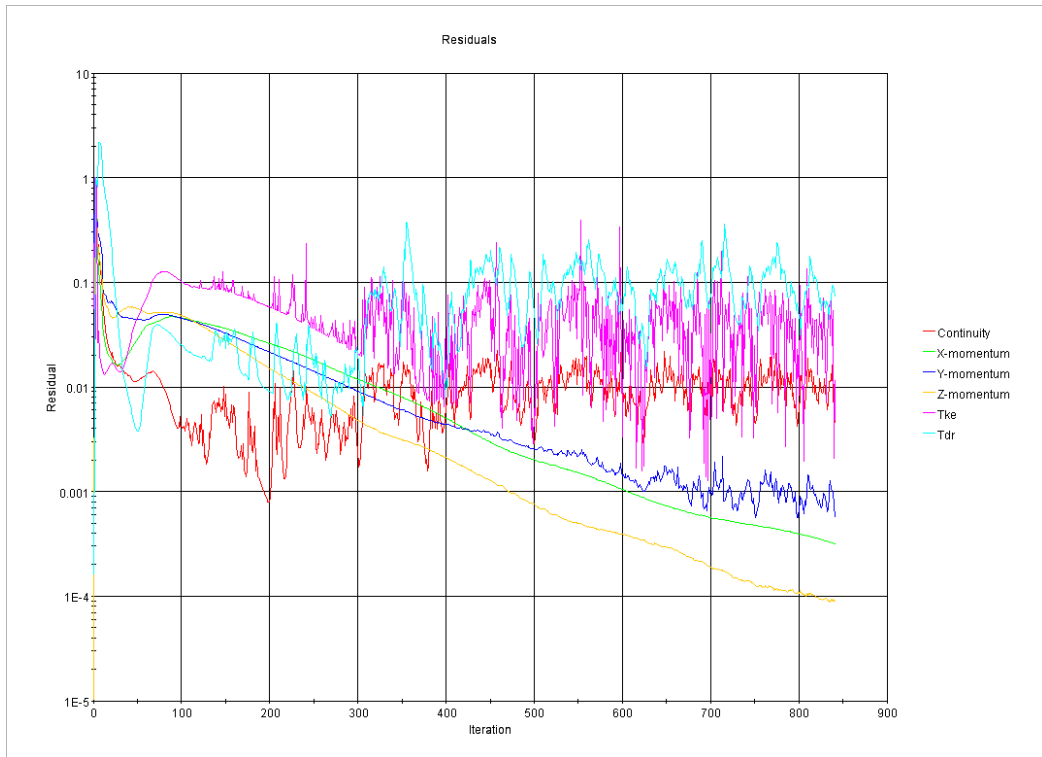
Detailed pressure contoured map on the horizontal plane B-B of 4 feet (1.2m) above the floor



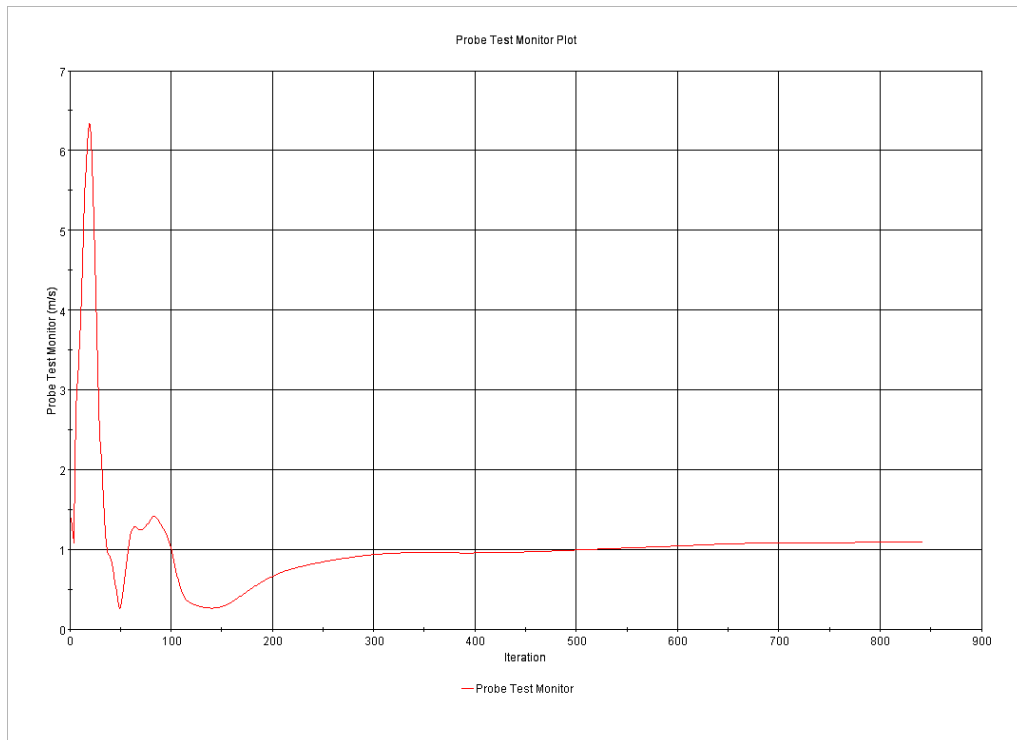
Detailed pressure contoured map on the vertical plane A-A



Solution ID	Coupled / Decoupled	With furniture	Turbulence model	Inlet	Outlet	Air density and dynamic viscosity	Test Scenario
B	Coupled	No	k-ε	Wind log profile	Constant mass flow rate (4.359kg/s)	Default	N/A

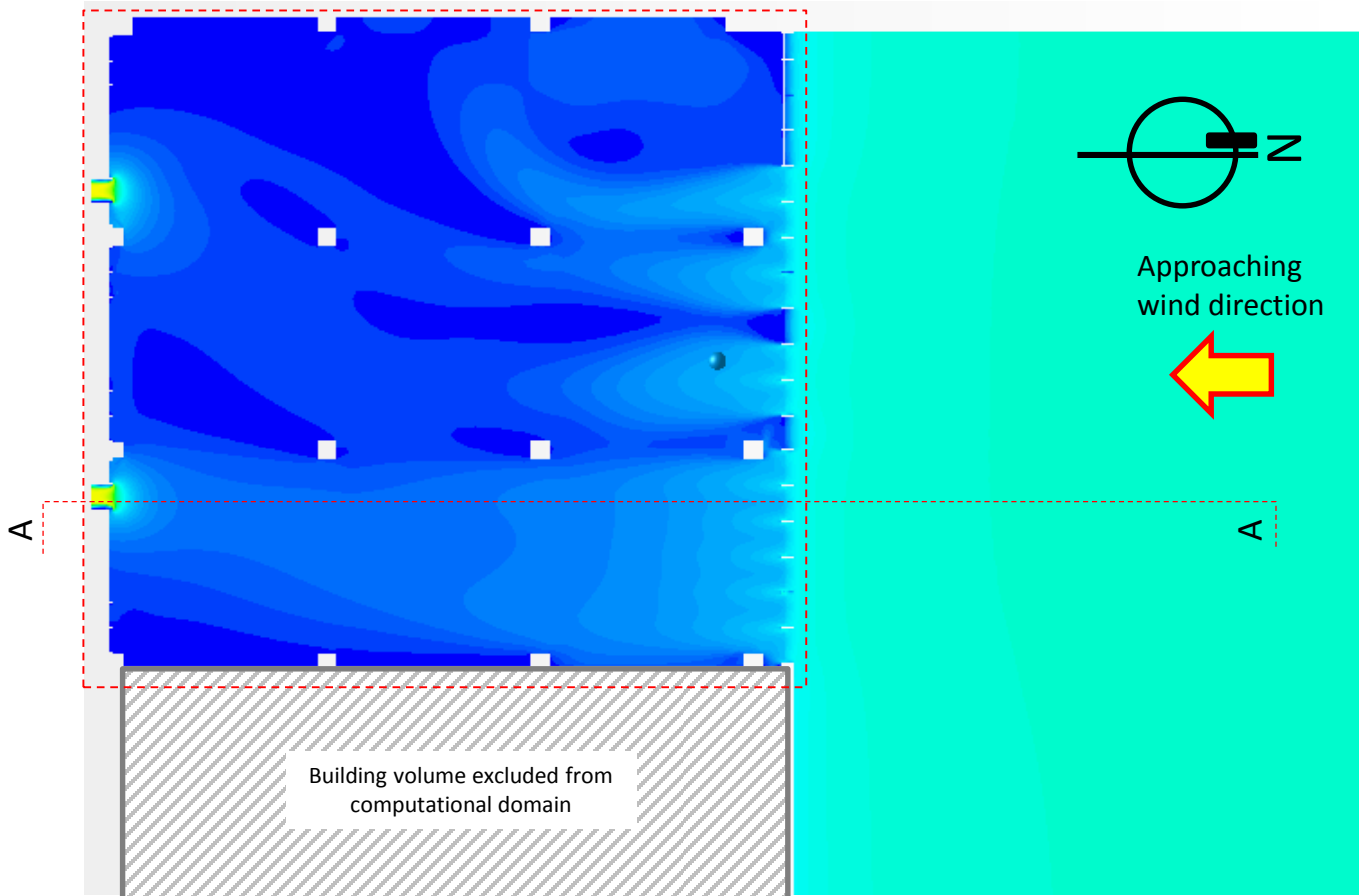


Residual plot

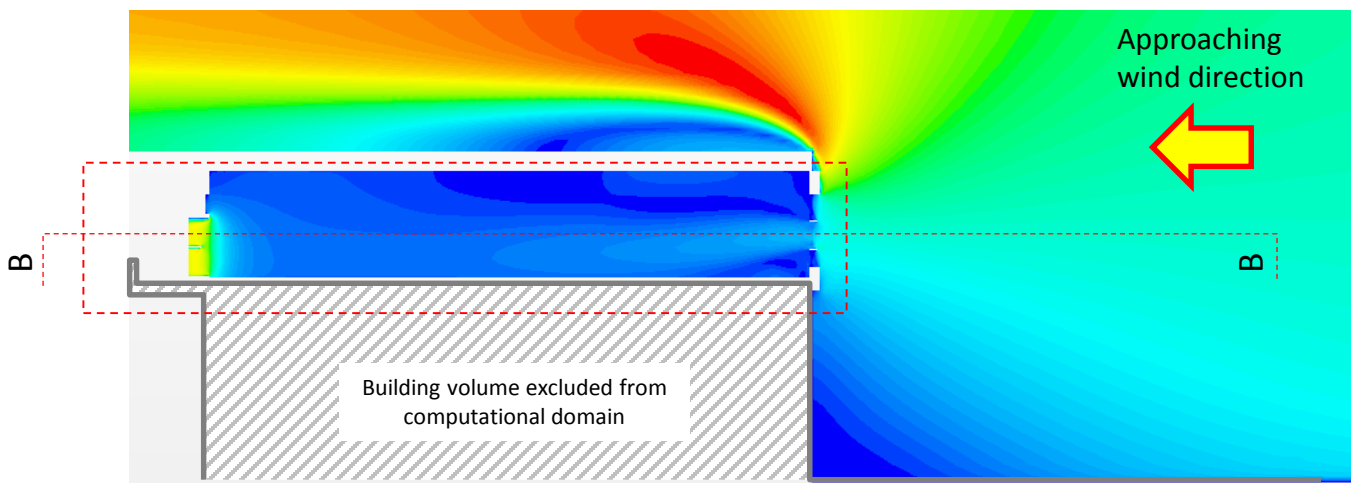


Monitoring plot of wind speed at the point-type probe for convergence checking

Solution ID	Coupled / Decoupled	With furniture	Turbulence model	Inlet	Outlet	Air density and dynamic viscosity	Test Scenario
B1	Coupled	No	k-ε	Wind log profile	Actual curve fan	Default	N/A



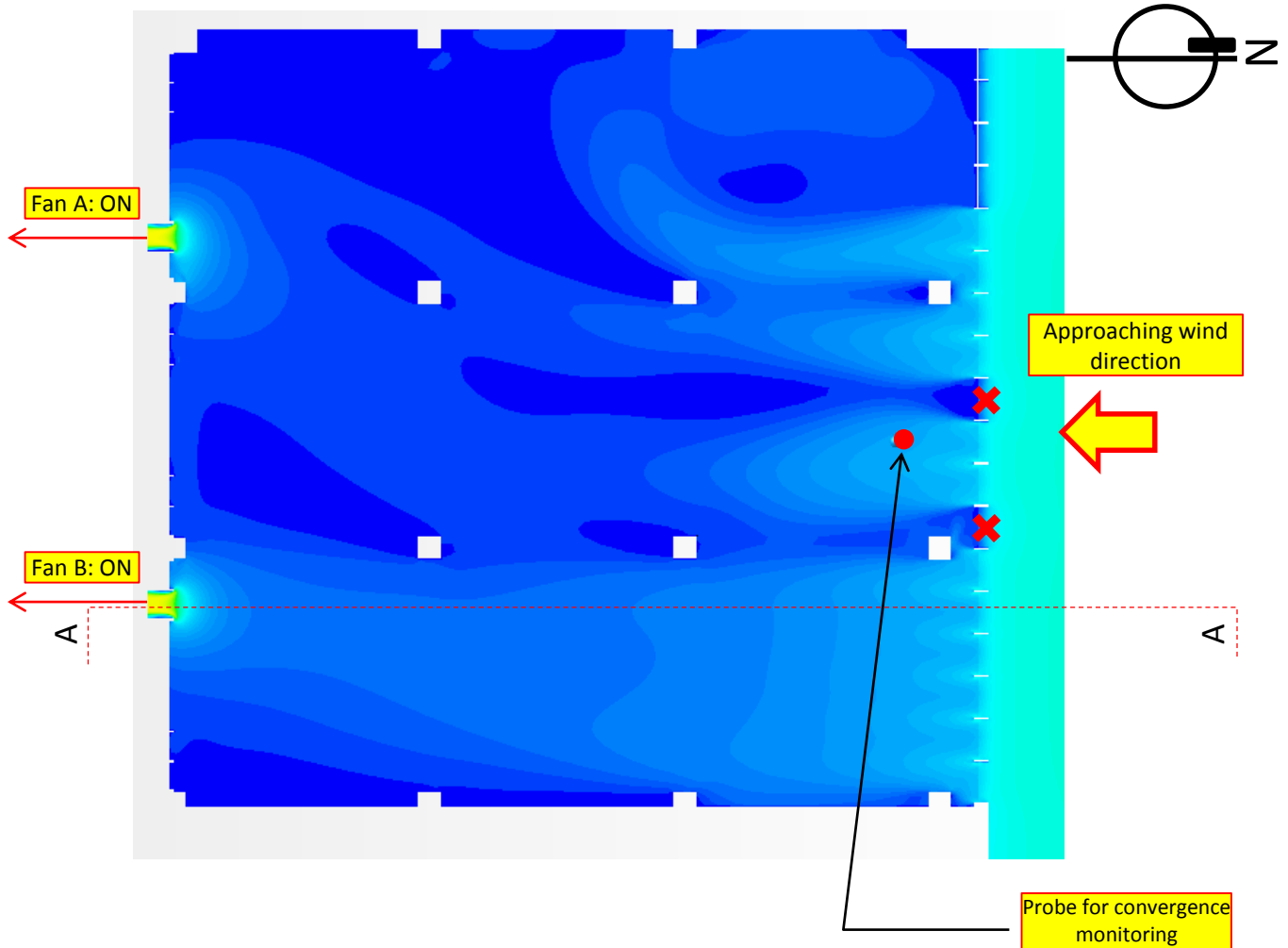
Velocity contoured map on the horizontal plane B-B of 4 feet (1.2m) above the floor (larger view)



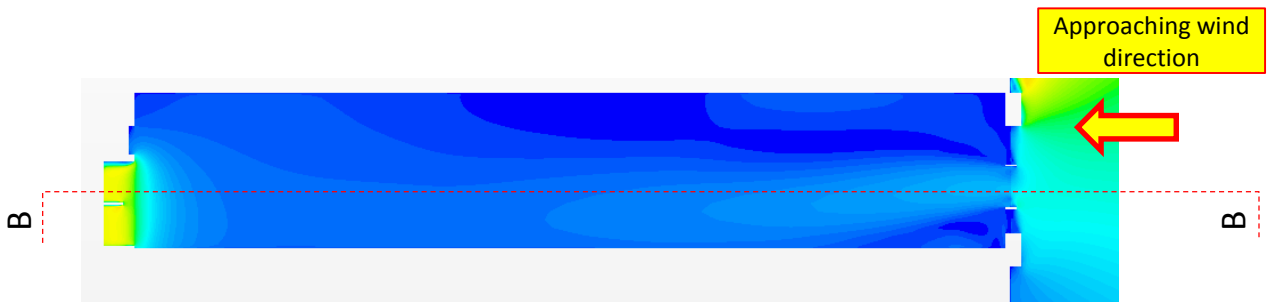
Velocity contoured map on the vertical plane A-A (larger view)



Solution ID	Coupled / Decoupled	With furniture	Turbulence model	Inlet	Outlet	Air density and dynamic viscosity	Test Scenario
B1	Coupled	No	k-ε	Wind log profile	Actual curve fan	Default	N/A



Detailed velocity contoured map on the horizontal plane B-B of 4 feet (1.2m) above the floor

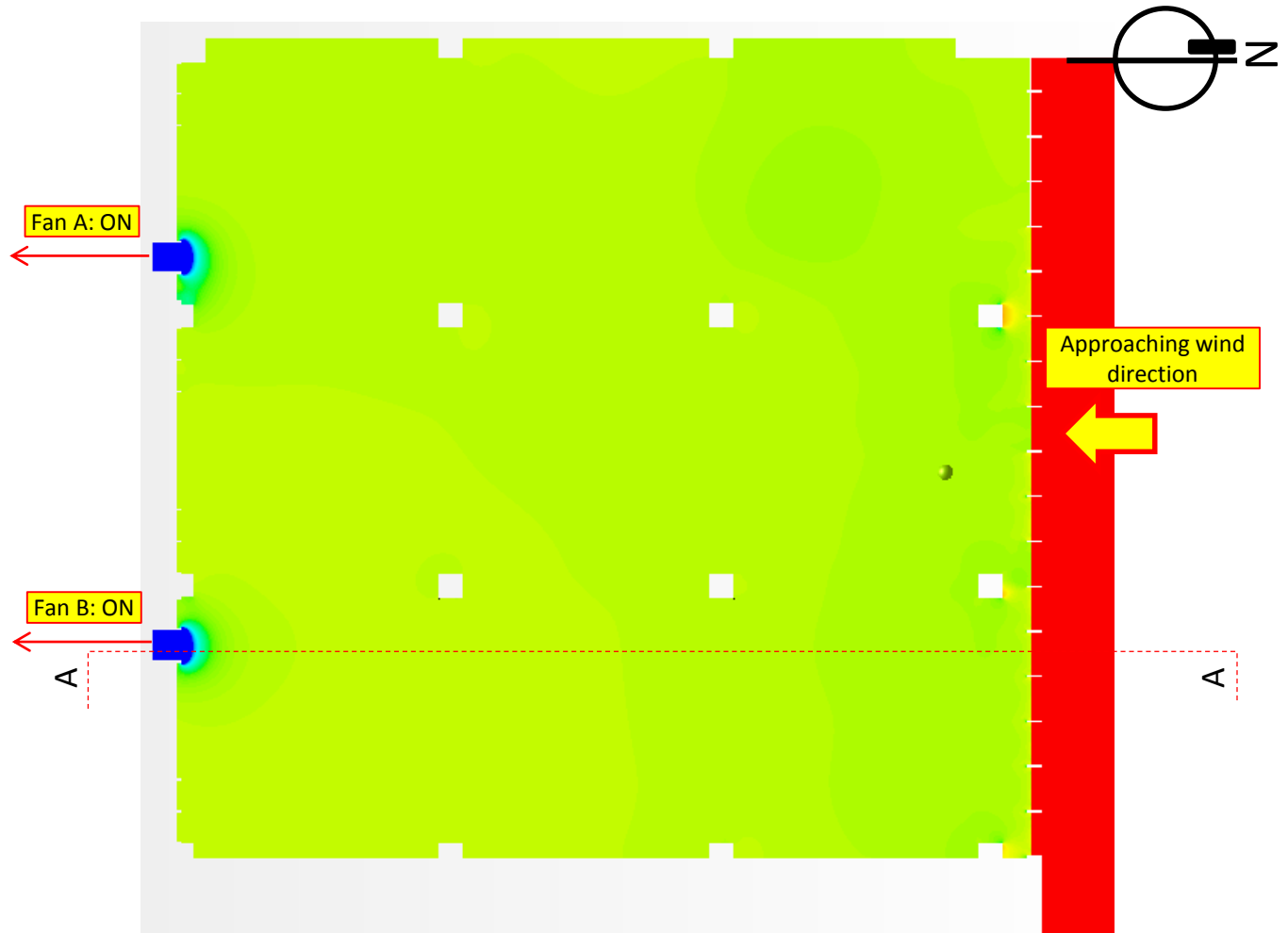


Detailed velocity contoured map on the vertical plane A-A



✘ Permanently closed non-working louvers

Solution ID	Coupled / Decoupled	With furniture	Turbulence model	Inlet	Outlet	Air density and dynamic viscosity	Test Scenario
B1	Coupled	No	k-ε	Wind log profile	Actual curve fan	Default	N/A



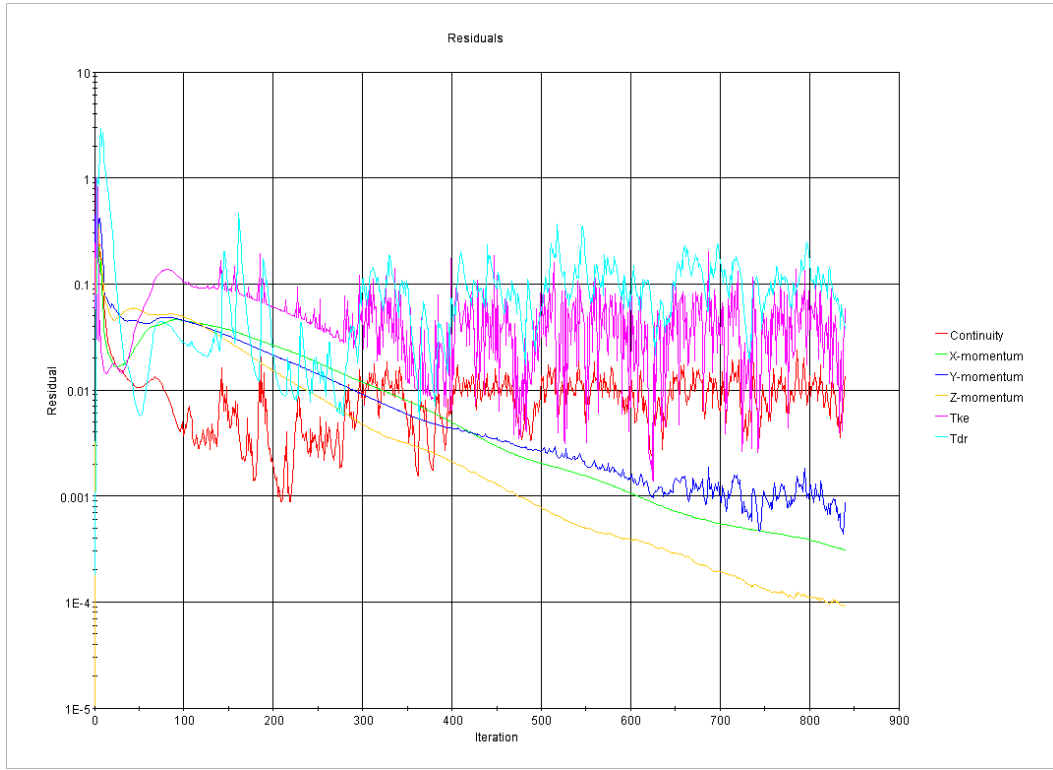
Detailed pressure contoured map on the horizontal plane B-B of 4 feet (1.2m) above the floor



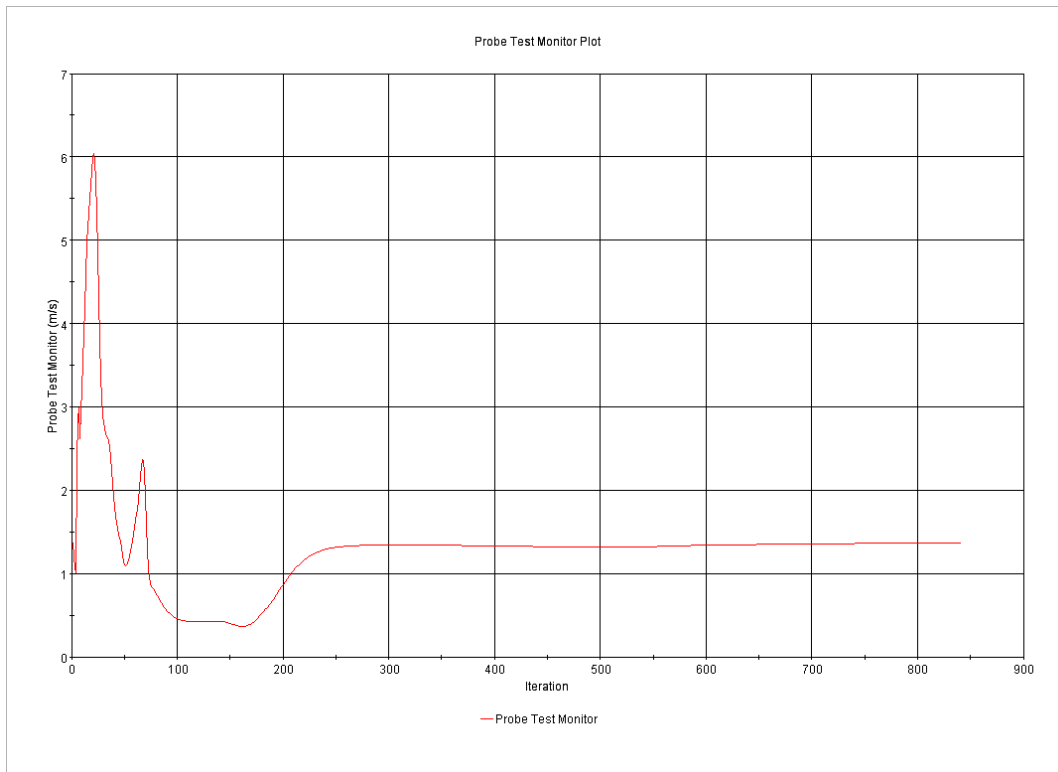
Detailed pressure contoured map on the vertical plane A-A



Solution ID	Coupled / Decoupled	With furniture	Turbulence model	Inlet	Outlet	Air density and dynamic viscosity	Test Scenario
B1	Coupled	No	k-ε	Wind log profile	Actual curve fan	Default	N/A

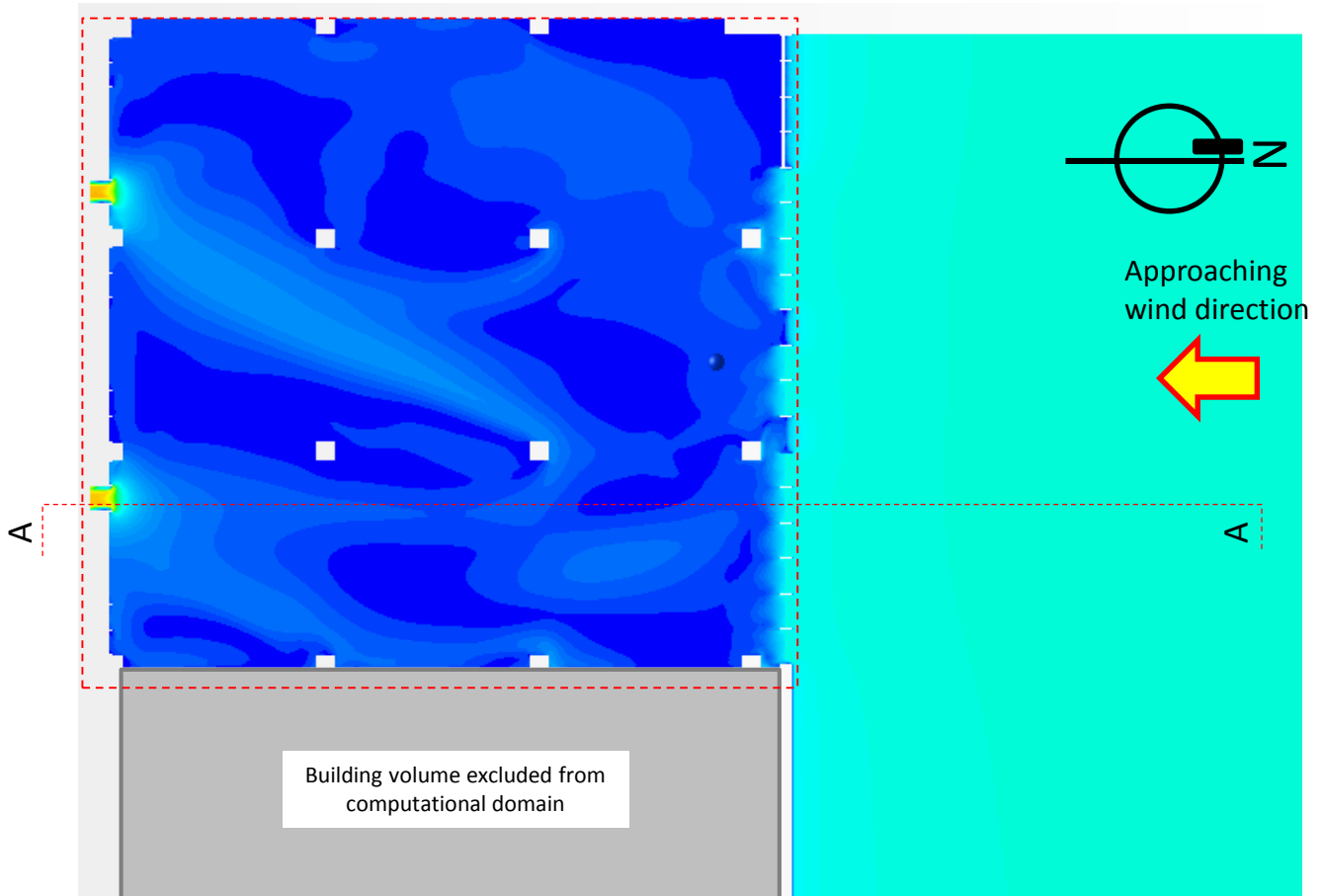


Residual plot

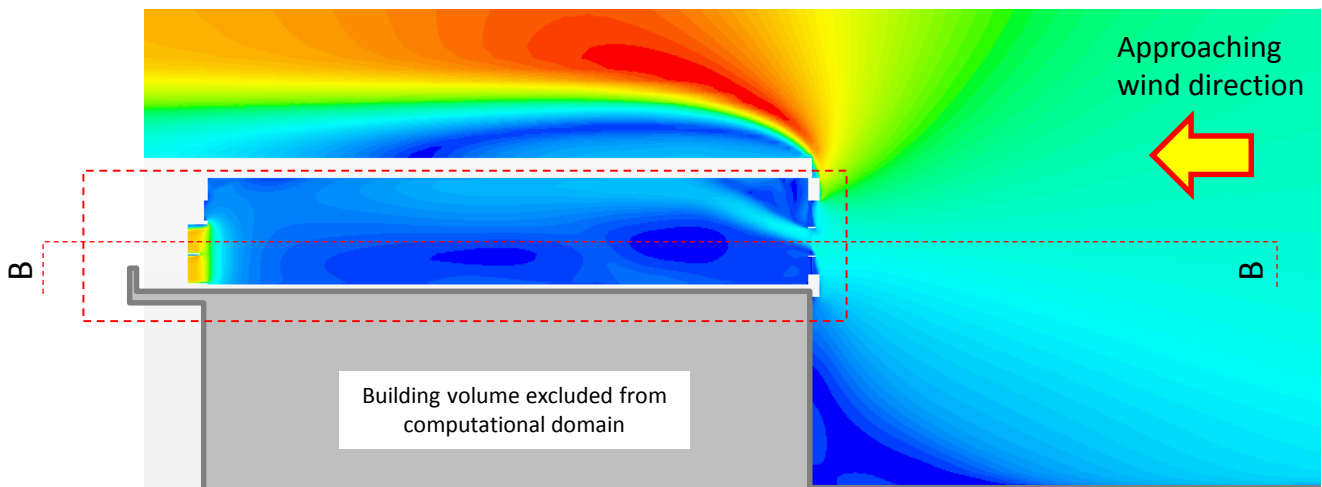


Monitoring plot of wind speed at the point-type probe for convergence checking

Solution ID	Coupled / Decoupled	With furniture	Turbulence model	Inlet	Outlet	Air density and dynamic viscosity	Test Scenario
B2	Coupled	No	k- ω	Wind log profile	Actual curve fan	Default	N/A



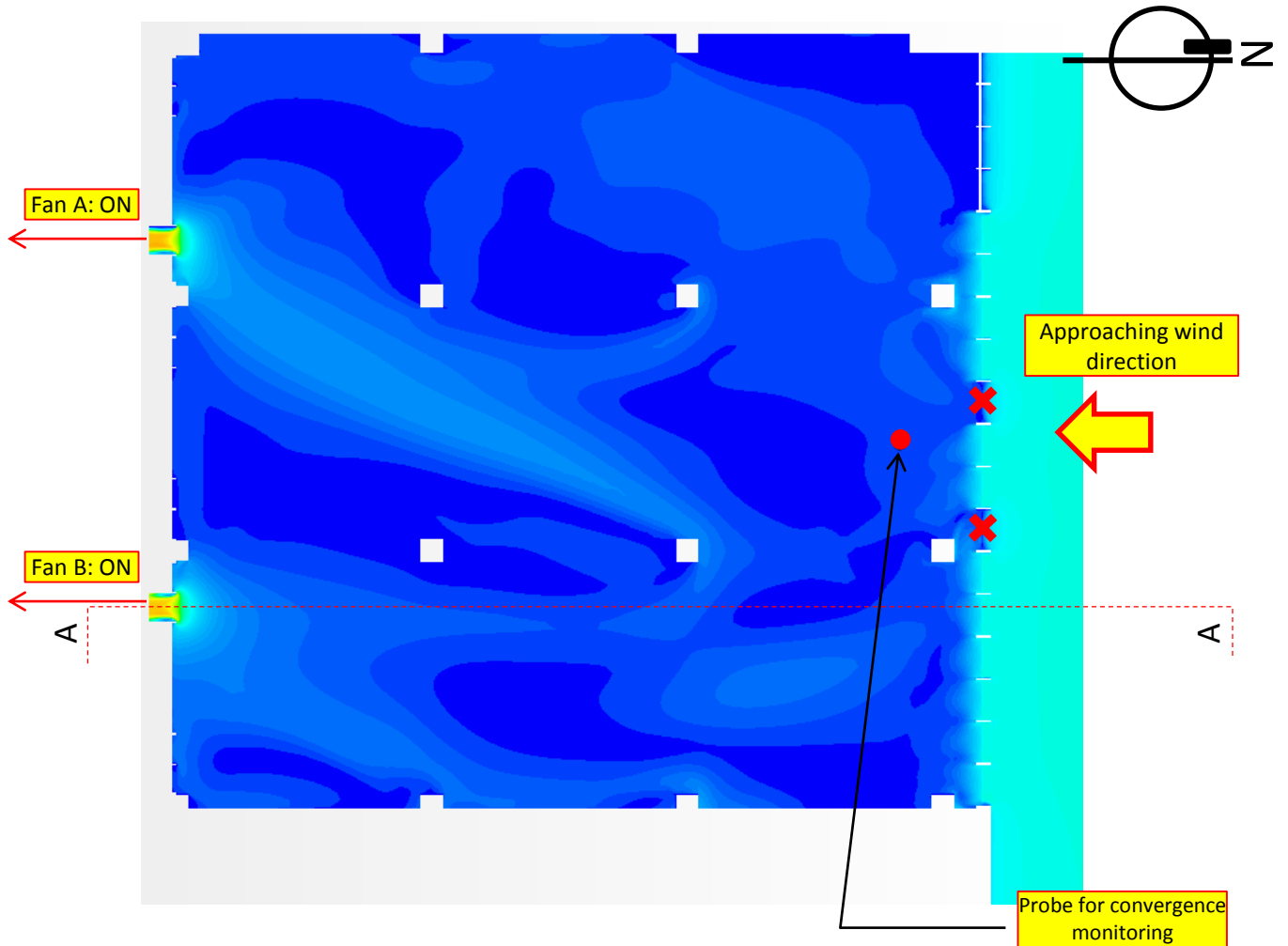
Velocity contoured map on the horizontal plane B-B of 4 feet (1.2m) above the floor (larger view)



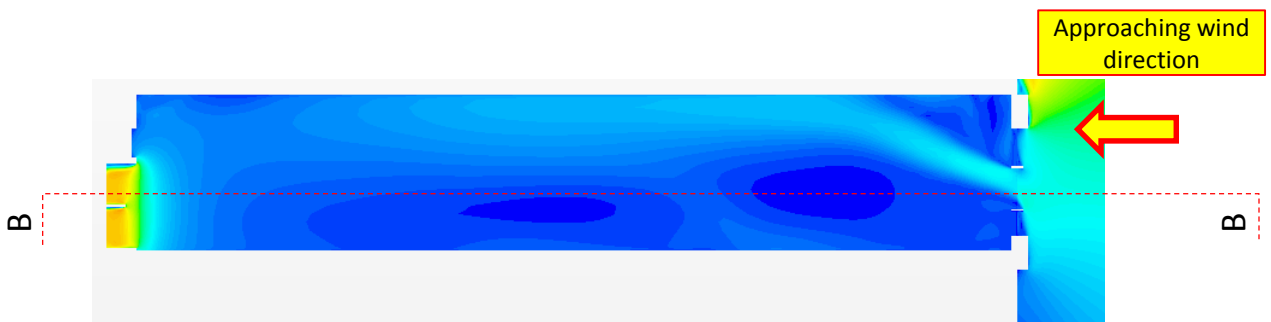
Velocity contoured map on the vertical plane A-A (larger view)



Solution ID	Coupled / Decoupled	With furniture	Turbulence model	Inlet	Outlet	Air density and dynamic viscosity	Test Scenario
B2	Coupled	No	k- ω	Wind log profile	Actual curve fan	Default	N/A



Detailed velocity contoured map on the horizontal plane B-B of 4 feet (1.2m) above the floor

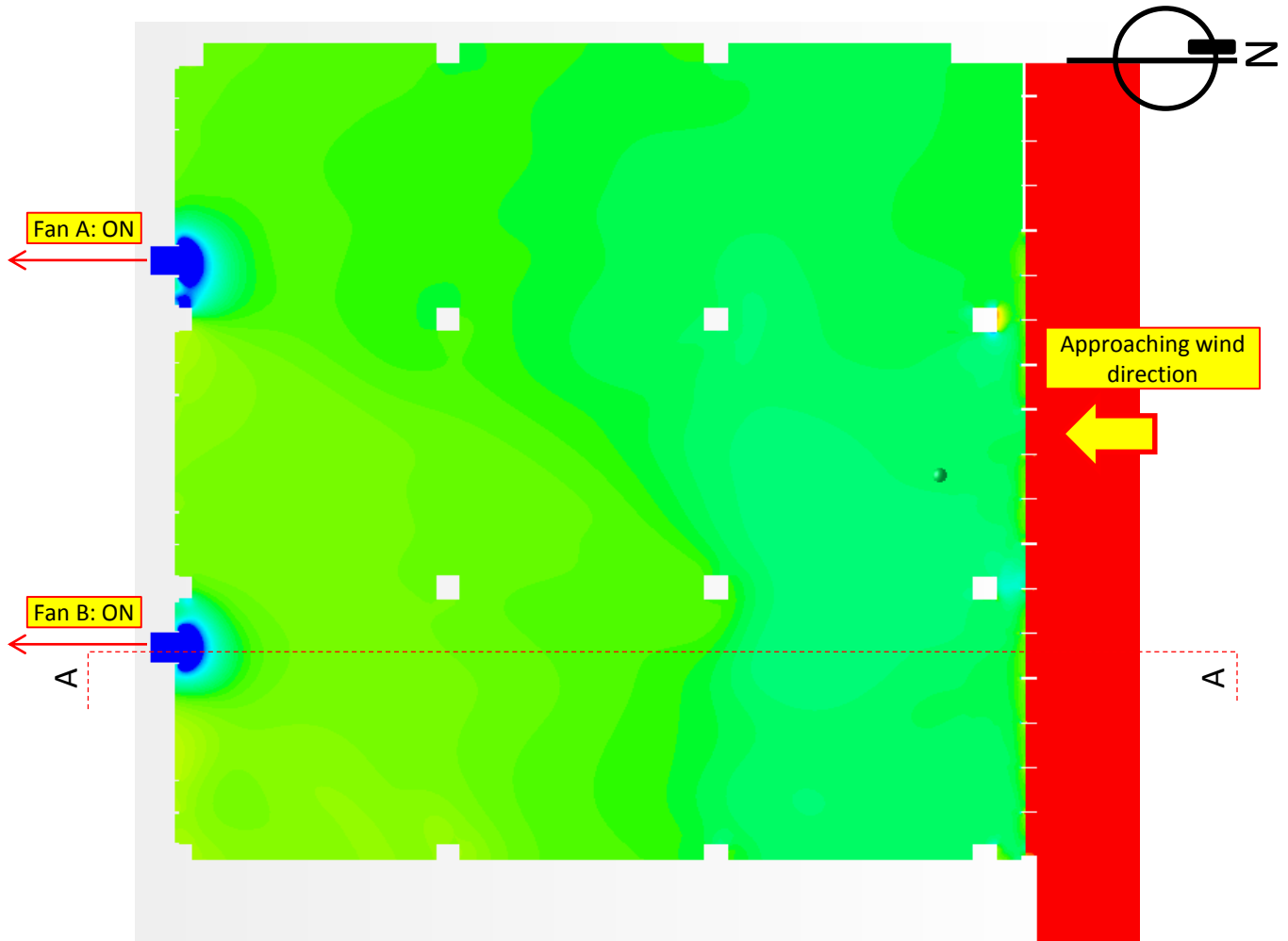


Detailed velocity contoured map on the vertical plane A-A

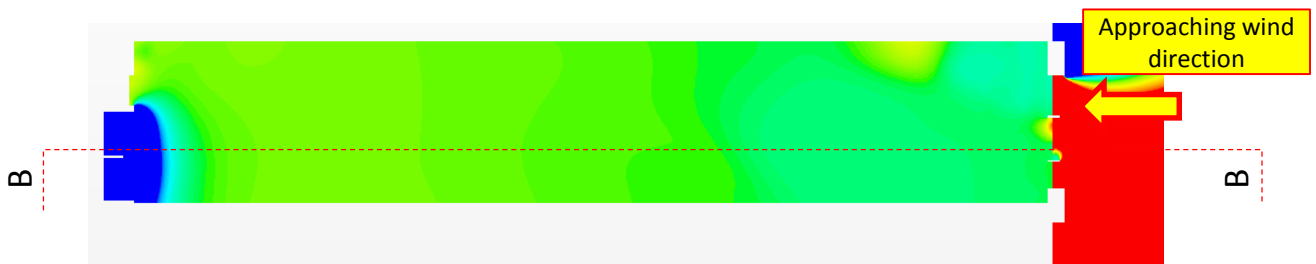


X Permanently closed non-working louvers

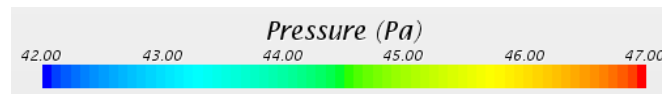
Solution ID	Coupled / Decoupled	With furniture	Turbulence model	Inlet	Outlet	Air density and dynamic viscosity	Test Scenario
B2	Coupled	No	k- ω	Wind log profile	Actual curve fan	Default	N/A



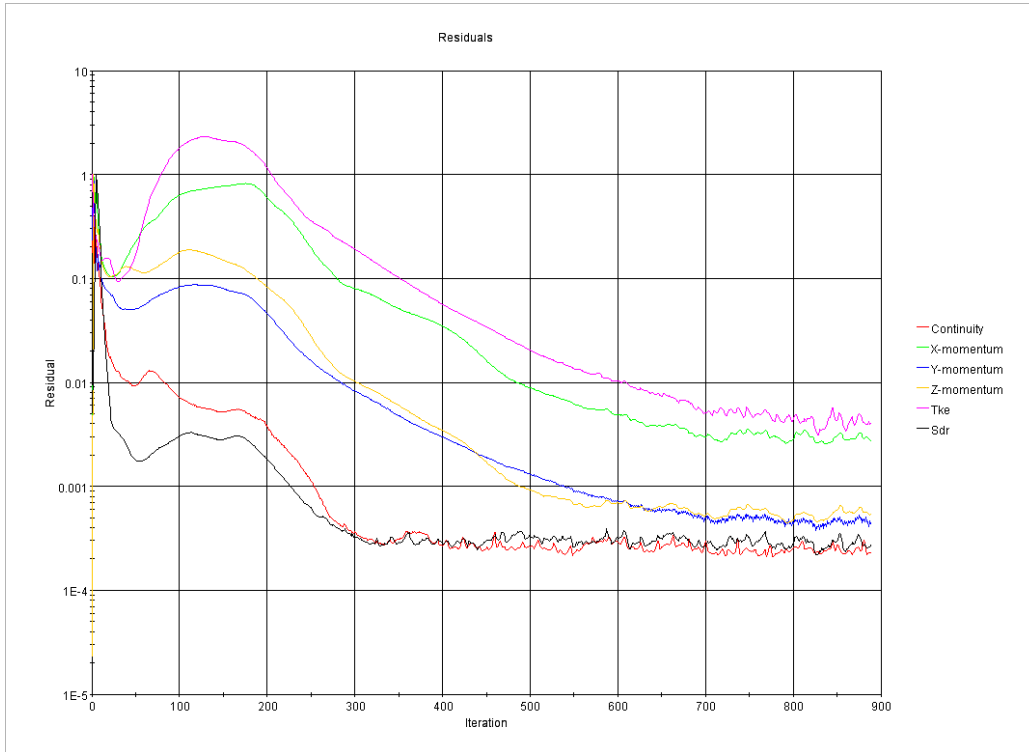
Detailed pressure contoured map on the horizontal plane B-B of 4 feet (1.2m) above the floor



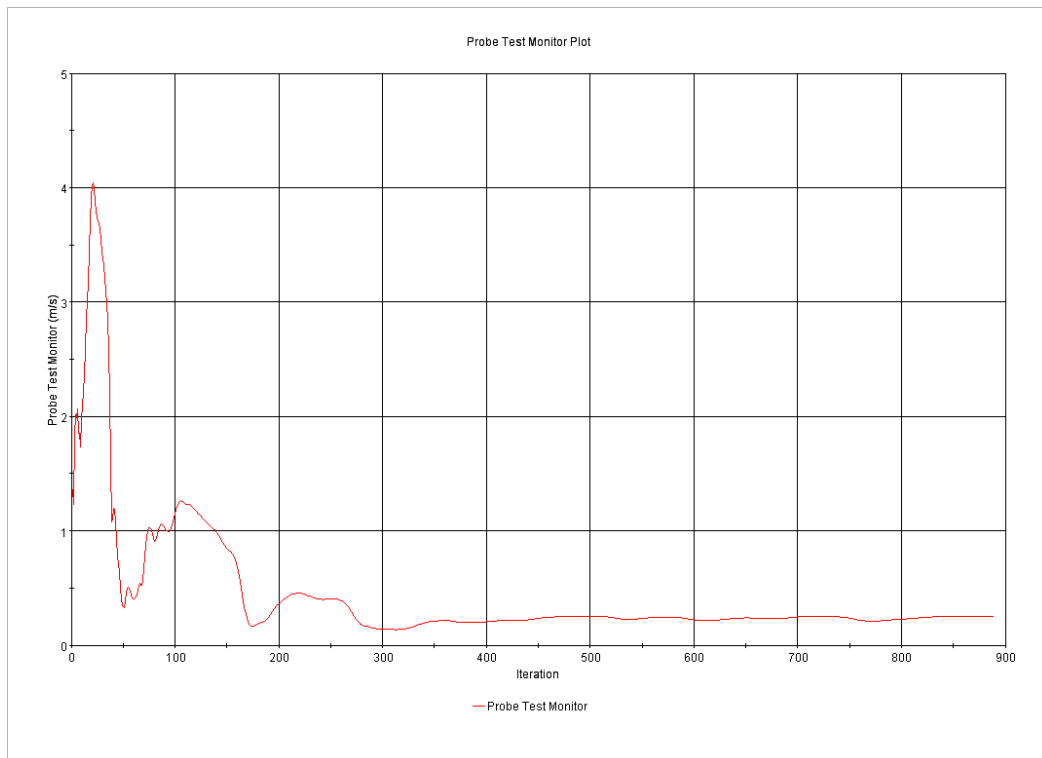
Detailed pressure contoured map on the vertical plane A-A



Solution ID	Coupled / Decoupled	With furniture	Turbulence model	Inlet	Outlet	Air density and dynamic viscosity	Test Scenario
B2	Coupled	No	k- ω	Wind log profile	Actual curve fan	Default	N/A

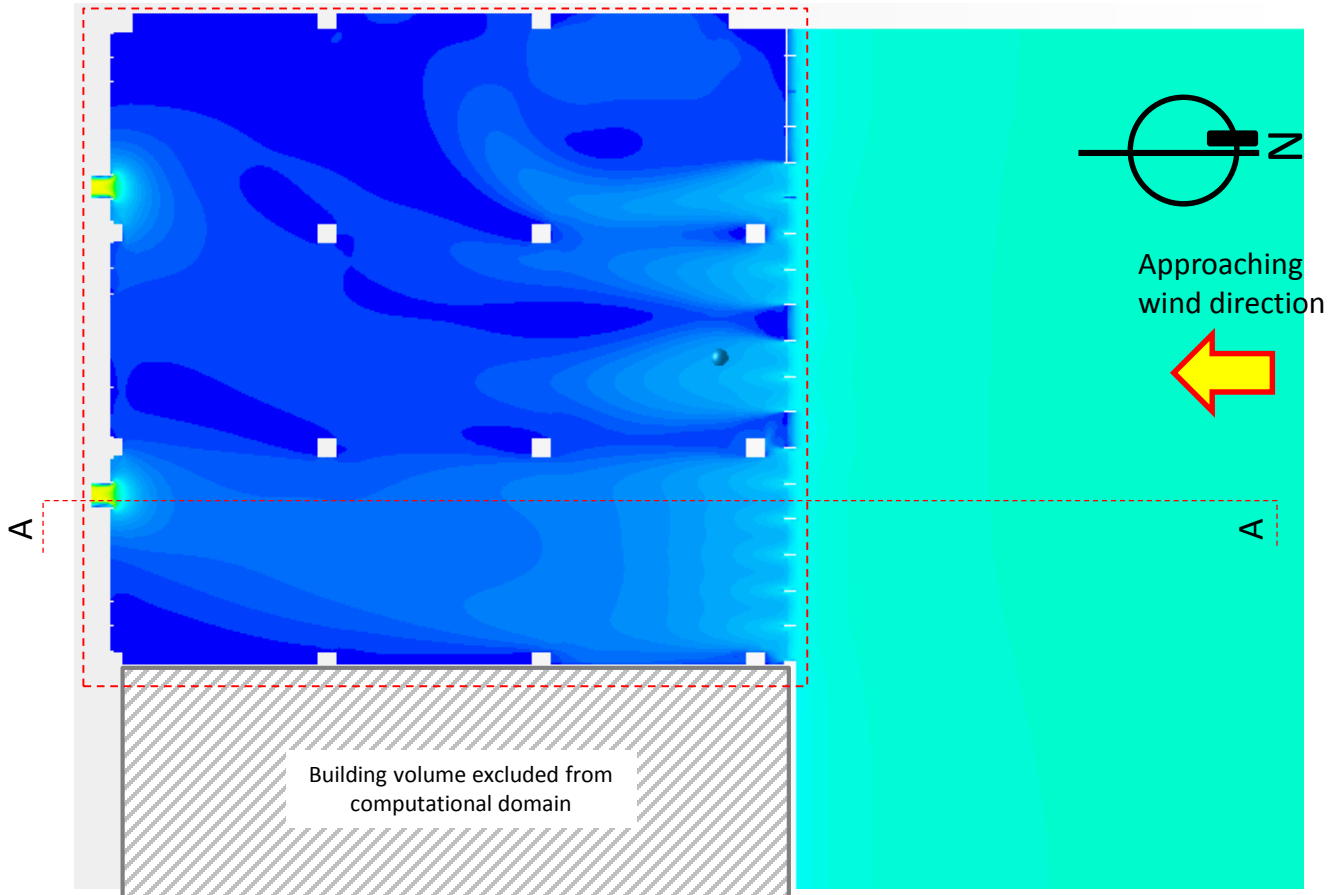


Residual plot

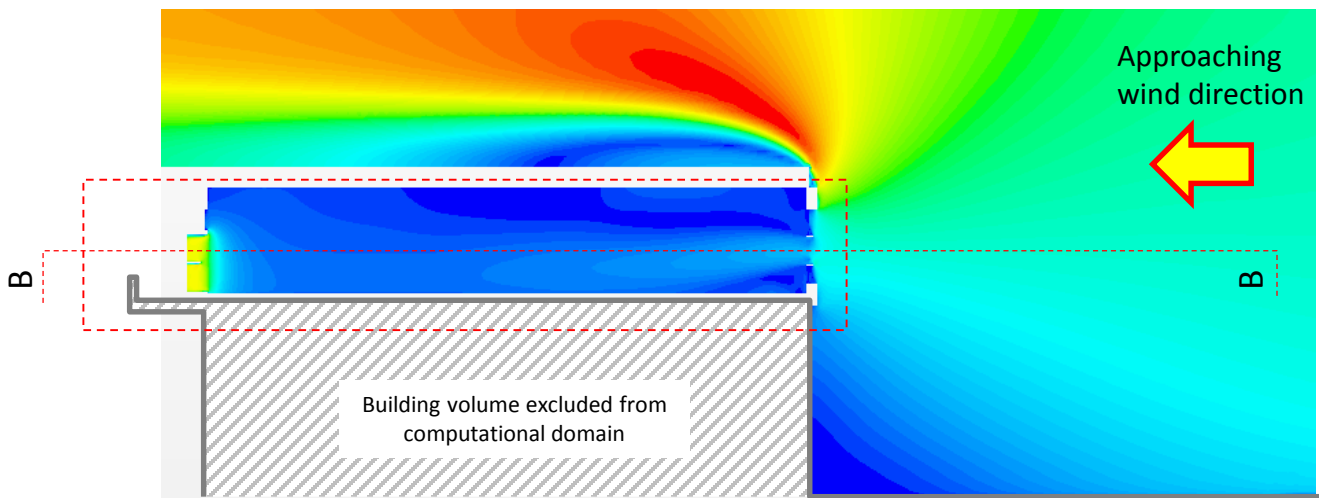


Monitoring plot of wind speed at the point-type probe for convergence checking

Solution ID	Coupled / Decoupled	With furniture	Turbulence model	Inlet	Outlet	Air density and dynamic viscosity	Test Scenario
B3	Coupled	No	k-ε	Wind log profile	Actual curve fan	Actual test condition	N/A



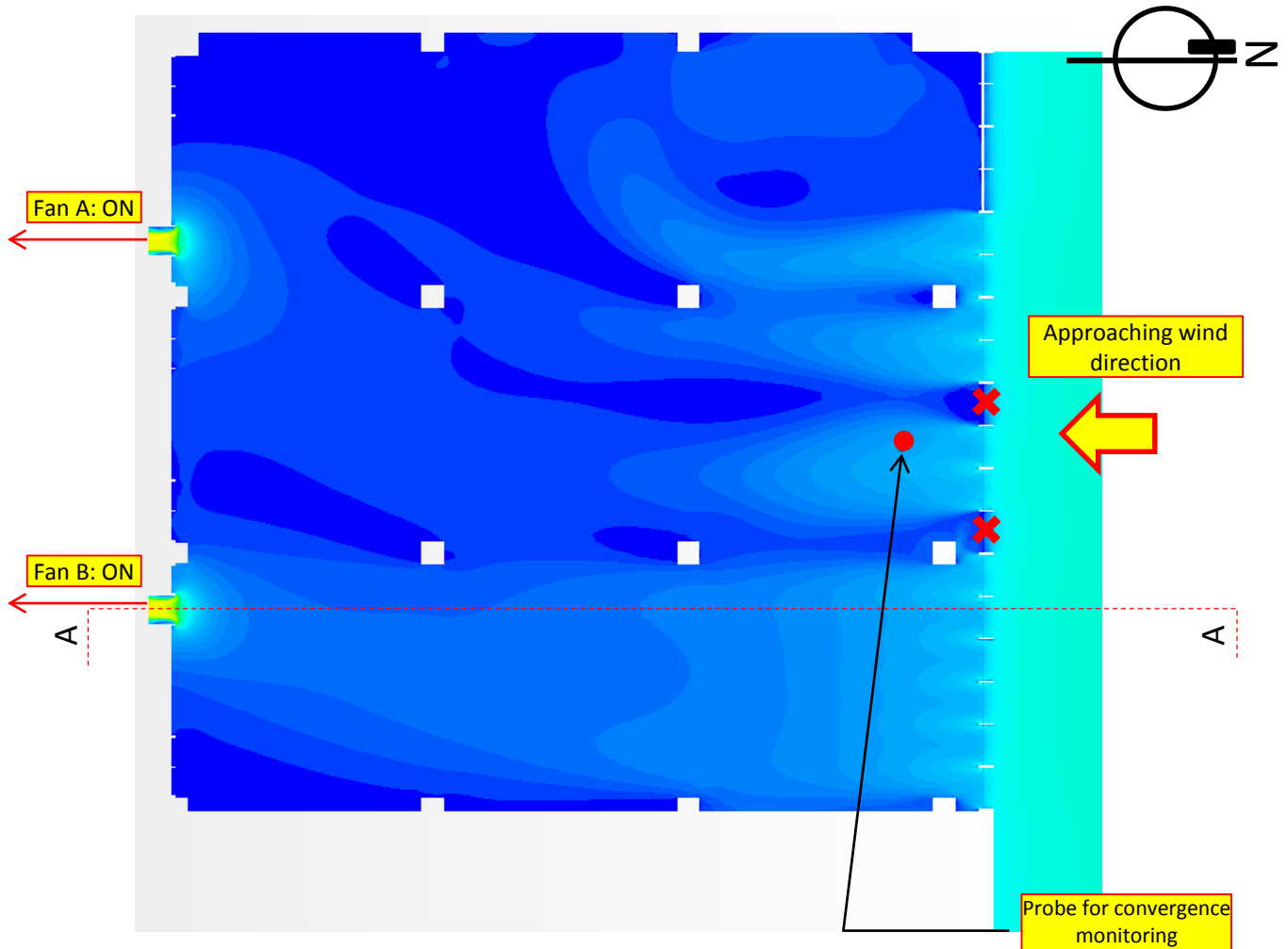
Velocity contoured map on the horizontal plane B-B of 4 feet (1.2m) above the floor (larger view)



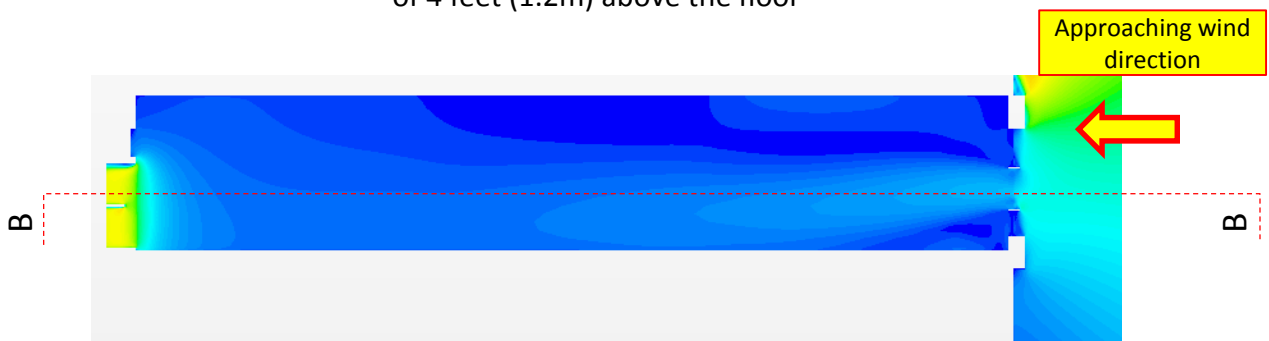
Velocity contoured map on the vertical plane A-A (larger view)



Solution ID	Coupled / Decoupled	With furniture	Turbulence model	Inlet	Outlet	Air density and dynamic viscosity	Test Scenario
B3	Coupled	No	k-ε	Wind log profile	Actual curve fan	Actual test condition	N/A



Detailed velocity contoured map on the horizontal plane B-B of 4 feet (1.2m) above the floor

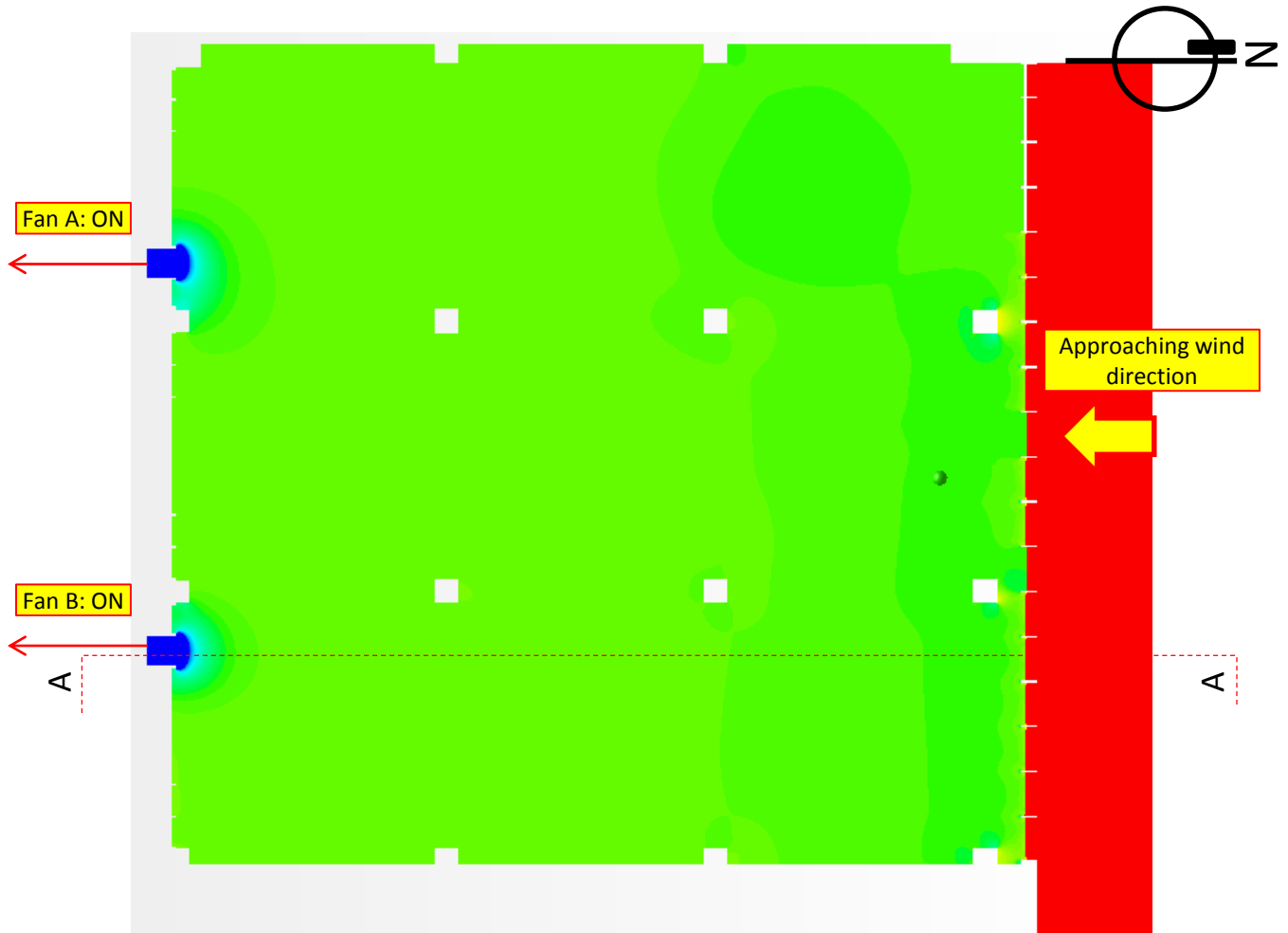


Detailed velocity contoured map on the vertical plane A-A



X Permanently closed non-working louvers

Solution ID	Coupled / Decoupled	With furniture	Turbulence model	Inlet	Outlet	Air density and dynamic viscosity	Test Scenario
B3	Coupled	No	k-ε	Wind log profile	Actual curve fan	Actual test condition	N/A



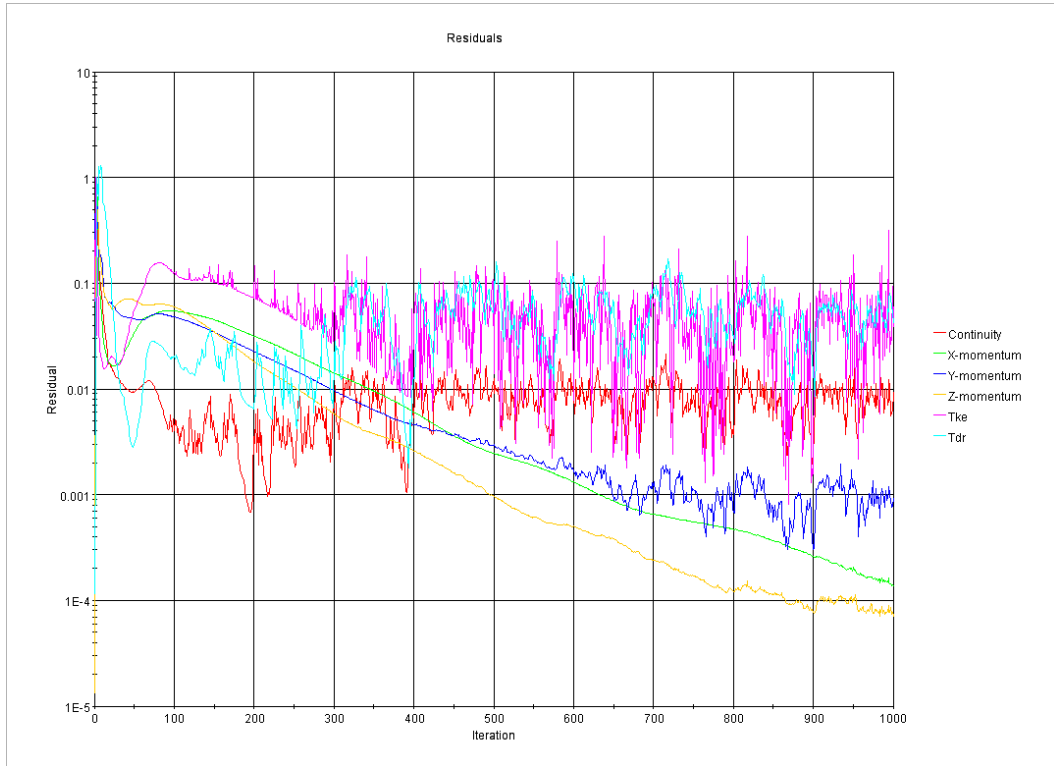
Detailed pressure contoured map on the horizontal plane B-B of 4 feet (1.2m) above the floor



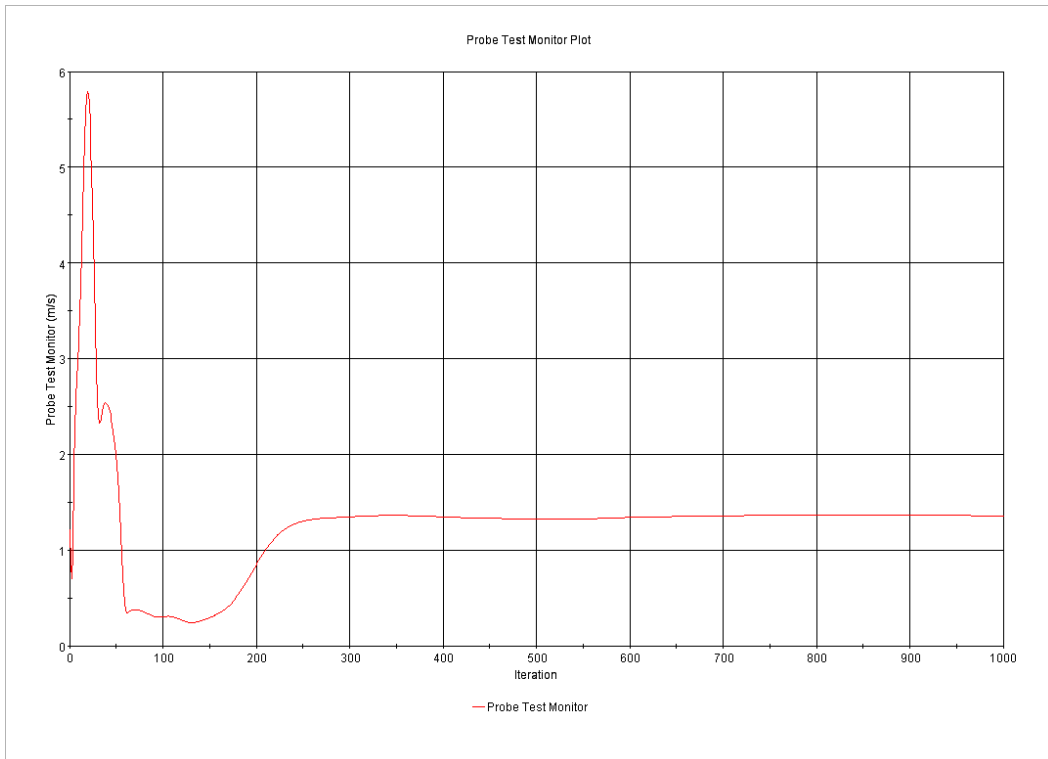
Detailed pressure contoured map on the vertical plane A-A



Solution ID	Coupled / Decoupled	With furniture	Turbulence model	Inlet	Outlet	Air density and dynamic viscosity	Test Scenario
B3	Coupled	No	k-ε	Wind log profile	Actual curve fan	Actual test condition	N/A

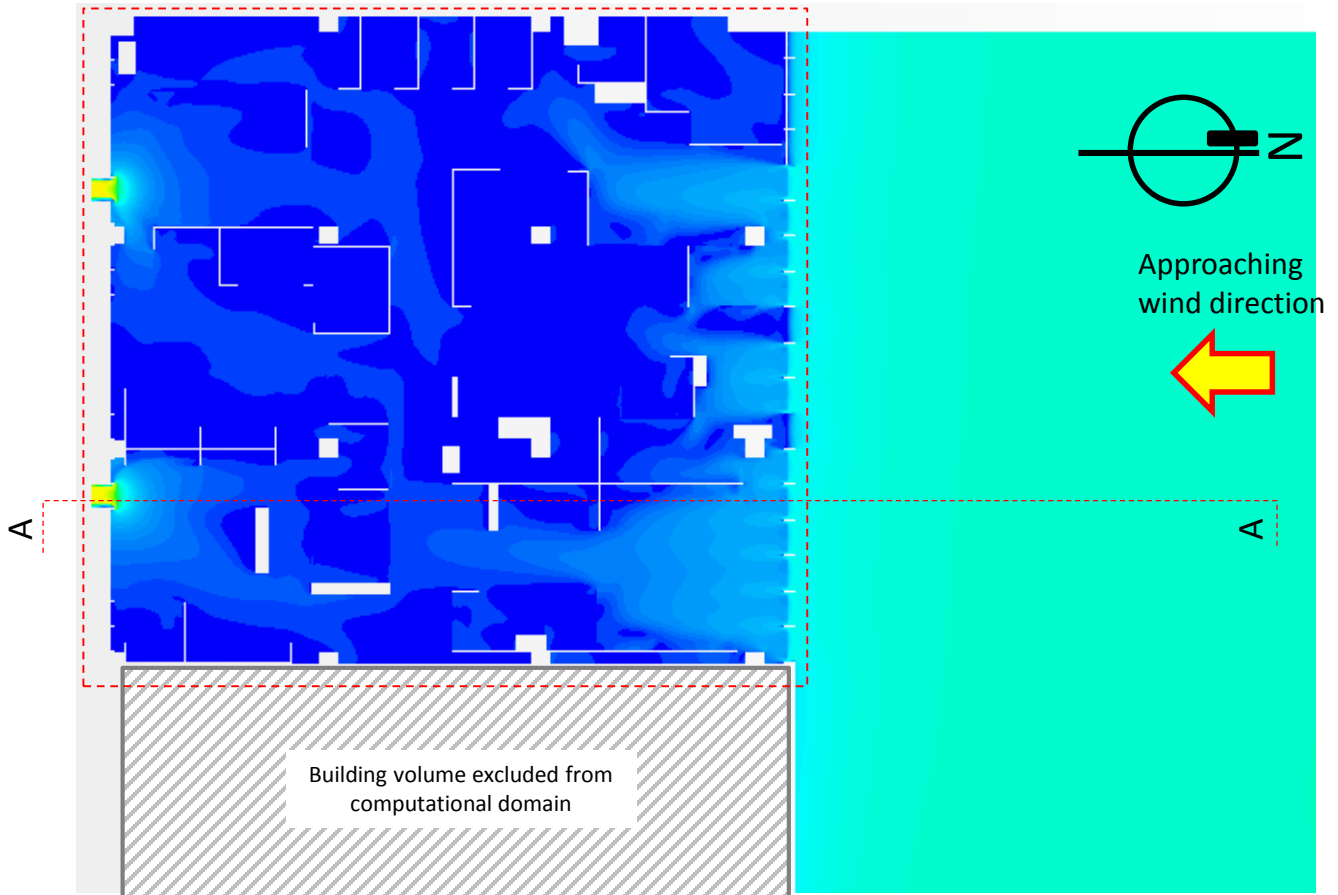


Residual plot

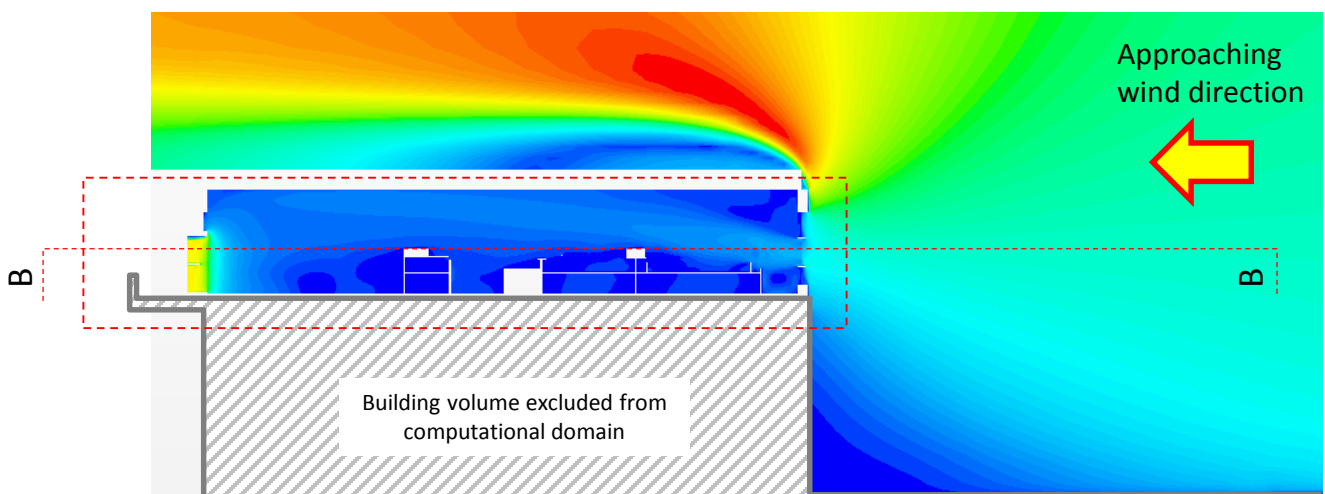


Monitoring plot of wind speed at the point-type probe for convergence checking

Solution ID	Coupled / Decoupled	With furniture	Turbulence model	Inlet	Outlet	Air density and dynamic viscosity	Test Scenario
C	Coupled	Yes	k-ε	Wind log profile	Actual curve fan	Default	N/A



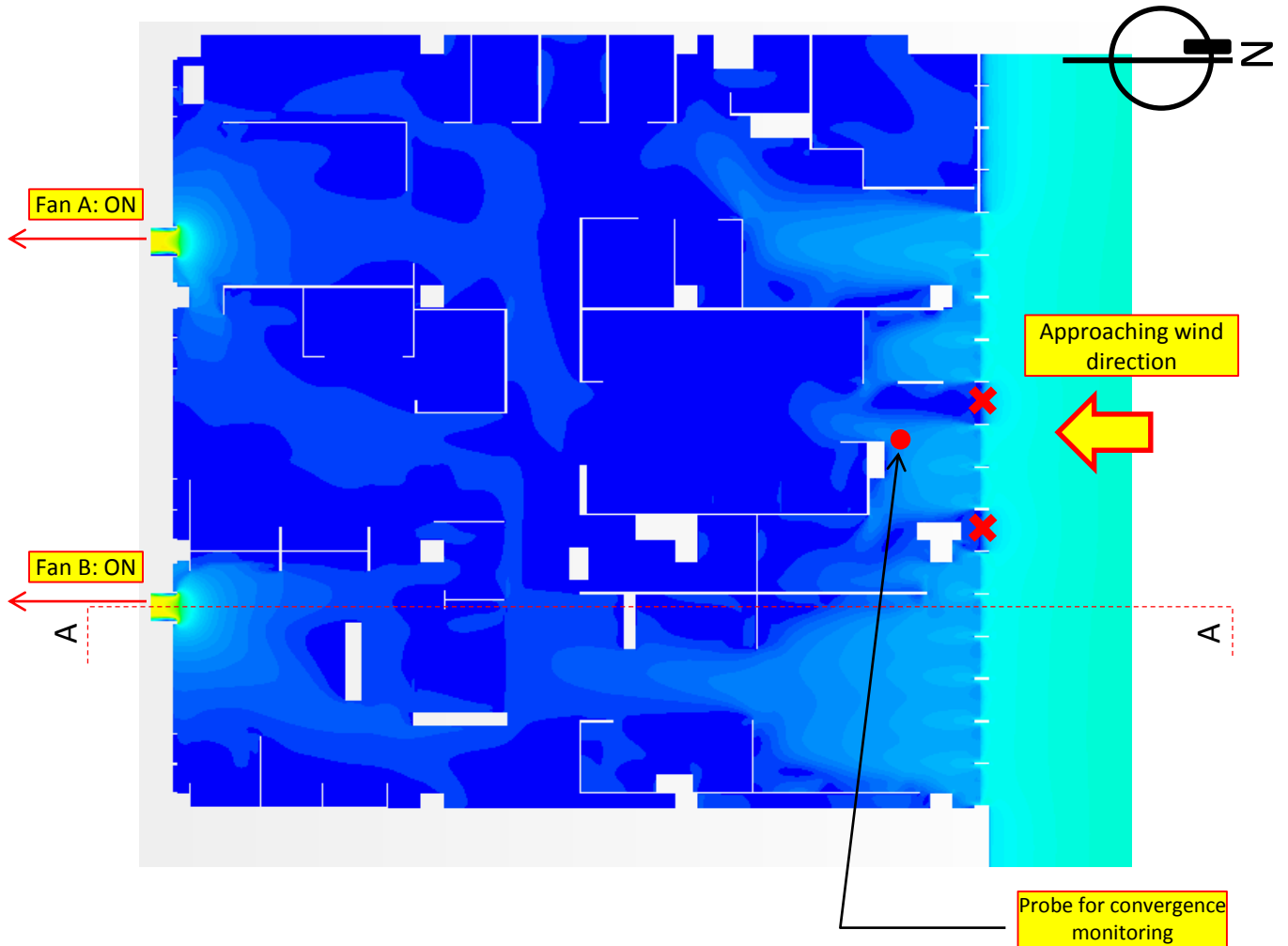
Velocity contoured map on the horizontal plane B-B of 4 feet (1.2m) above the floor (larger view)



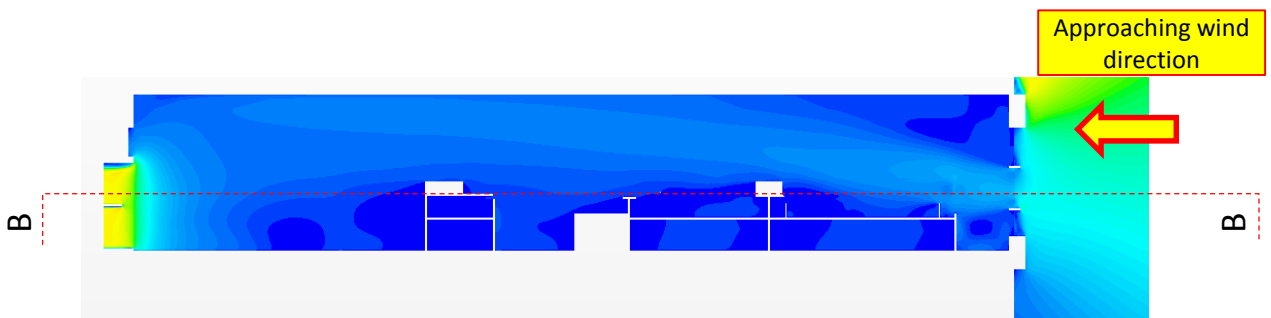
Velocity contoured map on the vertical plane A-A (larger view)



Solution ID	Coupled / Decoupled	With furniture	Turbulence model	Inlet	Outlet	Air density and dynamic viscosity	Test Scenario
C	Coupled	Yes	k-ε	Wind log profile	Actual curve fan	Default	N/A



Detailed velocity contoured map on the horizontal plane B-B of 4 feet (1.2m) above the floor

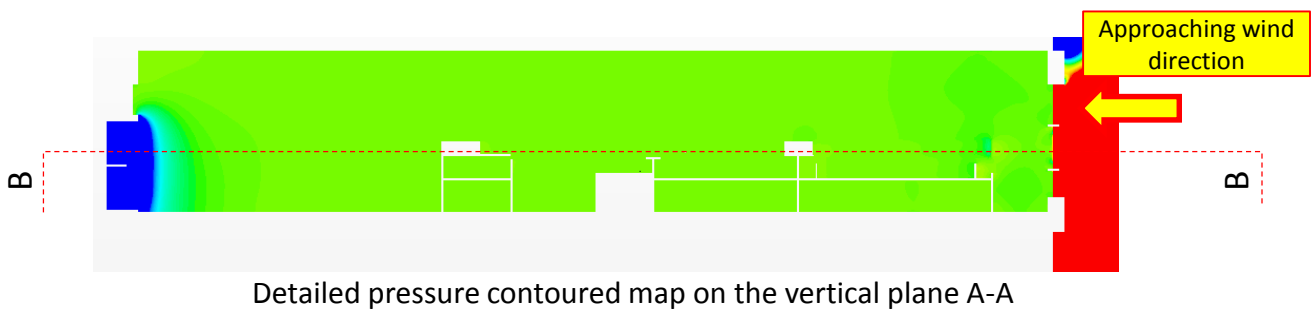
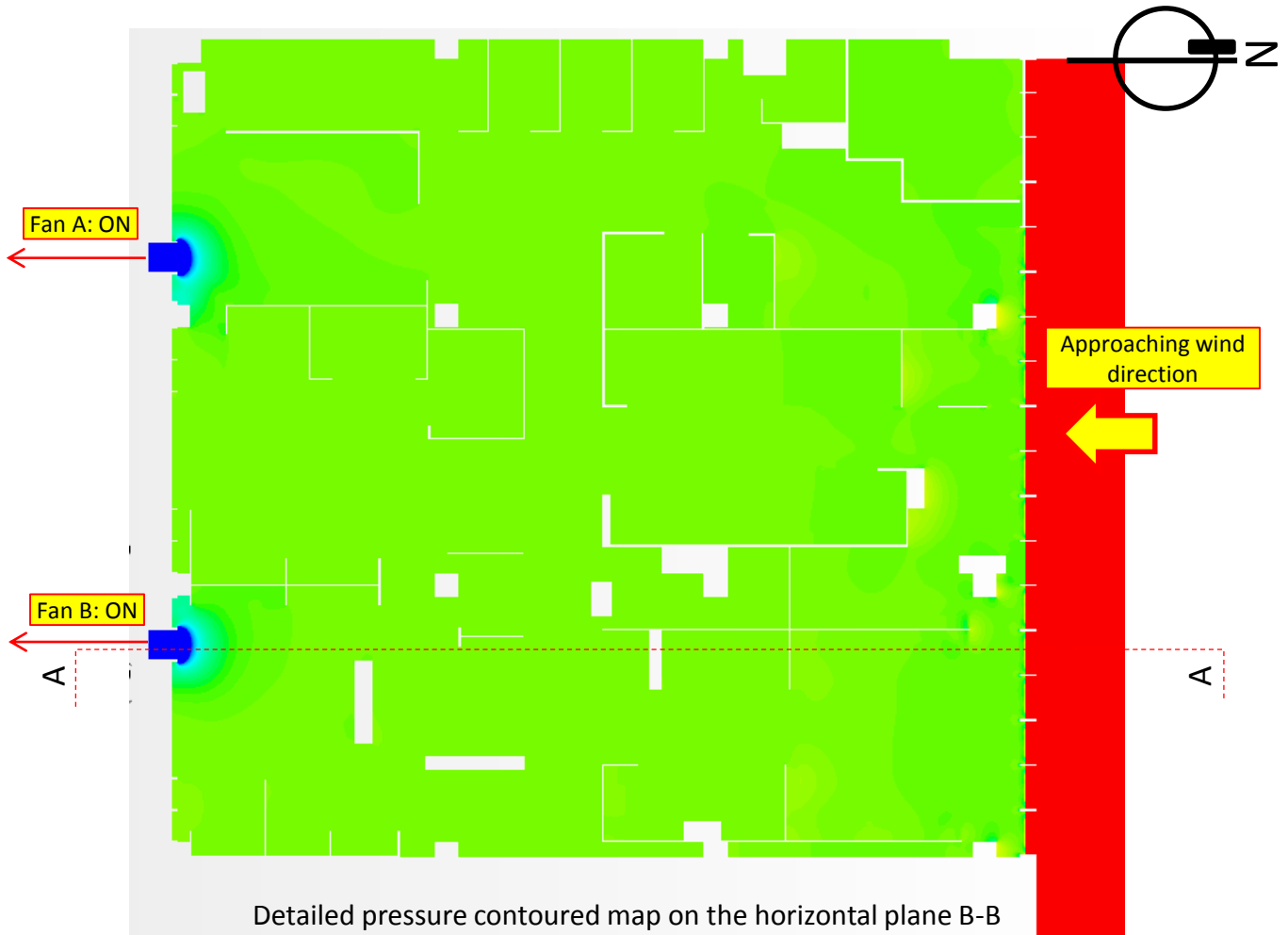


Detailed velocity contoured map on the vertical plane A-A

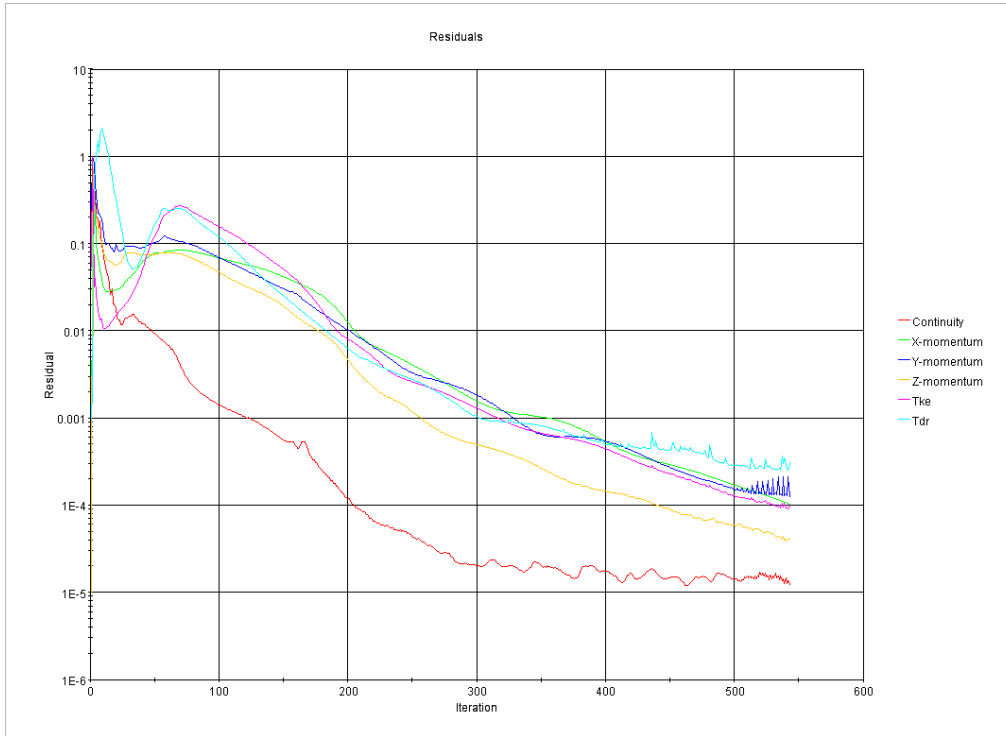


X Permanently closed non-working louvers

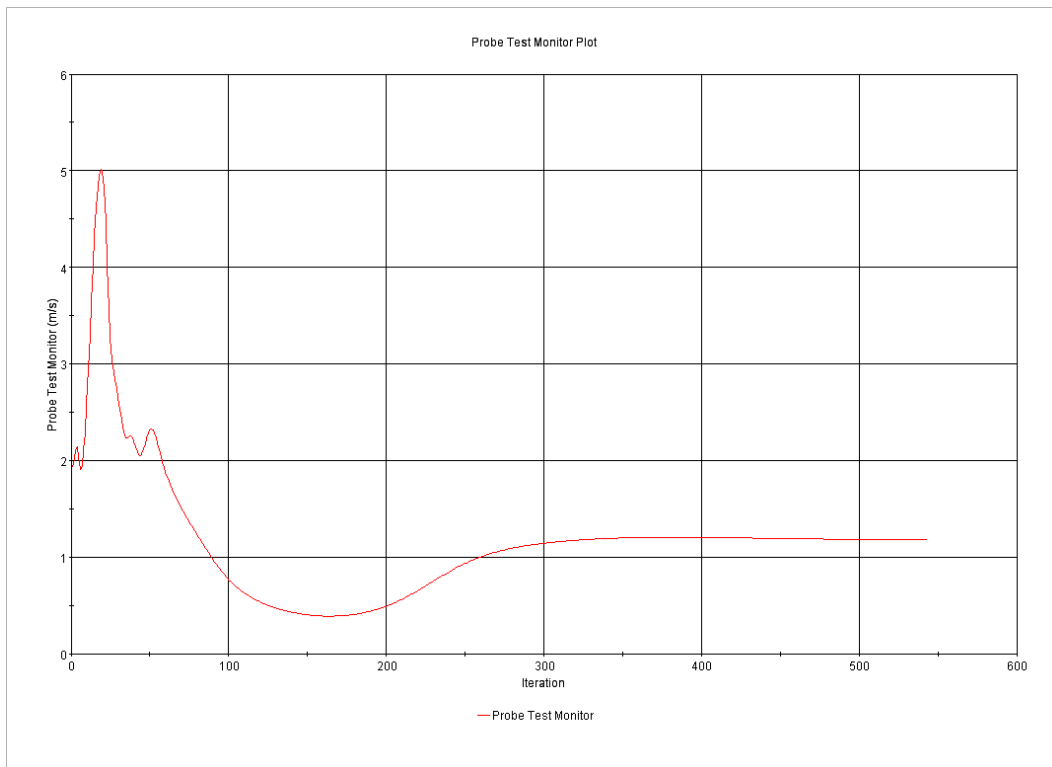
Solution ID	Coupled / Decoupled	With furniture	Turbulence model	Inlet	Outlet	Air density and dynamic viscosity	Test Scenario
C	Coupled	Yes	k-ε	Wind log profile	Actual curve fan	Default	N/A



Solution ID	Coupled / Decoupled	With furniture	Turbulence model	Inlet	Outlet	Air density and dynamic viscosity	Test Scenario
C	Coupled	Yes	k-ε	Wind log profile	Actual curve fan	Default	N/A

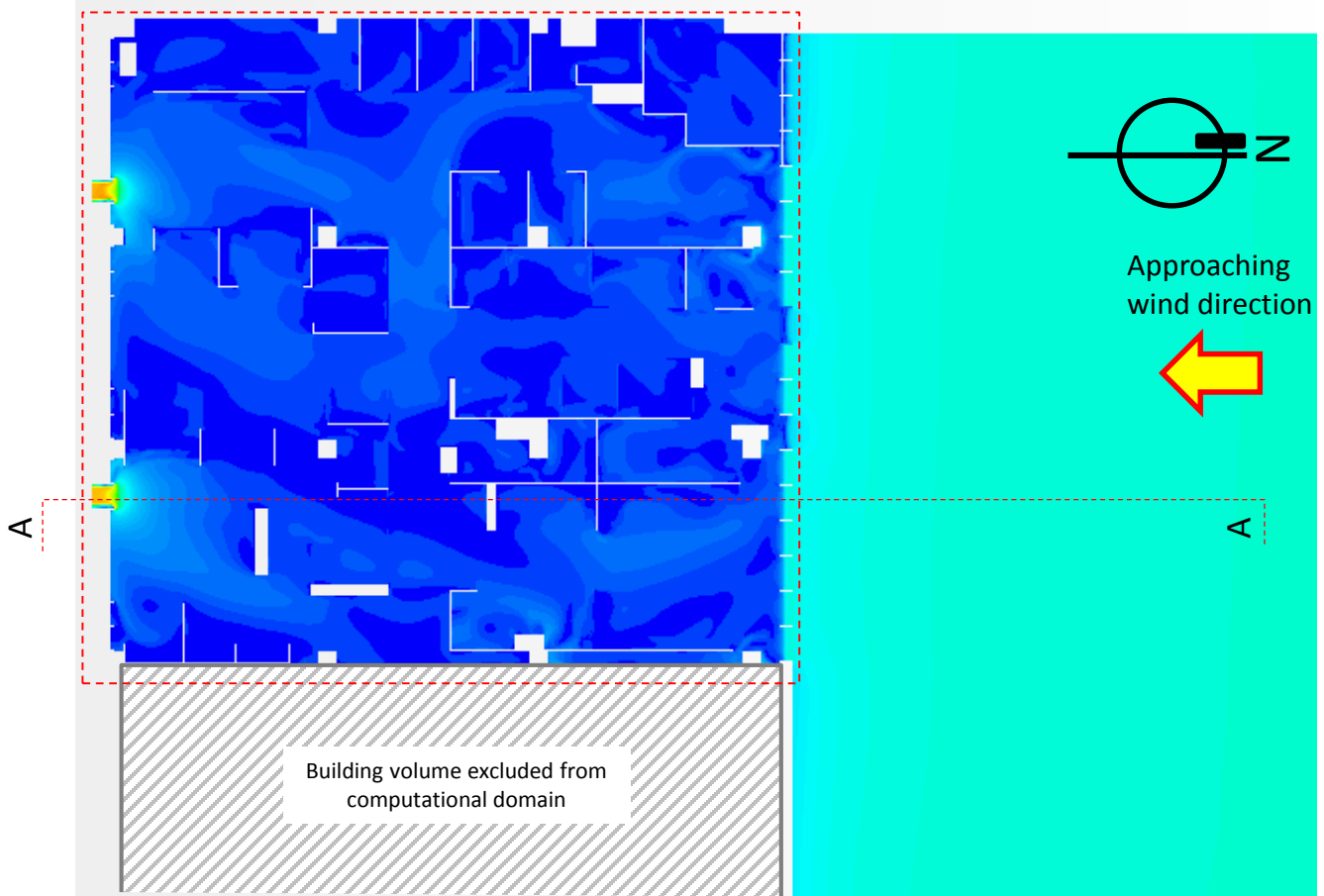


Residual plot

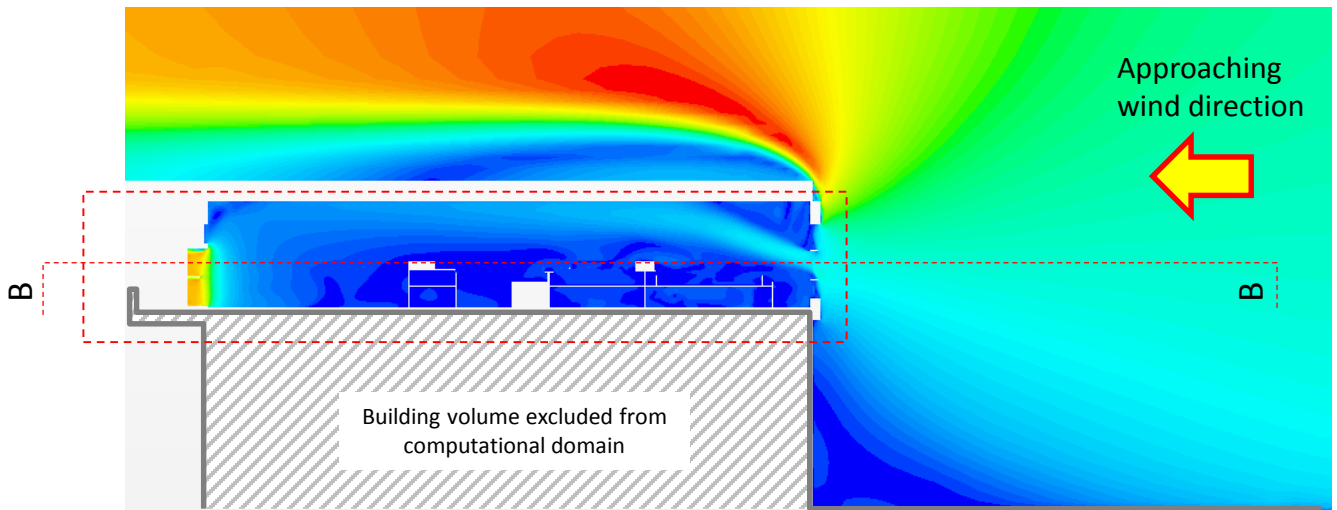


Monitoring plot of wind speed at the point-type probe for convergence checking

Solution ID	Coupled / Decoupled	With furniture	Turbulence model	Inlet	Outlet	Air density and dynamic viscosity	Test Scenario
C1	Coupled	Yes	k- ω	Wind log profile	Actual curve fan	Default	N/A



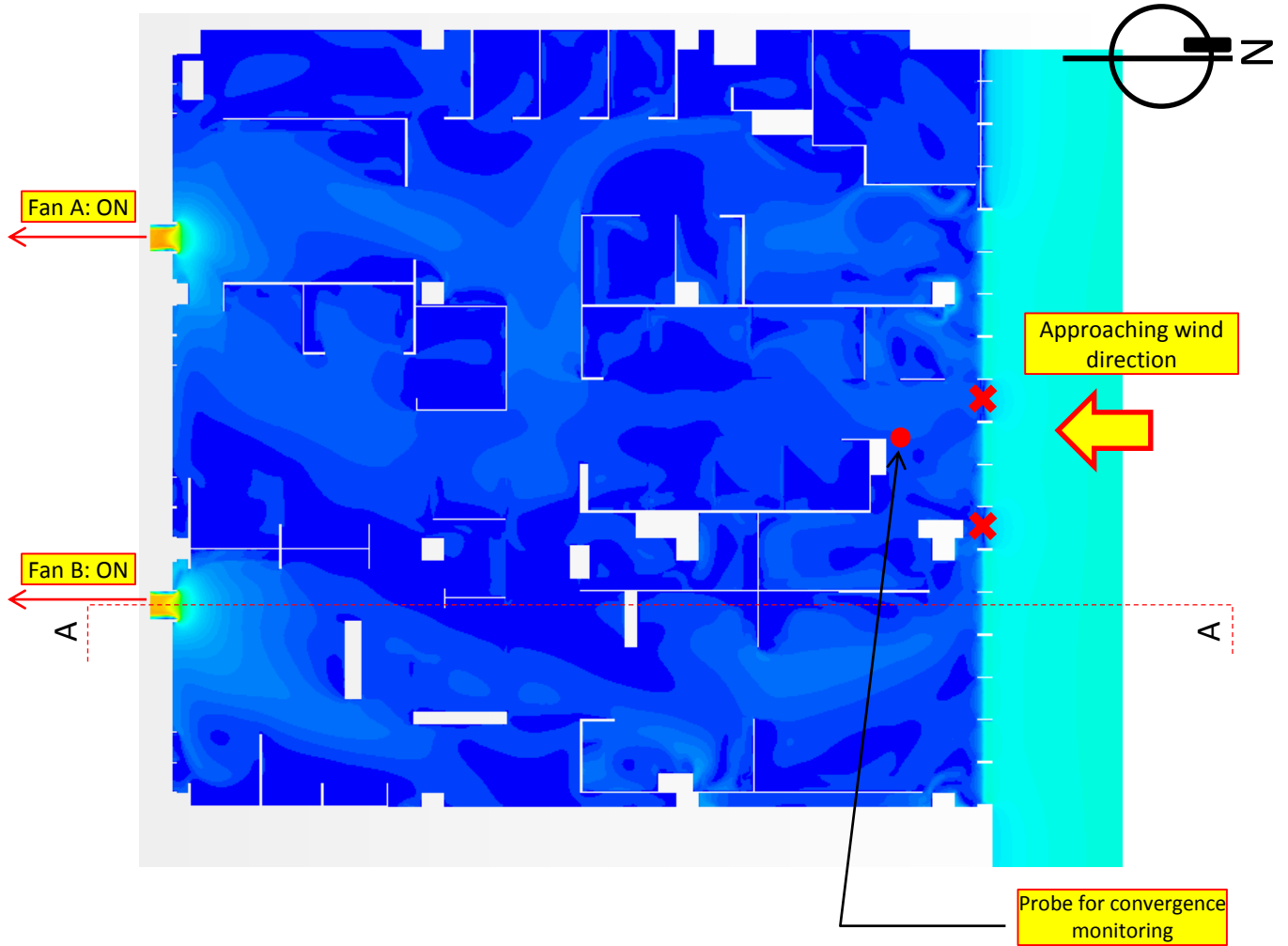
Velocity contoured map on the horizontal plane B-B of 4 feet (1.2m) above the floor (larger view)



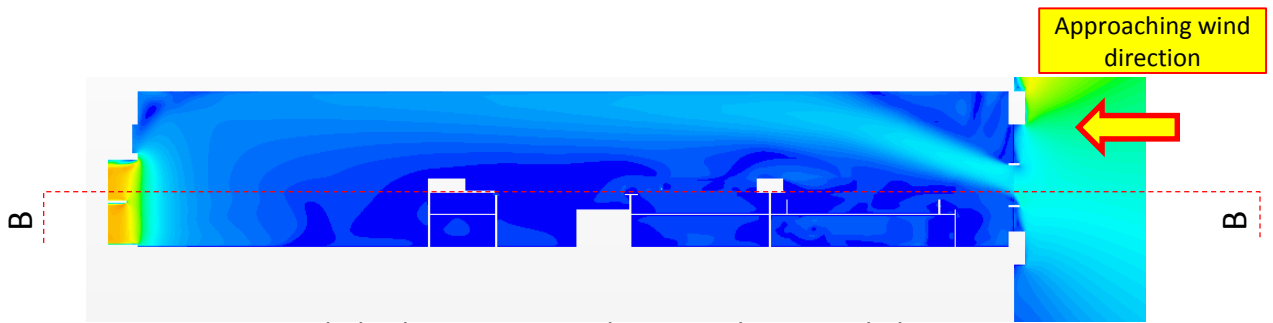
Velocity contoured map on the vertical plane A-A (larger view)



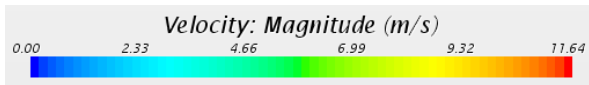
Solution ID	Coupled / Decoupled	With furniture	Turbulence model	Inlet	Outlet	Air density and dynamic viscosity	Test Scenario
C1	Coupled	Yes	k- ω	Wind log profile	Actual curve fan	Default	N/A



Detailed velocity contoured map on the horizontal plane B-B of 4 feet (1.2m) above the floor

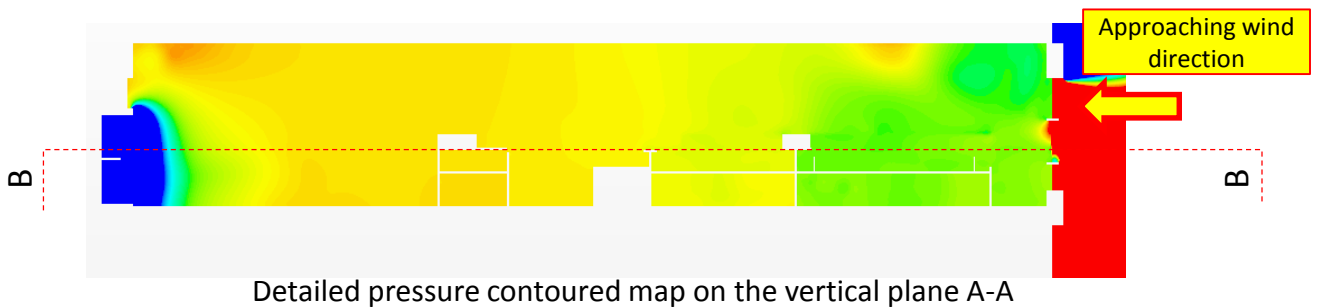
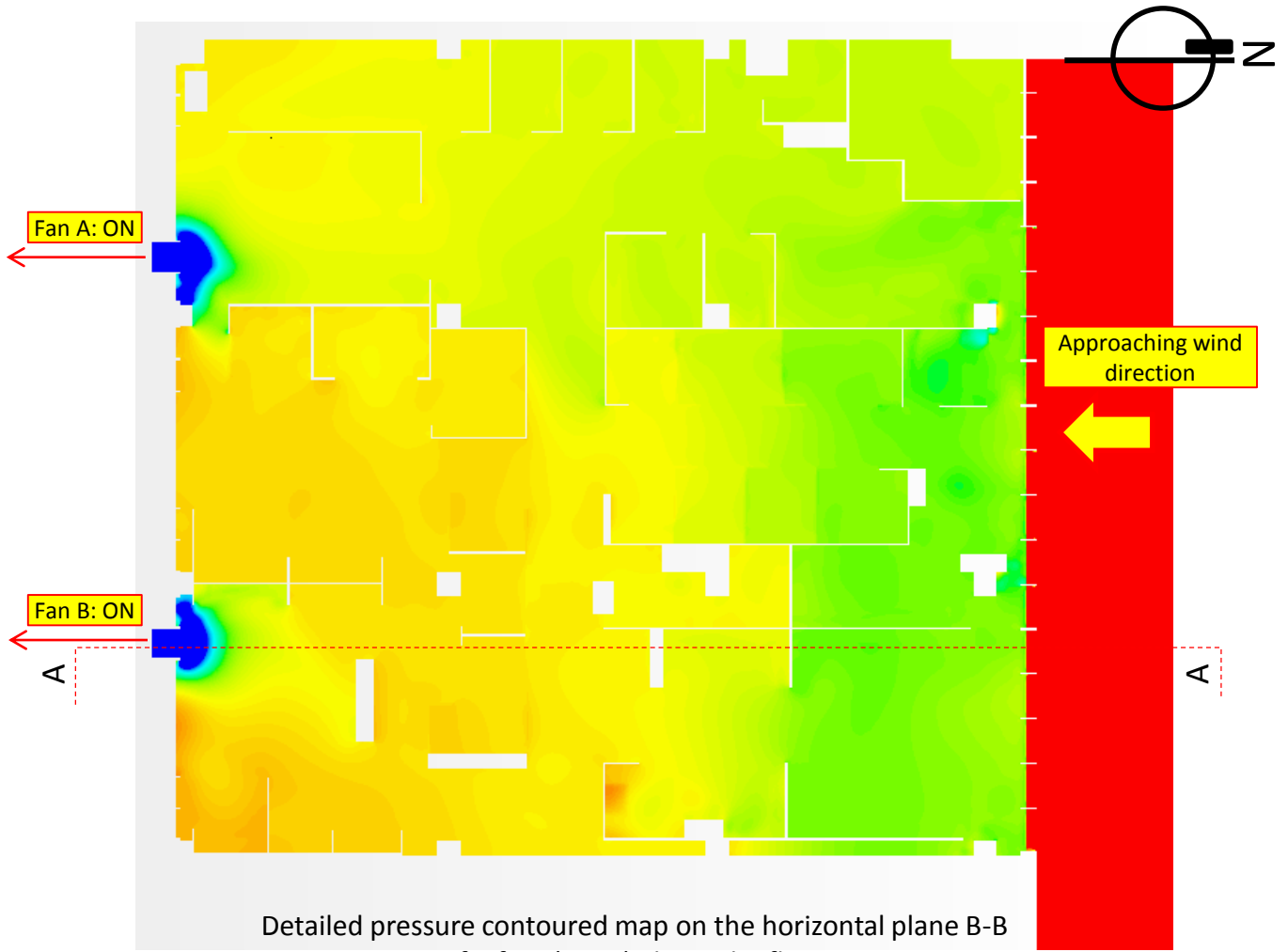


Detailed velocity contoured map on the vertical plane A-A

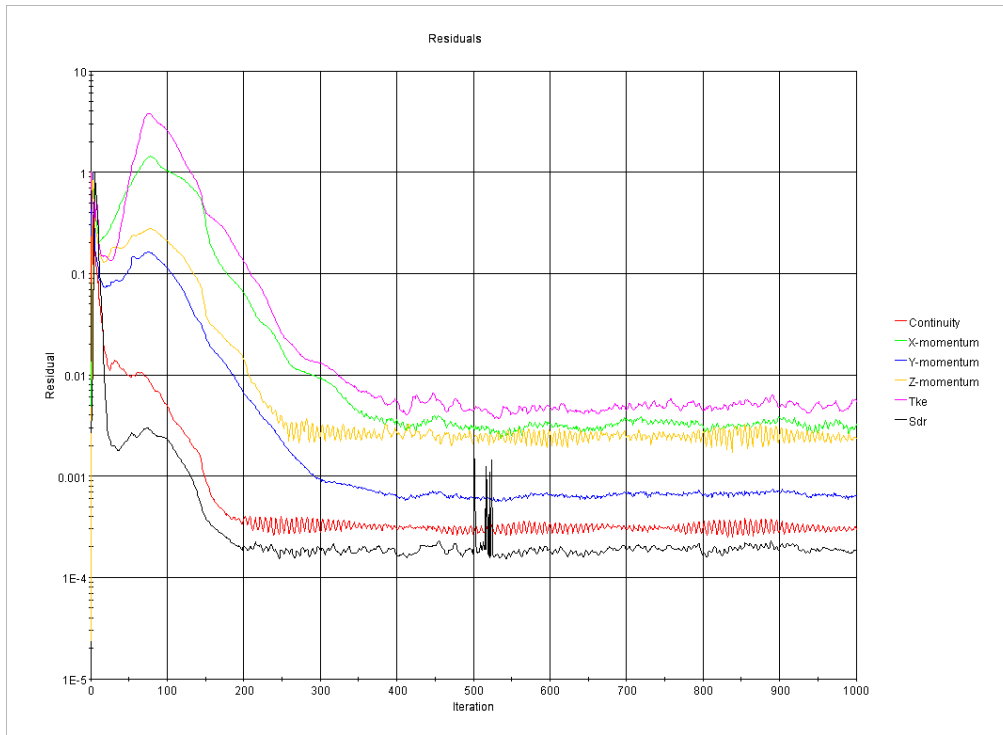


X Permanently closed non-working louvers

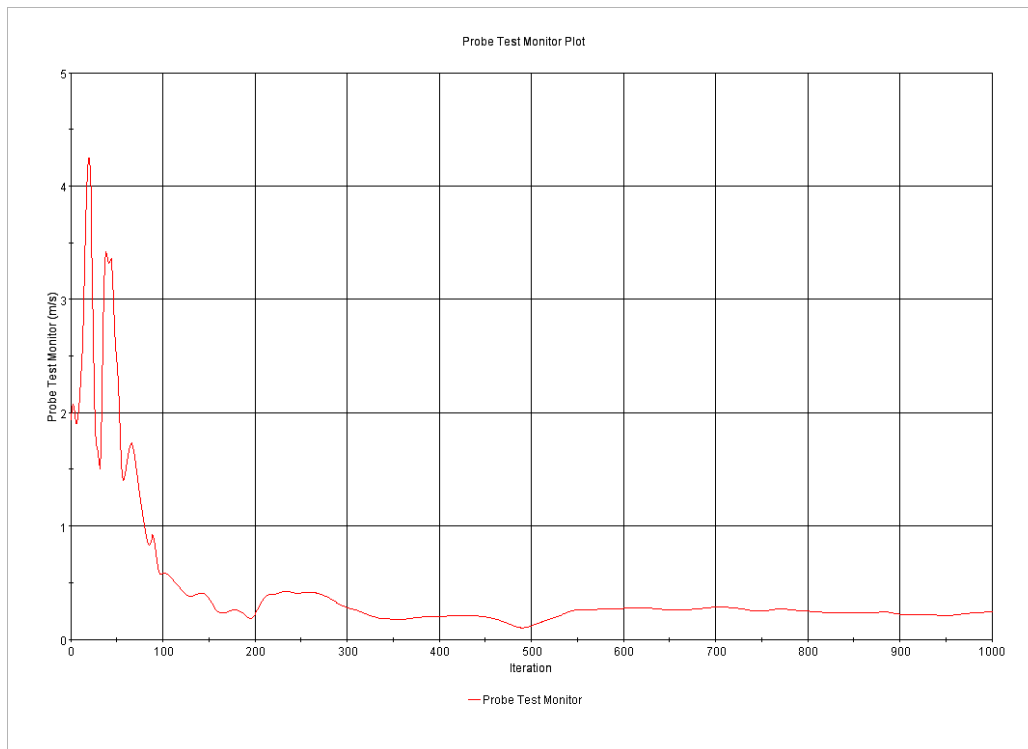
Solution ID	Coupled / Decoupled	With furniture	Turbulence model	Inlet	Outlet	Air density and dynamic viscosity	Test Scenario
C1	Coupled	Yes	k- ω	Wind log profile	Actual curve fan	Default	N/A



Solution ID	Coupled / Decoupled	With furniture	Turbulence model	Inlet	Outlet	Air density and dynamic viscosity	Test Scenario
C1	Coupled	Yes	k- ω	Wind log profile	Actual curve fan	Default	N/A

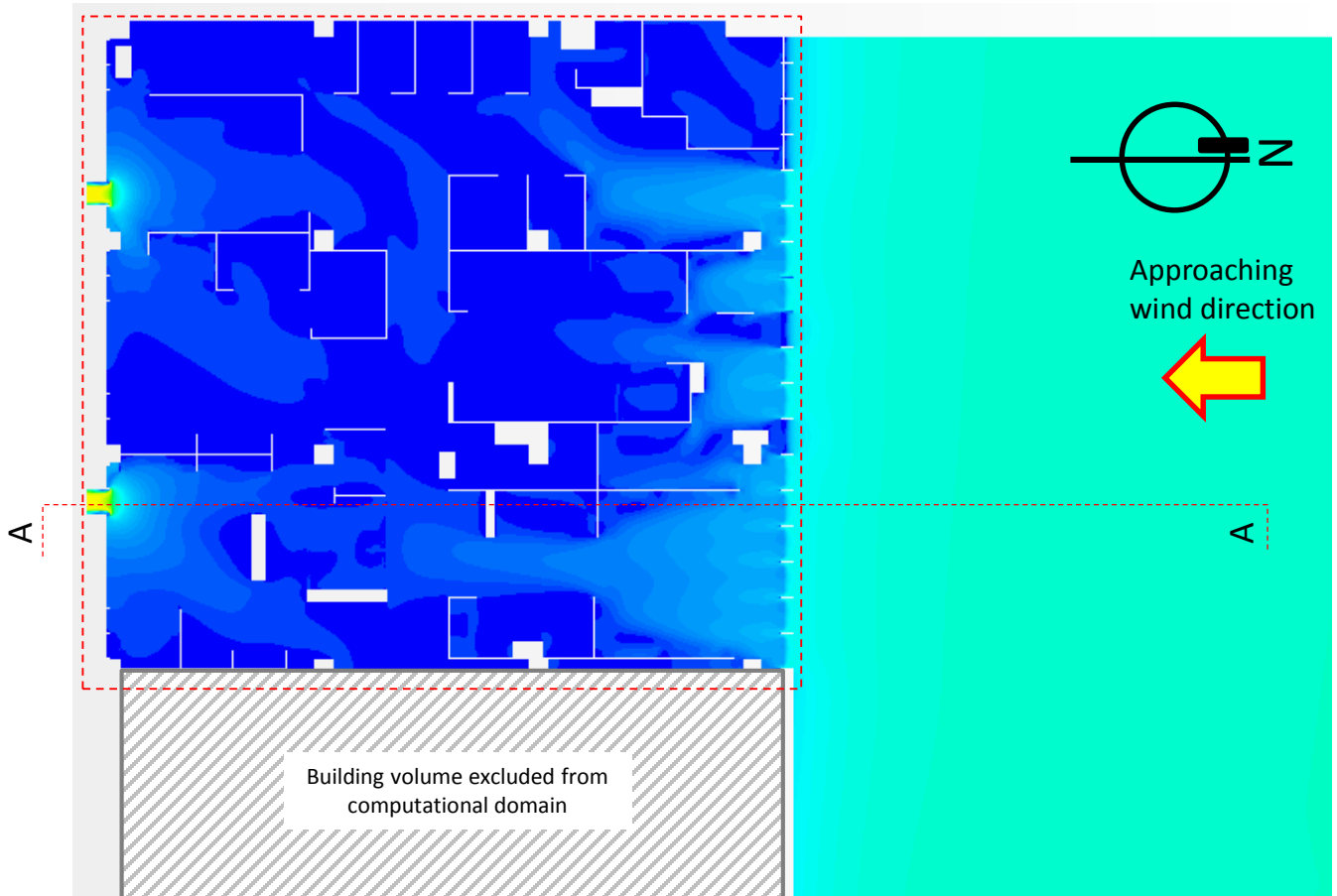


Residual plot

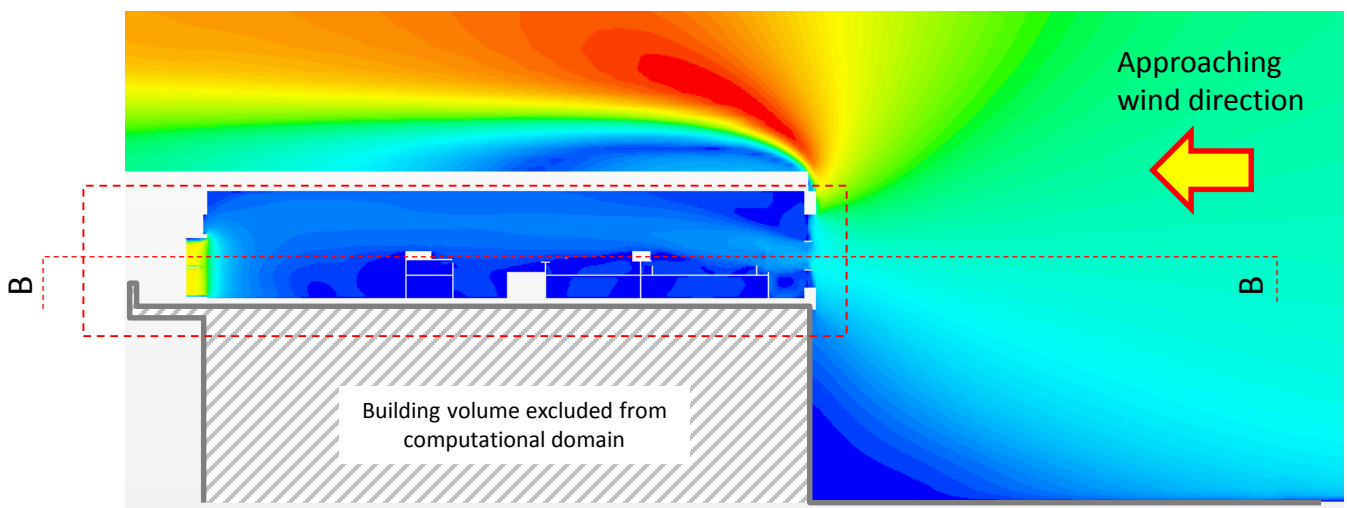


Monitoring plot of wind speed at the point-type probe for convergence checking

Solution ID	Coupled / Decoupled	With furniture	Turbulence model	Inlet	Outlet	Air density and dynamic viscosity	Test Scenario
C2	Coupled	Yes	k- ω	Wind log profile	Actual curve fan	Actual test condition	N/A



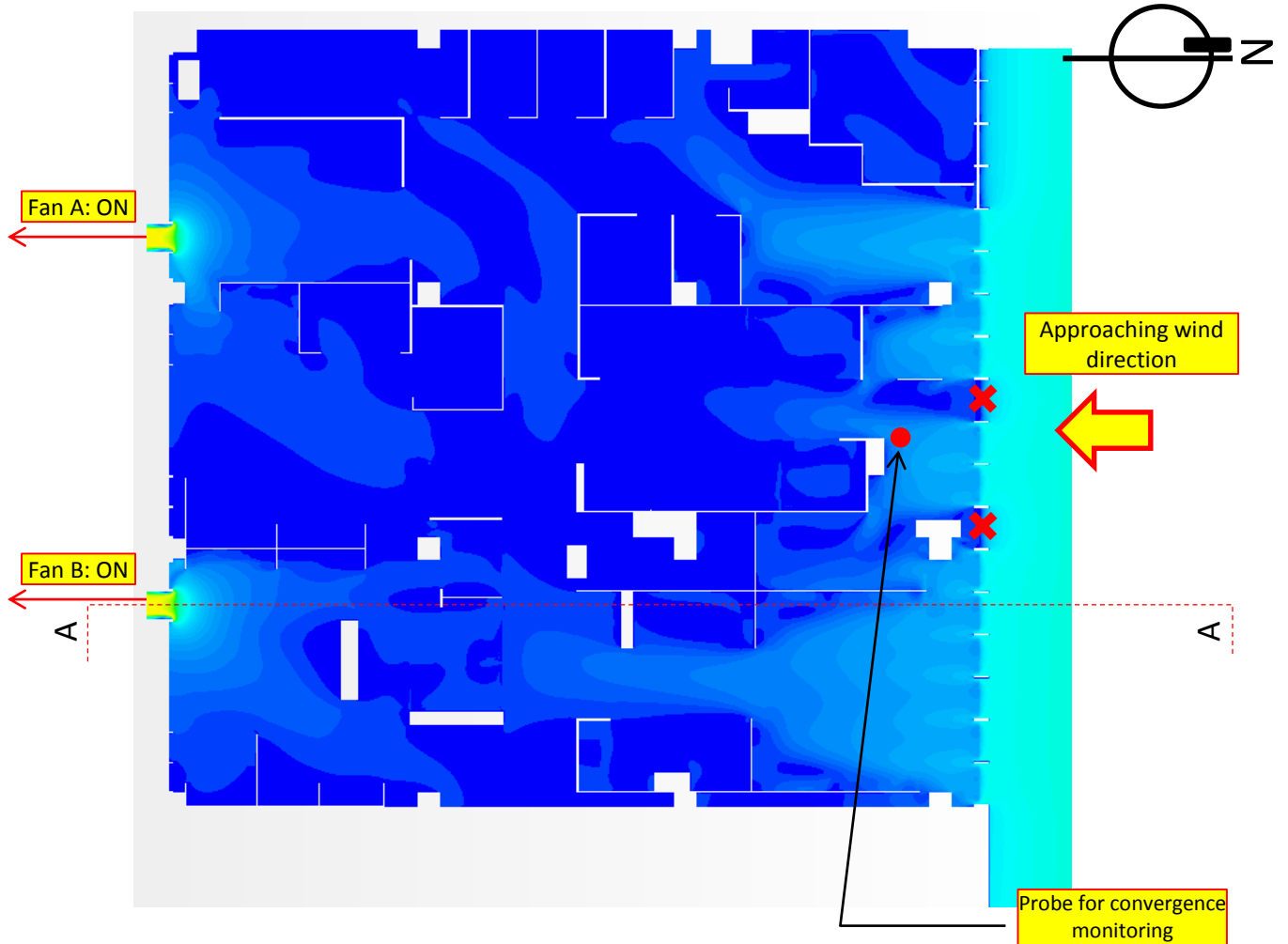
Velocity contoured map on the horizontal plane B-B of 4 feet (1.2m) above the floor (larger view)



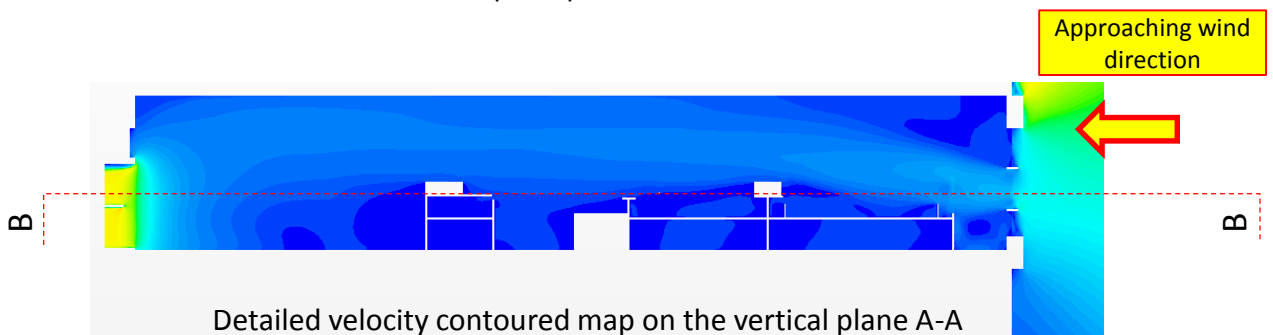
Velocity contoured map on the vertical plane A-A (larger view)



Solution ID	Coupled / Decoupled	With furniture	Turbulence model	Inlet	Outlet	Air density and dynamic viscosity	Test Scenario
C2	Coupled	Yes	k- ω	Wind log profile	Actual curve fan	Actual test condition	N/A



Detailed velocity contoured map on the horizontal plane B-B of 4 feet (1.2m) above the floor

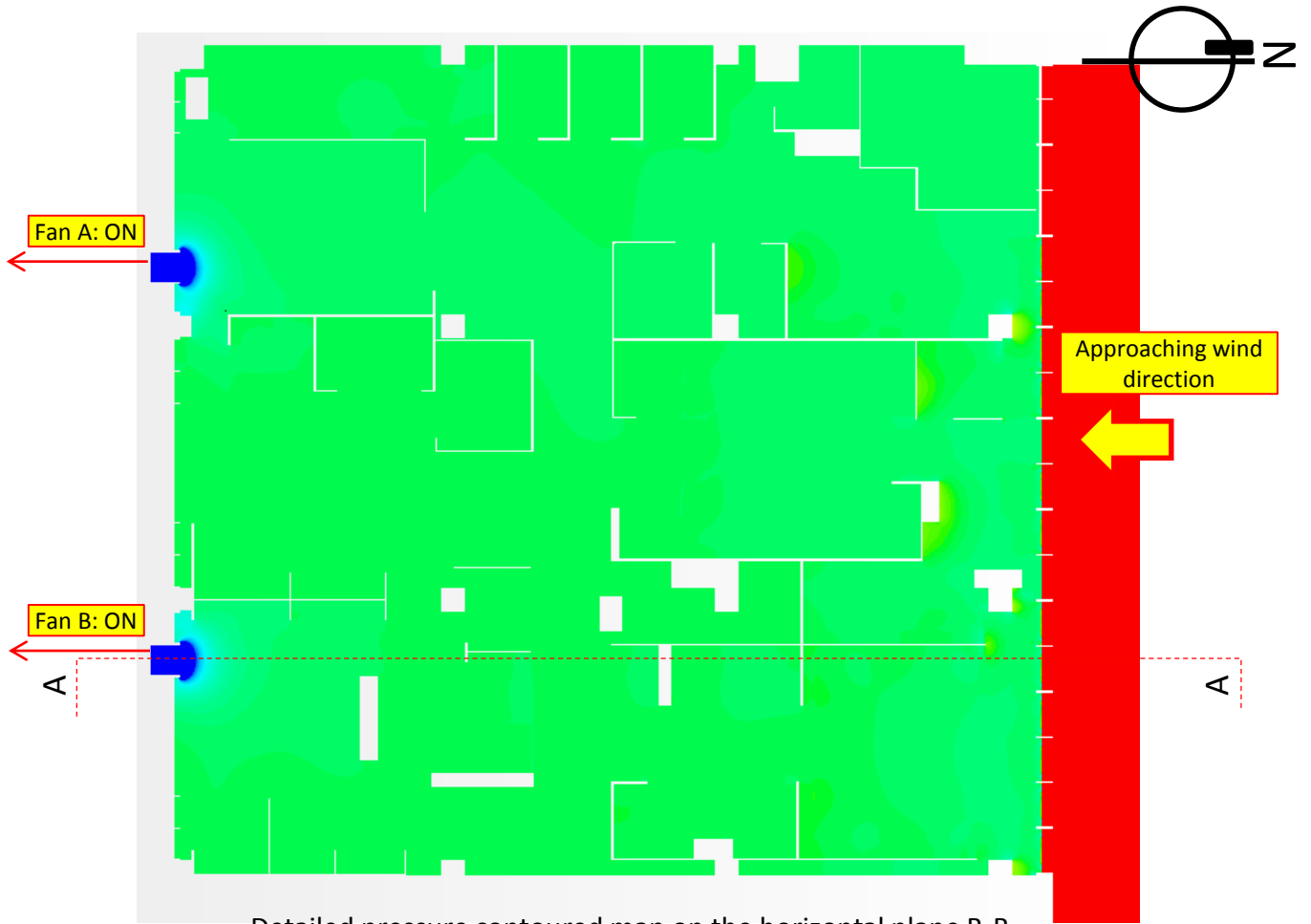


Detailed velocity contoured map on the vertical plane A-A

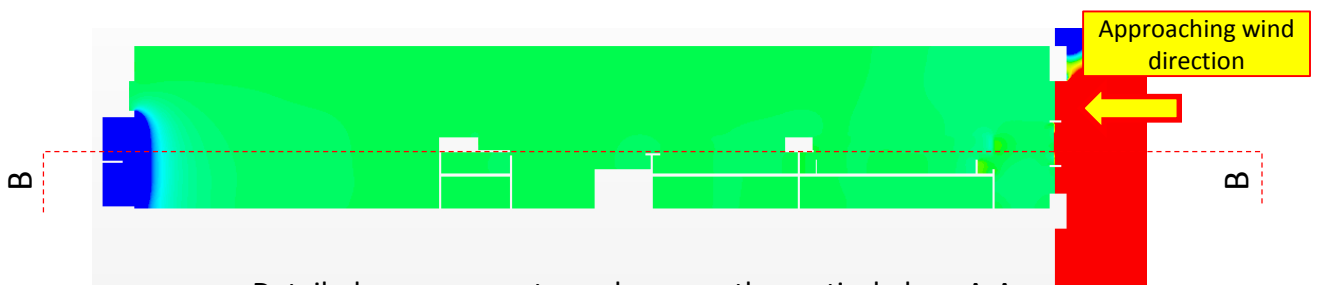


X Permanently closed non-working louvers

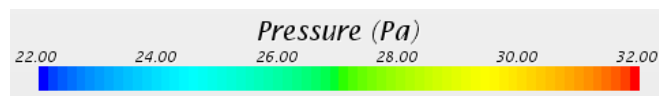
Solution ID	Coupled / Decoupled	With furniture	Turbulence model	Inlet	Outlet	Air density and dynamic viscosity	Test Scenario
C2	Coupled	Yes	k- ω	Wind log profile	Actual curve fan	Actual test condition	N/A



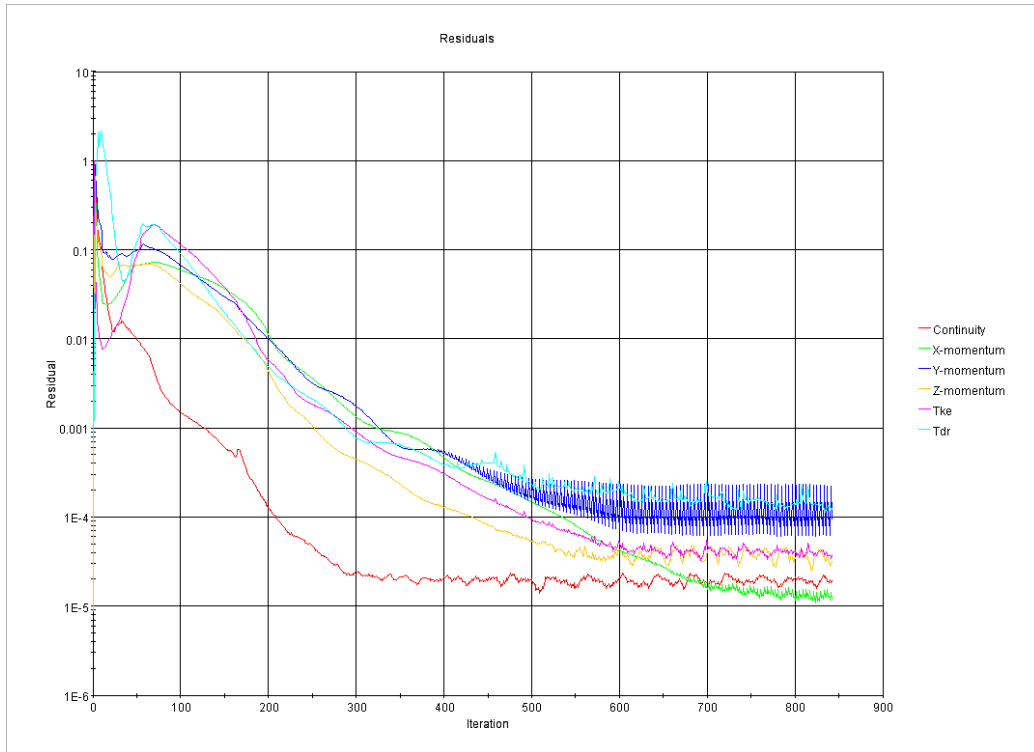
Detailed pressure contoured map on the horizontal plane B-B of 4 feet (1.2m) above the floor



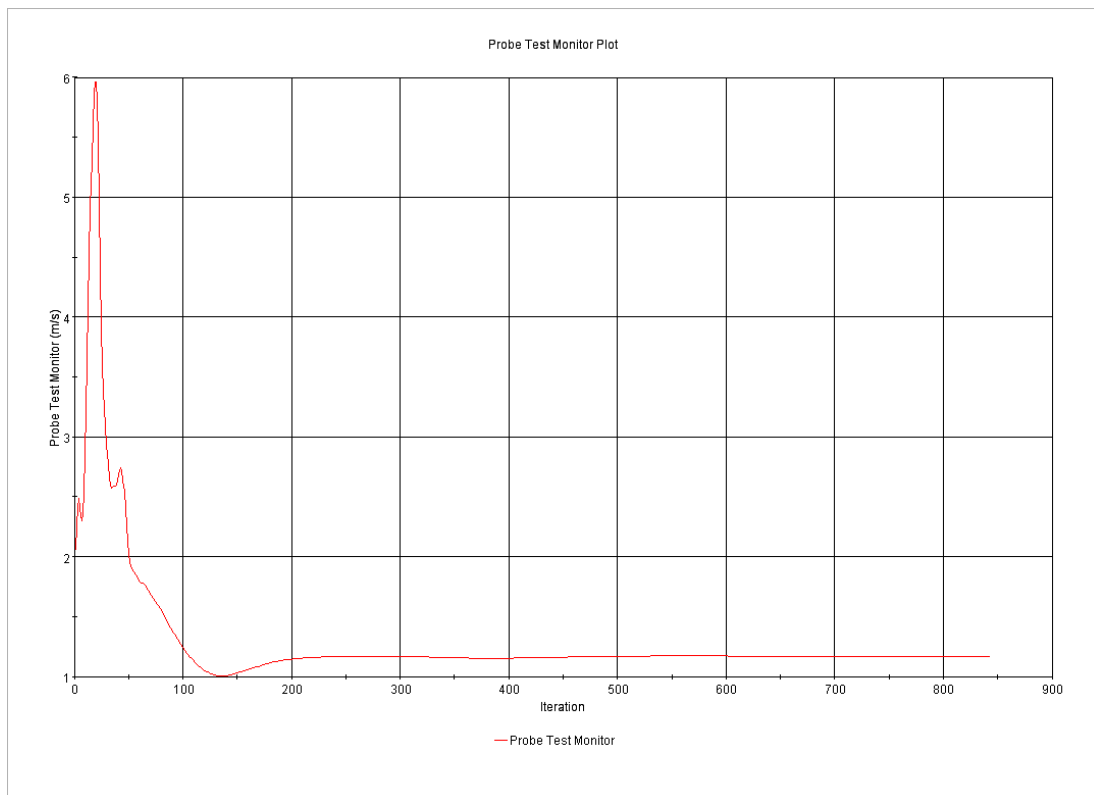
Detailed pressure contoured map on the vertical plane A-A



Solution ID	Coupled / Decoupled	With furniture	Turbulence model	Inlet	Outlet	Air density and dynamic viscosity	Test Scenario
C2	Coupled	Yes	k- ω	Wind log profile	Actual curve fan	Actual test condition	N/A

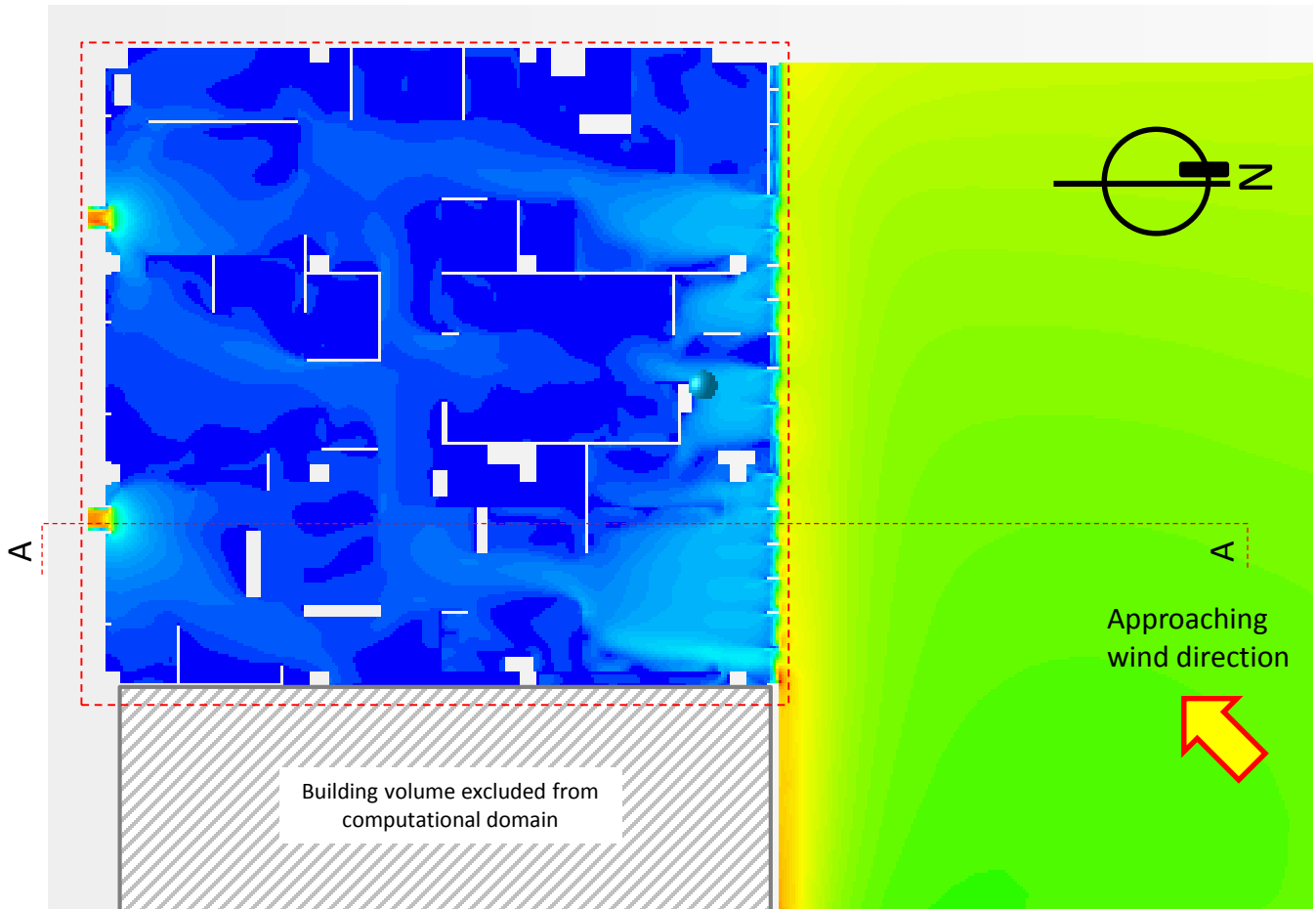


Residual plot

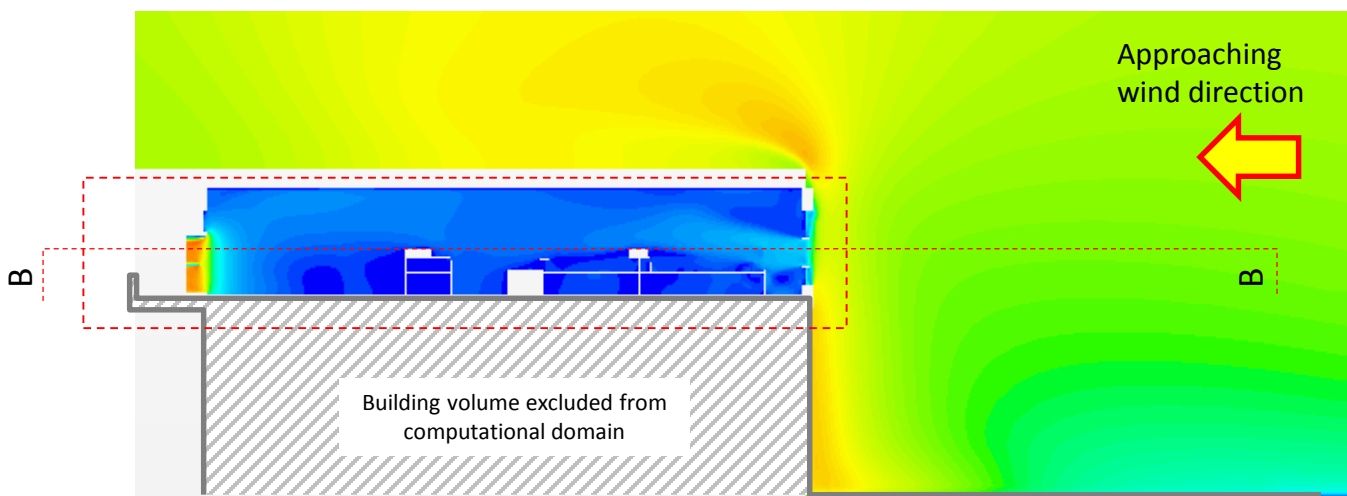


Monitoring plot of wind speed at the point-type probe for convergence checking

Solution ID	Coupled / Decoupled	With furniture	Turbulence model	Inlet	Outlet	Air density and dynamic viscosity	Test Scenario
D1	Coupled	Yes	k-ε	Wind log profile (NE direction)	Actual curve fan	Actual test condition	Scenario 1



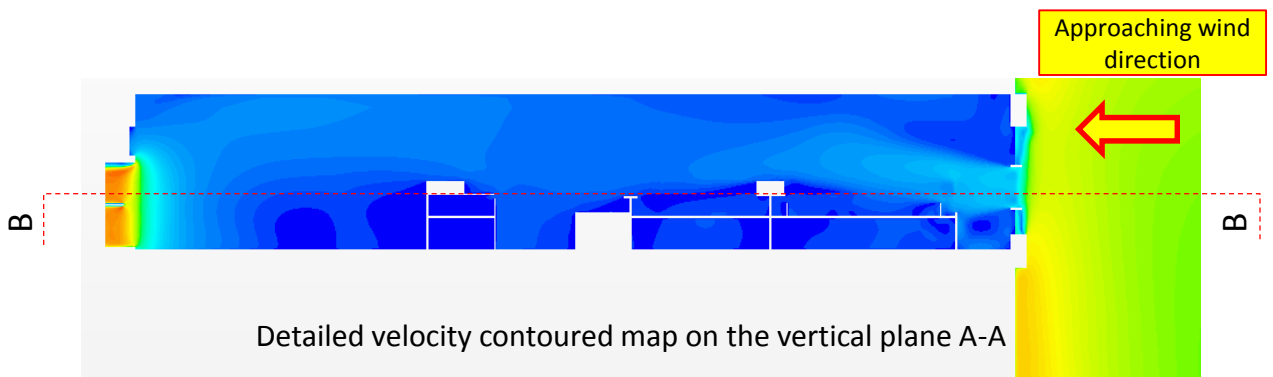
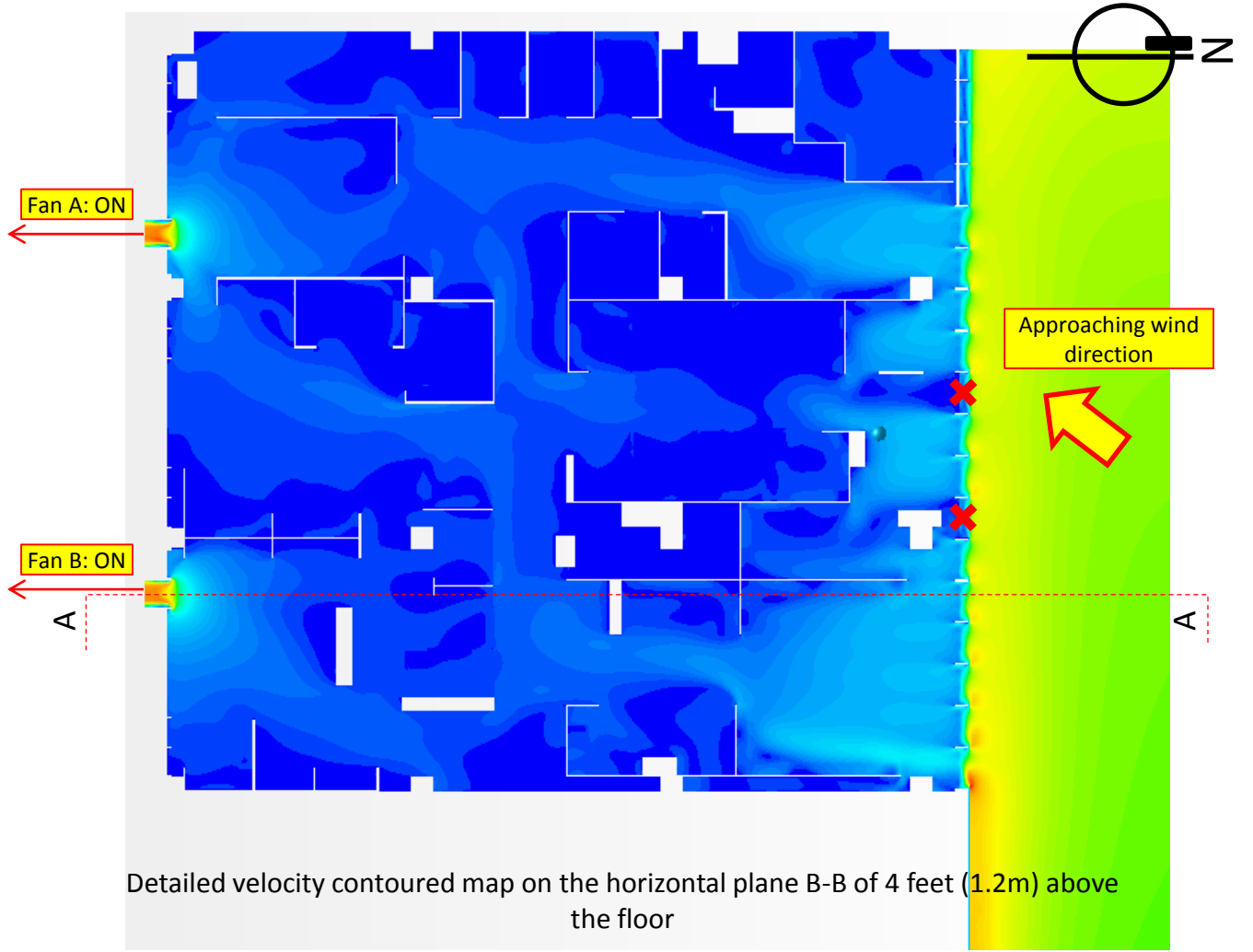
Velocity contoured map on the horizontal plane B-B of 4 feet (1.2m) above the floor (larger view)



Velocity contoured map on the vertical plane A-A (larger view)

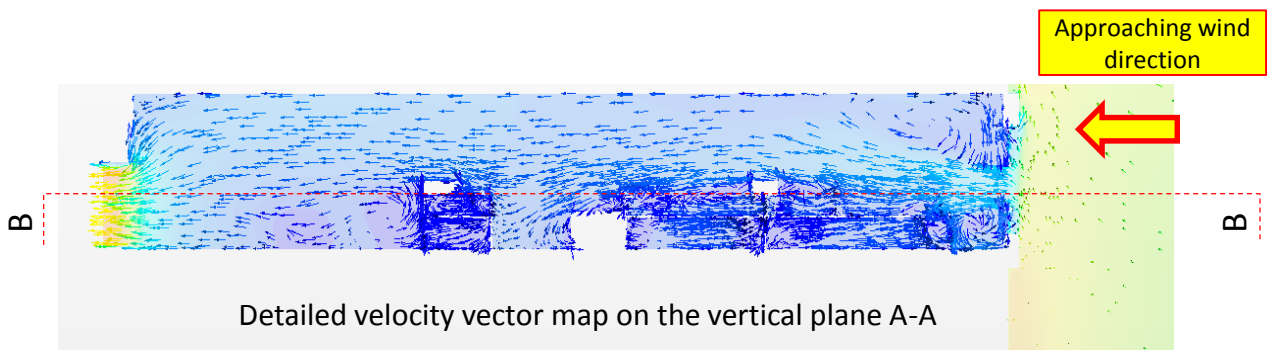
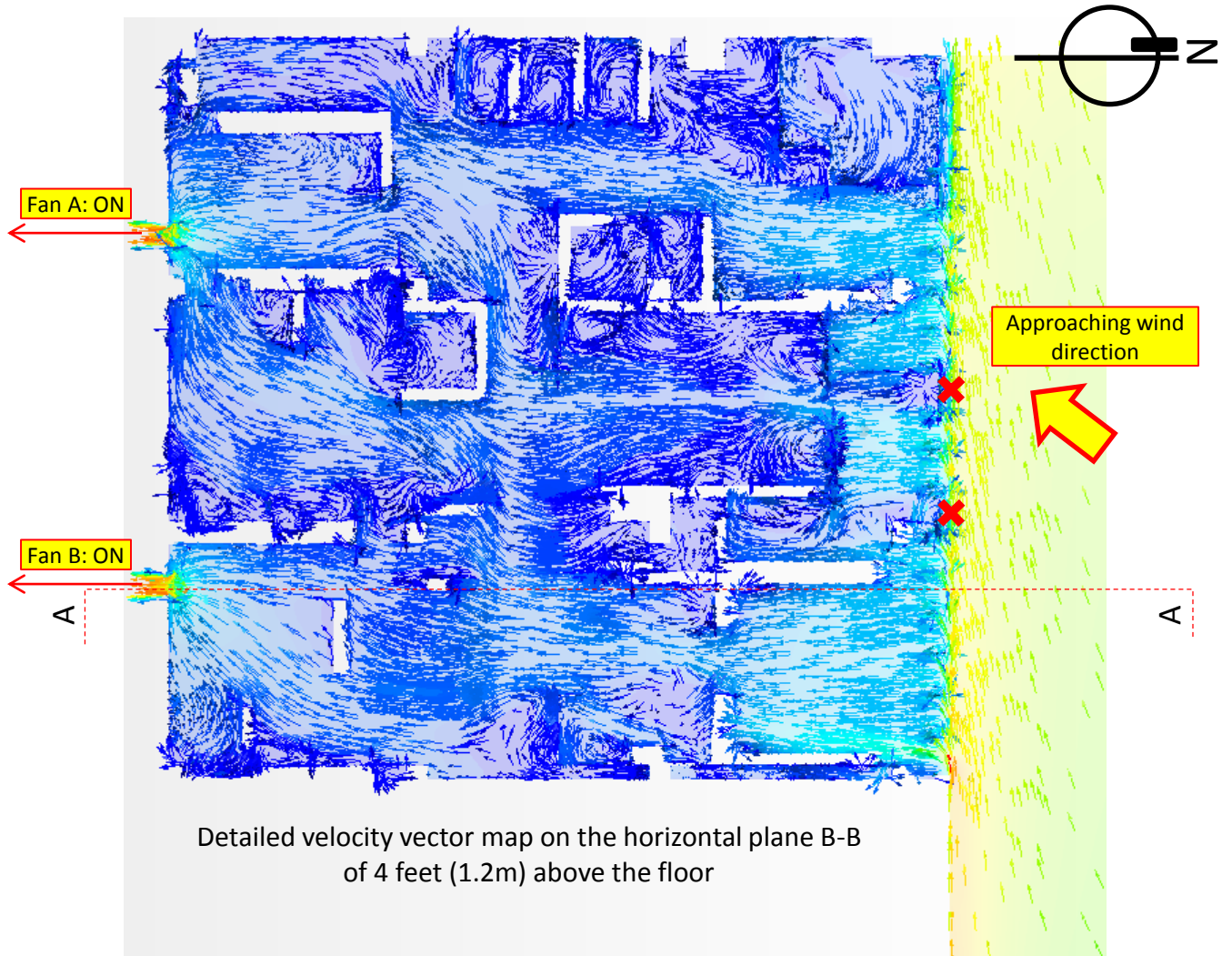


Solution ID	Coupled / Decoupled	With furniture	Turbulence model	Inlet	Outlet	Air density and dynamic viscosity	Test Scenario
D1	Coupled	Yes	k-ε	Wind log profile (NE direction)	Actual curve fan	Actual test condition	Scenario 1



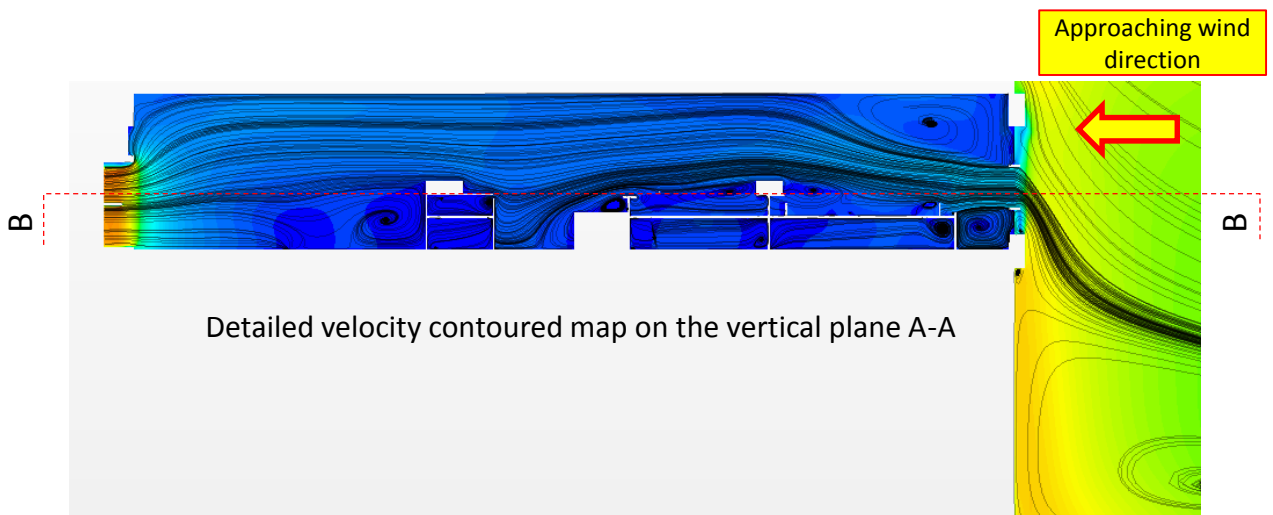
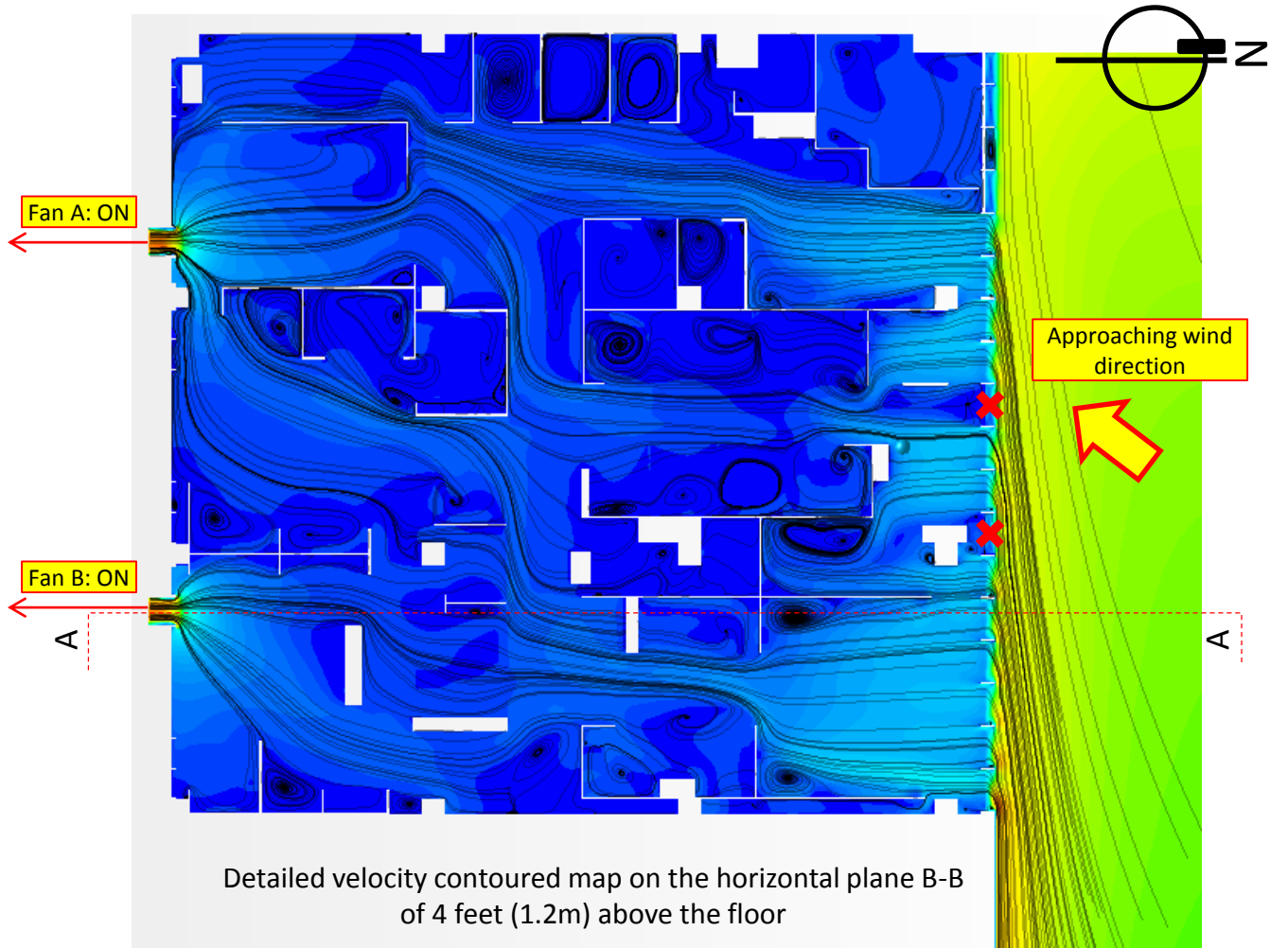
X Permanently closed non-working louvers

Solution ID	Coupled / Decoupled	With furniture	Turbulence model	Inlet	Outlet	Air density and dynamic viscosity	Test Scenario
D1	Coupled	Yes	k-ε	Wind log profile (NE direction)	Actual curve fan	Actual test condition	Scenario 1



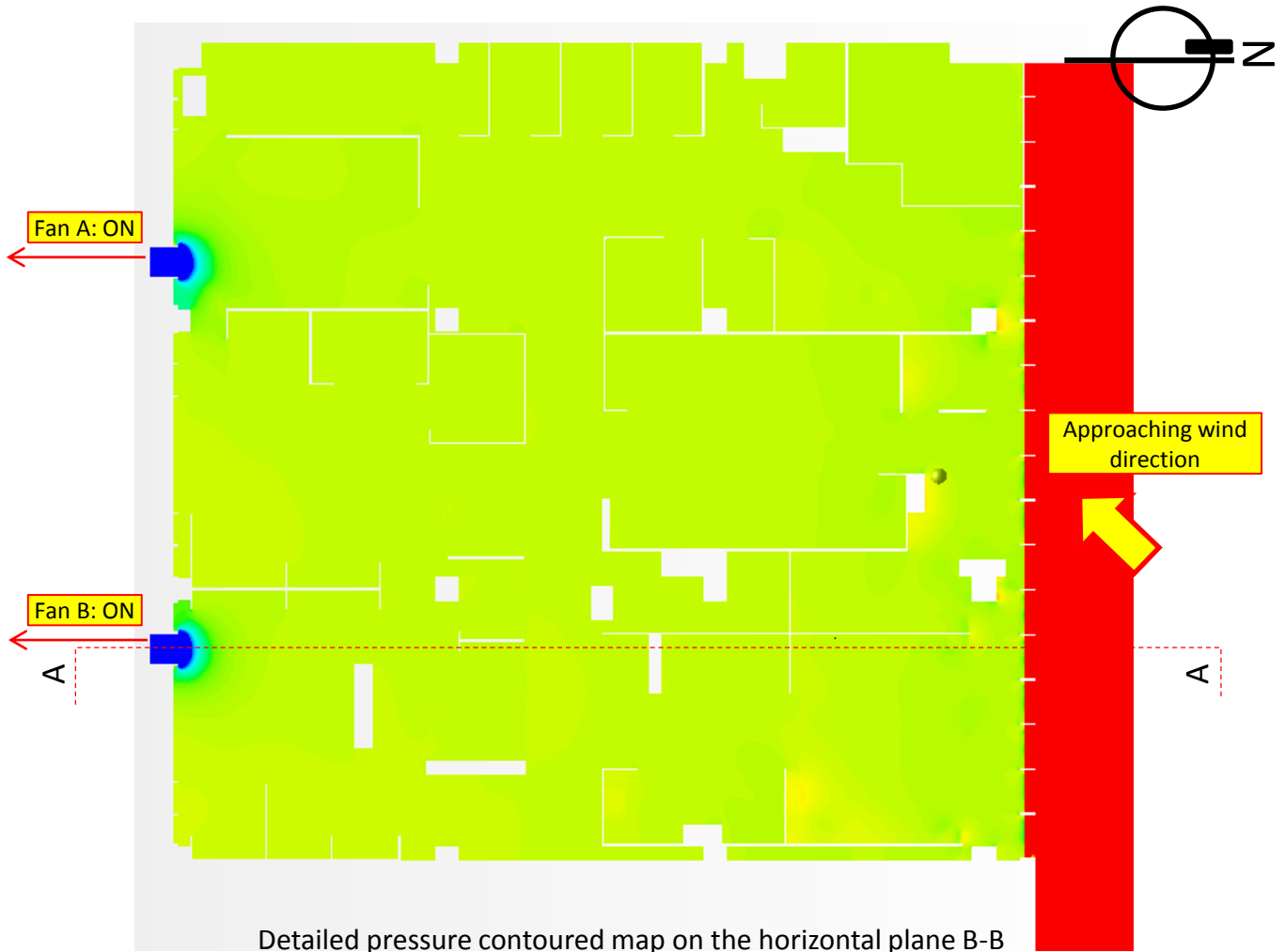
✗ Permanently closed non-working louvers

Solution ID	Coupled / Decoupled	With furniture	Turbulence model	Inlet	Outlet	Air density and dynamic viscosity	Test Scenario
D1	Coupled	Yes	k-ε	Wind log profile (NE direction)	Actual curve fan	Actual test condition	Scenario 1



✘ Permanently closed non-working louvers

Solution ID	Coupled / Decoupled	With furniture	Turbulence model	Inlet	Outlet	Air density and dynamic viscosity	Test Scenario
D1	Coupled	Yes	k-ε	Wind log profile (NE direction)	Actual curve fan	Actual test condition	Scenario 1



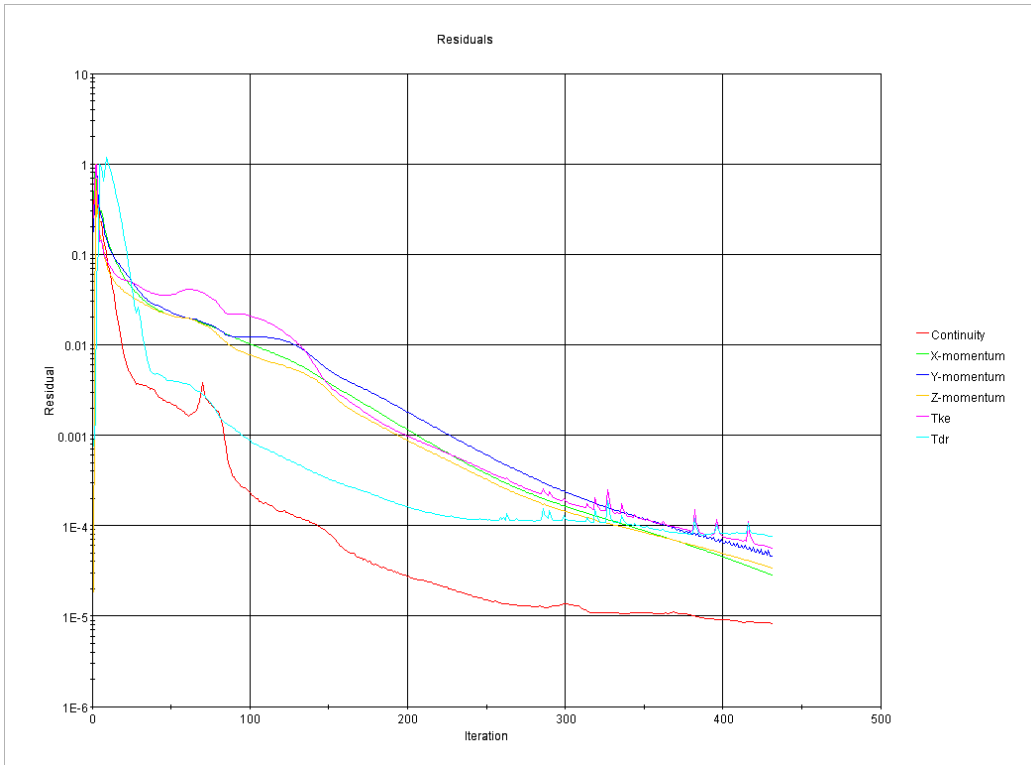
Detailed pressure contoured map on the horizontal plane B-B of 4 feet (1.2m) above the floor



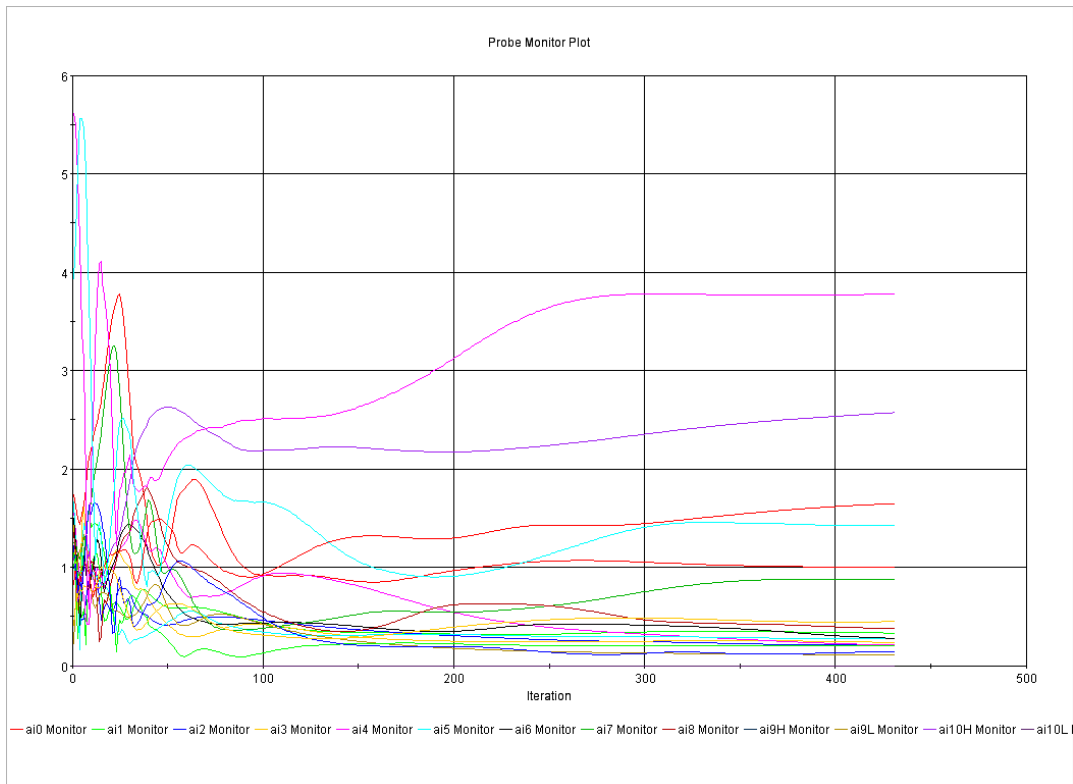
Detailed pressure contoured map on the vertical plane A-A



Solution ID	Coupled / Decoupled	With furniture	Turbulence model	Inlet	Outlet	Air density and dynamic viscosity	Test Scenario
D1	Coupled	Yes	k-ε	Wind log profile (NE direction)	Actual curve fan	Actual test condition	Scenario 1

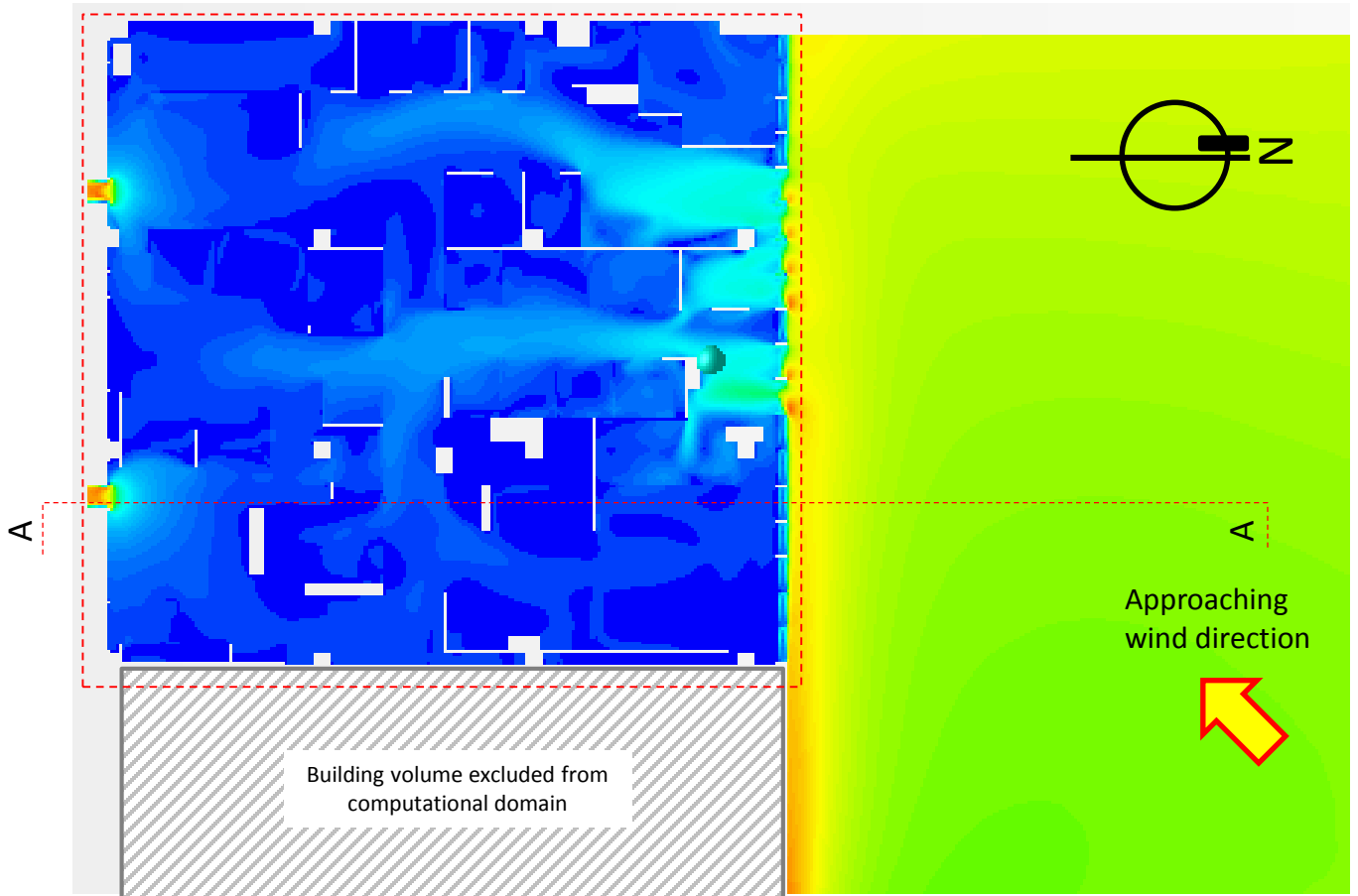


Residual plot

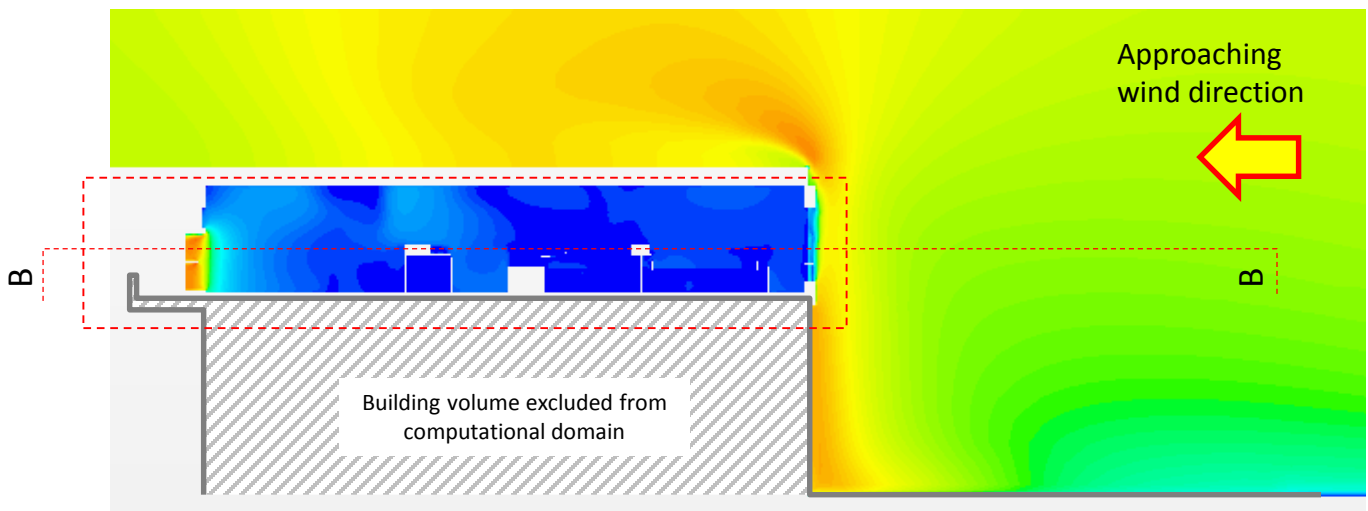


Monitoring plot of wind speed at the locations for placement of sensors for convergence checking

Solution ID	Coupled / Decoupled	With furniture	Turbulence model	Inlet	Outlet	Air density and dynamic viscosity	Test Scenario
D2	Coupled	Yes	k-ε	Wind log profile (NE direction)	Actual curve fan	Actual test condition	Scenario 2



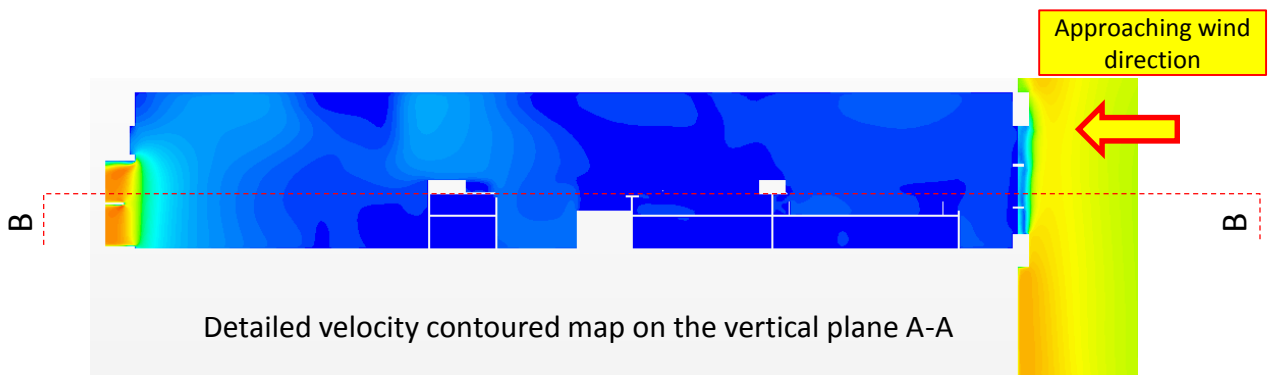
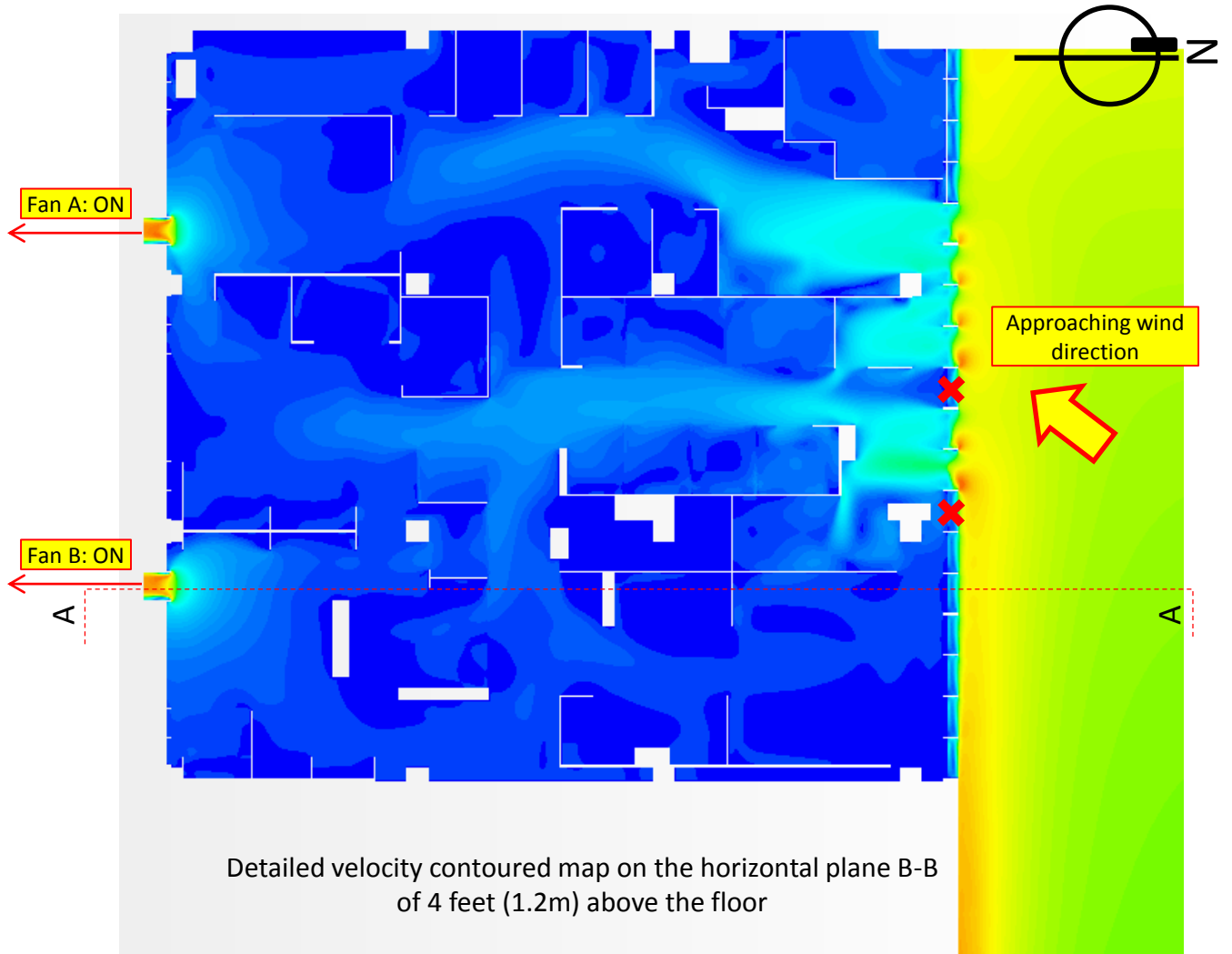
Velocity contoured map on the horizontal plane B-B of 4 feet (1.2m) above the floor (larger view)



Velocity contoured map on the vertical plane A-A (larger view)

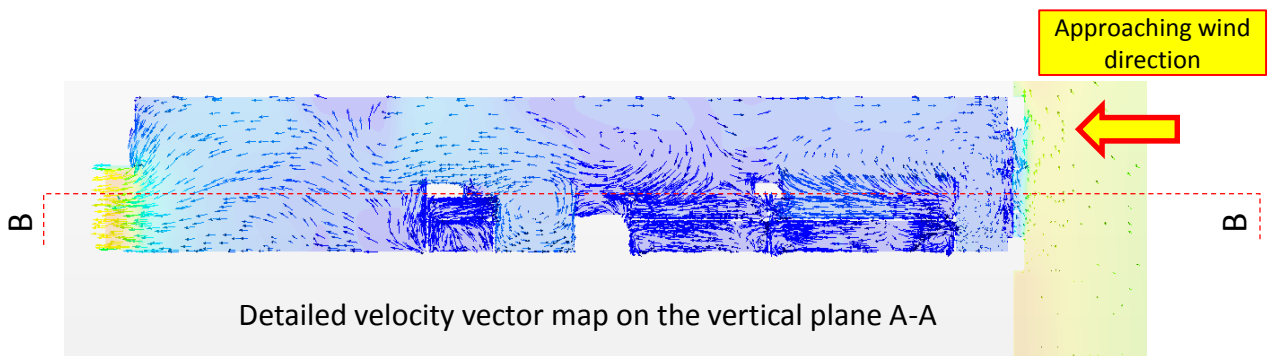
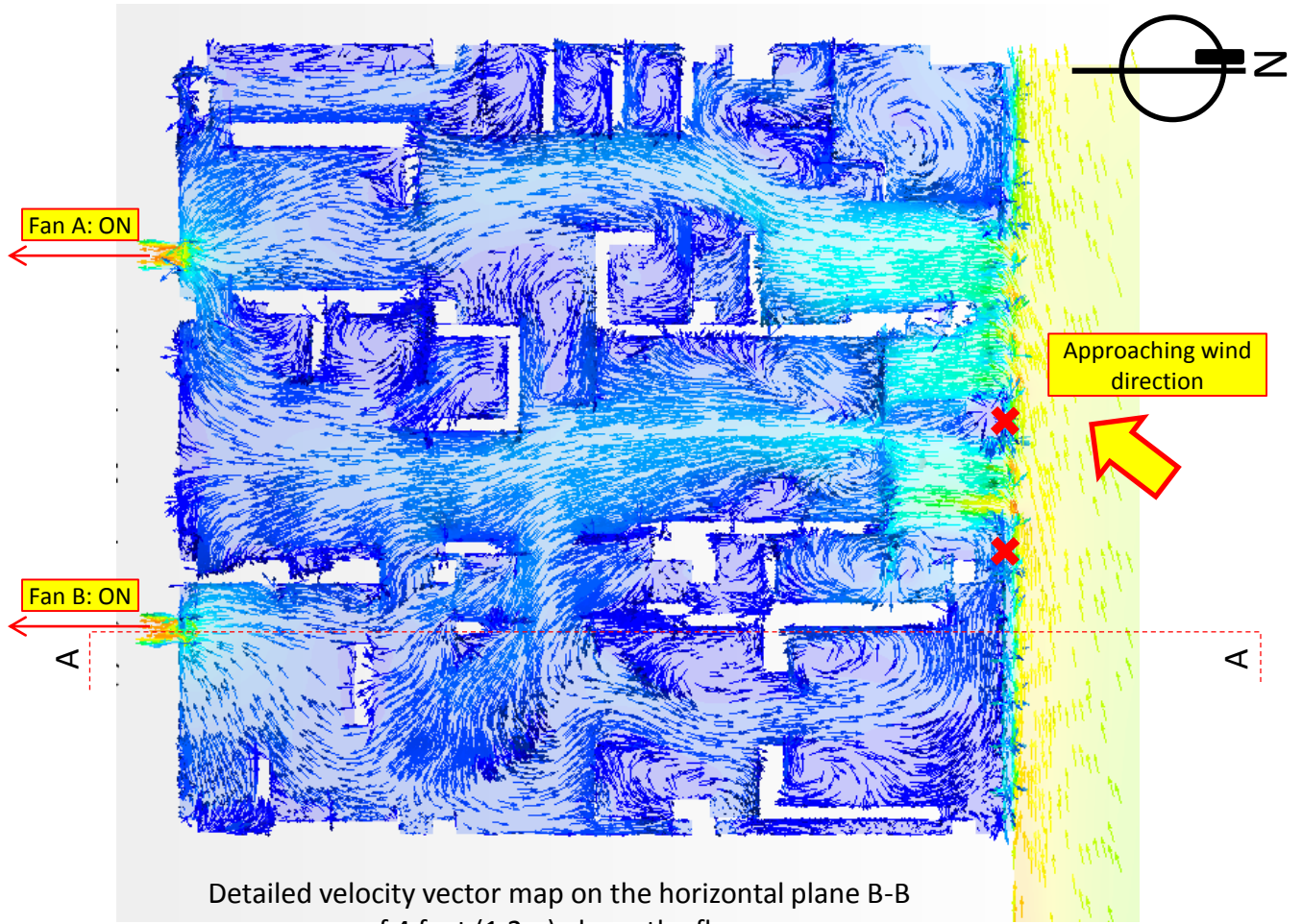


Solution ID	Coupled / Decoupled	With furniture	Turbulence model	Inlet	Outlet	Air density and dynamic viscosity	Test Scenario
D2	Coupled	Yes	k-ε	Wind log profile (NE direction)	Actual curve fan	Actual test condition	Scenario 2



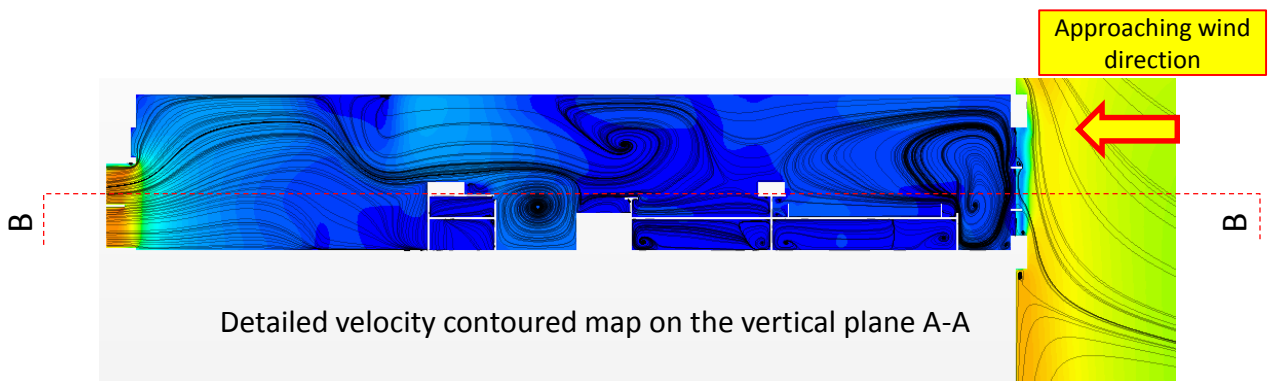
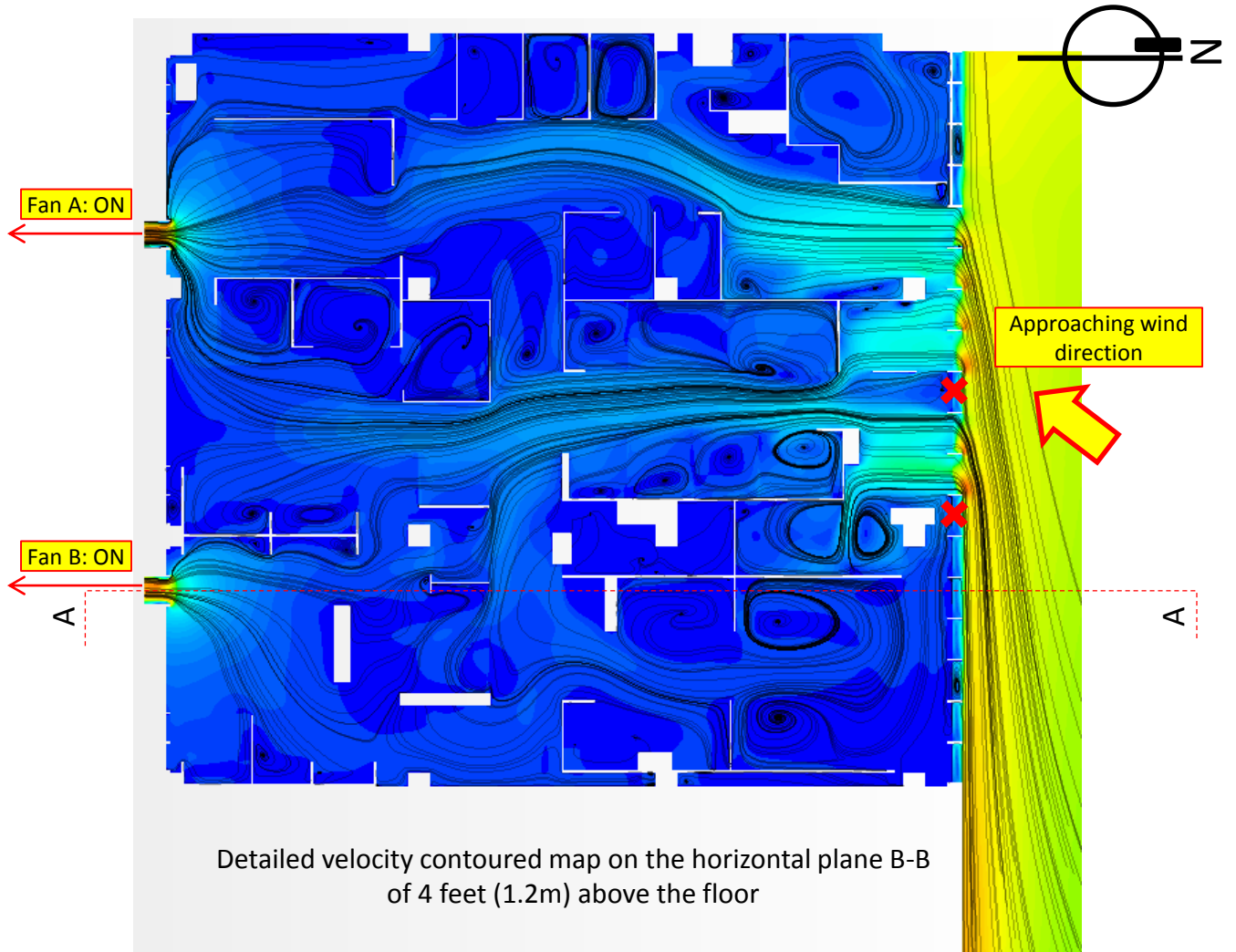
✘ Permanently closed non-working louvers

Solution ID	Coupled / Decoupled	With furniture	Turbulence model	Inlet	Outlet	Air density and dynamic viscosity	Test Scenario
D2	Coupled	Yes	k-ε	Wind log profile (NE direction)	Actual curve fan	Actual test condition	Scenario 2



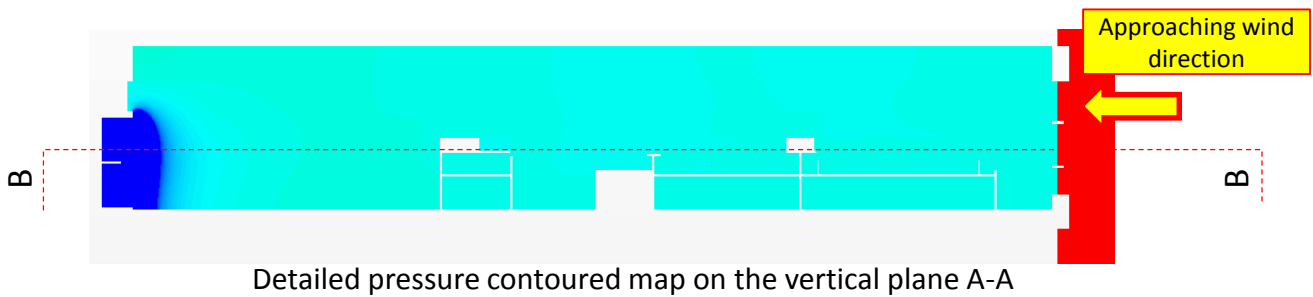
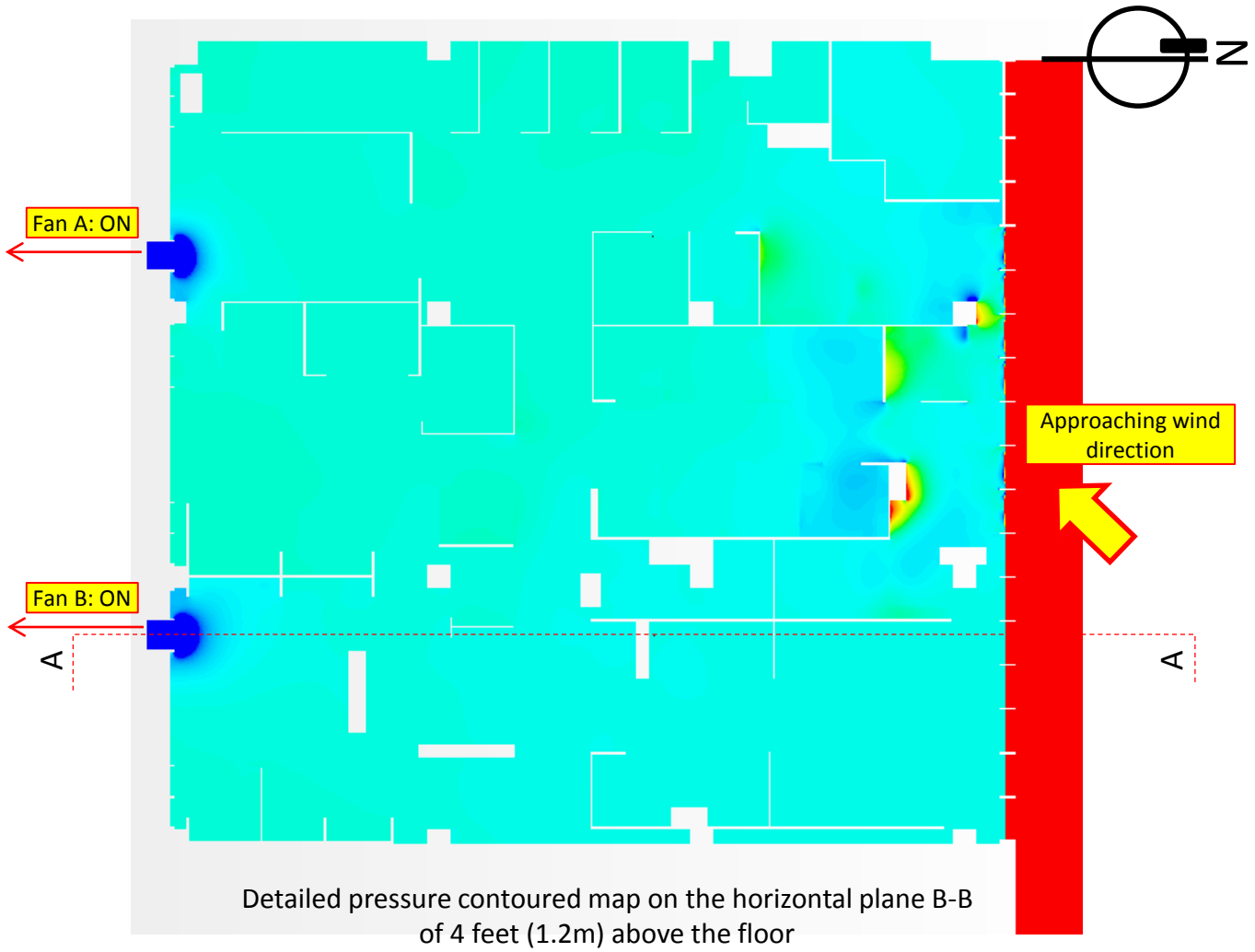
X Permanently closed non-working louvers

Solution ID	Coupled / Decoupled	With furniture	Turbulence model	Inlet	Outlet	Air density and dynamic viscosity	Test Scenario
D2	Coupled	Yes	k-ε	Wind log profile (NE direction)	Actual curve fan	Actual test condition	Scenario 2

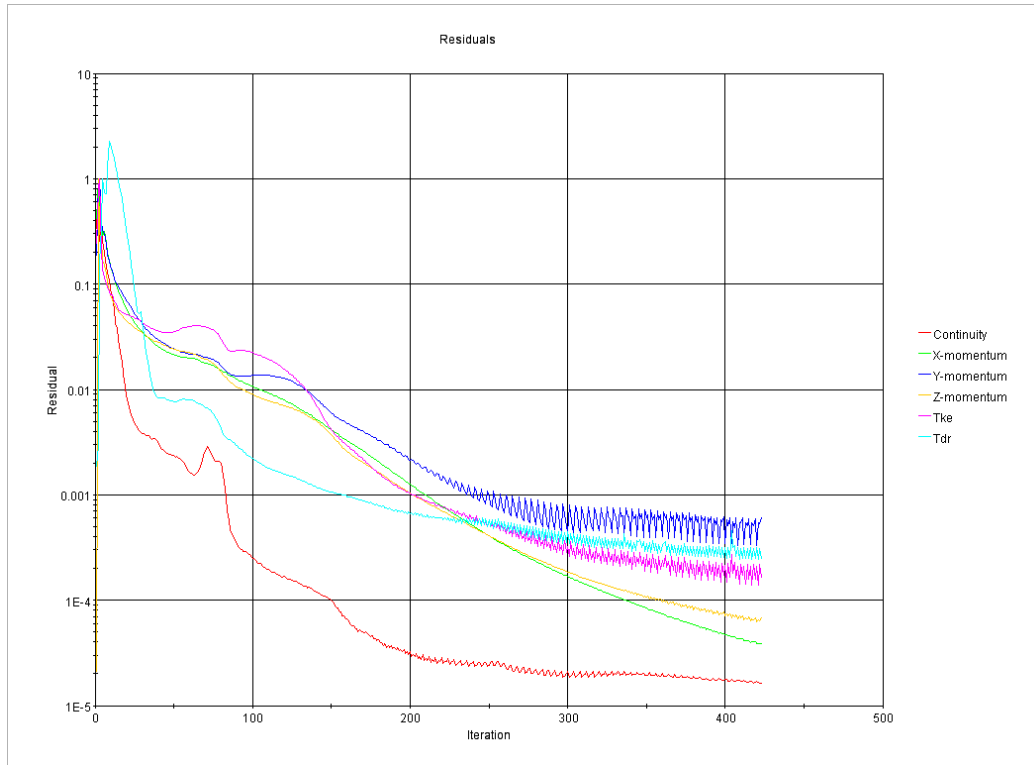


X Permanently closed non-working louvers

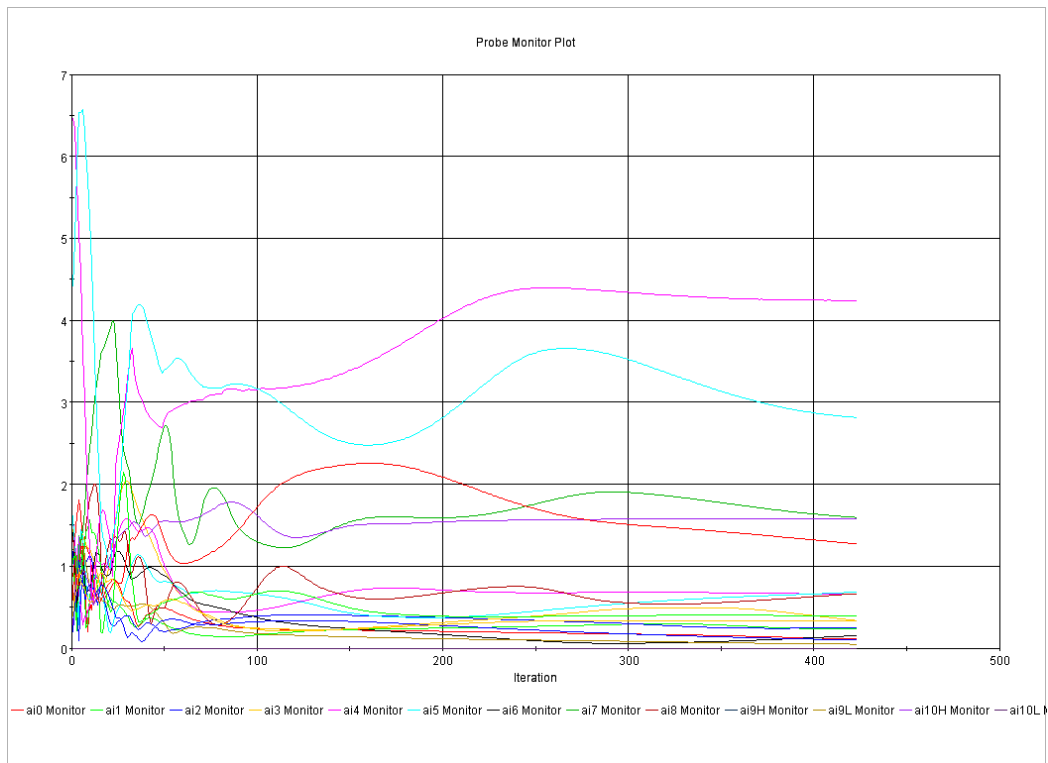
Solution ID	Coupled / Decoupled	With furniture	Turbulence model	Inlet	Outlet	Air density and dynamic viscosity	Test Scenario
D2	Coupled	Yes	k-ε	Wind log profile (NE direction)	Actual curve fan	Actual test condition	Scenario 2



Solution ID	Coupled / Decoupled	With furniture	Turbulence model	Inlet	Outlet	Air density and dynamic viscosity	Test Scenario
D2	Coupled	Yes	k-ε	Wind log profile (NE direction)	Actual curve fan	Actual test condition	Scenario 2

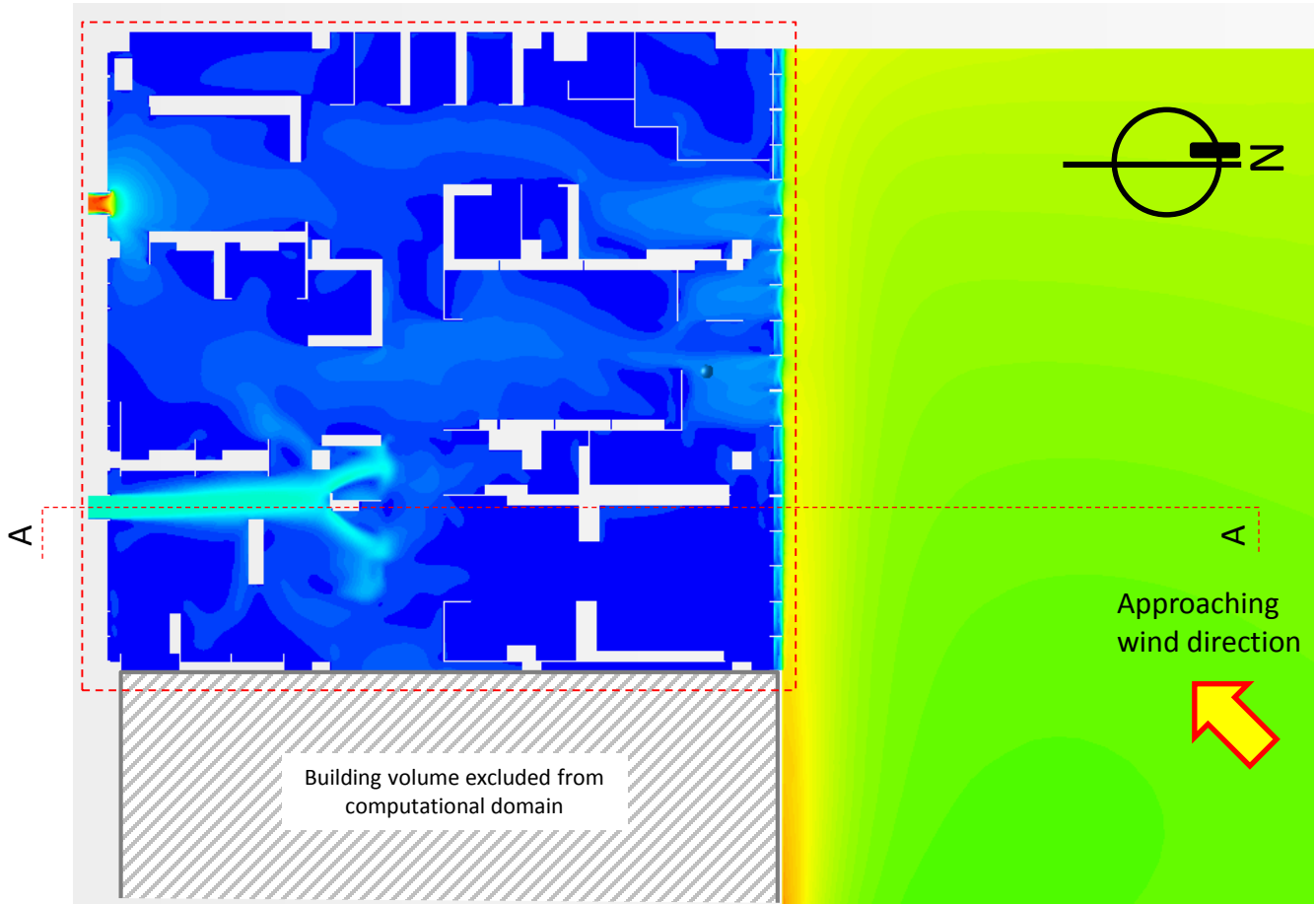


Residual plot

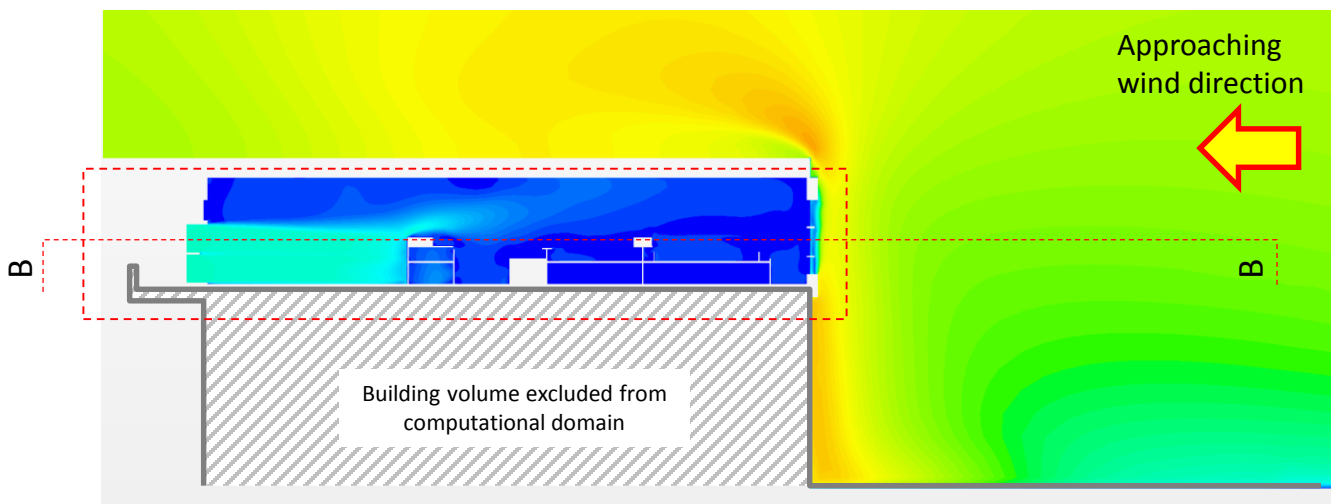


Monitoring plot of wind speed at the locations for placement of sensors for convergence checking

Solution ID	Coupled / Decoupled	With furniture	Turbulence model	Inlet	Outlet	Air density and dynamic viscosity	Test Scenario
D3	Coupled	Yes	k-ε	Wind log profile (NE direction)	Actual curve fan	Actual test condition	Scenario 3



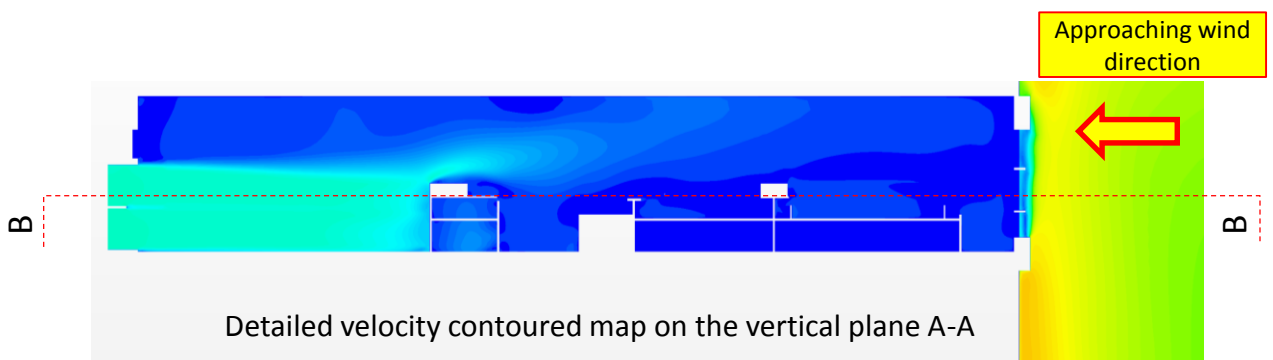
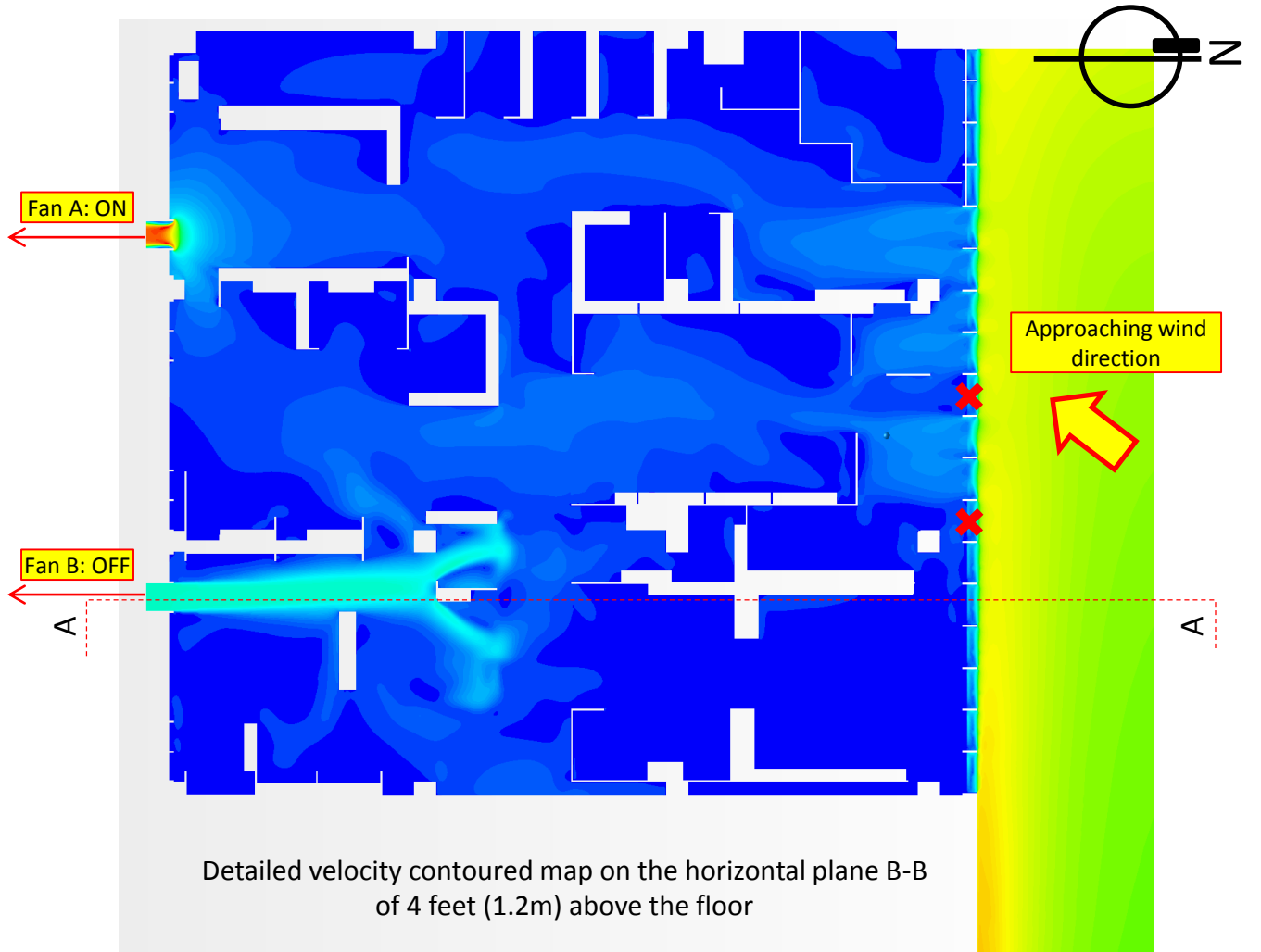
Velocity contoured map on the horizontal plane B-B of 4 feet (1.2m) above the floor (larger view)



Velocity contoured map on the vertical plane A-A (larger view)

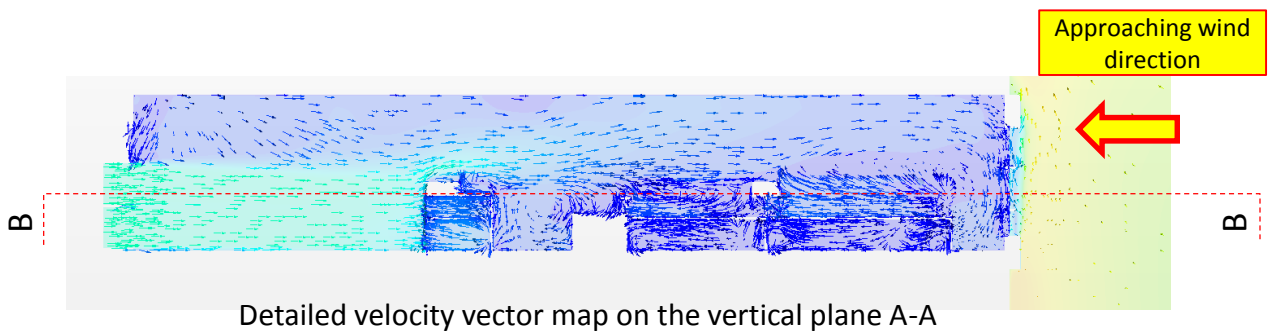
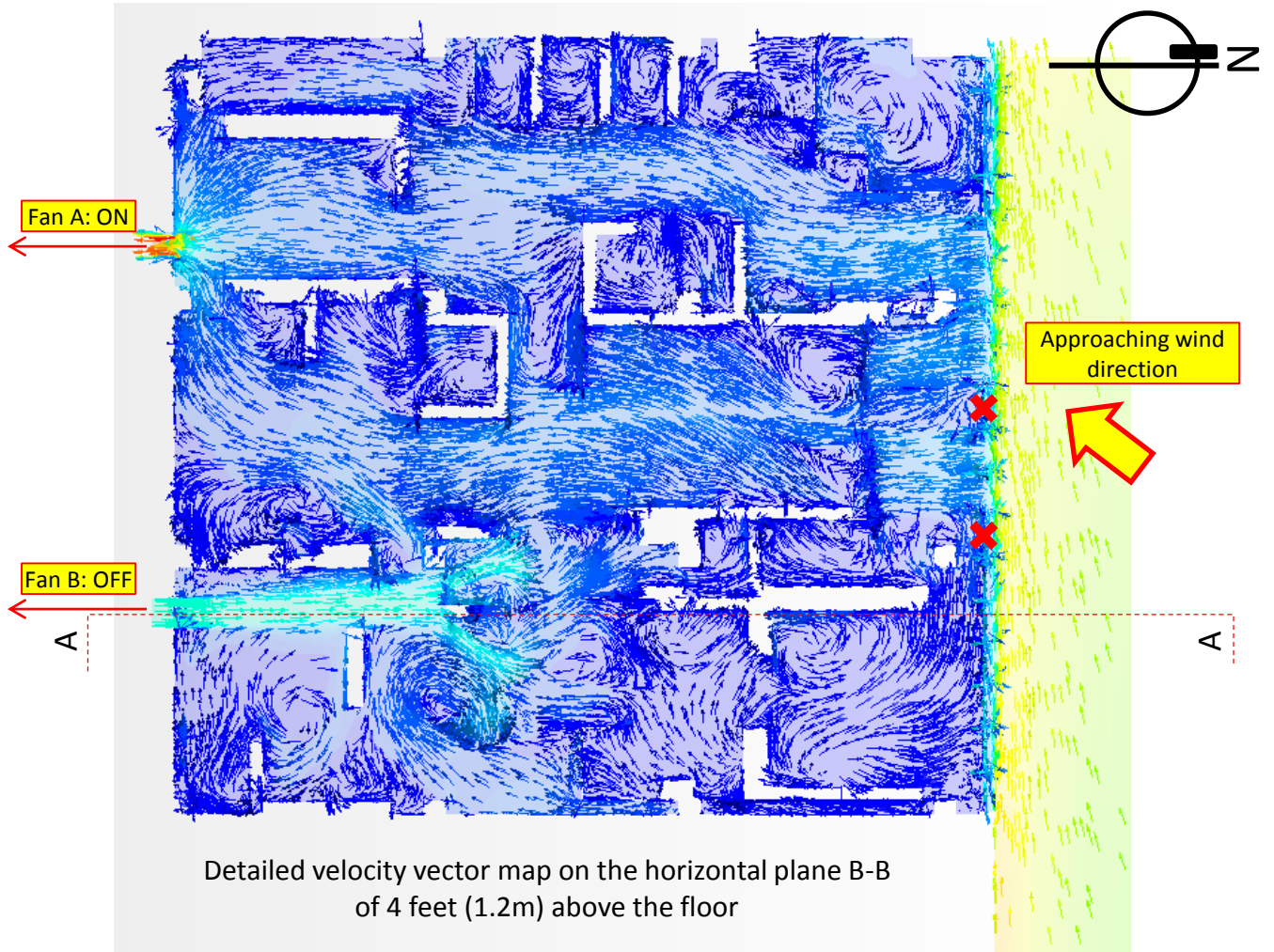


Solution ID	Coupled / Decoupled	With furniture	Turbulence model	Inlet	Outlet	Air density and dynamic viscosity	Test Scenario
D3	Coupled	Yes	k-ε	Wind log profile (NE direction)	Actual curve fan	Actual test condition	Scenario 3



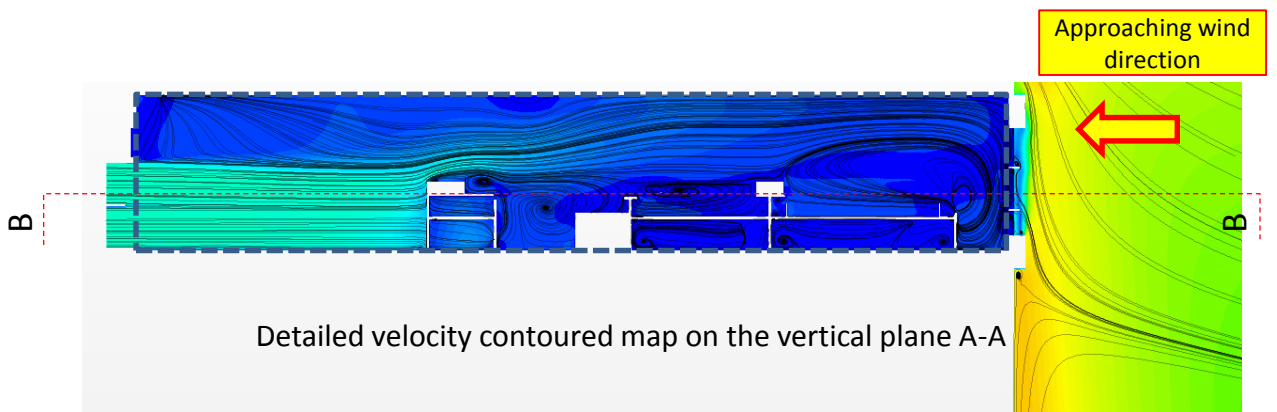
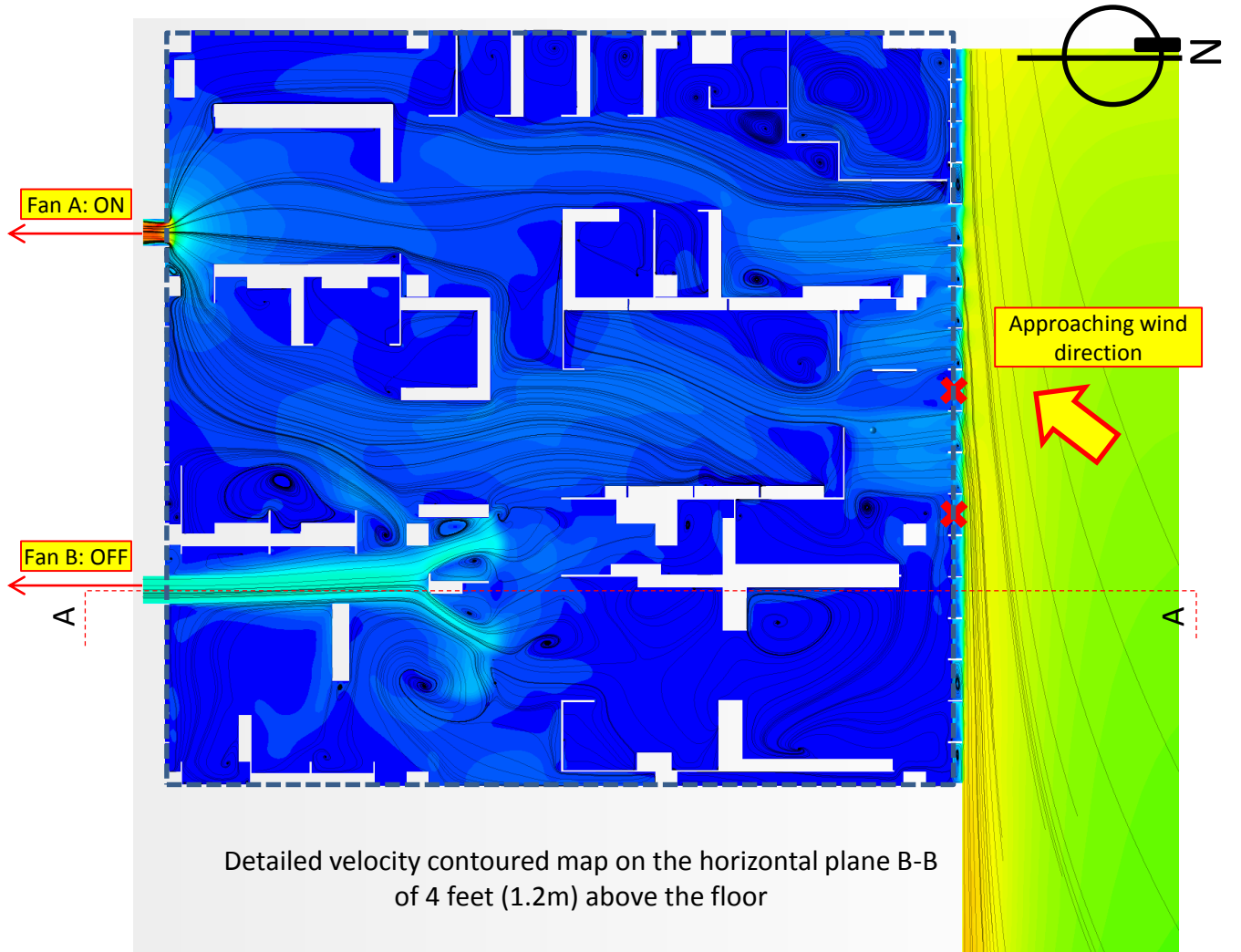
X Permanently closed non-working louvers

Solution ID	Coupled / Decoupled	With furniture	Turbulence model	Inlet	Outlet	Air density and dynamic viscosity	Test Scenario
D3	Coupled	Yes	k-ε	Wind log profile (NE direction)	Actual curve fan	Actual test condition	Scenario 3



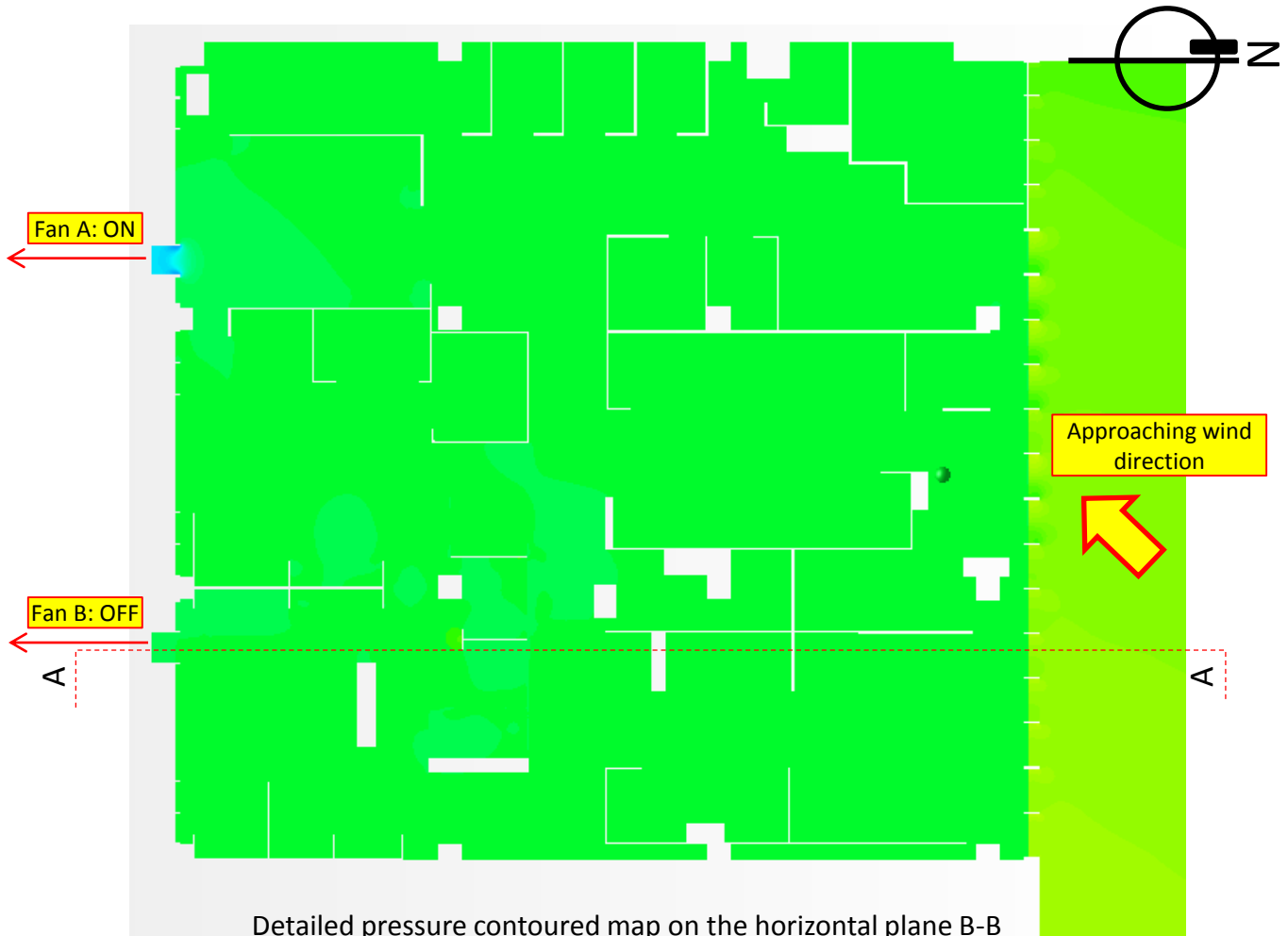
X Permanently closed non-working louvers

Solution ID	Coupled / Decoupled	With furniture	Turbulence model	Inlet	Outlet	Air density and dynamic viscosity	Test Scenario
D3	Coupled	Yes	k-ε	Wind log profile (NE direction)	Actual curve fan	Actual test condition	Scenario 3

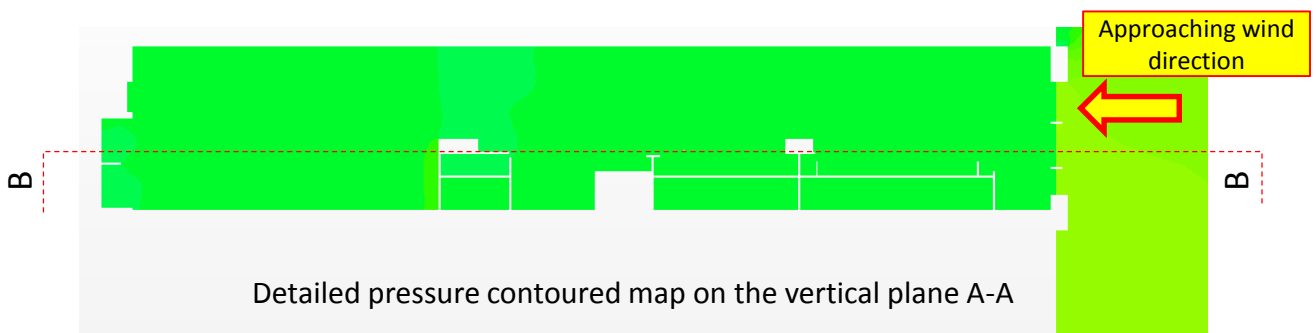


X Permanently closed non-working louvers

Solution ID	Coupled / Decoupled	With furniture	Turbulence model	Inlet	Outlet	Air density and dynamic viscosity	Test Scenario
D3	Coupled	Yes	k-ε	Wind log profile (NE direction)	Actual curve fan	Actual test condition	Scenario 3



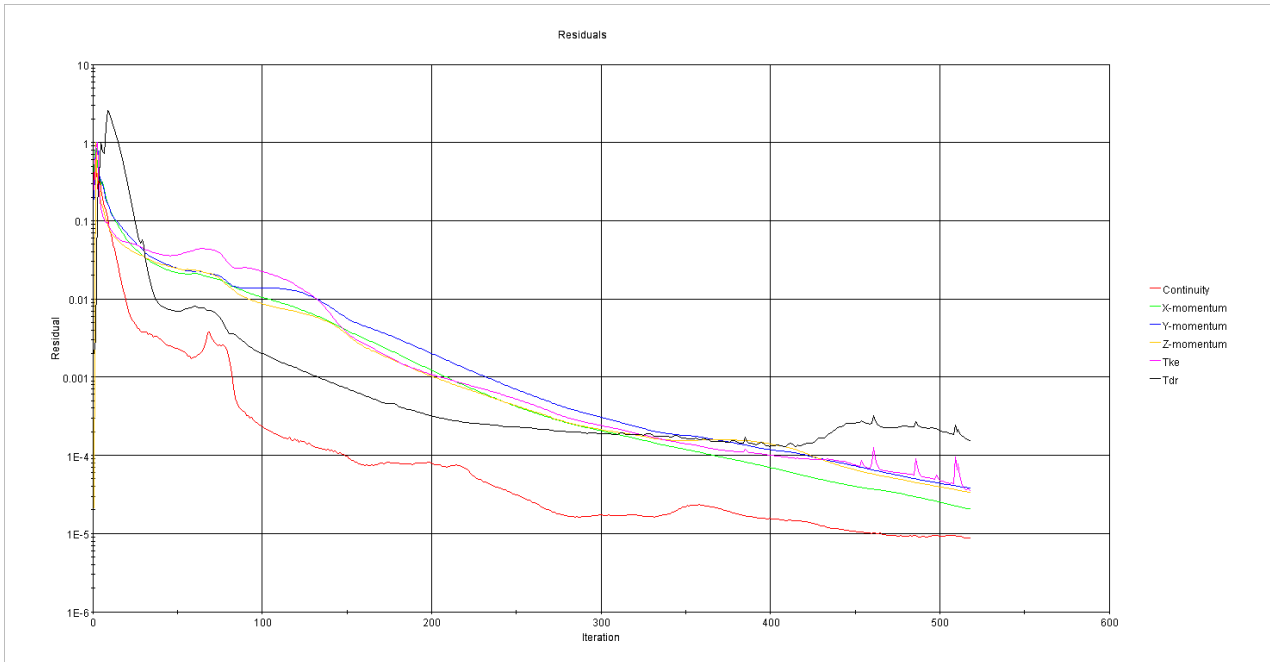
Detailed pressure contoured map on the horizontal plane B-B of 4 feet (1.2m) above the floor



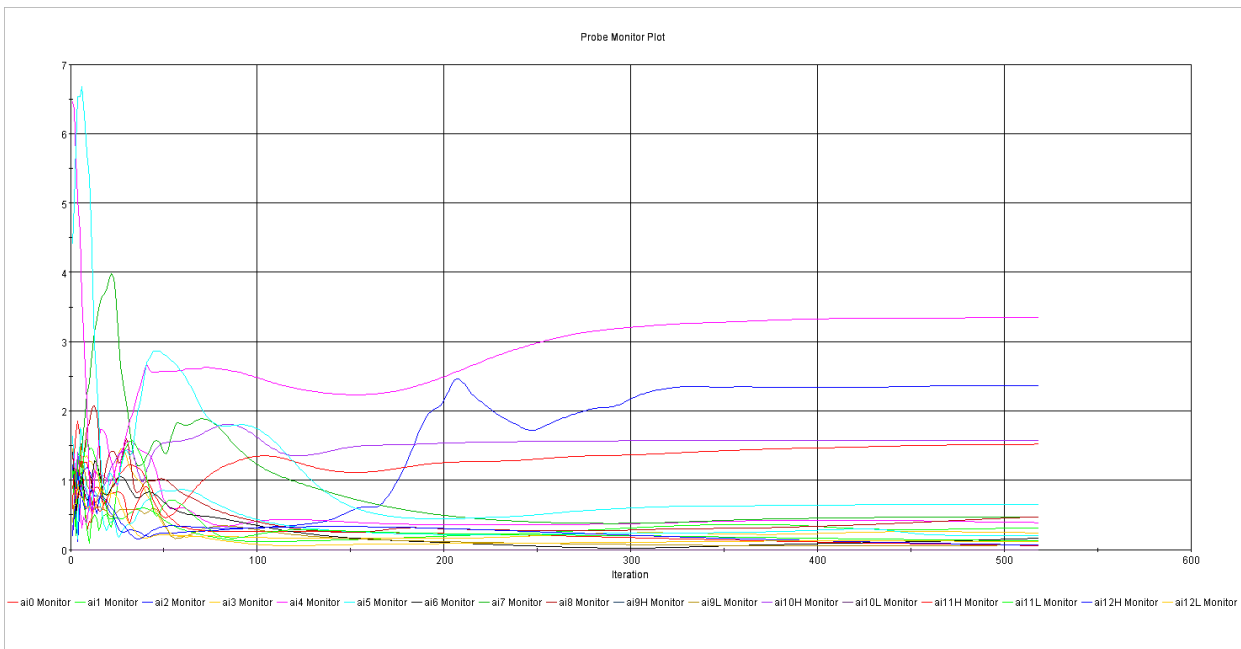
Detailed pressure contoured map on the vertical plane A-A



Solution ID	Coupled / Decoupled	With furniture	Turbulence model	Inlet	Outlet	Air density and dynamic viscosity	Test Scenario
D3	Coupled	Yes	k-ε	Wind log profile (NE direction)	Actual curve fan	Actual test condition	Scenario 3

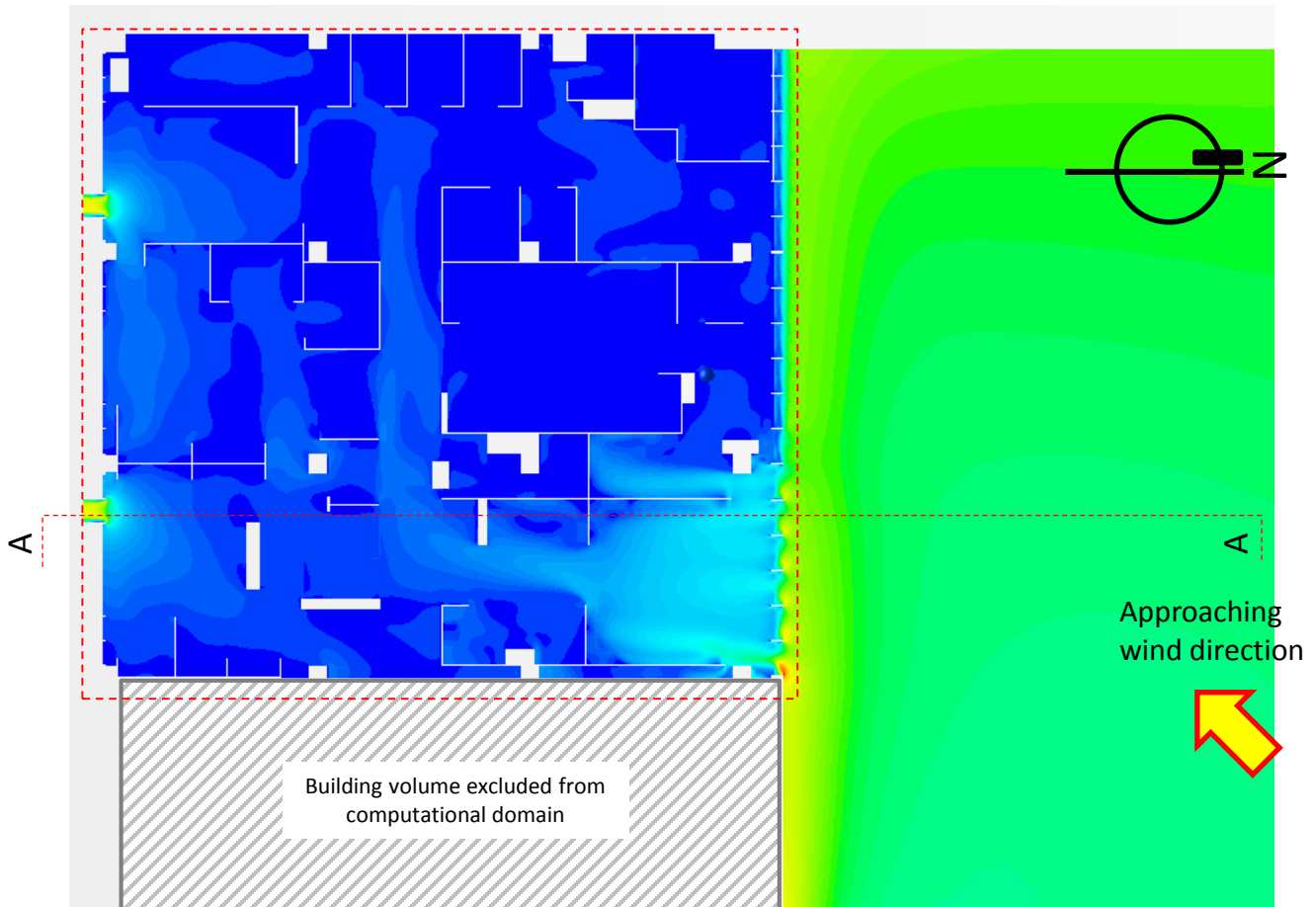


Residual plot

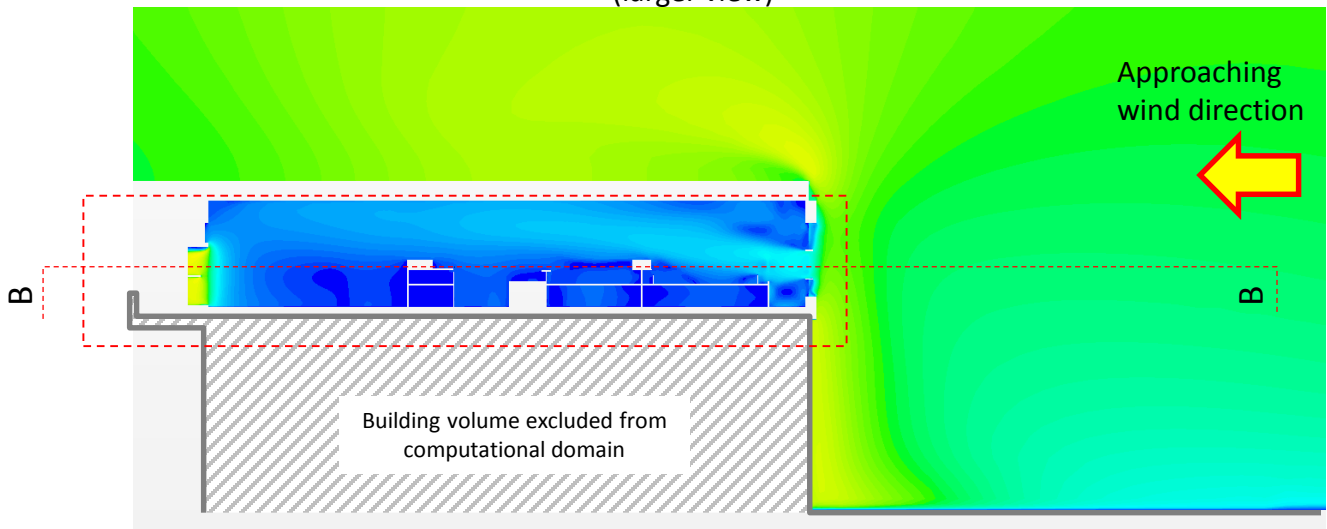


Monitoring plot of wind speed at the locations for placement of sensors for convergence checking

Solution ID	Coupled / Decoupled	With furniture	Turbulence model	Inlet	Outlet	Air density and dynamic viscosity	Test Scenario
D4	Coupled	Yes	k-ε	Wind log profile (NE direction)	Actual curve fan	Actual test condition	Scenario 4



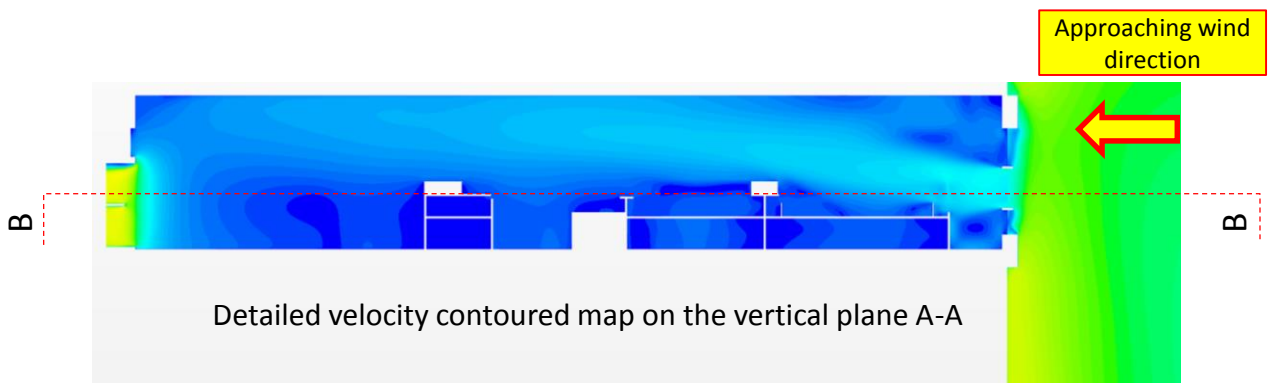
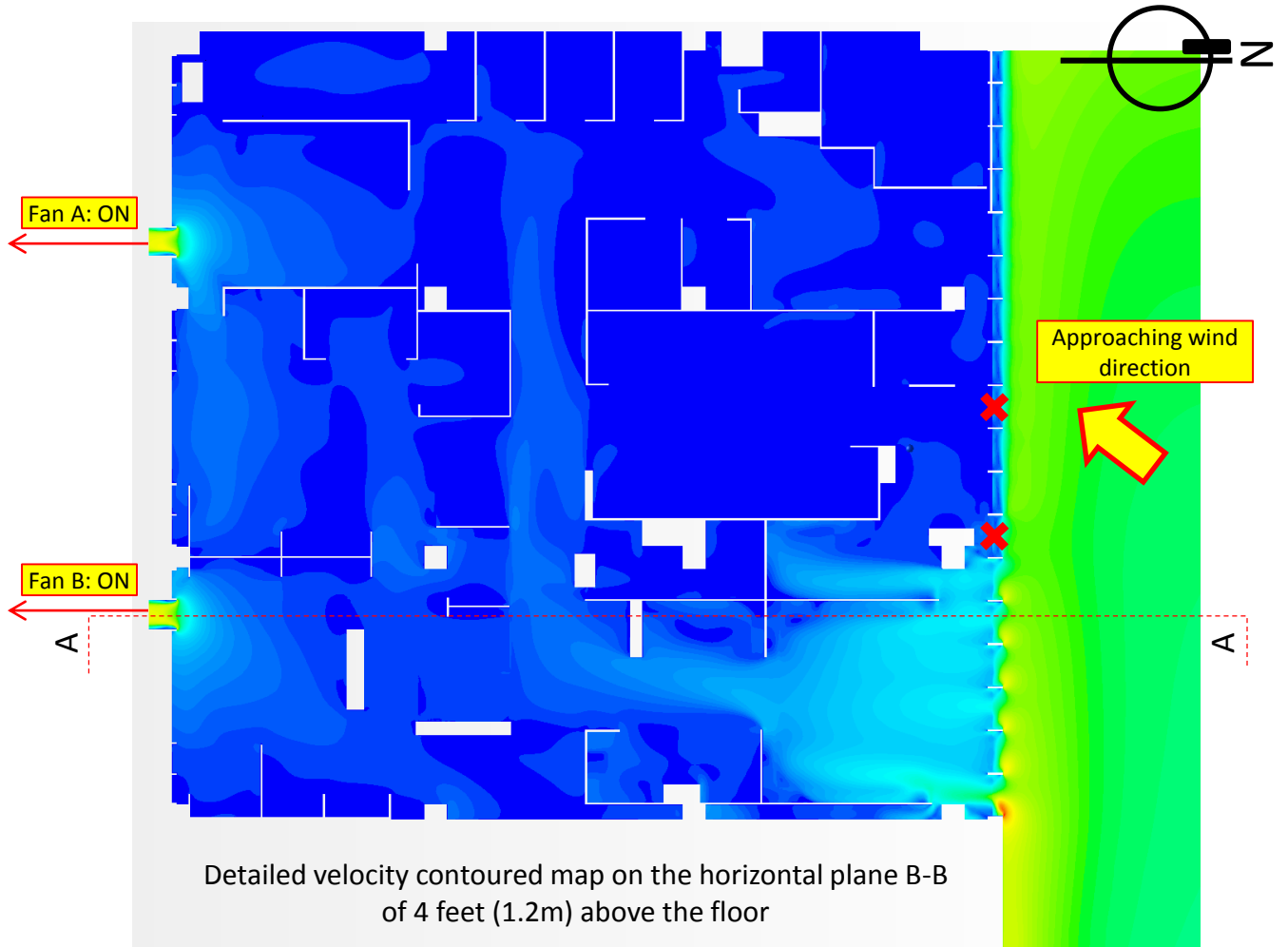
Velocity contoured map on the horizontal plane B-B of 4 feet (1.2m) above the floor (larger view)



Velocity contoured map on the vertical plane A-A (larger view)

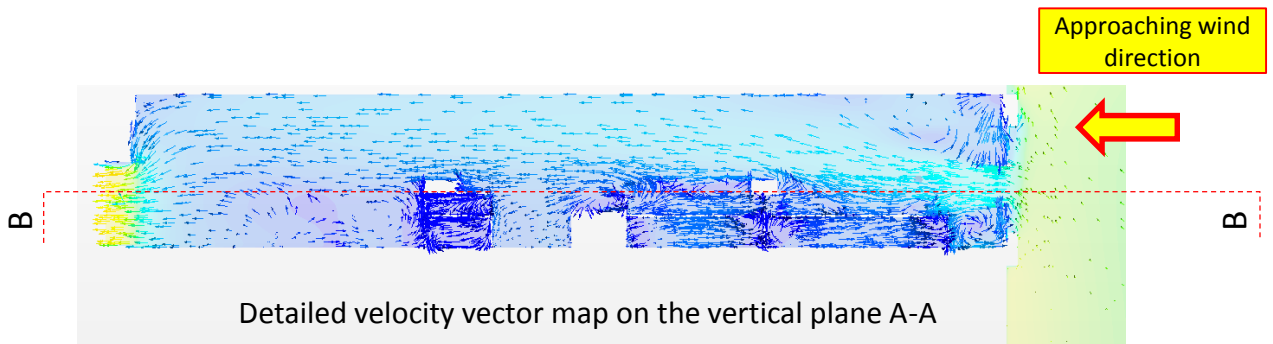
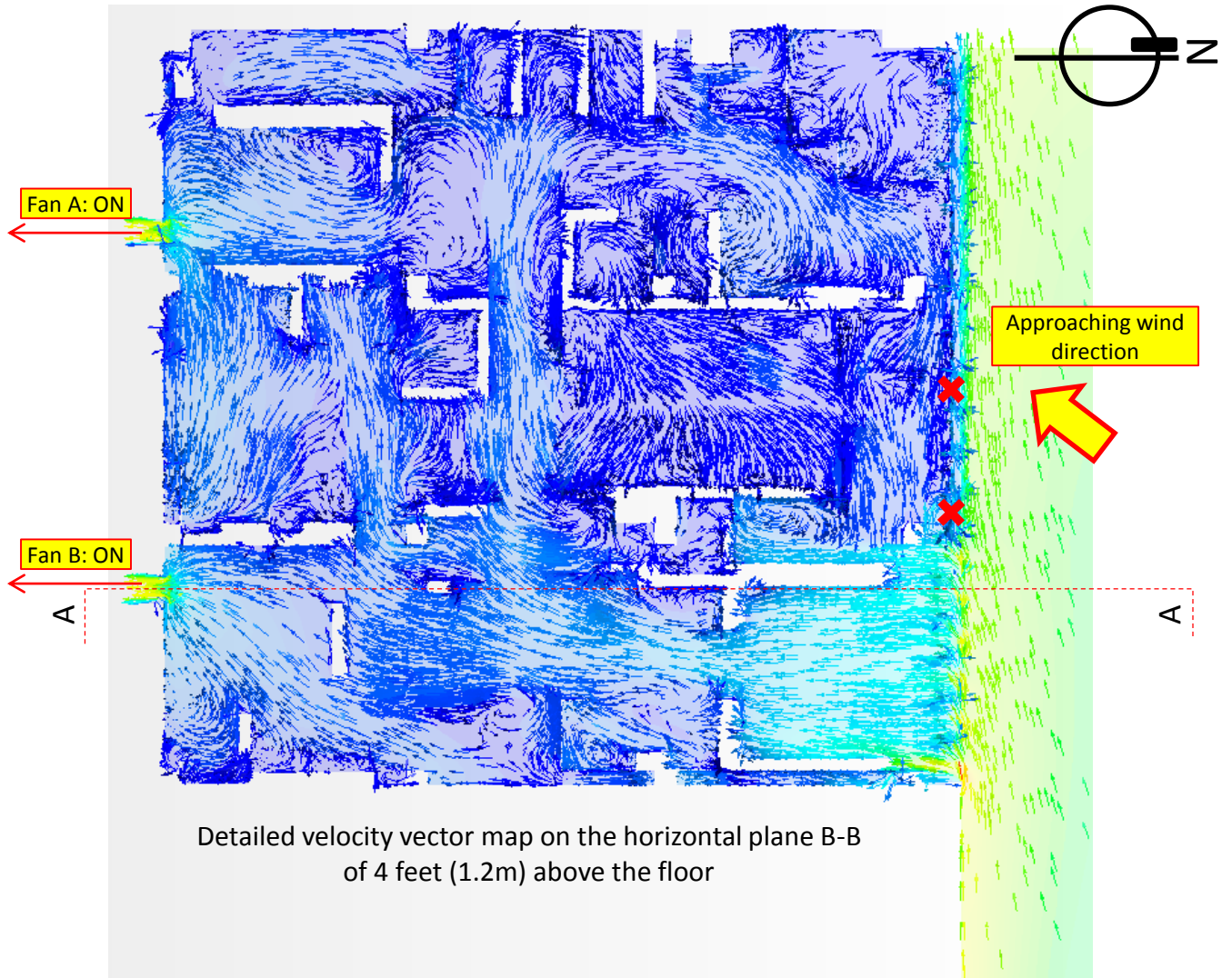


Solution ID	Coupled / Decoupled	With furniture	Turbulence model	Inlet	Outlet	Air density and dynamic viscosity	Test Scenario
D4	Coupled	Yes	k-ε	Wind log profile (NE direction)	Actual curve fan	Actual test condition	Scenario 4



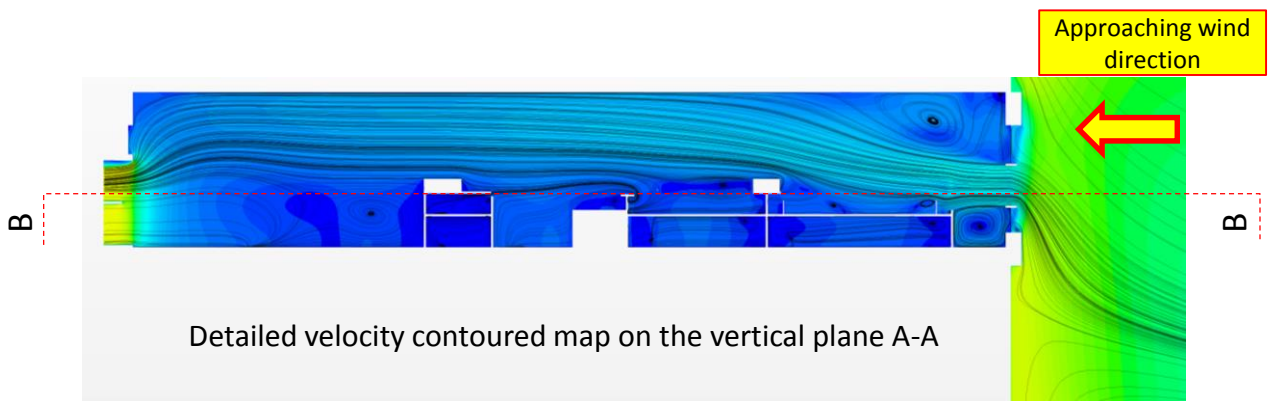
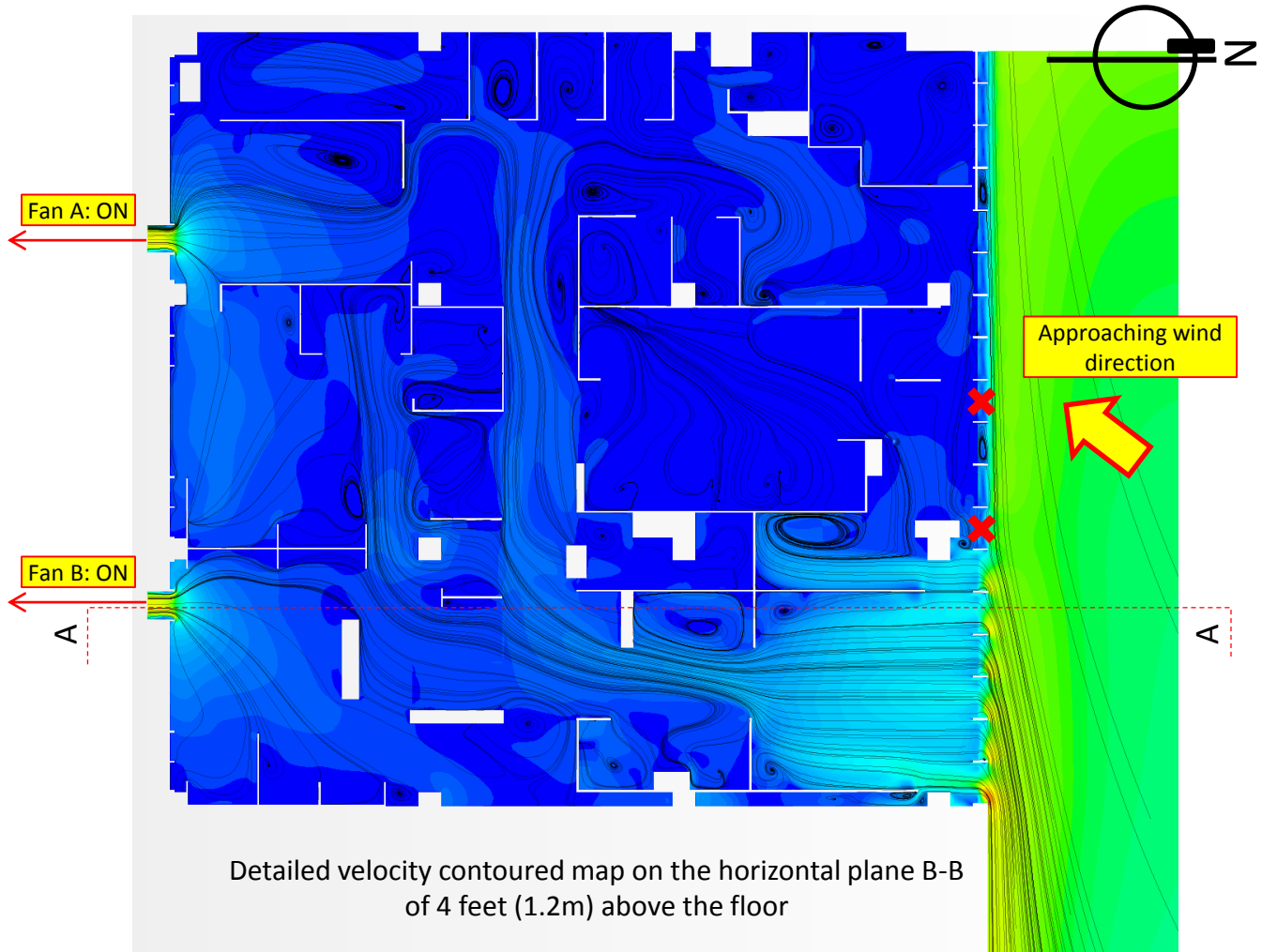
✗ Permanently closed non-working louvers

Solution ID	Coupled / Decoupled	With furniture	Turbulence model	Inlet	Outlet	Air density and dynamic viscosity	Test Scenario
D4	Coupled	Yes	k-ε	Wind log profile (NE direction)	Actual curve fan	Actual test condition	Scenario 4



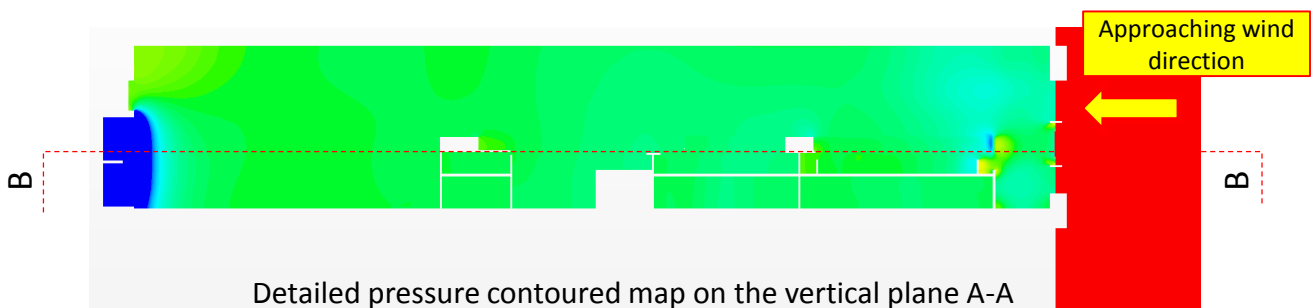
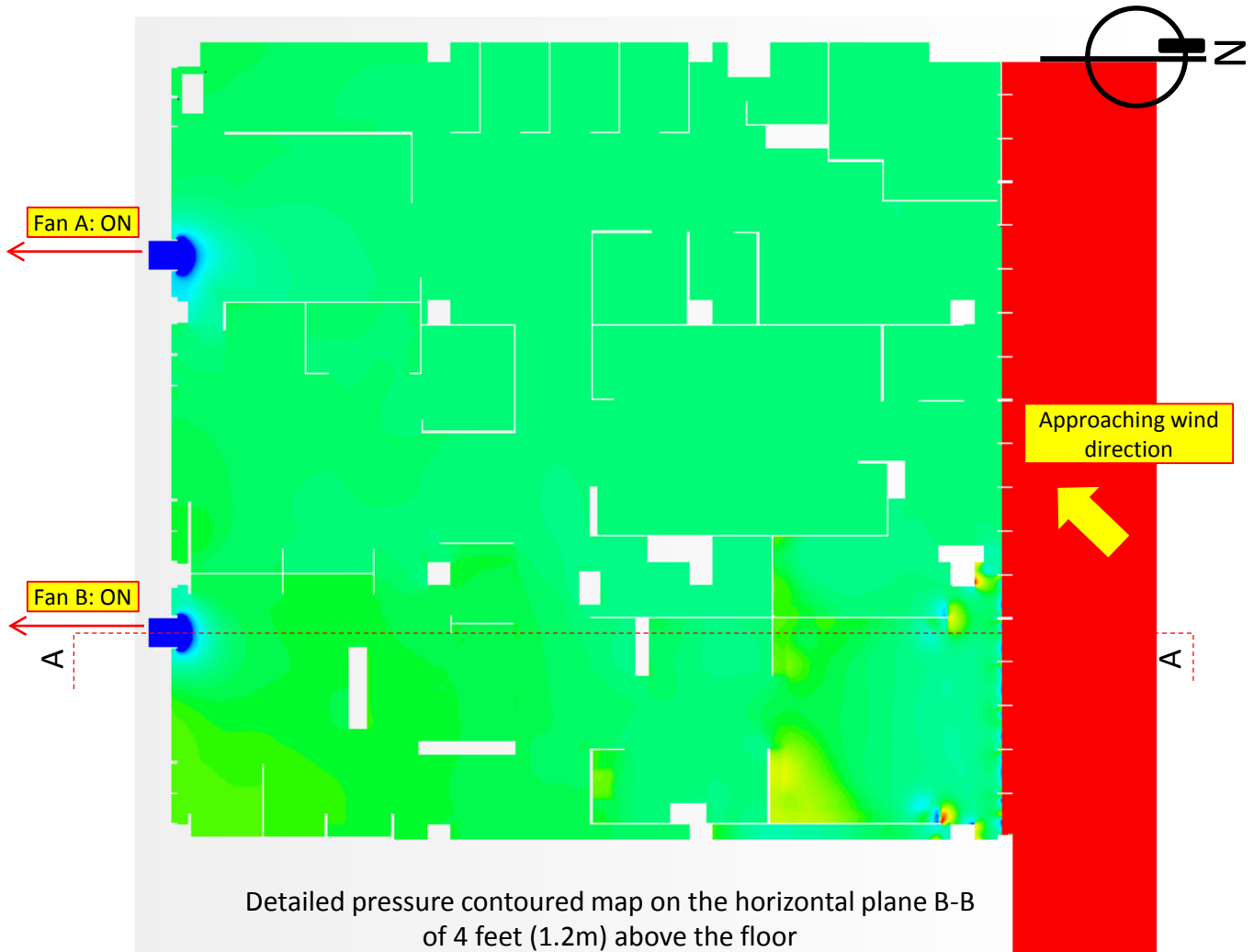
✘ Permanently closed non-working louvers

Solution ID	Coupled / Decoupled	With furniture	Turbulence model	Inlet	Outlet	Air density and dynamic viscosity	Test Scenario
D4	Coupled	Yes	k-ε	Wind log profile (NE direction)	Actual curve fan	Actual test condition	Scenario 4

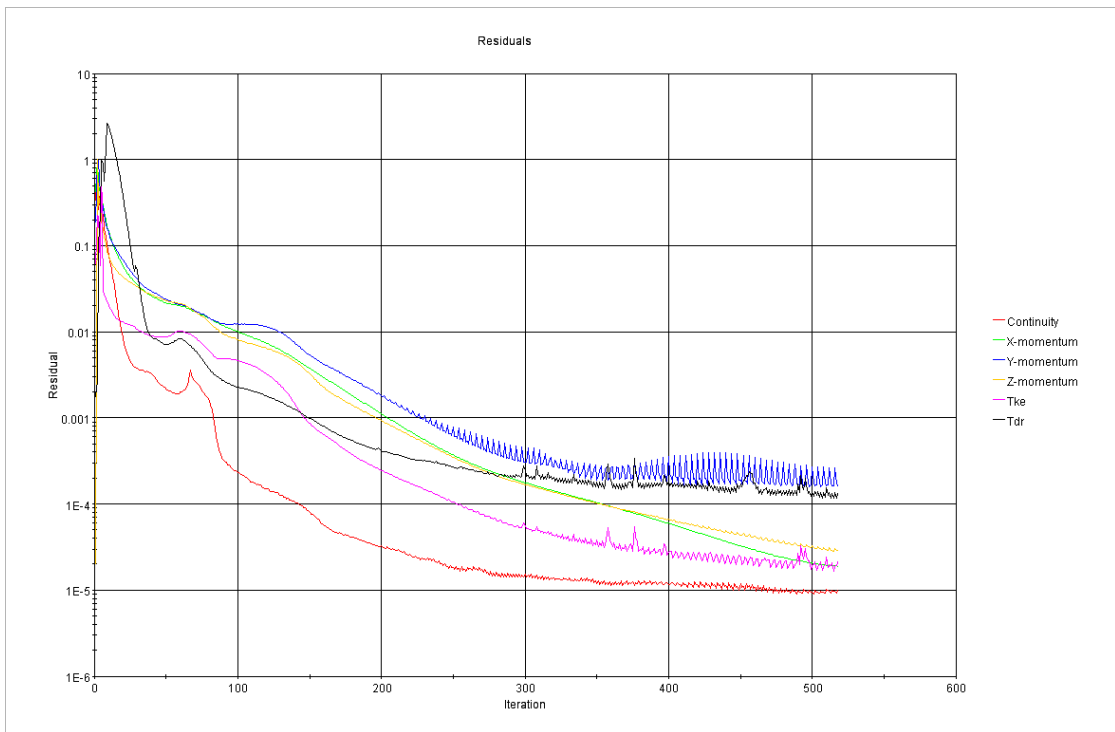


✘ Permanently closed non-working louvers

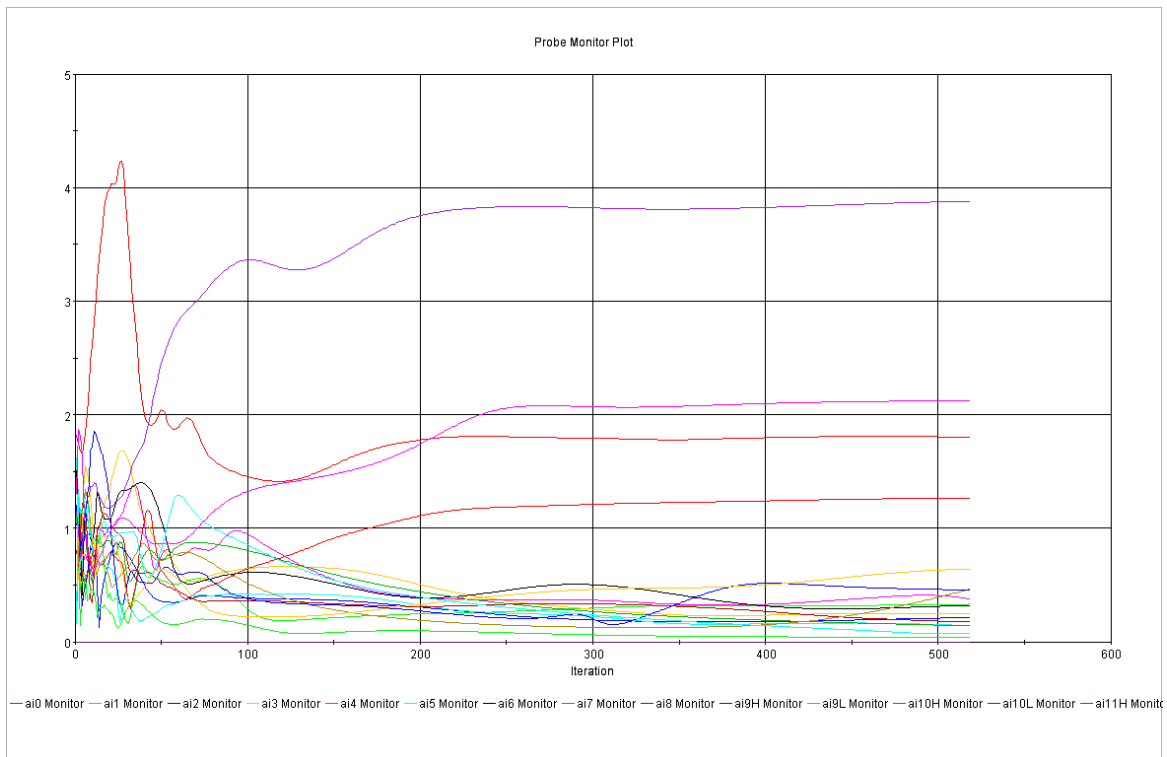
Solution ID	Coupled / Decoupled	With furniture	Turbulence model	Inlet	Outlet	Air density and dynamic viscosity	Test Scenario
D4	Coupled	Yes	k-ε	Wind log profile (NE direction)	Actual curve fan	Actual test condition	Scenario 4



Solution ID	Coupled / Decoupled	With furniture	Turbulence model	Inlet	Outlet	Air density and dynamic viscosity	Test Scenario
D4	Coupled	Yes	k-ε	Wind log profile (NE direction)	Actual curve fan	Actual test condition	Scenario 4

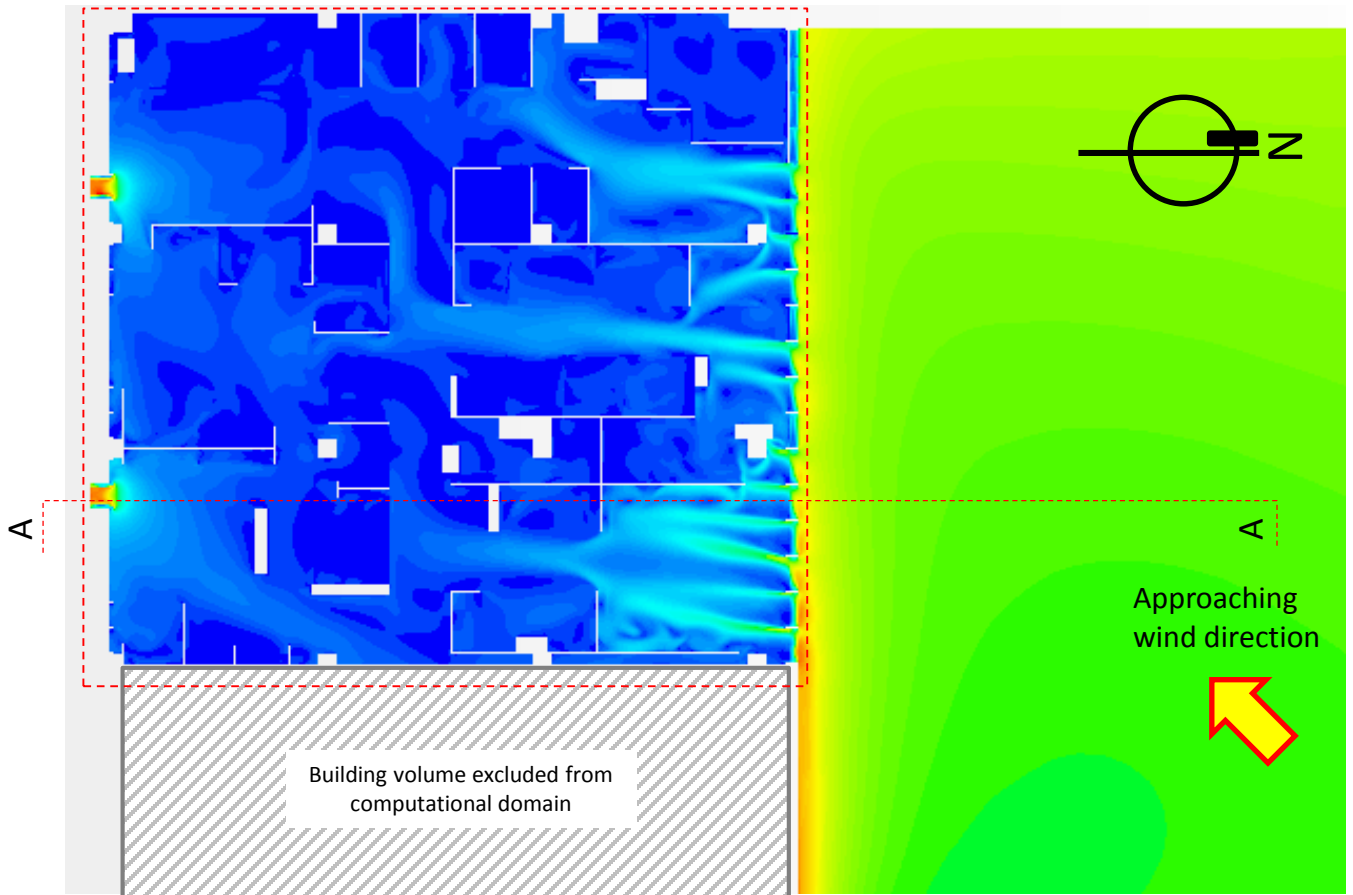


Residual plot

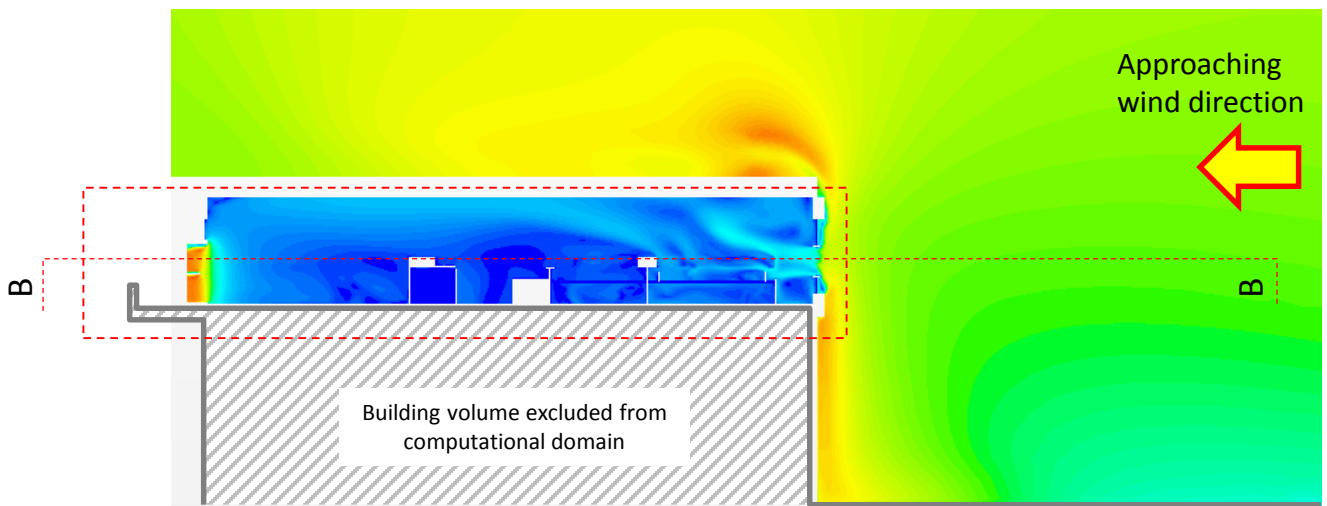


Monitoring plot of wind speed at the locations for placement of sensors for convergence checking

Solution ID	Coupled / Decoupled	With furniture	Turbulence model	Inlet	Outlet	Air density and dynamic viscosity	Test Scenario
E1	Coupled	Yes	k- ω	Wind log profile (NE direction)	Actual curve fan	Actual test condition	Scenario 1



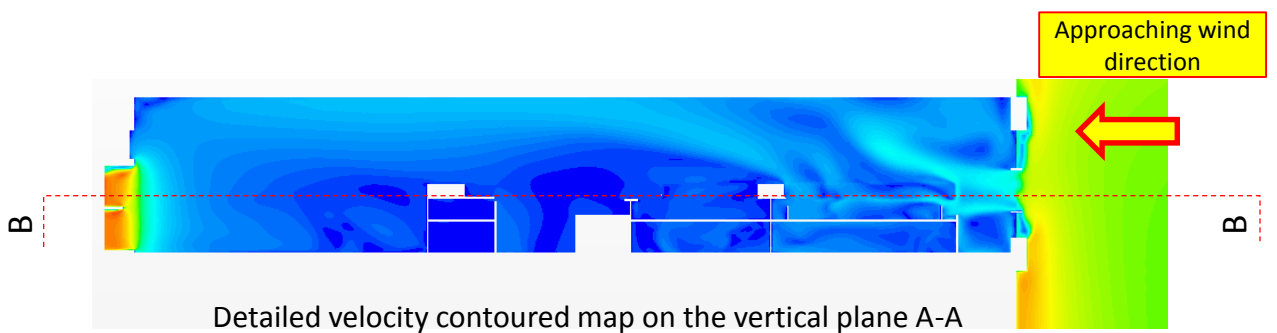
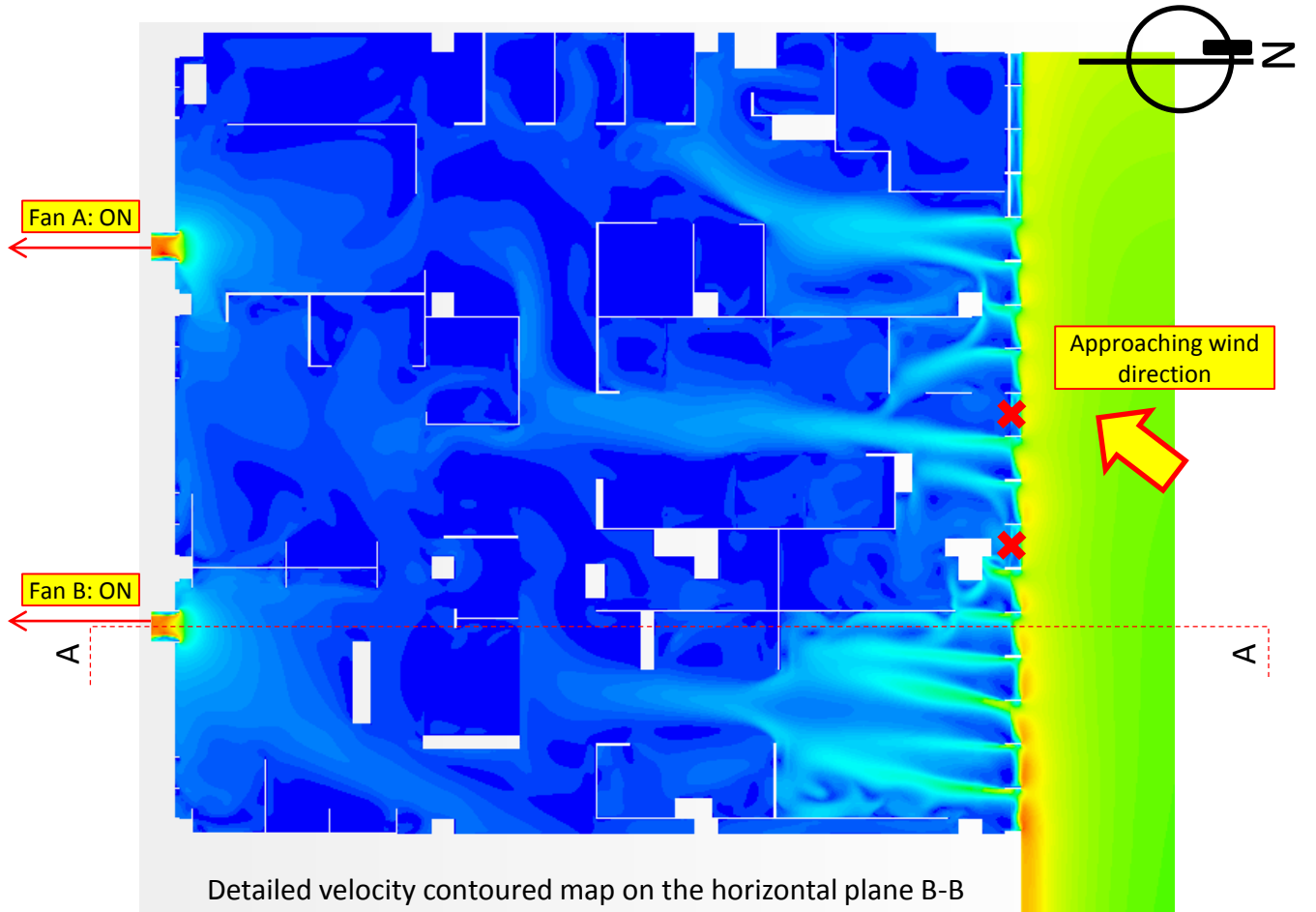
Velocity contoured map on the horizontal plane B-B of 4 feet (1.2m) above the floor (larger view)



Velocity contoured map on the vertical plane A-A (larger view)

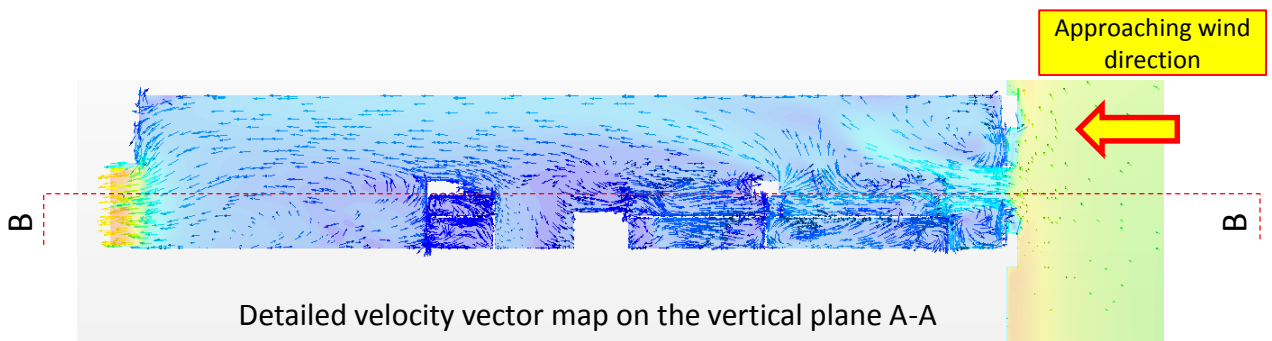
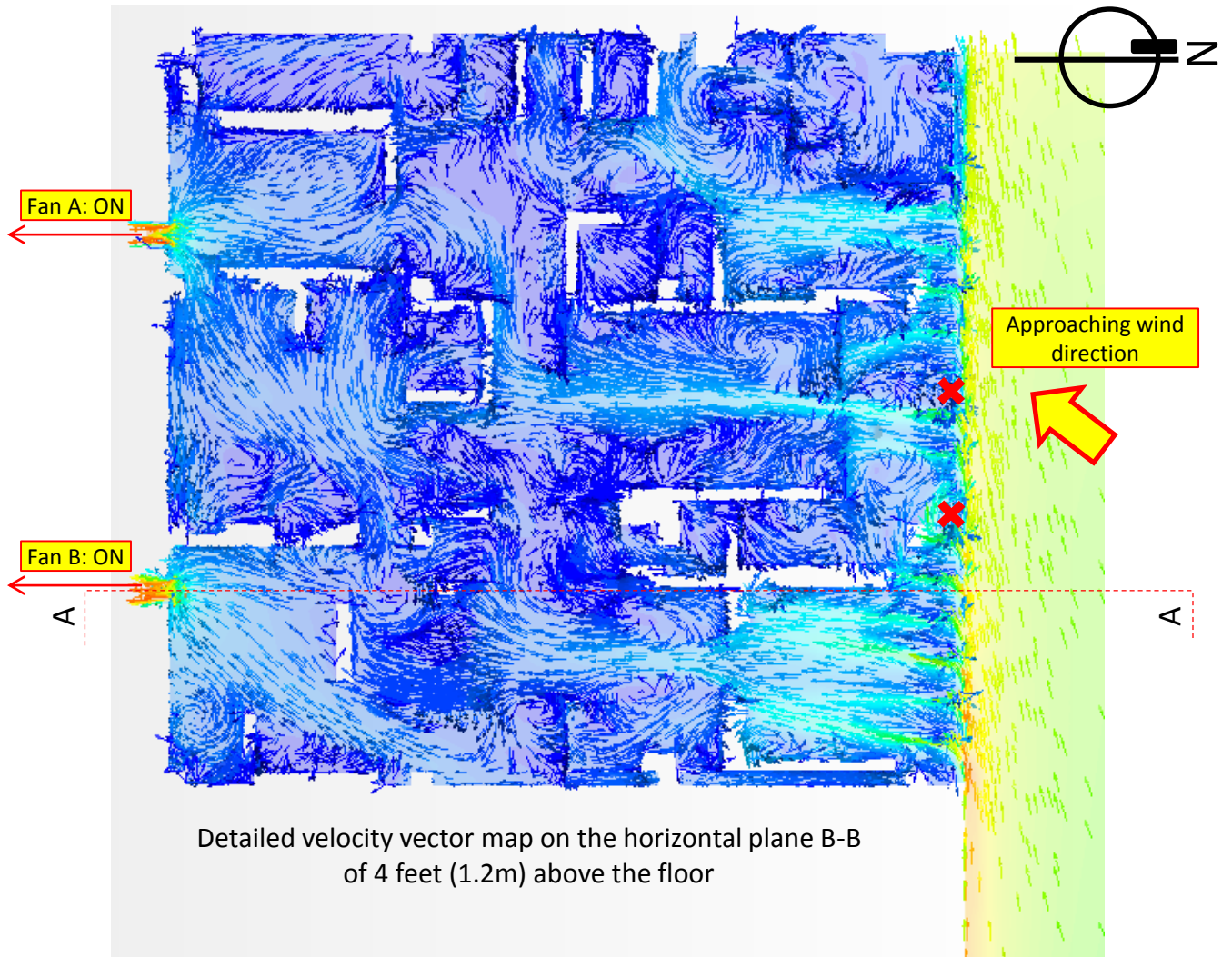


Solution ID	Coupled / Decoupled	With furniture	Turbulence model	Inlet	Outlet	Air density and dynamic viscosity	Test Scenario
E1	Coupled	Yes	k- ω	Wind log profile (NE direction)	Actual curve fan	Actual test condition	Scenario 1



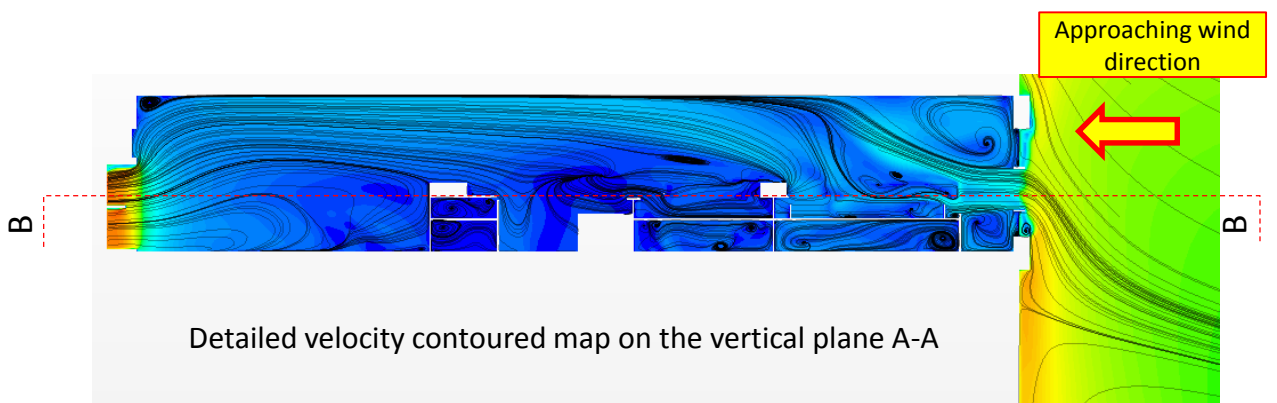
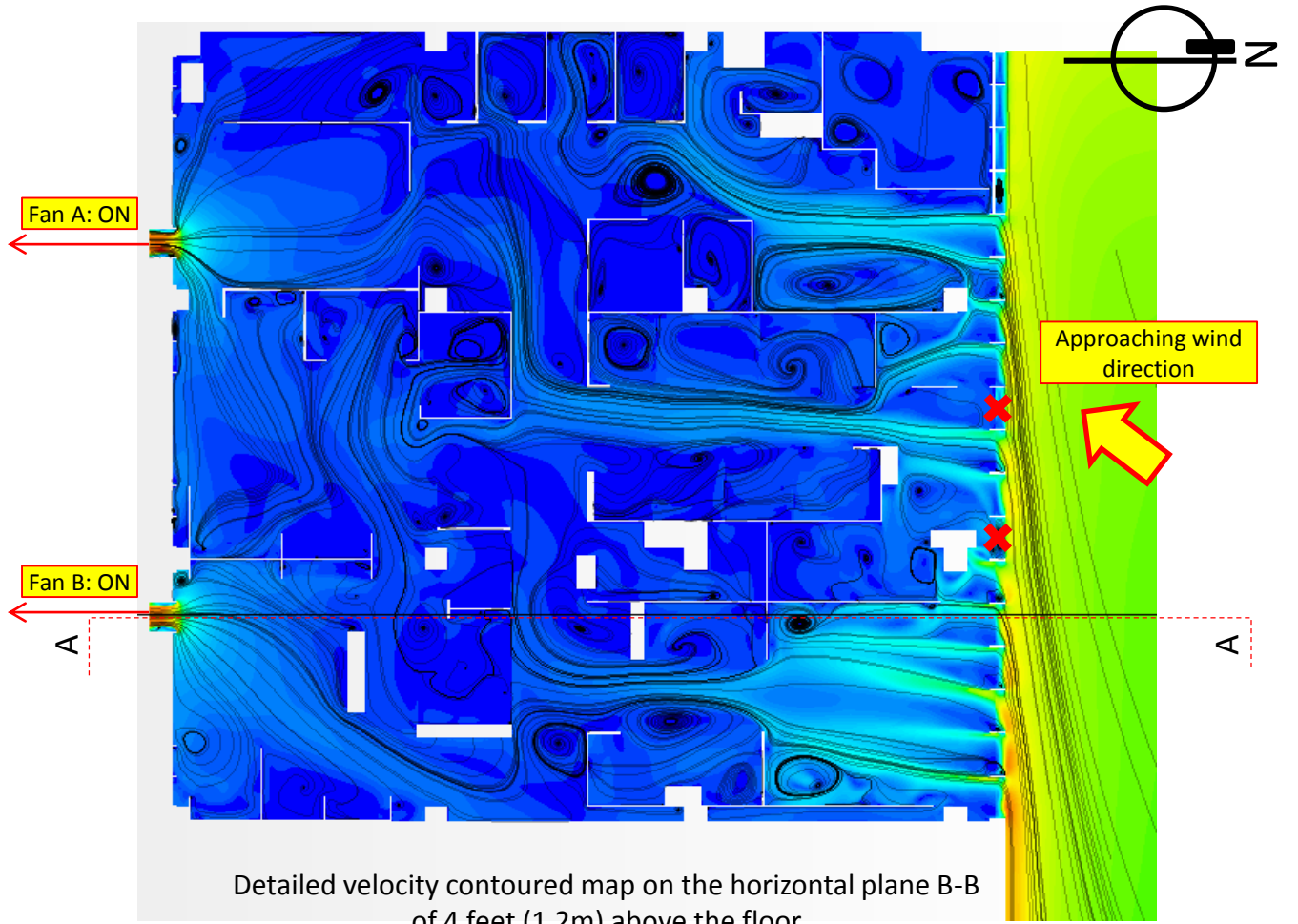
X Permanently closed non-working louvers

Solution ID	Coupled / Decoupled	With furniture	Turbulence model	Inlet	Outlet	Air density and dynamic viscosity	Test Scenario
E1	Coupled	Yes	k- ω	Wind log profile (NE direction)	Actual curve fan	Actual test condition	Scenario 1



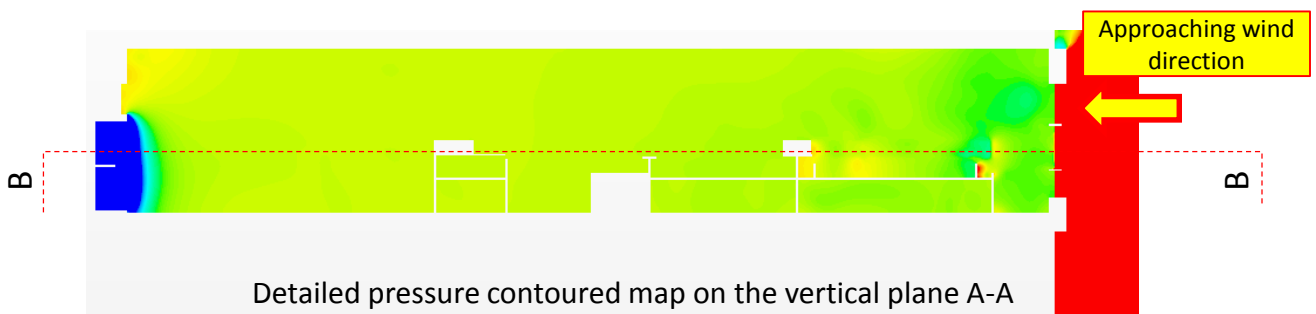
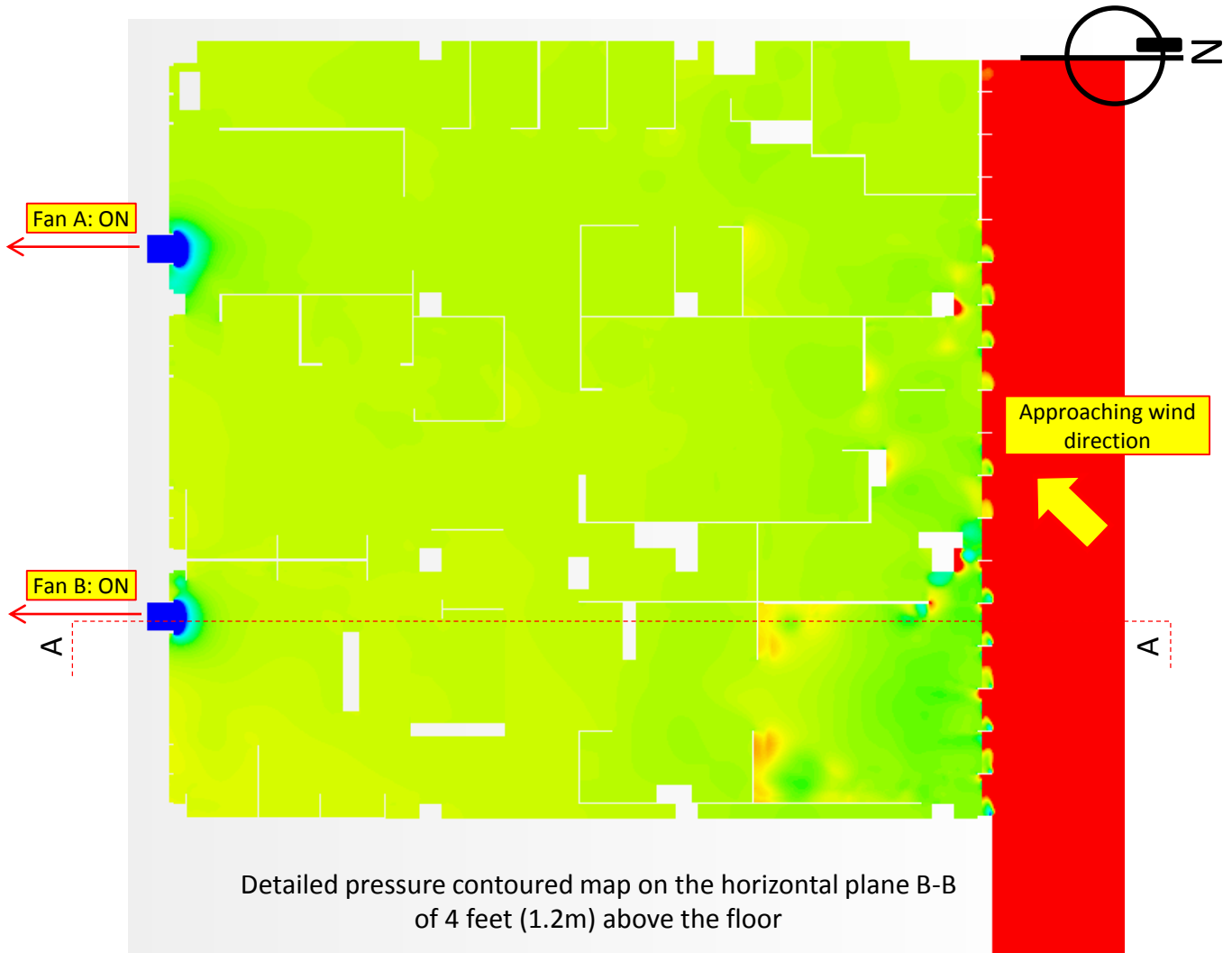
✘ Permanently closed non-working louvers

Solution ID	Coupled / Decoupled	With furniture	Turbulence model	Inlet	Outlet	Air density and dynamic viscosity	Test Scenario
E1	Coupled	Yes	k- ω	Wind log profile (NE direction)	Actual curve fan	Actual test condition	Scenario 1

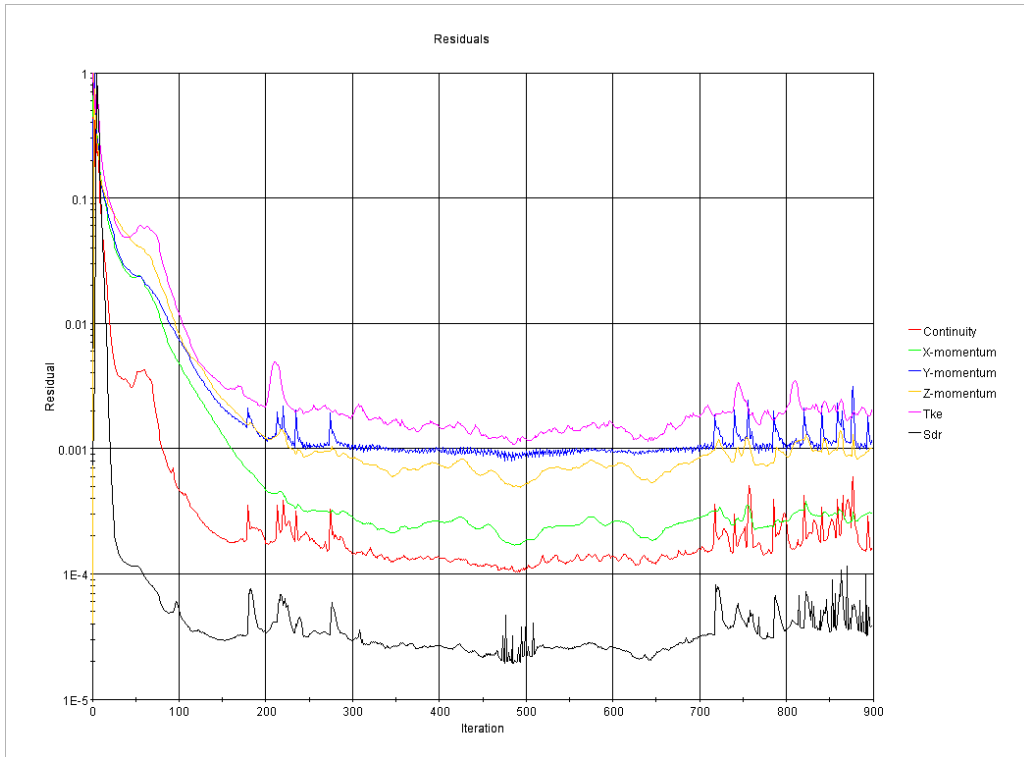


✘ Permanently closed non-working louvers

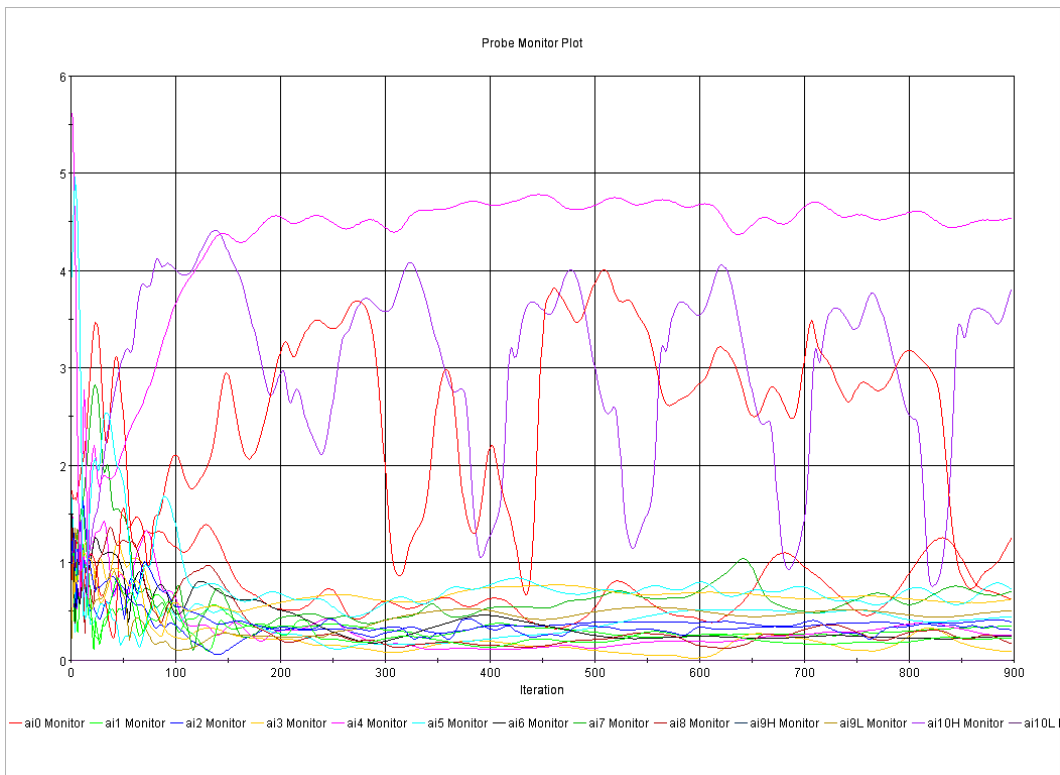
Solution ID	Coupled / Decoupled	With furniture	Turbulence model	Inlet	Outlet	Air density and dynamic viscosity	Test Scenario
E1	Coupled	Yes	k- ω	Wind log profile (NE direction)	Actual curve fan	Actual test condition	Scenario 1



Solution ID	Coupled / Decoupled	With furniture	Turbulence model	Inlet	Outlet	Air density and dynamic viscosity	Test Scenario
E1	Coupled	Yes	k- ω	Wind log profile (NE direction)	Actual curve fan	Actual test condition	Scenario 1

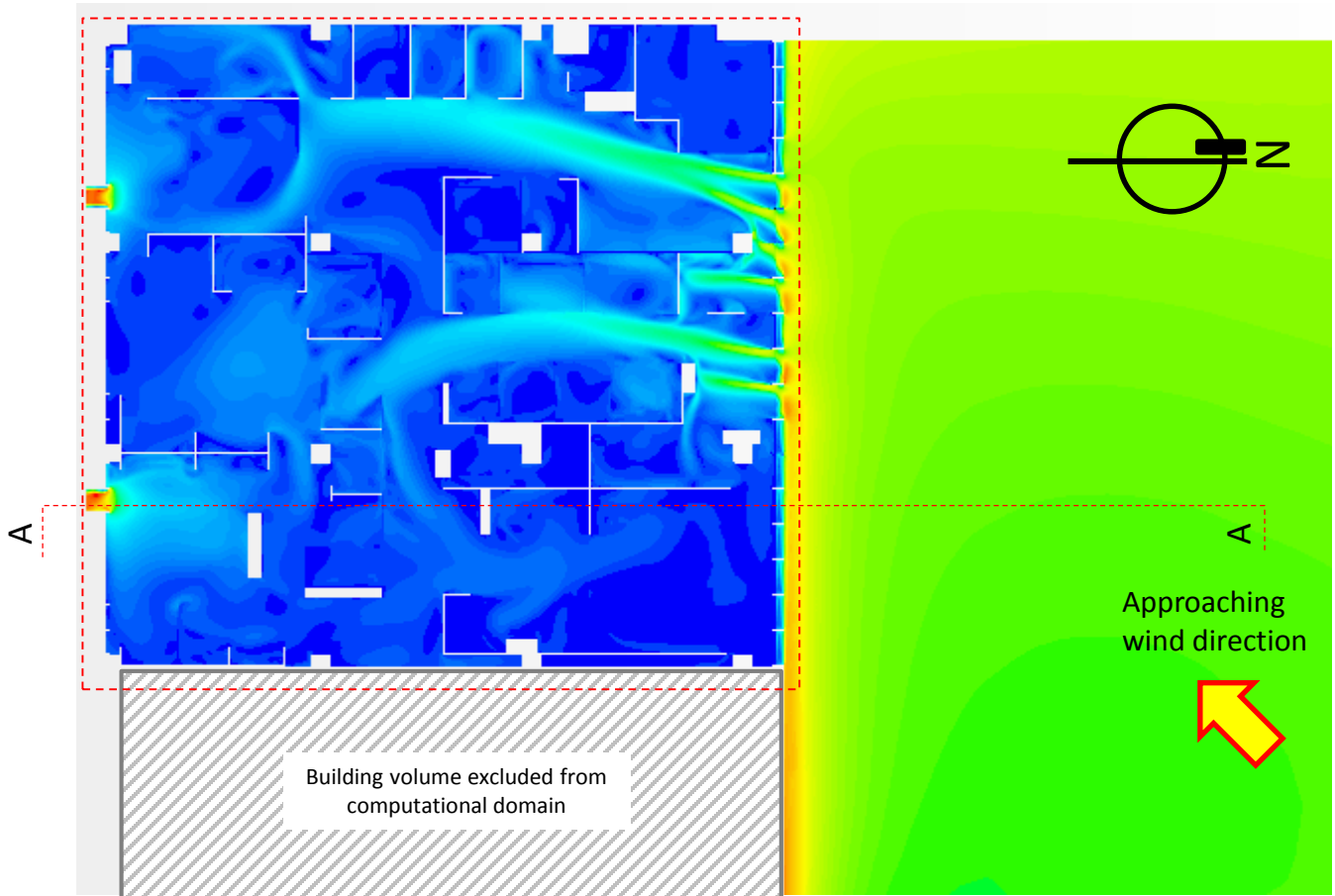


Residual plot

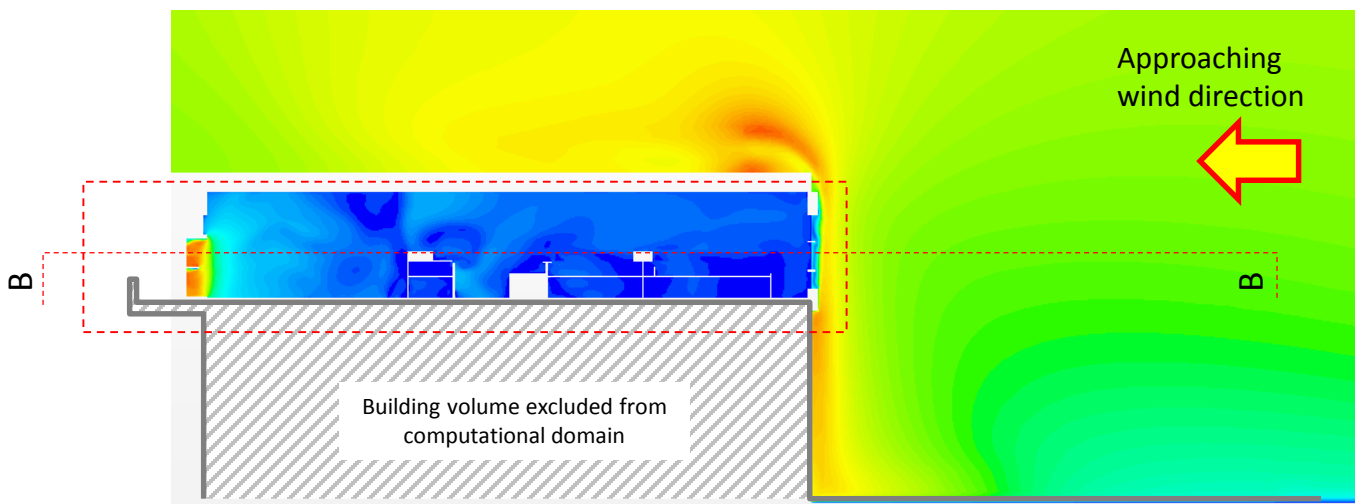


Monitoring plot of wind speed at the locations for placement of sensors for convergence checking

Solution ID	Coupled / Decoupled	With furniture	Turbulence model	Inlet	Outlet	Air density and dynamic viscosity	Test Scenario
E2	Coupled	Yes	k- ω	Wind log profile (NE direction)	Actual curve fan	Actual test condition	Scenario 2



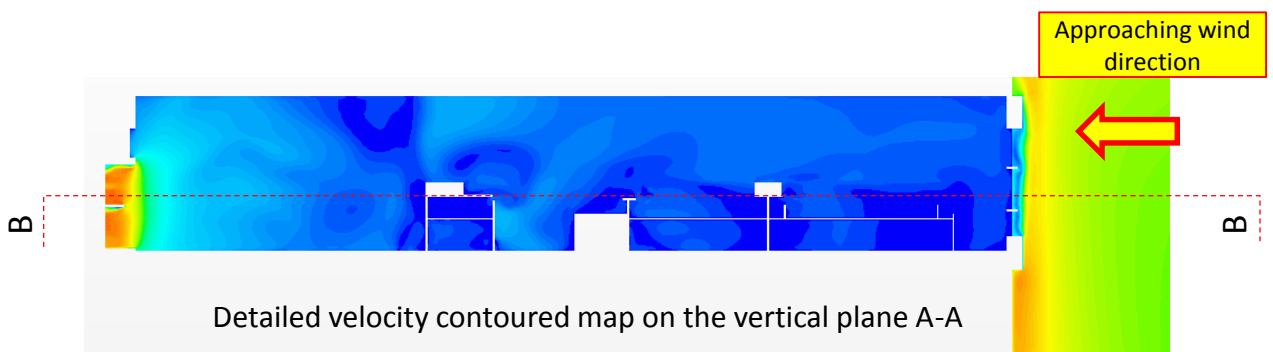
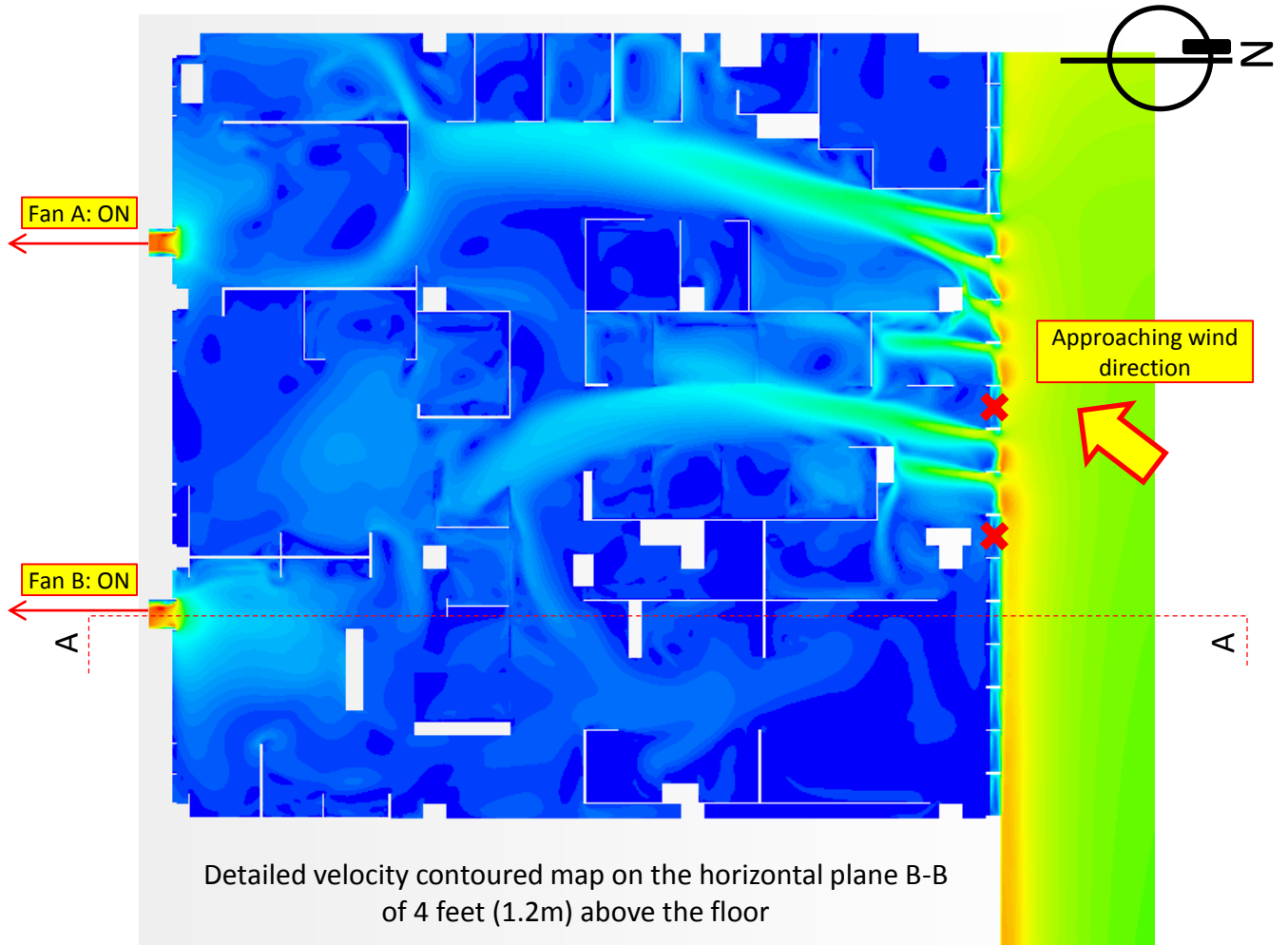
Velocity contoured map on the horizontal plane B-B of 4 feet (1.2m) above the floor (larger view)



Velocity contoured map on the vertical plane A-A (larger view)

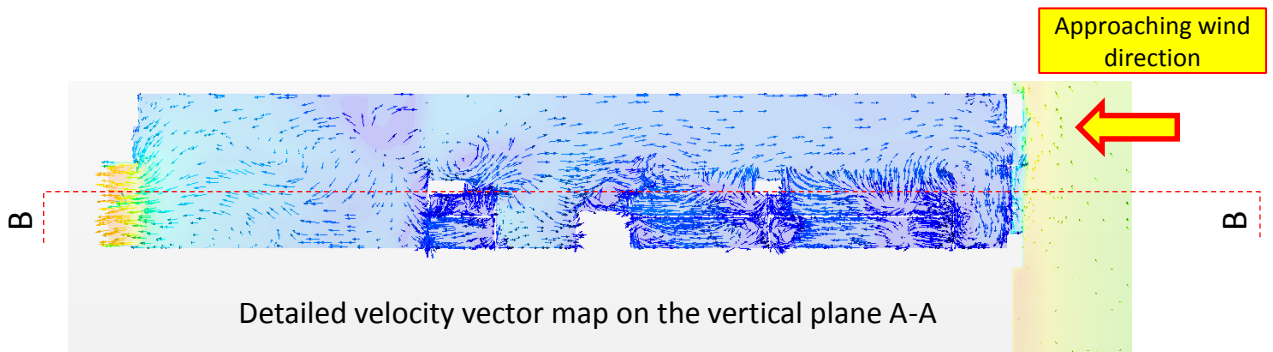
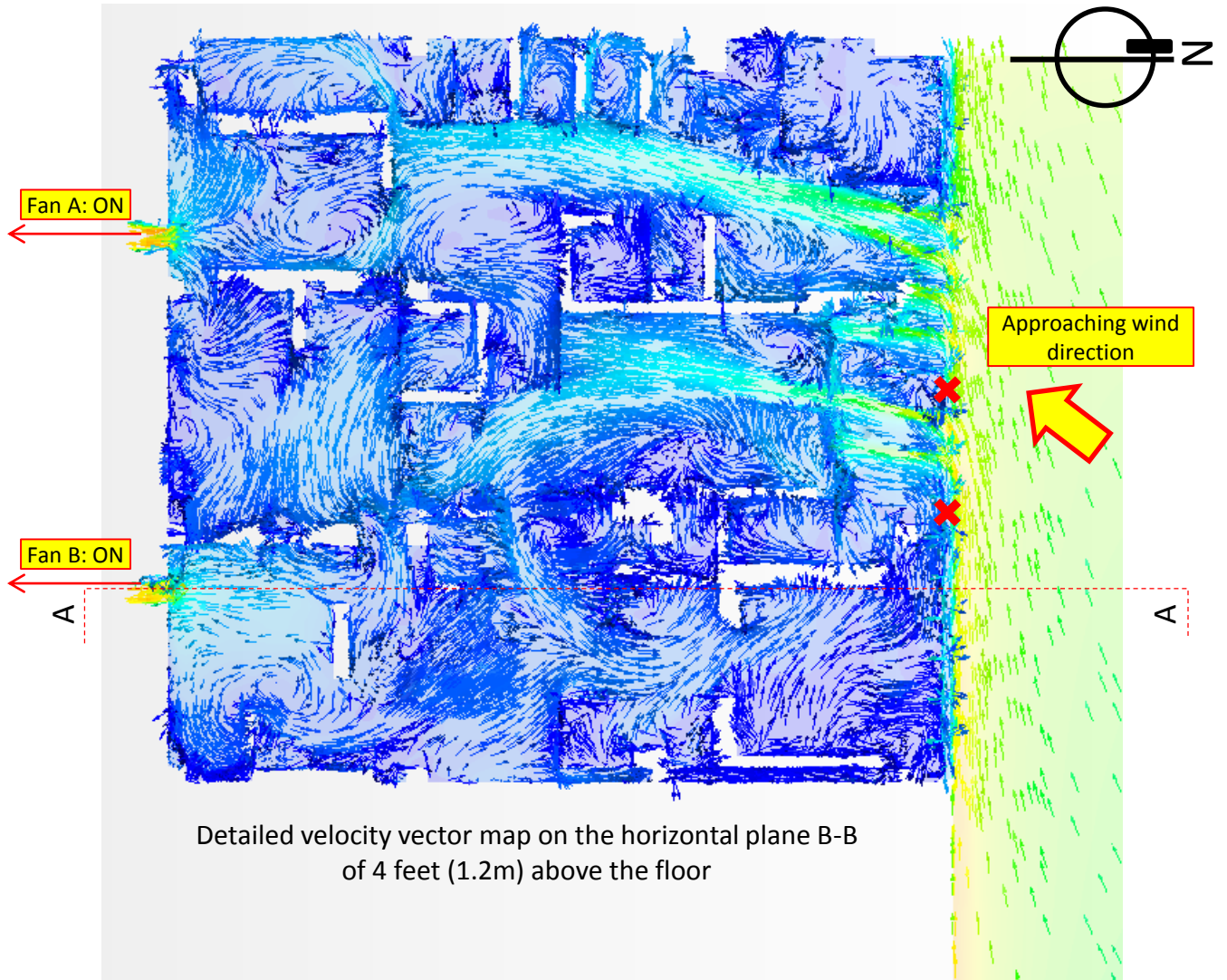


Solution ID	Coupled / Decoupled	With furniture	Turbulence model	Inlet	Outlet	Air density and dynamic viscosity	Test Scenario
E2	Coupled	Yes	k- ω	Wind log profile (NE direction)	Actual curve fan	Actual test condition	Scenario 2



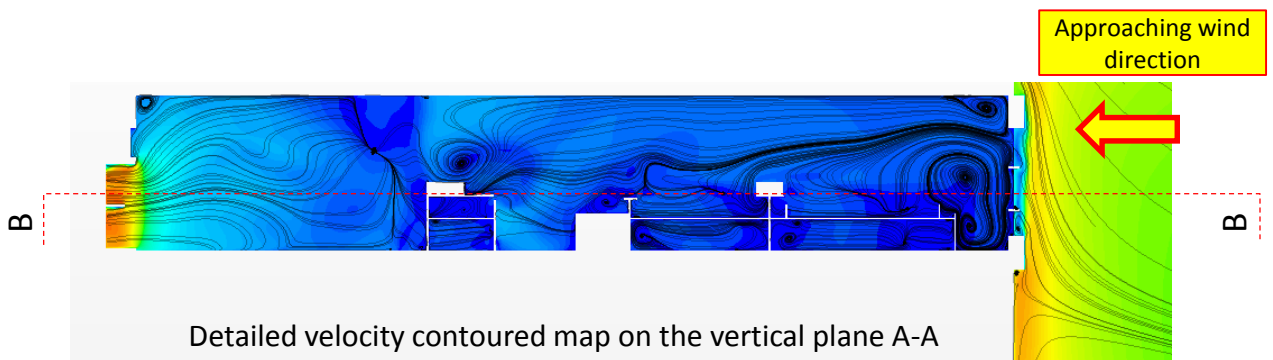
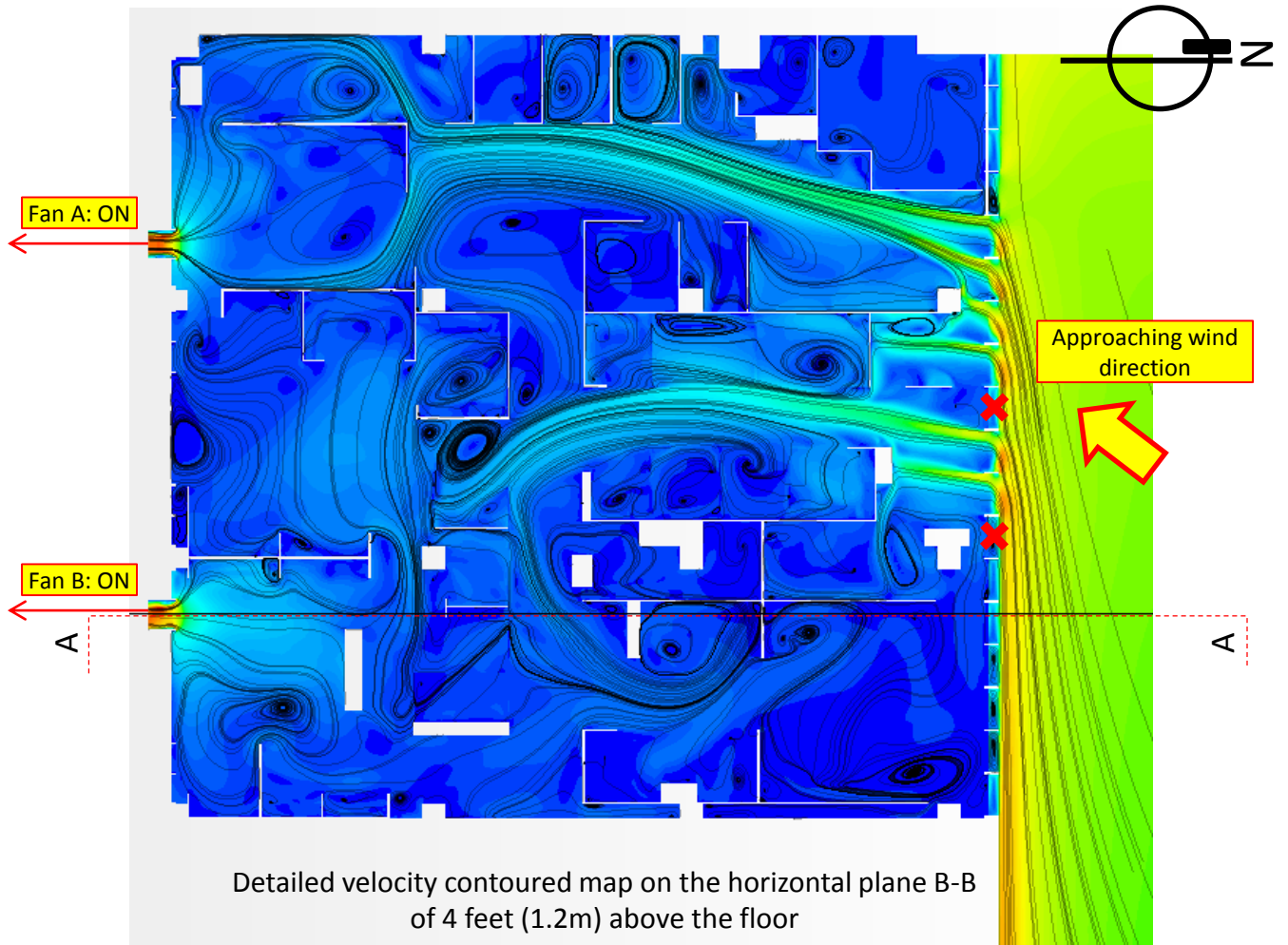
✘ Permanently closed non-working louvers

Solution ID	Coupled / Decoupled	With furniture	Turbulence model	Inlet	Outlet	Air density and dynamic viscosity	Test Scenario
E2	Coupled	Yes	k- ω	Wind log profile (NE direction)	Actual curve fan	Actual test condition	Scenario 2



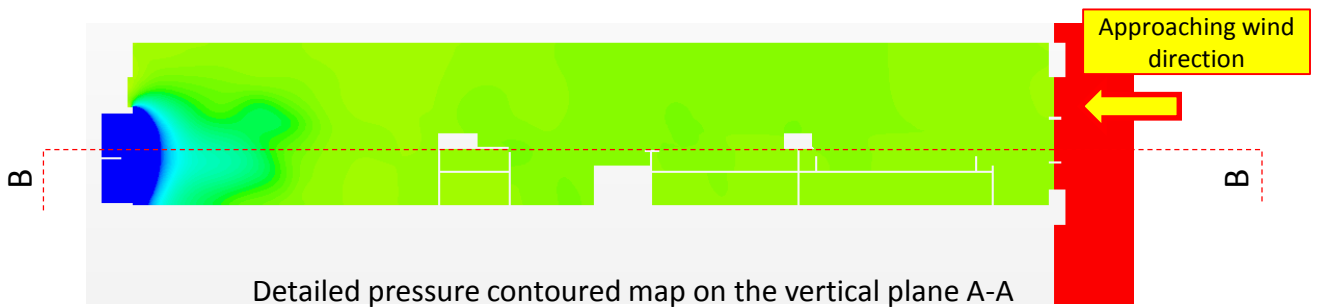
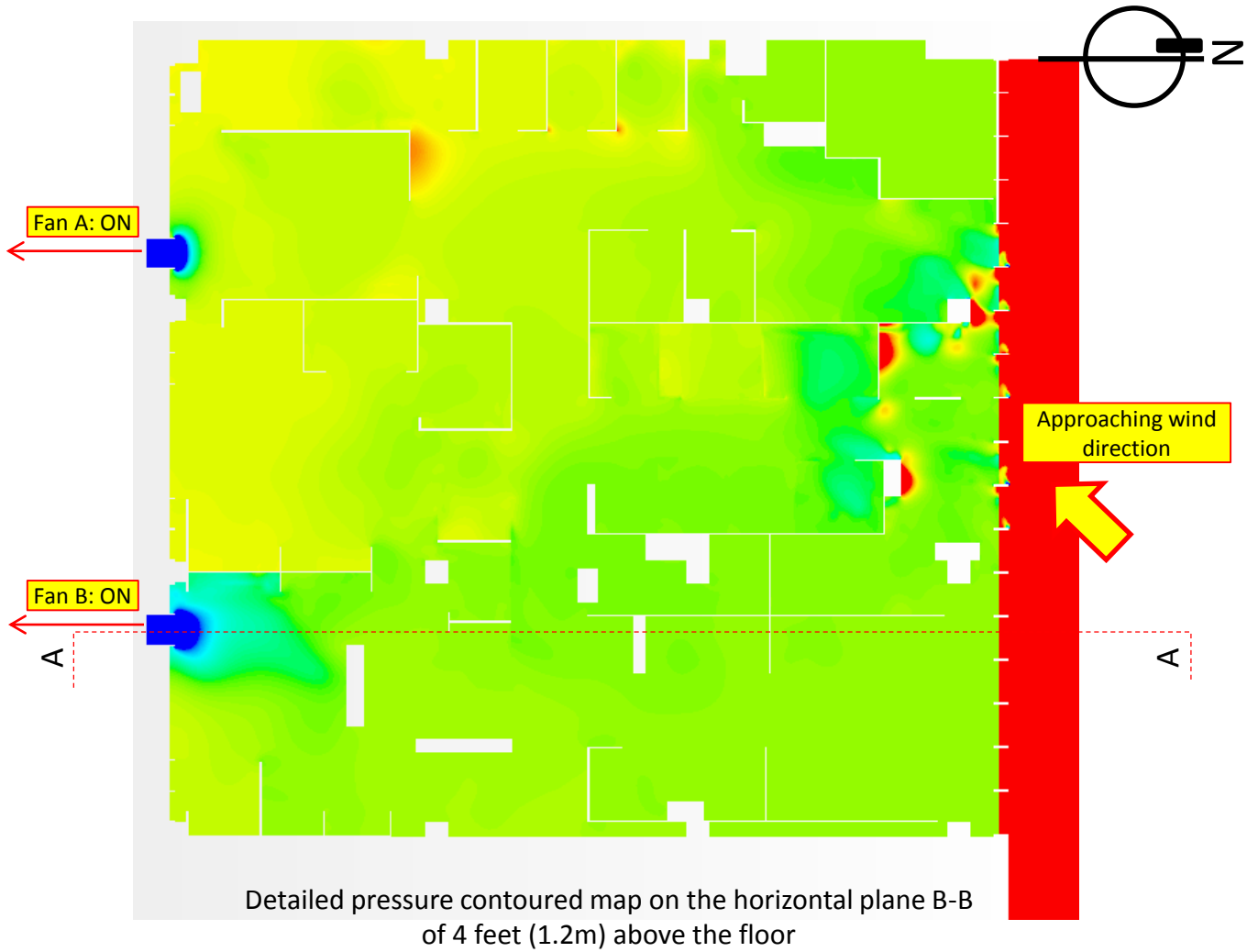
X Permanently closed non-working louvers

Solution ID	Coupled / Decoupled	With furniture	Turbulence model	Inlet	Outlet	Air density and dynamic viscosity	Test Scenario
E2	Coupled	Yes	k- ω	Wind log profile (NE direction)	Actual curve fan	Actual test condition	Scenario 2

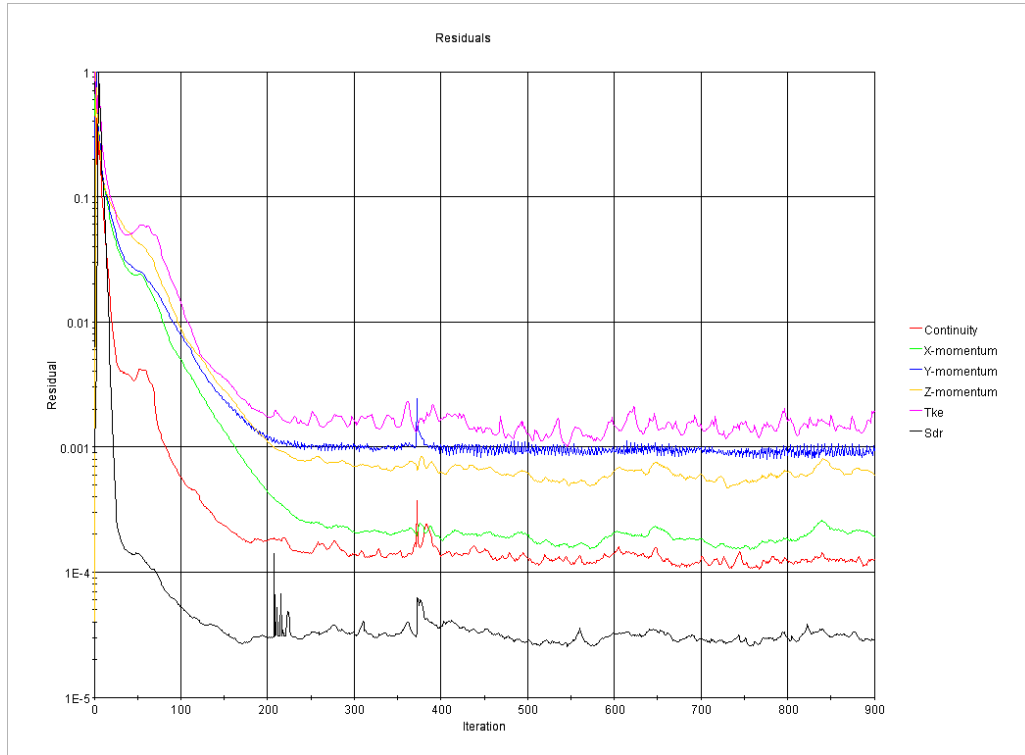


✘ Permanently closed non-working louvers

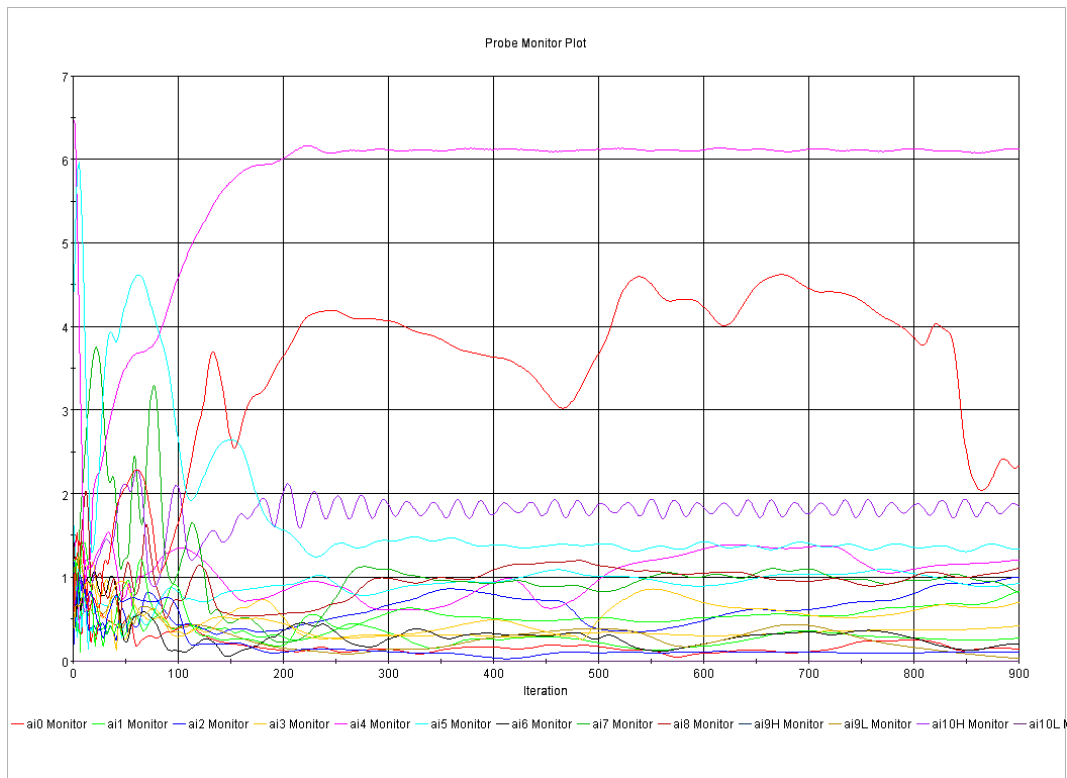
Solution ID	Coupled / Decoupled	With furniture	Turbulence model	Inlet	Outlet	Air density and dynamic viscosity	Test Scenario
E2	Coupled	Yes	k- ω	Wind log profile (NE direction)	Actual curve fan	Actual test condition	Scenario 2



Solution ID	Coupled / Decoupled	With furniture	Turbulence model	Inlet	Outlet	Air density and dynamic viscosity	Test Scenario
E2	Coupled	Yes	k- ω	Wind log profile (NE direction)	Actual curve fan	Actual test condition	Scenario 2

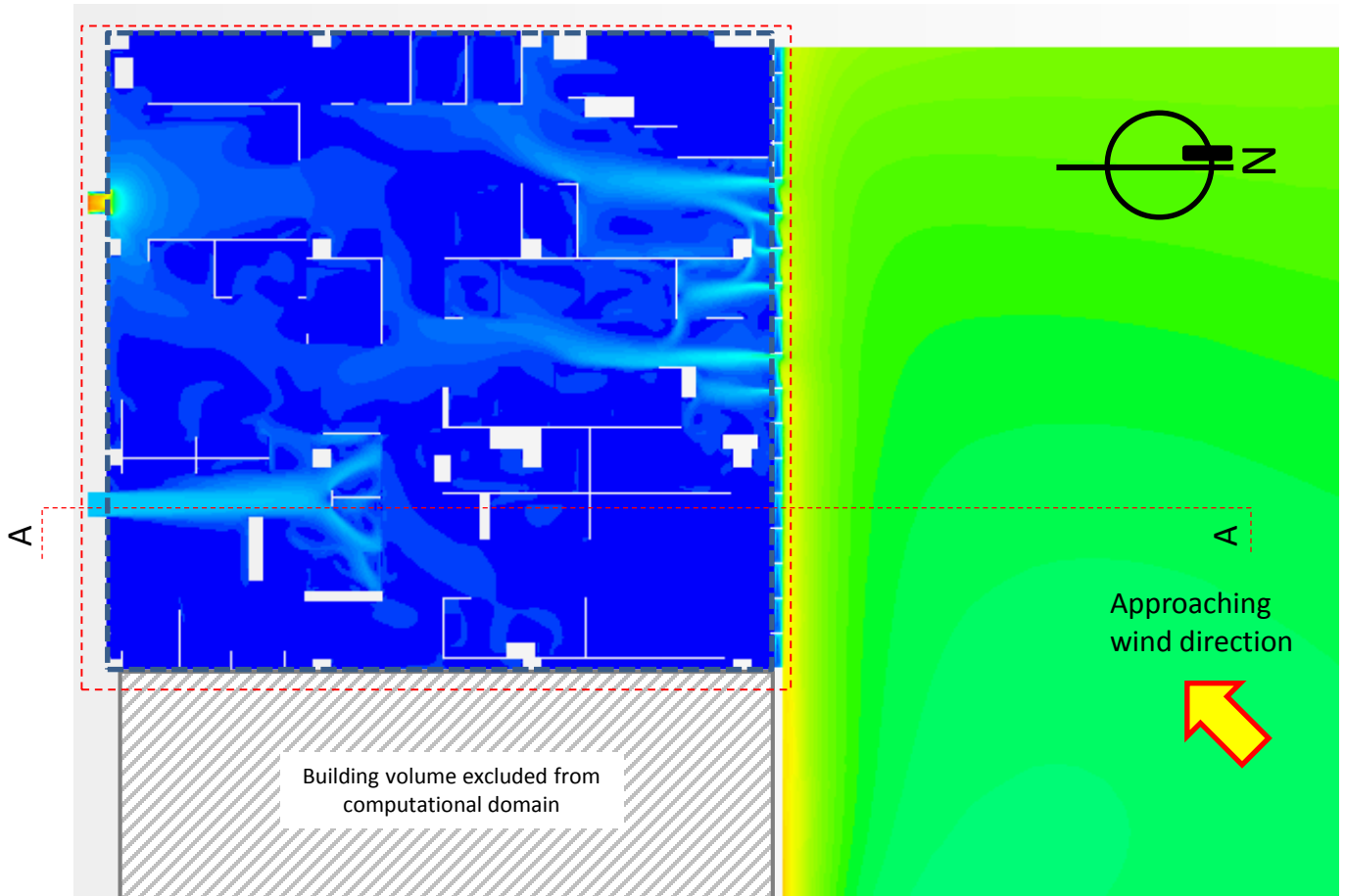


Residual plot

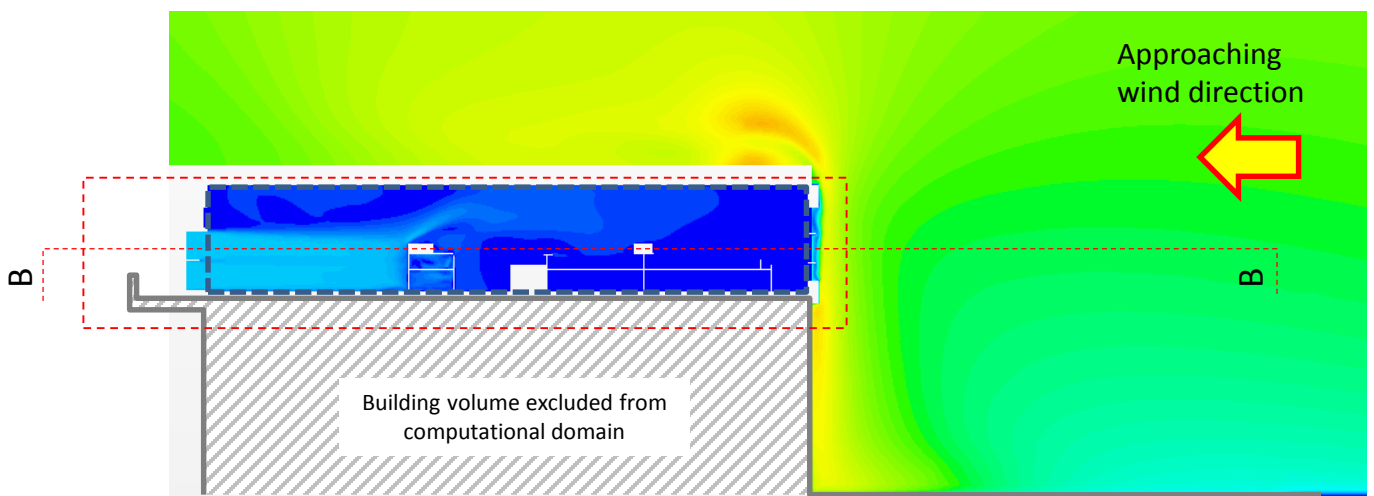


Monitoring plot of wind speed at the locations for placement of sensors for convergence checking

Solution ID	Coupled / Decoupled	With furniture	Turbulence model	Inlet	Outlet	Air density and dynamic viscosity	Test Scenario
E3	Coupled	Yes	k- ω	Wind log profile (NE direction)	Actual curve fan	Actual test condition	Scenario 3



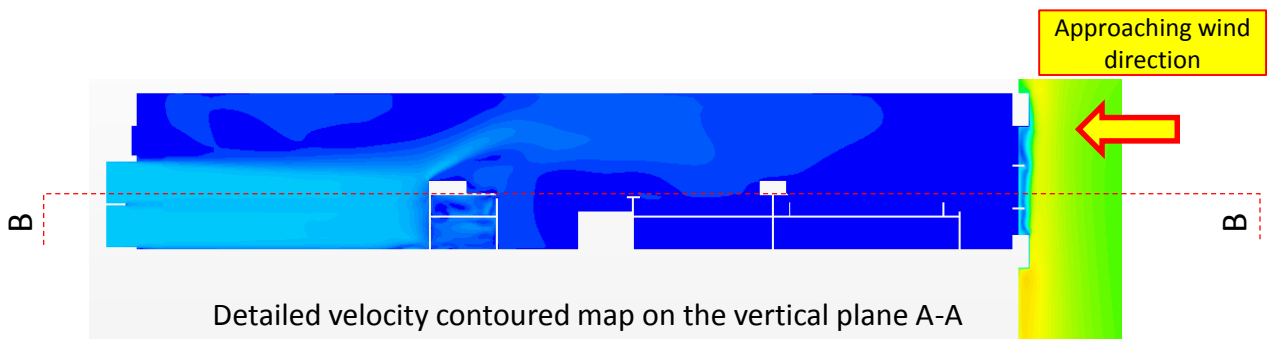
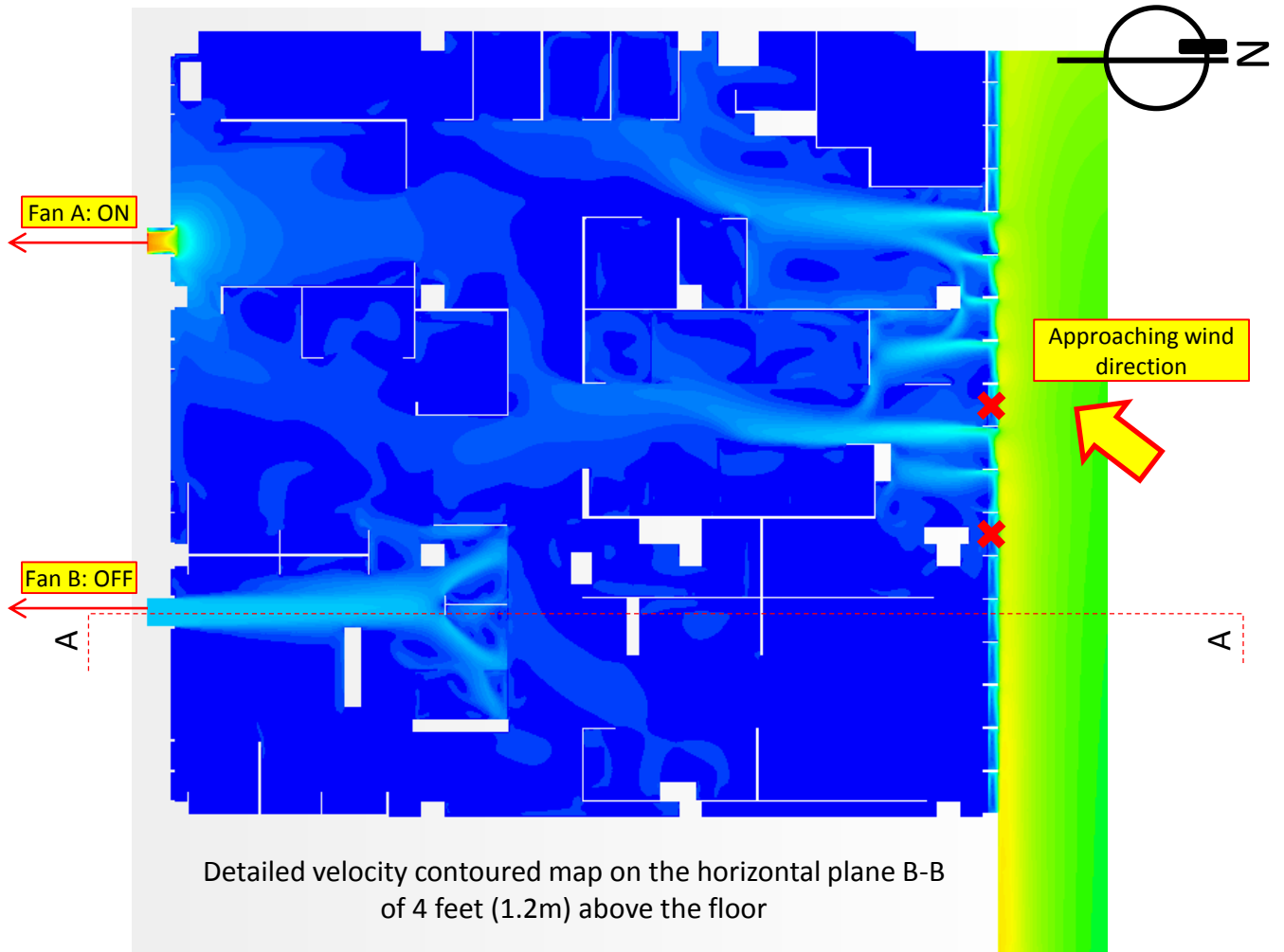
Velocity contoured map on the horizontal plane B-B of 4 feet (1.2m) above the floor (larger view)



Velocity contoured map on the vertical plane A-A (larger view)

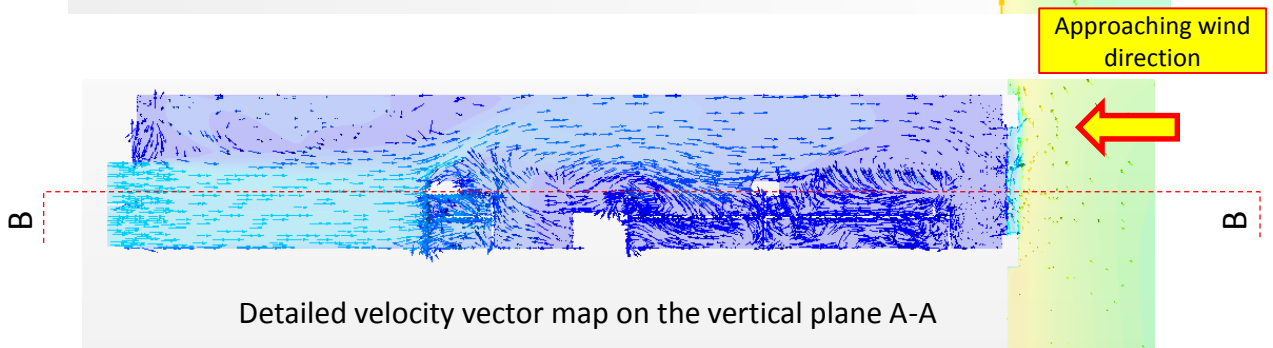
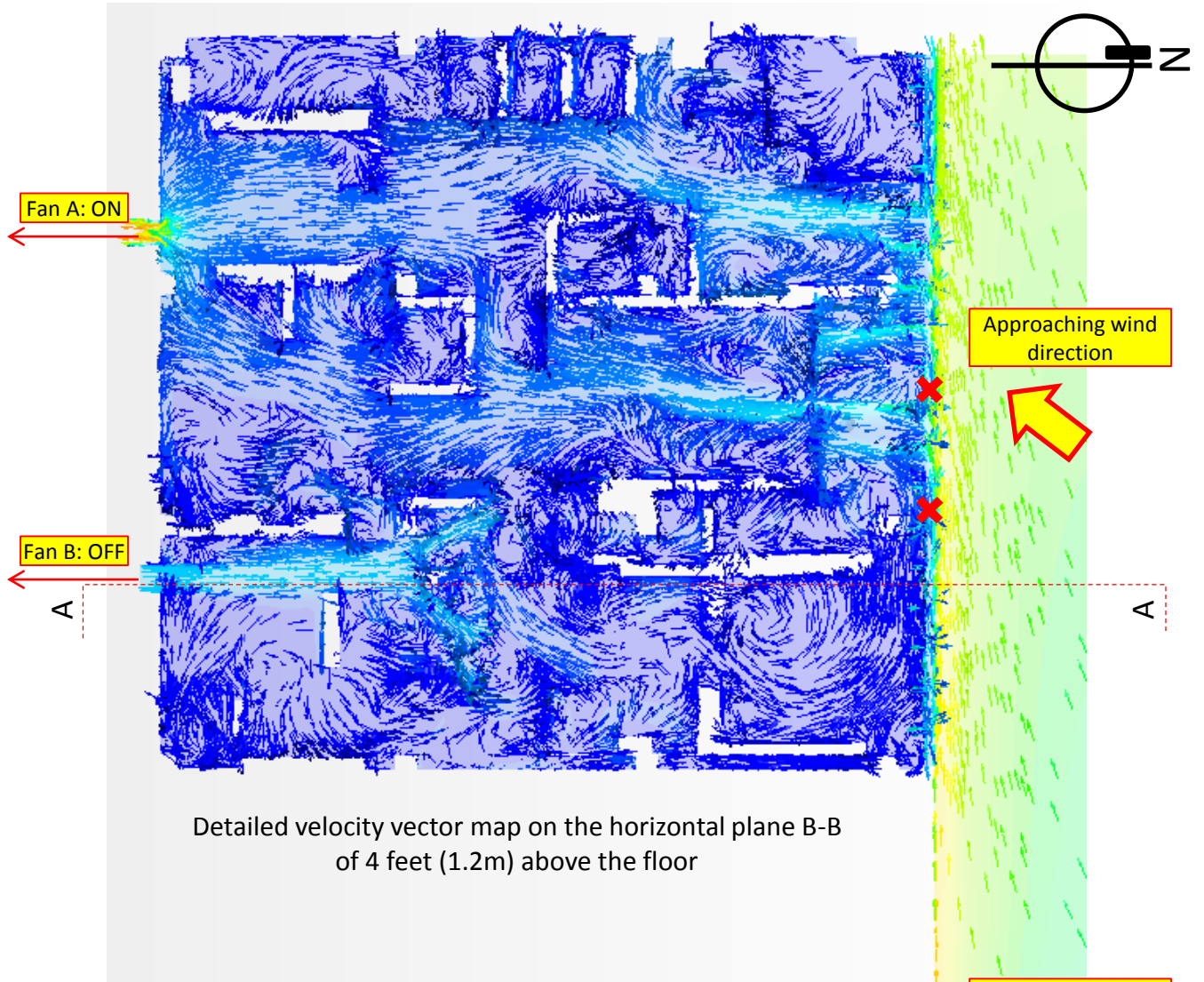


Solution ID	Coupled / Decoupled	With furniture	Turbulence model	Inlet	Outlet	Air density and dynamic viscosity	Test Scenario
E3	Coupled	Yes	k- ω	Wind log profile (NE direction)	Actual curve fan	Actual test condition	Scenario 3



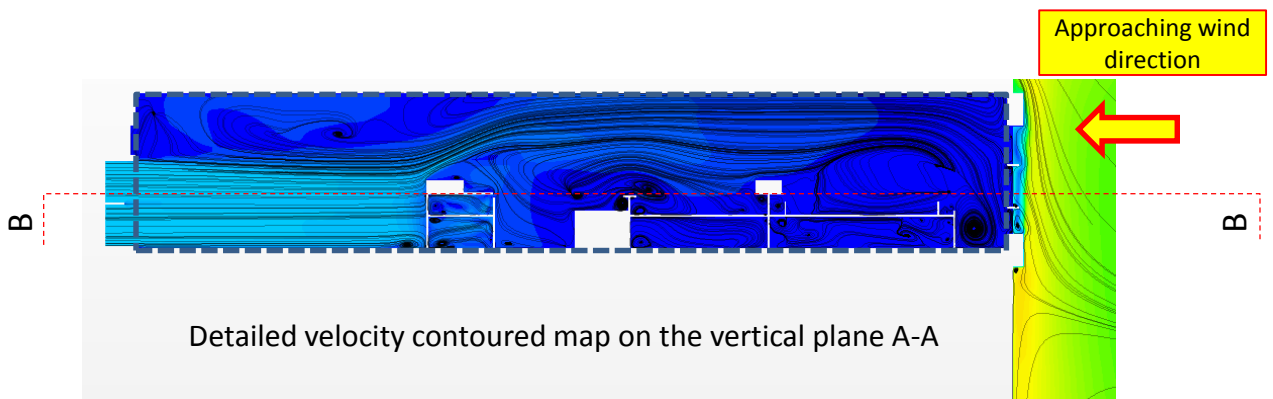
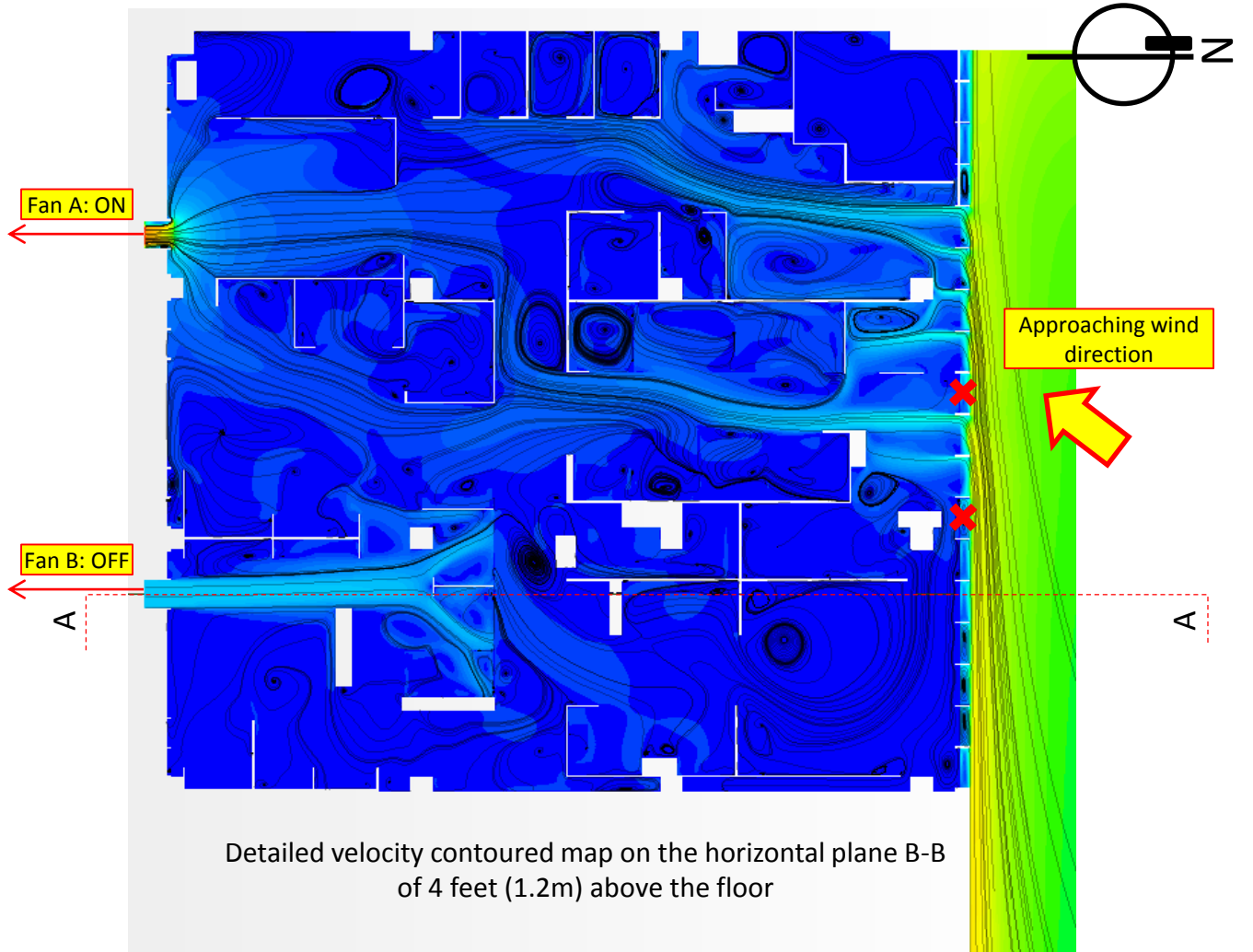
X Permanently closed non-working louvers

Solution ID	Coupled / Decoupled	With furniture	Turbulence model	Inlet	Outlet	Air density and dynamic viscosity	Test Scenario
E3	Coupled	Yes	k- ω	Wind log profile (NE direction)	Actual curve fan	Actual test condition	Scenario 3



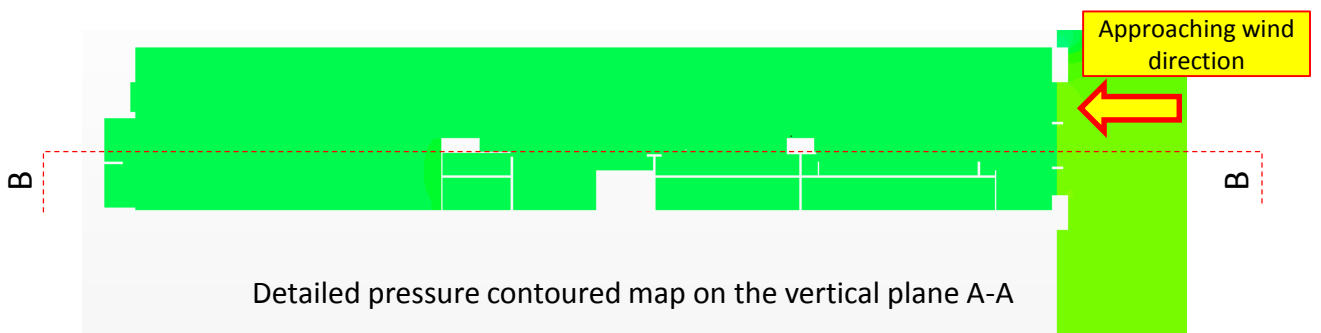
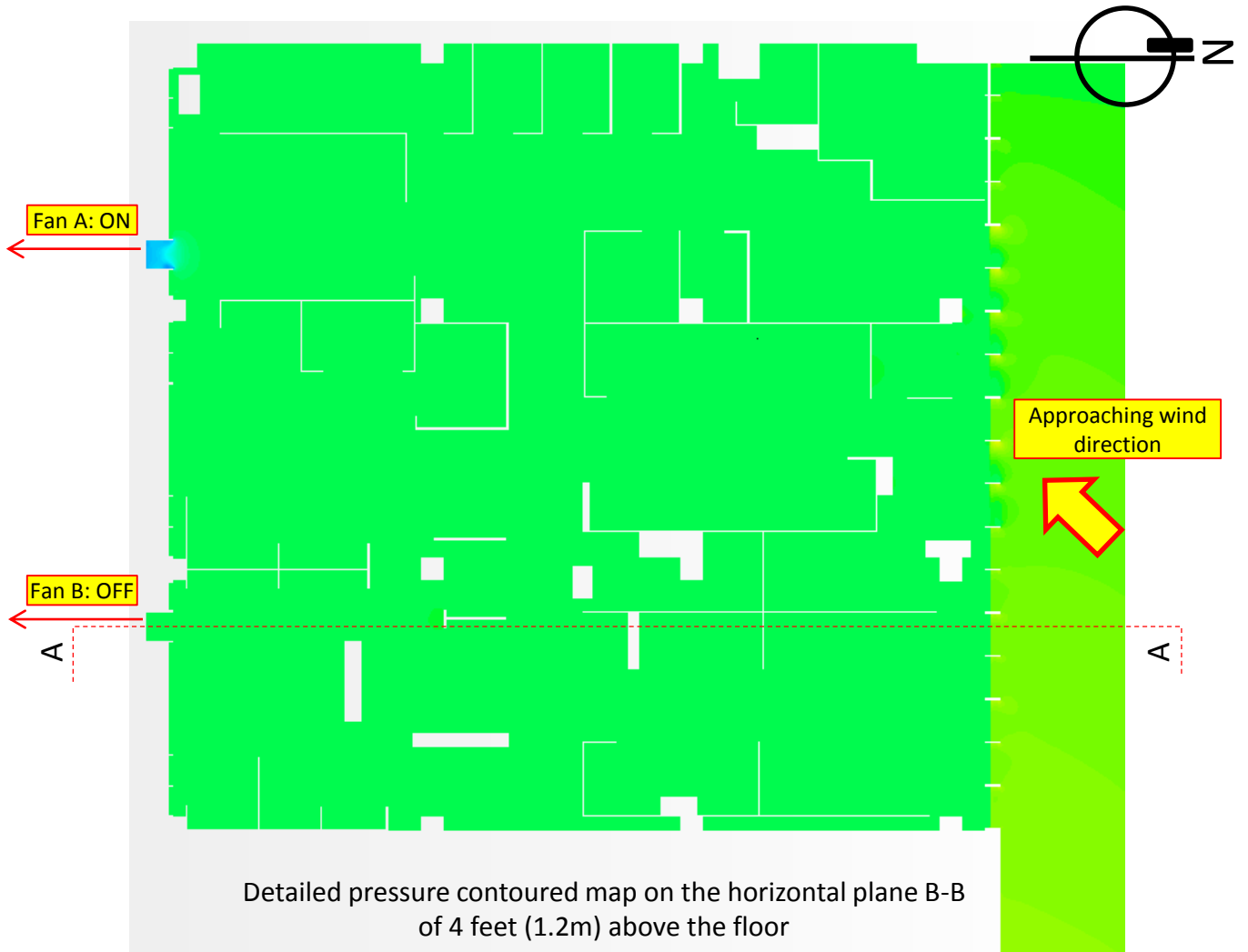
X Permanently closed non-working louvers

Solution ID	Coupled / Decoupled	With furniture	Turbulence model	Inlet	Outlet	Air density and dynamic viscosity	Test Scenario
E3	Coupled	Yes	k- ω	Wind log profile (NE direction)	Actual curve fan	Actual test condition	Scenario 3

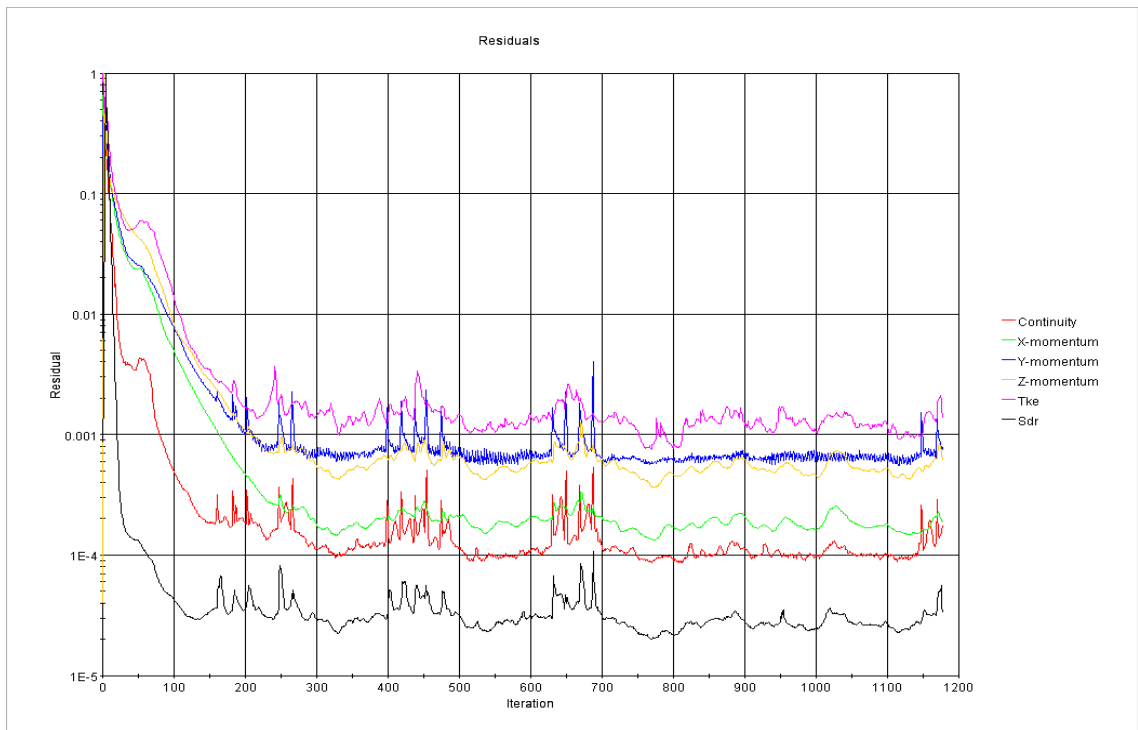


✘ Permanently closed non-working louvers

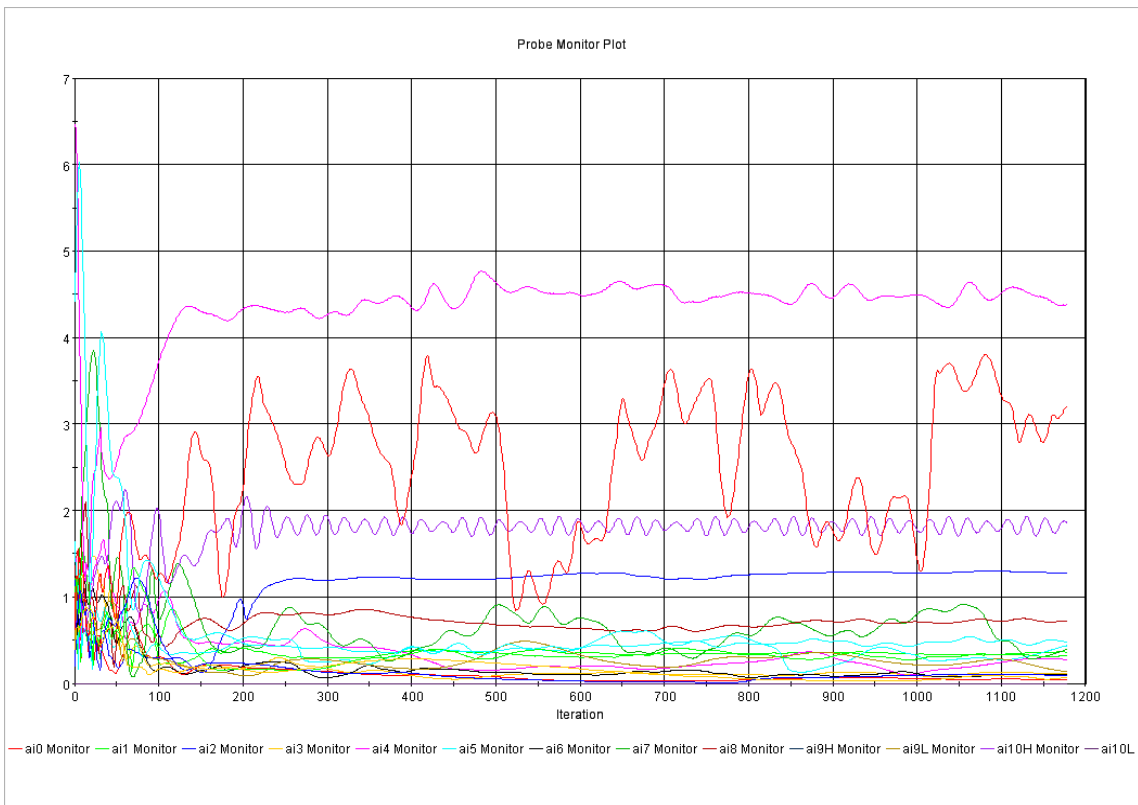
Solution ID	Coupled / Decoupled	With furniture	Turbulence model	Inlet	Outlet	Air density and dynamic viscosity	Test Scenario
E3	Coupled	Yes	k- ω	Wind log profile (NE direction)	Actual curve fan	Actual test condition	Scenario 3



Solution ID	Coupled / Decoupled	With furniture	Turbulence model	Inlet	Outlet	Air density and dynamic viscosity	Test Scenario
E3	Coupled	Yes	k- ω	Wind log profile (NE direction)	Actual curve fan	Actual test condition	Scenario 3

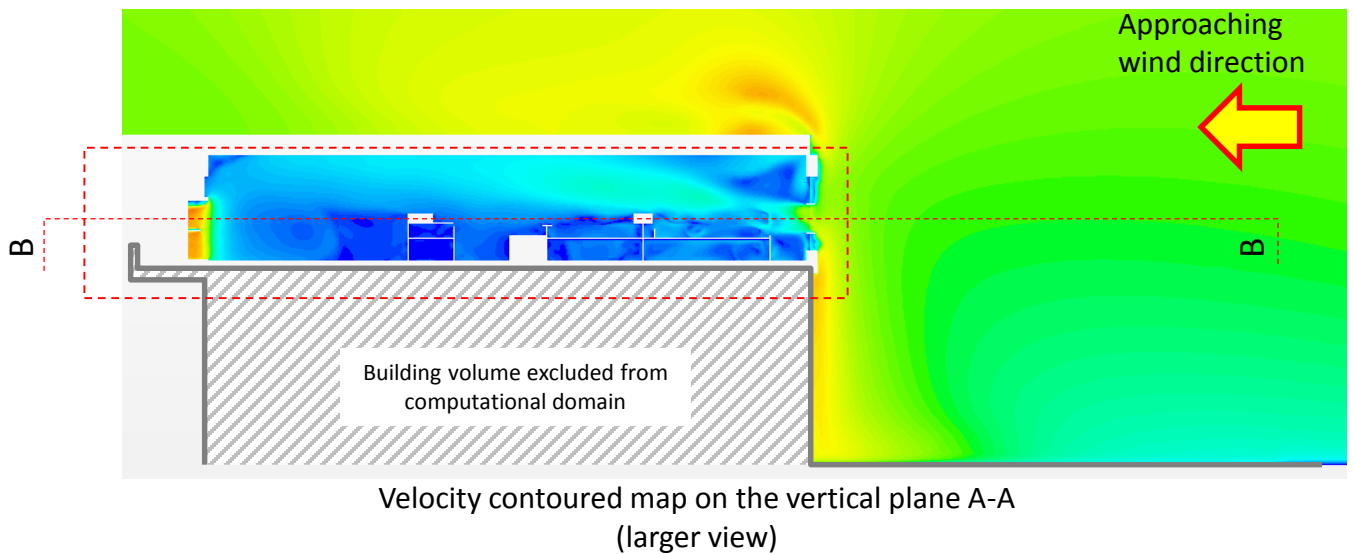
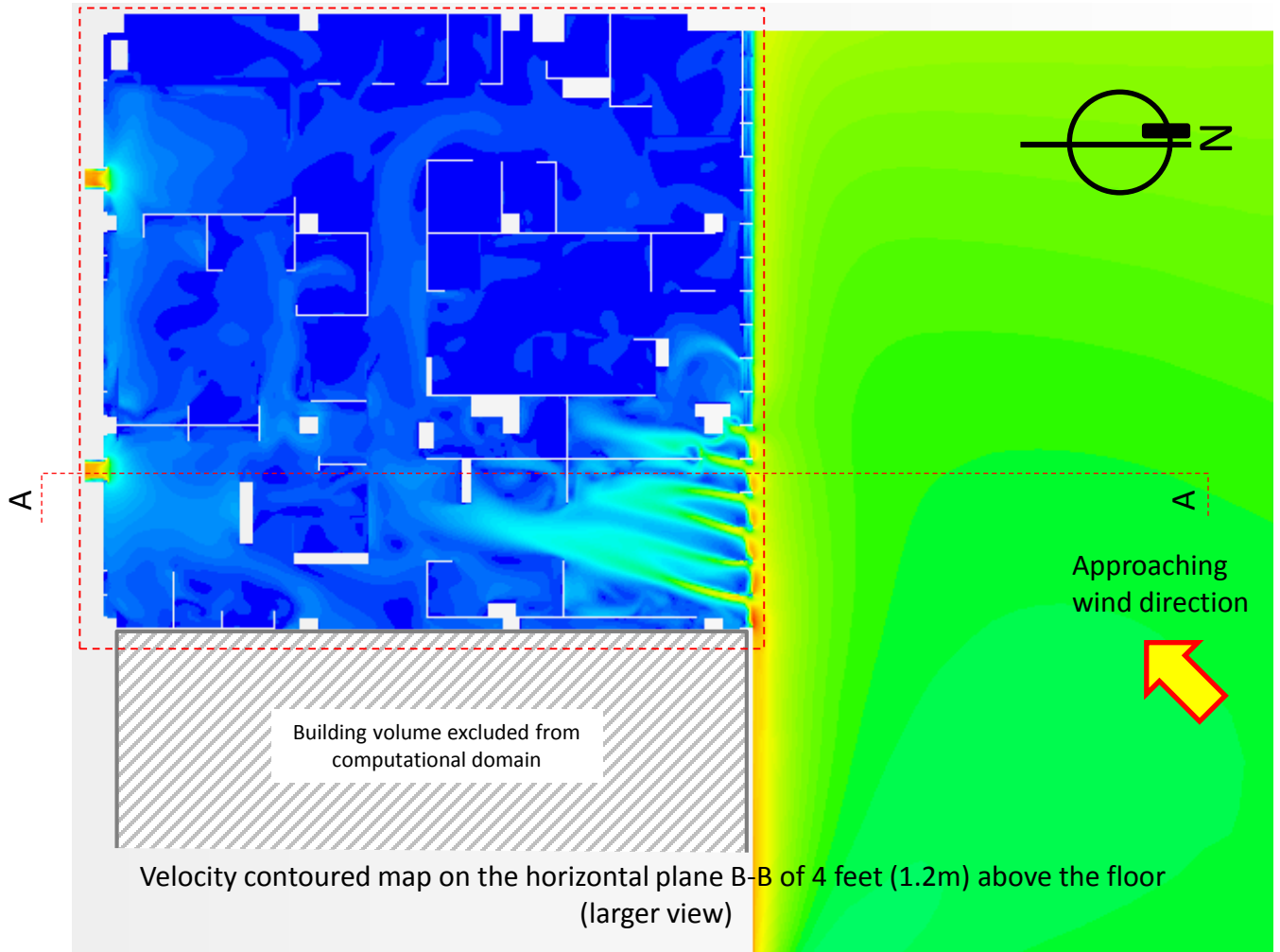


Residual plot

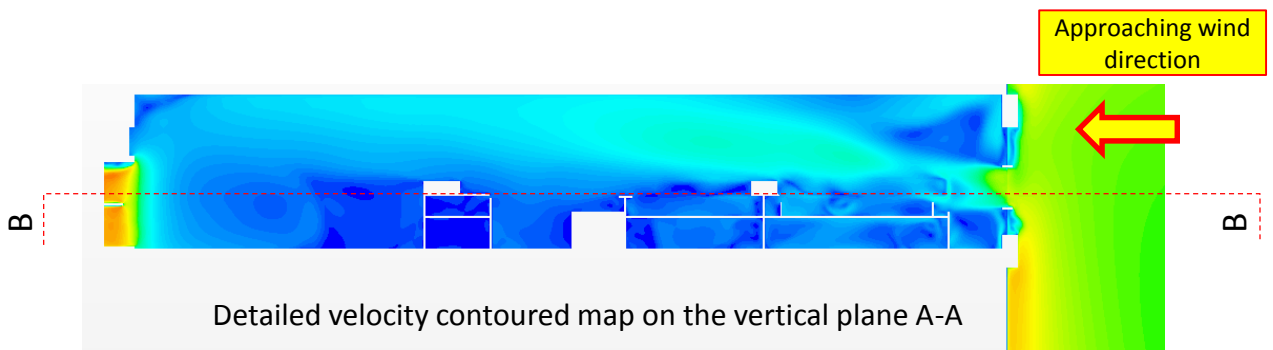
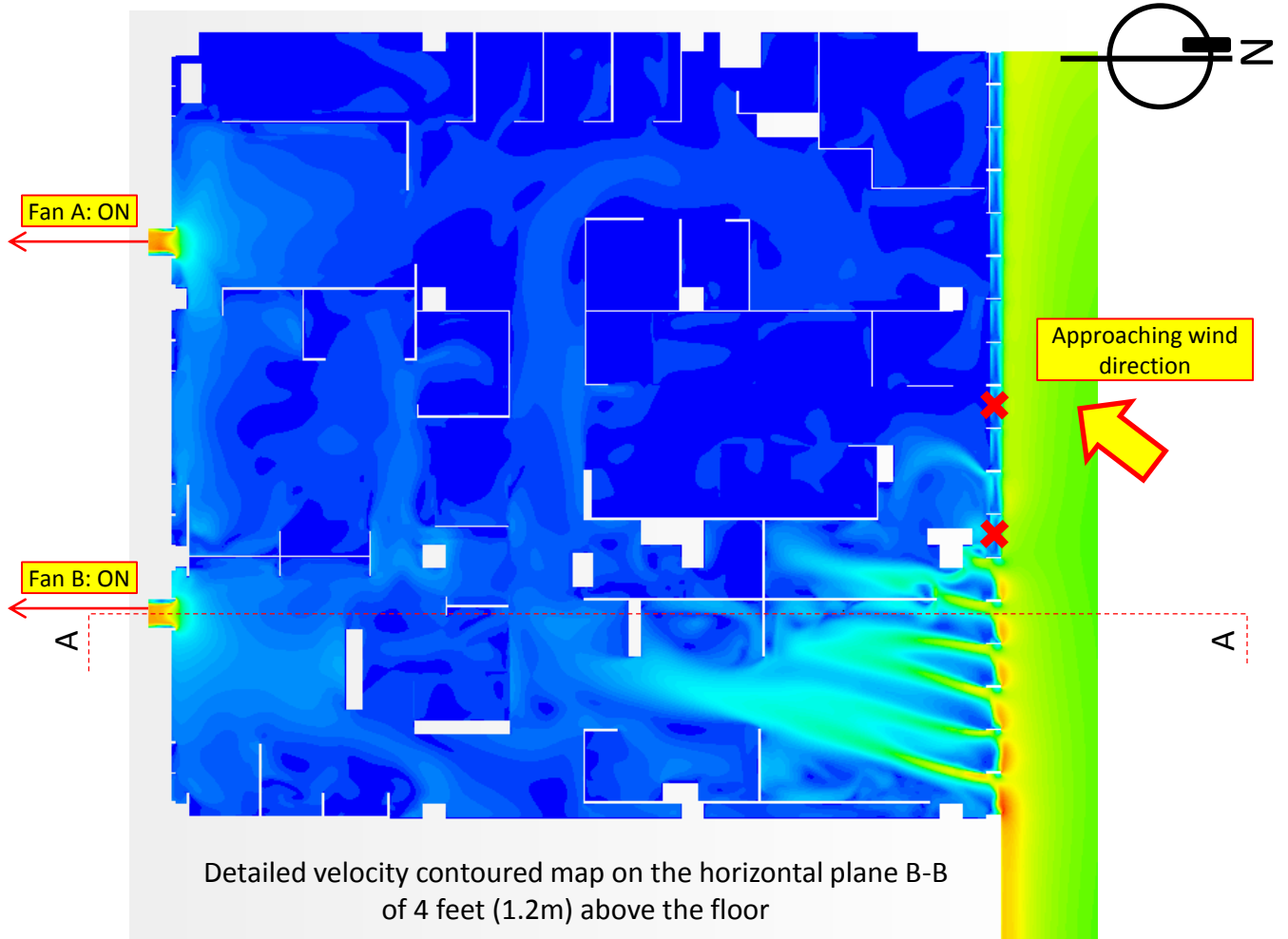


Monitoring plot of wind speed at the locations for placement of sensors for convergence checking

Solution ID	Coupled / Decoupled	With furniture	Turbulence model	Inlet	Outlet	Air density and dynamic viscosity	Test Scenario
E4	Coupled	Yes	k- ω	Wind log profile (NE direction)	Actual curve fan	Actual test condition	Scenario 4

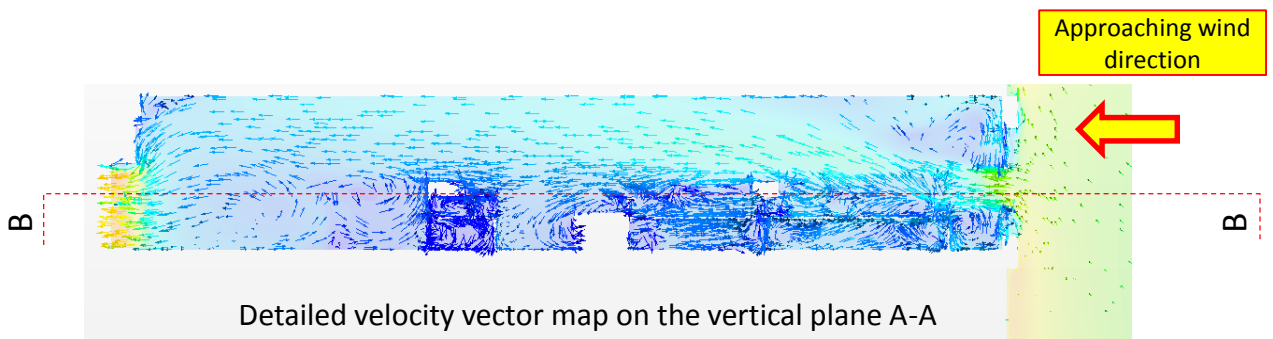
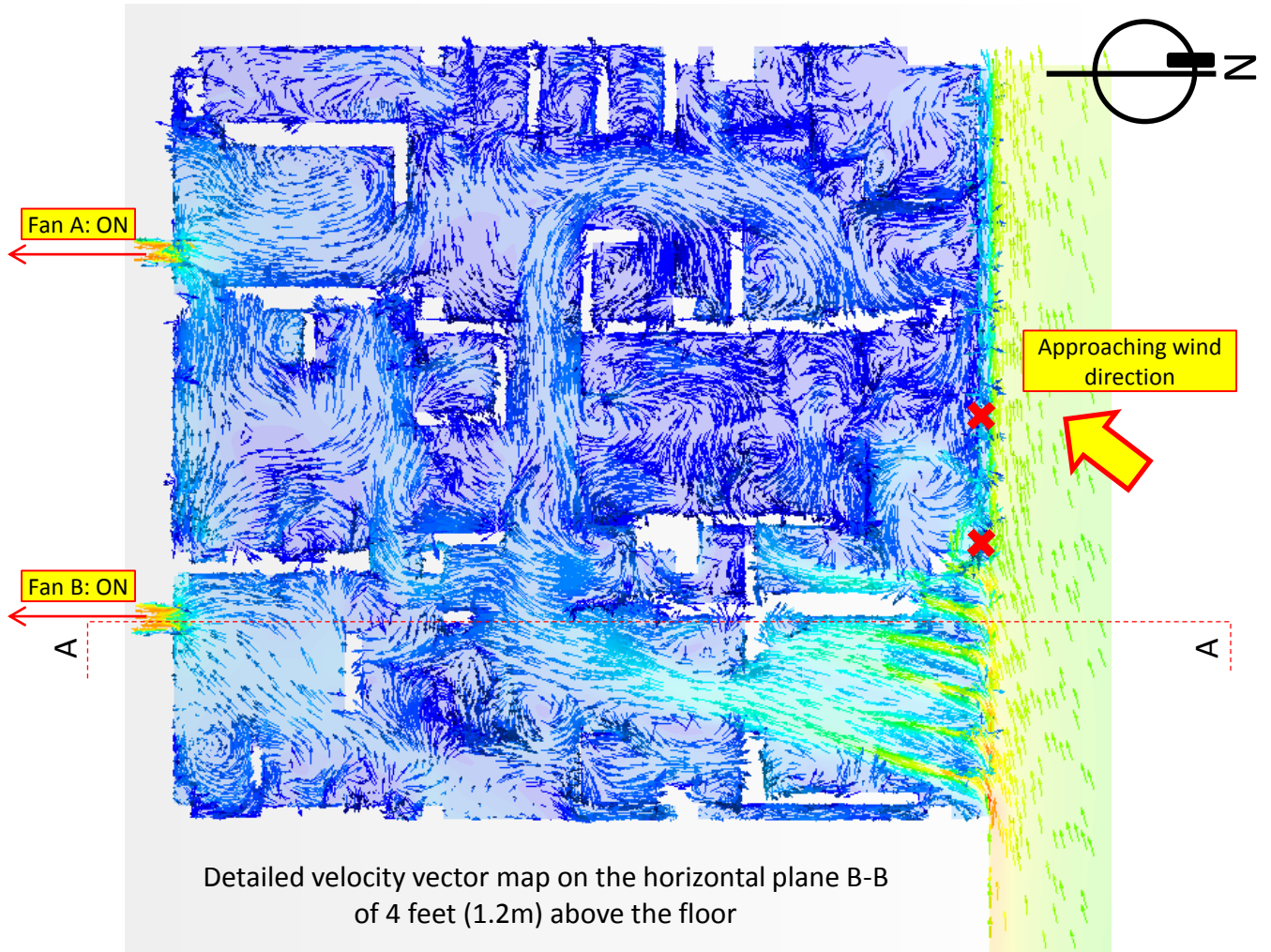


Solution ID	Coupled / Decoupled	With furniture	Turbulence model	Inlet	Outlet	Air density and dynamic viscosity	Test Scenario
E4	Coupled	Yes	k- ω	Wind log profile (NE direction)	Actual curve fan	Actual test condition	Scenario 4



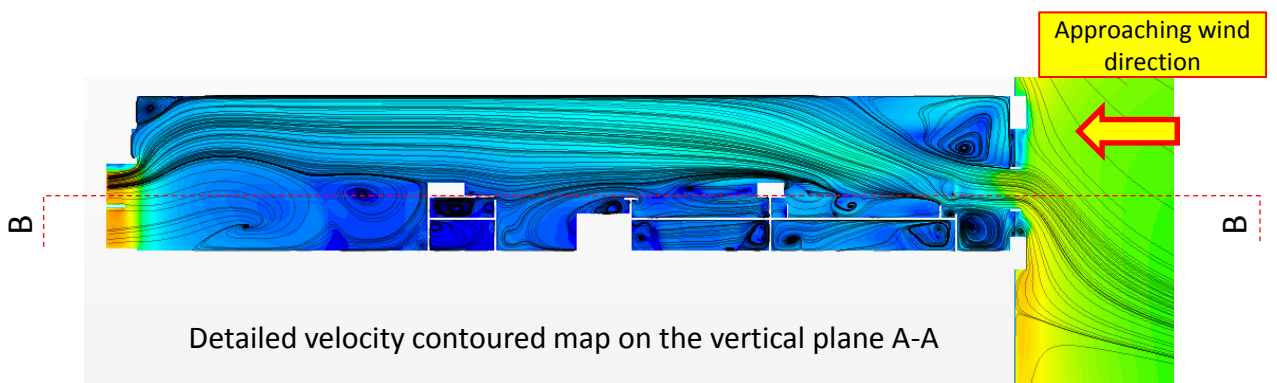
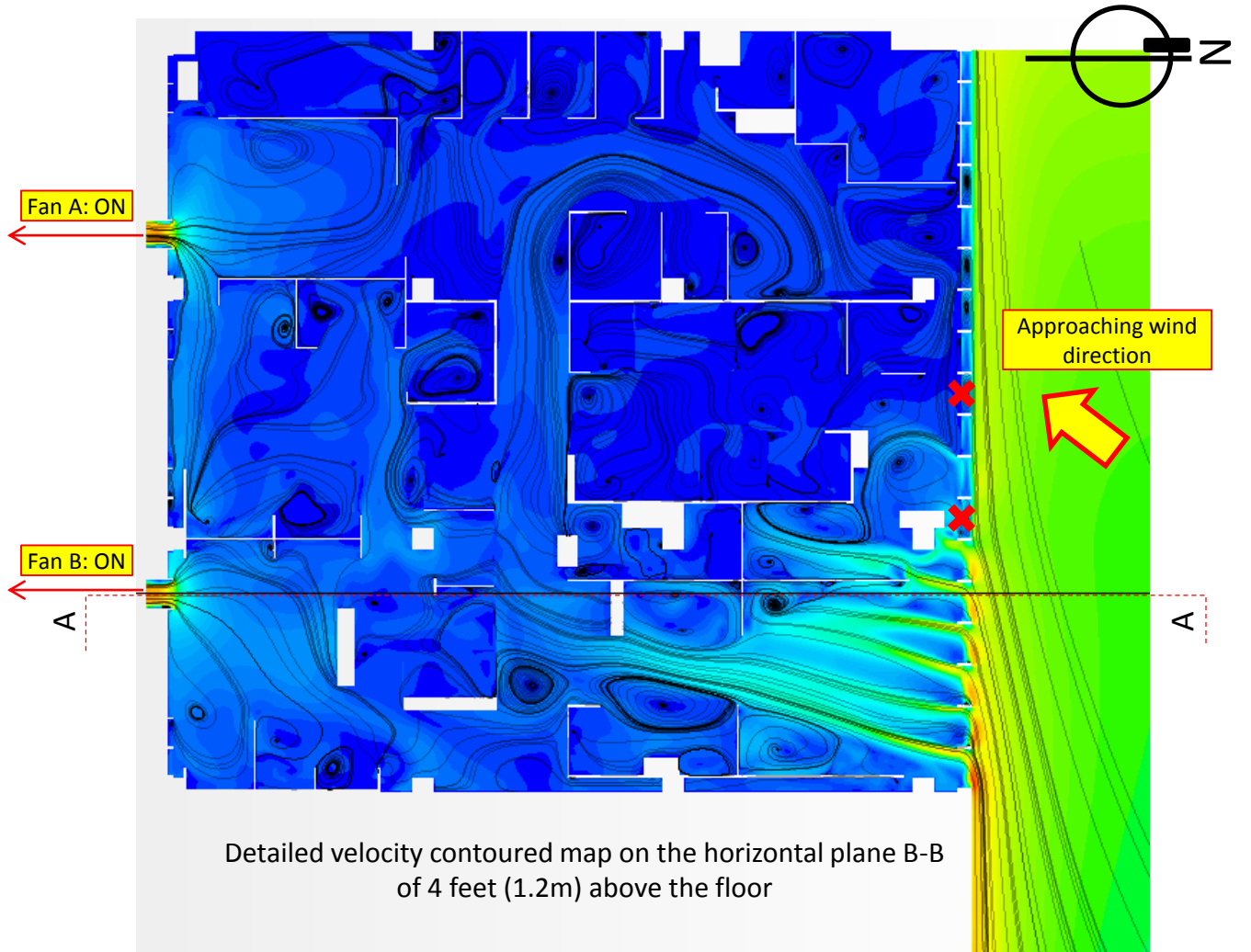
✘ Permanently closed non-working louvers

Solution ID	Coupled / Decoupled	With furniture	Turbulence model	Inlet	Outlet	Air density and dynamic viscosity	Test Scenario
E4	Coupled	Yes	k- ω	Wind log profile (NE direction)	Actual curve fan	Actual test condition	Scenario 4



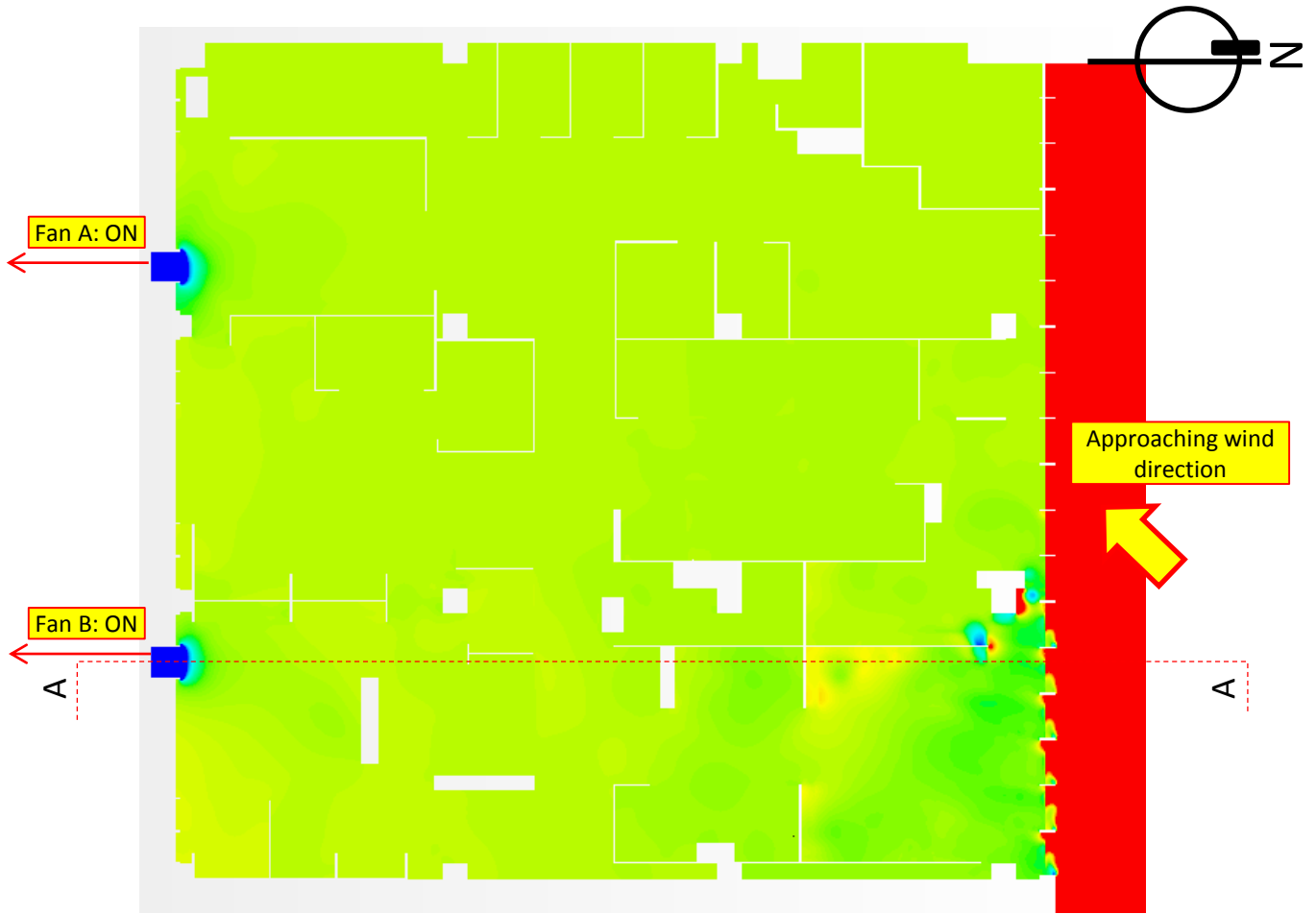
X Permanently closed non-working louvers

Solution ID	Coupled / Decoupled	With furniture	Turbulence model	Inlet	Outlet	Air density and dynamic viscosity	Test Scenario
E4	Coupled	Yes	k- ω	Wind log profile (NE direction)	Actual curve fan	Actual test condition	Scenario 4

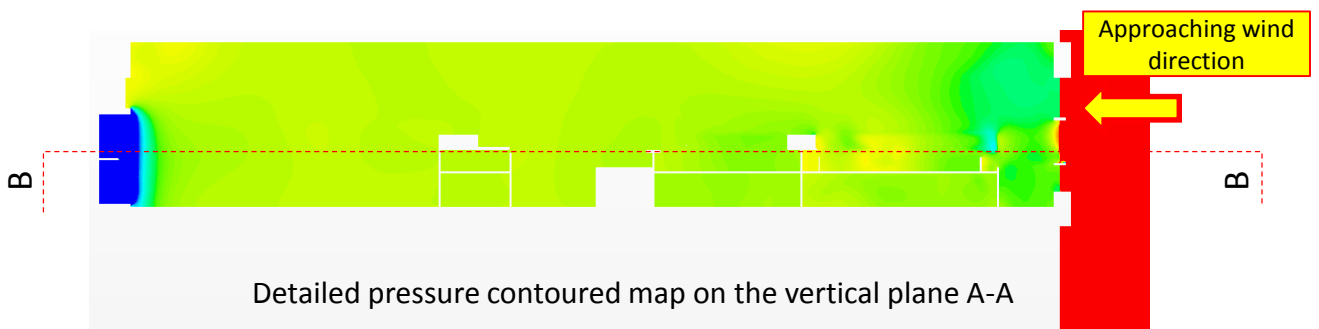


✘ Permanently closed non-working louvers

Solution ID	Coupled / Decoupled	With furniture	Turbulence model	Inlet	Outlet	Air density and dynamic viscosity	Test Scenario
E4	Coupled	Yes	k- ω	Wind log profile (NE direction)	Actual curve fan	Actual test condition	Scenario 4



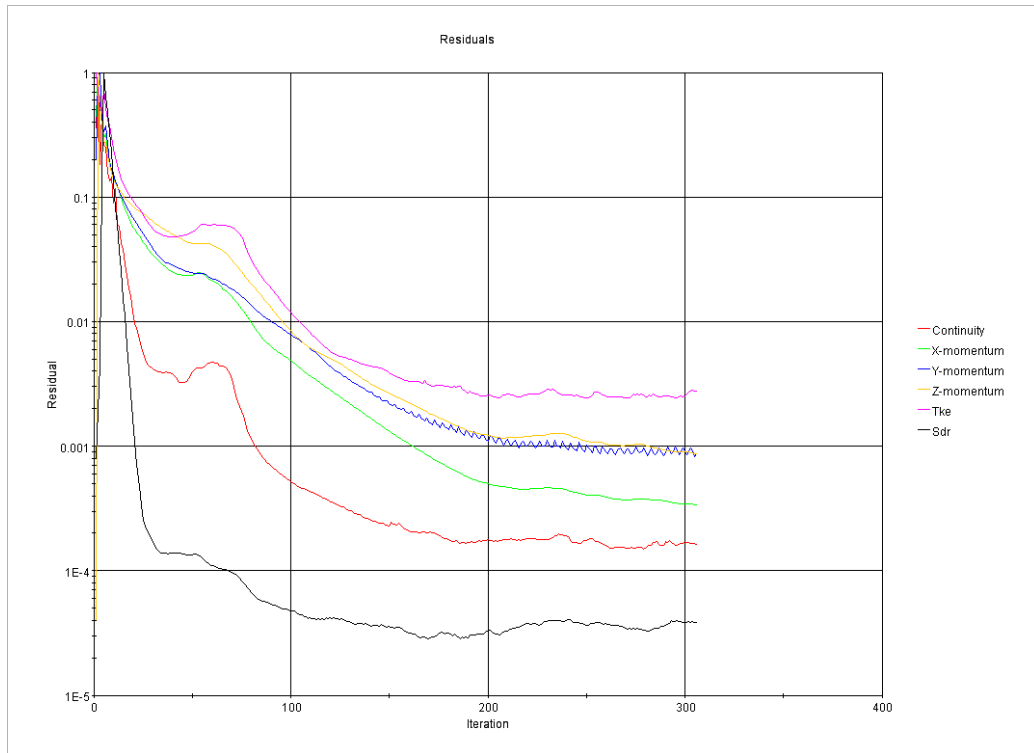
Detailed pressure contoured map on the horizontal plane B-B of 4 feet (1.2m) above the floor



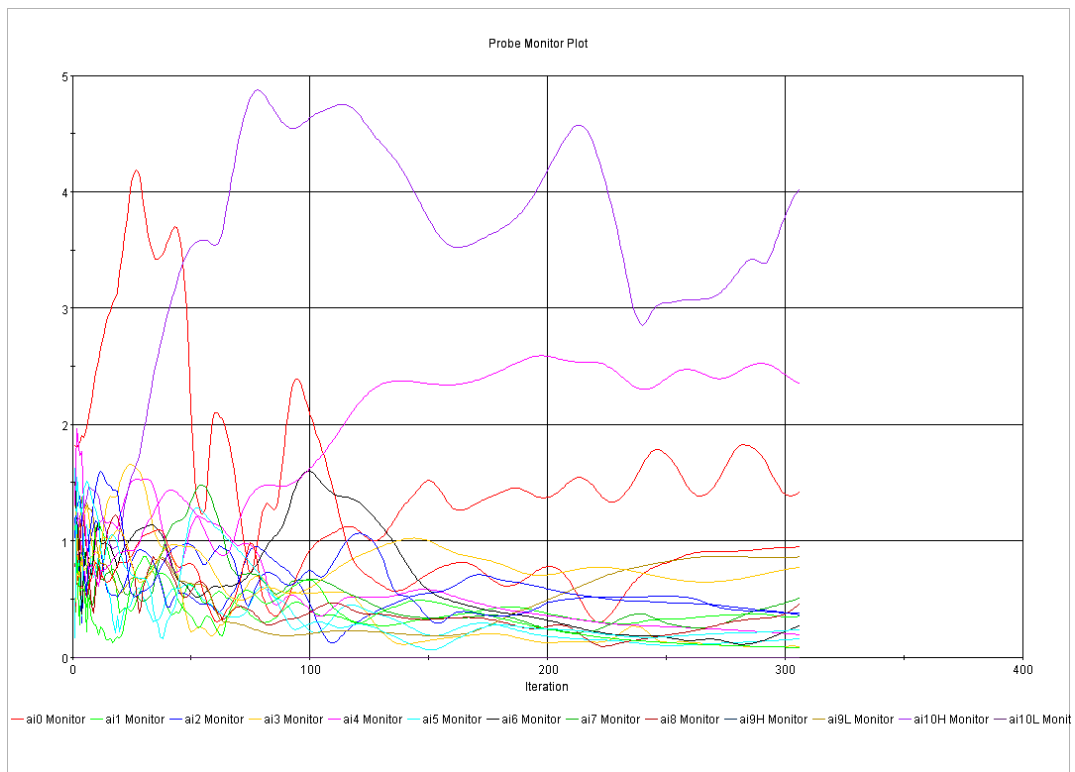
Detailed pressure contoured map on the vertical plane A-A



Solution ID	Coupled / Decoupled	With furniture	Turbulence model	Inlet	Outlet	Air density and dynamic viscosity	Test Scenario
E4	Coupled	Yes	k- ω	Wind log profile (NE direction)	Actual curve fan	Actual test condition	Scenario 4



Residual plot



Monitoring plot of wind speed at the locations for placement of sensors for convergence checking